The preparation of encapsulated fluoride anion in T8 silsesquiocane cages

Thesis

UNRESTRICTED

The preparation of encapsulated fluoride anion in T8 silsesquioxane cages

A thesis submitted for the degree of

Doctor of Philosophy in Chemistry

to

The Open University

by

Manuel Pourny, BSc, AMRSC

April 2005

Department of Chemistry

The Open University

Walton Hall

Milton Keynes MK7 6AA

United Kingdom

DATE OF SUBMISSION 28 APRIL 2005
DATE OF AWARD 12 AUGUST 2005

To Annaick, Morgane and Thiphaine

HUMANS HAVE GOT SO MUCH KNOWLEDGE AND TOO LITTLE UNDERSTANDING.

STATEMENT

I declare that the work included in this thesis was carried out by the author at the Open University Chemistry Department between 1st February 2001 and 29th April 2005 under the supervision of Dr Peter Taylor and Dr Alan Bassindale. The material embodied in this thesis has not been submitted nor is currently being submitted for any other degree.

The work is the result of my own investigations apart from the following which are fully acknowledged:

Elemental analyses carried out by Medac Ltd
Solid State ^{19}F NMR by Dr David Apperley from the Industrial Research Laboratories, University of Durham

Parts of the work have been presented or published as listed below:

A. Bassindale, M. Pourny, P.G. Taylor et al.; *Angewandte Chemie*, 42 (**2003**), 3488, Fluoride ion encapsulated in a silsesquioxane cage – a novel molecular anion.

A. Bassindale, M. Pourny, P.G. Taylor et al.; *Organometallics*, 23 (**2004**) 19, 4400-4405, Fluoride ion encapsulation in octasilsesquioxane cages as models for ion entrapment in zeolites. Further examples, X-ray crystal structure studies and investigations into how and why they may be formed.

London, UK, June 2002 (poster)
New Orleans, USA, March 2003 (poster)
London, UK, June 2003 (poster)

Manuel Pourny, April 2005

ACKNOWLEDGEMENTS

I would like to thank my supervisors, Peter Taylor and Alan Bassindale, not only for their continuous support and guidance through my studies but also for their friendship, discussion and nice company over some pints of nice English beer.

I would also like to express my sincere gratitude, and the word is small, to Sharon Moore for her continous help in and outside the lab but mainly for her friendship and for making me so nicely welcome in her house during the last year. I must thank Rebecca and Sean for their great company and laugh during this time at theirs.

I would also like to thank Jenny for her help in Shakespeare's language and her friendship during these four years.

I must also thank the staff of the Research School Department of The Open University, and particularly Alison Robinson, Paula Piggott and Samantha Quinn for their help and support through my time at the Open University.

I must thank The Open University Chemistry Department and particularly all the technicians, Gordon Howell, Jim Gibbs, Brandon Cook, Graham Jeffs, Colin Haynes, Pravin Patel for their assistance and help in the lab without which it would not have been possible to complete this work. I must also thank Mike Mortimer for his assistance in obtaining the solid state ^{19}F NMR.

Finally, I must thank my parents, Franz, Emmanuelle and my lovely nieces for all their encouragement, not only during my PhD but also for all the years spent too far from them. I would especially thank Sophie who has been of an immense support and patience through these four years.

ABSTRACT

A great number of reactions leading to the formation of polyhedral silsesquioxanes are known. Because this is a complex and multistep process, these reactions also lead to polymers and oligomers, which may include polyhedral silsesquioxanes and some homo derivatives. Our work has focused on the synthesis of octasilsesquioxanes by the hydrolytic condensation of trifunctional monomers using tetra-*n*-butylammonium fluoride as a catalyst. We have studied the influence of solvent and the nature of the alkoxy leaving group in the starting material, trialkoxysilane, on the yields in the synthesis of octacyclopentyloctasilsesquioxanes and octaphenyloctasilsesquioxanes. Using the TBAF route, we also prepared a phenyl-T8, a vinyl-T8 and *para*-tolyl-T8 cage with a fluoride anion which is perfectly centred in the middle of the cage. For all of these fluoride encapsulated cages, we have obtained single crystal X-Ray structures as shown below.

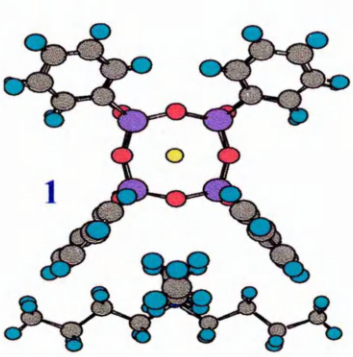

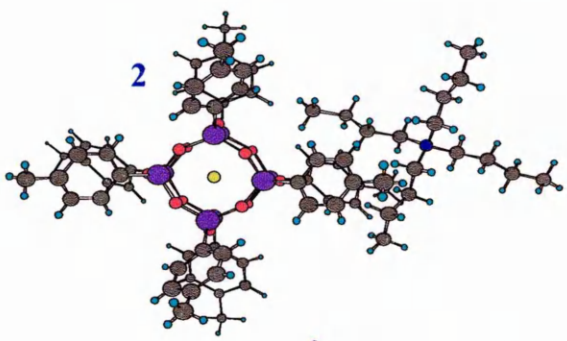

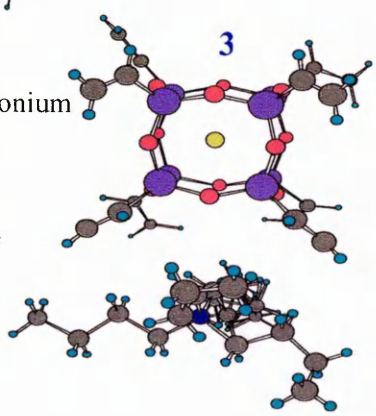

Compounds **1**, **2** and **3**. Structure of tetra-*n*-butylammonium octaphenyloctasilsesquioxane fluoride (**1**), tetra-*n*-butylammonium octa-*para*-tolylsilsesquioxane fluoride (**2**) and tetra-*n*-butylammonium octavinyloctasilsesquioxane fluoride (**3**)

We were also able to synthesize octa-*para*-chloromethylphenyloctasilsesquioxane cage with an encapsulated fluoride anion. For this latter structure we only obtained ^{29}Si and ^{19}F NMR data and Mass Spectrometry data which are in agreement with data from the phenyl and vinyl cages. The four tetra-*n*-butylammonium octasilsesquioxane fluoride cages obtained so far all have an sp^2 carbon atom bonded to the silicon atom. We thus attempted to prepare fluoride-encapsulated cages where the R group at silicon is bound by an sp^3 carbon, such as cyclohexyl, cyclopentyl, *iso*butyl, n-octyl or benzyl. Unfortunately using these groups, we have only been able to isolate the conventional octasilsesquioxane fluoride ion free cages. However, experimental attempts to synthesize Q8 cages with fluoride ion inside have been successful and even though we were unable to obtain a single X-ray crystal structure, ^{29}Si and ^{19}F NMR spectroscopy and Mass Spectrometry data demonstrated that tetra-*n*-butylammonium fluoride Q8 cages were the main product of the reaction and were obtained in reasonable yields. In order to understand the encapsulation mechanism we investigated the possibility of the entrapment of different anions using other sources of catalyst. None of these investigations showed the encapsulation of an anion other than fluoride ion. This highlighted the peculiar role of TBAF and so we looked further at the mechanism of the encapsulation and its requirements in terms of physical and environmental parameters.

Finally we carried out some physical studies and in particular Thermo Gravimetric Analysis (TGA) of some of materials synthesized by our research group, namely pure hexa, octa and dodecasilsesquioxane cages and compared them with the corresponding fluoride-encapsulated cages where possible.

SYMBOLS AND ABBREVIATIONS

λ	Wavelength of absorption
Ar	Aryl group
br	Broad
bp	Boiling point
Cp	Cyclopentyl
Cy	Cyclohexyl
d	Doublet
DCM	Dichloromethane
DMF	Dimethylformamide
DMSO	Dimethyl Sulfoxide
EI	Electron Ionisation
ELSD	Evaporative Light Scatter Detector
ET	Electron Transfer
FTIR	Fourier Transform Infrared Spectroscopy
GC	Gas Chromatography
HPLC	High Performance Liquid Chromatography
Hz	Hertz
J	Coupling constants
LC-MS	Liquid Chromatography-Mass Spectrometry
m	Multiplet
M	Molar
MALDI-TOF	Matrix-Assisted Laser Desorption Ionisation Time of Flight

MAS NMR	Magic Angle Spinning Nuclear Magnetic Resonance
MS	Mass Spectrometry
NMR	Nuclear Magnetic Resonance
NOBA	3-nitrobenzyl alcohol
ppm	Parts per million
q	Quartet
s	Singlet
TASF	Tris(dimethylamino)sulfonium difluorotrimethylsilicate
TBAF	Tetra-*n*-butylammonium fluoride
TEA	Triethylamine
TGA	Thermo Gravimetric Analysis
THF	Tetrahydrofuran
TMS	Tetramethylsilane, also Trimethylsilyl
Ts or tosyl	*p*-toluenesulfonyl
UV-vis	Ultra violet-visible spectroscopie
VR	Vibrational relaxation

New compounds will be named as followed and I will use the following abbreviations:

Tetrabutylammonium octaphenyloctasilsesquioxane fluoride **Ph_8T_8-TBAF**

Tetrabutylammonium octavinyloctasilsesquioxane fluoride **vinylT_8-TBAF**

Tetrabutylammonium octa-*para*-tolyloctasilsesquioxane fluoride ***para*-tolylT_8-TBAF**

Tetrabutylammonium octa-*para*-chloromethylphenyloctasilsesquioxane fluoride

(*para*-chloromethyl)phenylT_8-TBAF

Tetrabutylammonium octaethoxyoctasilsesquioxane fluoride **Et_8Q_8-TBAF**

Tetrabutylammonium octapropoxyoctasilsesquioxane fluoride **Pr_8Q_8-TBAF**

To aid the organisation of the text, I have numbered the experiments as MPXXX (ex: MP08) in the text and their details will be reported in the experimental section.

Contents

Chapter 1: Introduction

1.1 Introduction

A major objective of modern science is to build new molecules and materials of technological and biochemical interest. One class of these new materials of particular interest is the silicones where the first commercialisation began with the production of linear polymers. The silicone industry began with the commercialisation of silicone resins, consisting primarily of silsesquioxanes, for electrical insulation at high temperature. Developmental Research was started in the 1930's in Corning Glass Works and the General Electric Company[1]. The research work at Corning Glass Work resulted in formation of the Dow Corning Corporation in 1943. General Electric started commercial production of silicones in 1946. Since then silicone sales world wide have reached multibillion dollar levels and the number of silicone products are measured in thousands.

In understanding the background to silicone chemistry it is necessary to look at the atomic properties of silicon and the occurrence of silicon in the natural world. The presence of silicon and carbon in group 14 of the periodic table suggests that the chemistry of these two elements should be similar. In fact, the electronic structures are similar with $2s^2 2p^2$ for carbon and $3s^2 3p^2$ for silicon which shows why silicon and carbon share the most common bonding configuration, the sp^3 hybridization configuration. While carbon atoms tend to form more stable π bonds than silicon atoms, silicon atoms participate much better in extracoordinate bonding as pentad-[2,3,4,5] or hexacoordinate[6].

Silicon atoms form the largest number of bonds with other elements, second only to carbon. Unlike carbon, for which the C–C, C–O and C–H bond energies are close, the Si–O bond is considerably stronger than the Si–H bond and much stronger than the Si–Si bond. Additionally, silicon and oxygen are the two most abundant elements to be found in the earth's crust, therefore, chains of Si–O– and Si–O–Si readily make up the skeletons of most silicates[7]. As a main topic of this thesis is polyhedral silsesquioxane cages with organic groups attached to the silicon atoms, it is interesting to notice the higher bond strength of the silicon-oxygen bond (~130 kcal/mol) in comparison with the silicon-carbon bond strength (~90 kcal/mol) reported by R. Walsh and R. Becerra[8].

Most of the silicon in nature is present in the form of silica (SiO_2) or silicate minerals with crystalline silica being the main constituent of sand. Given the availability of silica, some bioorganisms such as sponges and diatoms have processed it in silica exoskeleta[9] from dissolved silicic acid (with general formula, $[SiO_x(OH)_{4-2x}]_n$, such as *metasilicic acid* (H_2SiO_3), *orthosilicic acid* (H_4SiO_4), *disilicic acid* ($H_2Si_2O_5$), and *pyrosilicic acid* ($H_6Si_2O_7$)).

So most of the naturally-occurring compounds containing silicon atoms on earth are made up of a skeleton of Si-O bonds and Si-O-Si chains as in silica and silicate minerals.

Another family of important and largely used compounds containing silicon atoms are silicones $(RR'SiO)_n$. Silicones have been known since the early part of the twentieth century and Frederick Stanley Kipping[10,11] were among the first to prepare, name and characterize them. The popularity of silicones is due in part to their properties:

- High thermostability and resistance to chemical degradation[12] which made them used as in seals of kitchen appliances or hair dryers.

- Electrical resistance[13,14] for which they are used as wire coating or motor insulators.
- Hydrophobicity[15] for which property silicones are used as release agents to prevent adhesion or as surfactants when combined with hydrophilic species.

Silicones possess a large array of useful properties which led to intense research for the synthesis of new compounds with even greater ranges of properties. Polymerization and crosslinking processes of silicones have been used in the discovery of new classes of compounds such as dendrimers[16], polymers and copolymers[17]. Such synthesis has been made possible by the presence of functional groups on the side chain, R and R', in the silicone oligomers $(RR'SiO)_n$. All these silicone products have very high molecular weight and quite random network structures. Even more highly crosslinked network polymers have been prepared by the condensation of trifunctional silanes ($RSiX_3$) alone with the resulting network containing only one functional organic residue on each silicon atom. These specific compounds are called silsesquioxanes[1,18]. The term silsesquioxanes refers to all structures with the empirical formula $RSiO_{3/2}$ where R is hydrogen (hydrosilsesquioxanes or hydridosphero-silsesquioxanes), alkyl, alkylene, aryl, arylene or organo-functional derivatives of alkyl, alkylene, aryl or arylene groups. The structures of silsesquioxanes have been reported as random structures, ladder structures or cage structures as illustrated in Figure 1.

Figure 1 Random and ladder structure of silsesquioxanes

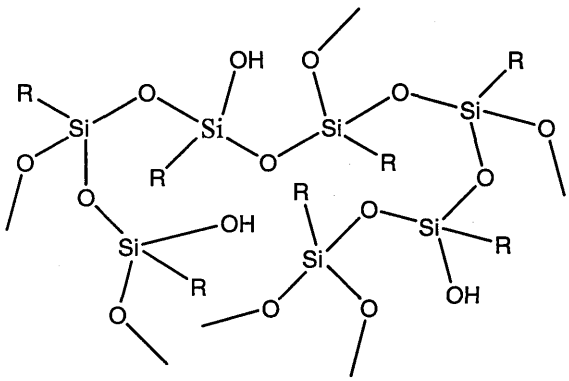

Random structure

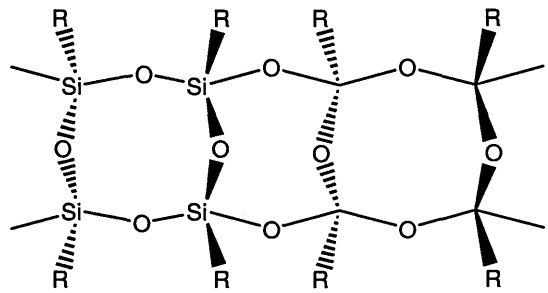

Ladder structure

In the case of cage structures, the number of $\{RSiO_{3/2}\}$ units sets the shape of the frame, which is unstrained for eight and ten units. Silsesquioxane cage compounds $(RSiO_{3/2})_n$ represent a rather versatile class of potential three-dimensional building blocks for the synthesis of new materials, and therefore they are of considerable theoretical and practical interest. These compounds are known as polyhedral silsesquioxanes (sometimes referred to as POSS)[19]. The structures of the lower oligosilsesquioxanes are represented by the structural formulae in the Figure 2 below.

Figure 2 Structure of lower oligosilsesquioxanes

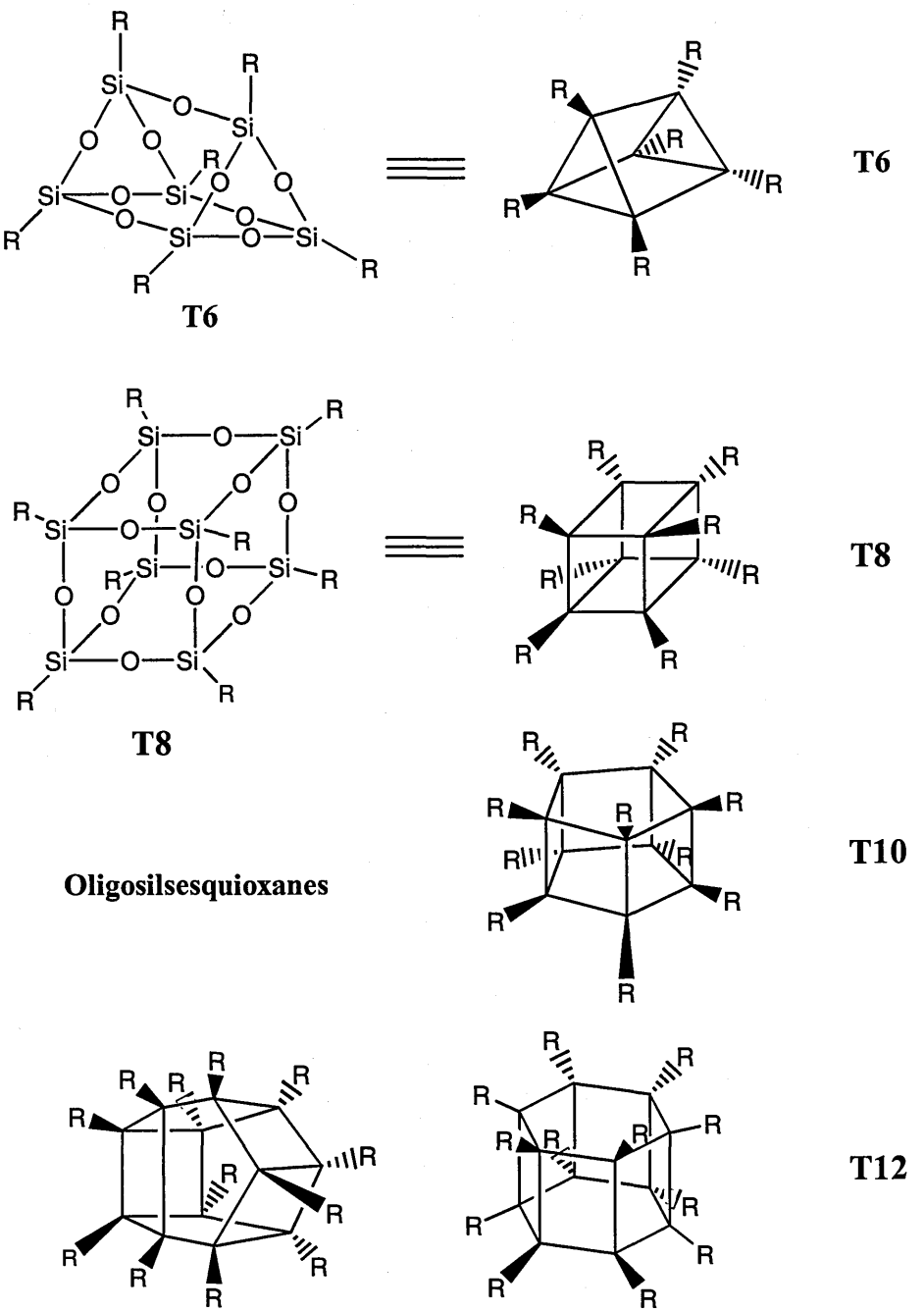

A great number of reactions leading to the formation of polyhedral silsesquioxanes are known. Depending on the nature of the starting material, these reactions can be divided in two groups: the first group involves the construction of Si-O-Si bonds from $RSiX_3$ precursors with subsequent formation of polyhedral silsesquioxanes. These reactions,

because of a complex and multistep process, lead to polymers and oligomers, which may include polyhedral silsesquioxanes and, when R_2SiX_2 compounds are also used as precursors, some homo derivatives, homooligosilsesquioxanes[18,20]. Homooligosilsesquioxanes are structurally similar to oligosilsesquioxanes. They differ from regularly built oligosilsesquioxanes in that one of the Si-O bond of the latter is inserted by an RR'SiO group. Homooligosilsesquioxanes are described by the general formula $(RSiO_{3/2})_nO$-SiR'R'' and the structures of their lower members are shown in Figure 3.

Figure 3 Lower Homooligosilsesquioxanes

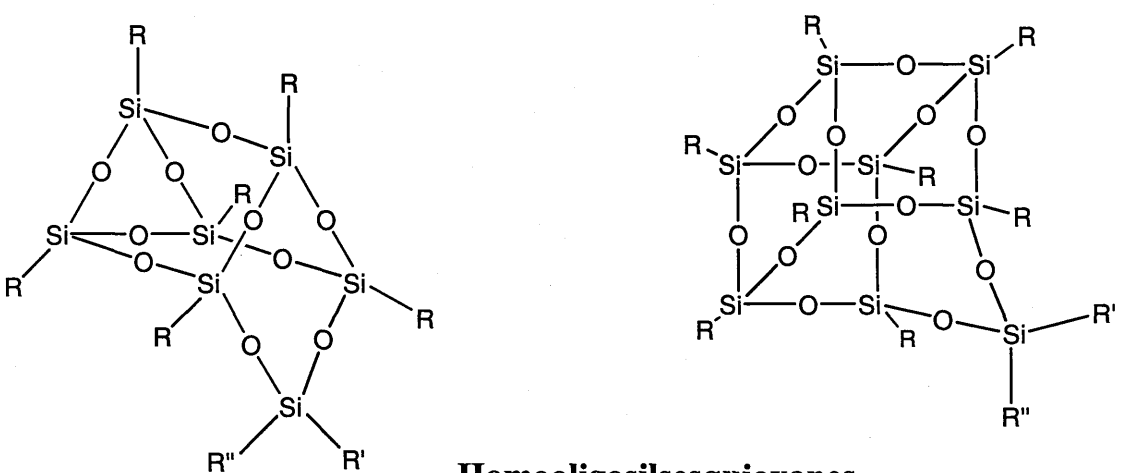

Homooligosilsesquioxanes

The second group of reactions is based on the modification of a pre-existing silicon-oxygen framework, such as hydrosilsesquioxanes[21,22,23], in other words this second type of synthesis involves only variation of the structure and composition of substituents at the silicon without affecting the Si-O-Si skeleton of the molecule. Calzaferri and co-workers[24] have obtained octahexylsilsesquioxane and octa-cyclo-hexylmethylsilsesquioxane by reacting $H_8Si_8O_{12}$ with 1-hexene and methylenecyclohexene respectively.

The silsesquioxanes can be divided into two classes, functional and non-functional. The first group involved methyl-[25] and other alkyl-silsesquioxane (ethyl, propyl, *cyclo*-hexyl etc.), aryl-silsesquioxanes (phenyl) and mixed silsesquioxanes[19]. The second and more interesting class of silsesquioxanes contain functional groups at the silicon atoms as vinyl, Si-OH or Si-H group. The hydridosilsesquioxane cage, $(HSiO_{3/2})_8$, was the first octasilsesquioxane cage structure to be characterised unequivocally by Larsson in 1960 using single crystal X-ray crystallography[26].

Since then, the novel physical and chemical properties as well as the interesting cage structure have enriched the research on this novel class of compounds. Improvements in analytical chemistry and method of chemistry investigation have led to the synthesis and characterization of a wide range of new polyhedral silsesquioxane frameworks. Some new examples and their characterisation are reported later in this thesis.

1.2 Nomenclature

As a detailed summary of silane nomenclature can be found in Eaborn's book[27], we limit interest in this section to the nomenclature of silicones. Silicone components are differentiated by the number of oxygen attachments as monofunctional (M), difunctional (D), trifunctional (T) and tetrafunctional (Q), as shown in Figure 4. In this simplified nomenclature, it is assumed that, unless otherwise specified, the groups at the silicon are methyl groups. In case of a methyl is replaced by a different residue, this will be indicated by a superscripted symbol as D^H represents -OSiMeHO-.

Figure 4 Nomenclature for silicone components

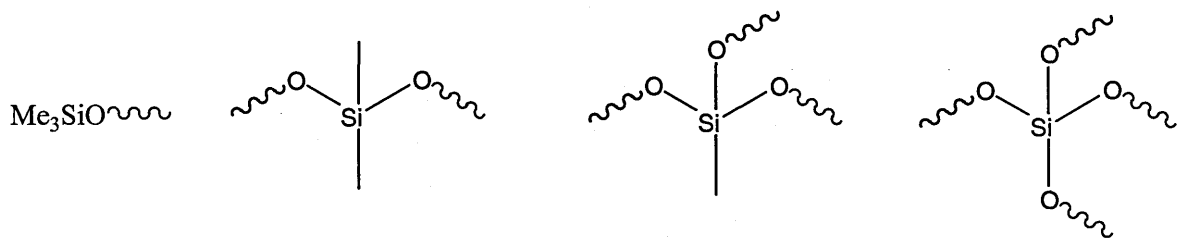

M **D** **T** **Q**

Silicones poly(dialkylsiloxanes) **Silsesquioxanes** **Silicates Silica etc.**

As this thesis will focus on polyhedral silsesquioxanes, we will describe now the nomenclature most commonly used for such compounds. The general name of these compounds contains indications about its silicon atom: "sil" for silicon, "sesqui" means 1.5 and "oxane" for linked to oxygen atom. This indicates that each silicon atom in these polyhedral silsesquioxanes is connected to three oxygen atoms, each of which is part of a SiOSi group giving rise to a general formula for the SiO unit of $SiO_{3/2}$. The basic silicon unit in the polyhedral silsesquioxane, $(RSiO_{3/2})_n$, will thus be represented by the letter T and the silsesquioxane cages will be thus represented by the letter T_n. When n = 6, 8, 10 and 12, these polyhedral silsesquioxanes are called hexa, octa, deca and dodecasilsesquioxanes, respectively, i.e. T_6R_6, T_8R_8, $T_{10}R_{10}$ and $T_{12}R_{12}$. In the same way, spherosilicate cages, $(ROSiO_{3/2})_n$, will be represented by the letter Q_n.

In this thesis, all of silsesquioxane formulae are simplified as follows;

Hexacyclopentylsilsesquioxane: Cp_6T_6

Octaphenylsilsesquioxane: Ph_8T_8

Decylphenylsilsesquioxane: $Ph_{10}T_{10}$

Dodecylphenylsilsesquioxane: $Ph_{12}T_{12}$

For the spherosilicate cages,

Spherosilicate, $(SiO_{3/2})_8[OEt]_8$: $(EtO)_8Q_8$

1.3 Synthesis of Polyhedral Silsesquioxanes Cages

Silsesquioxanes are a unique class of three dimensional polyhedral silicon oligomers that present very interesting chemical and physical properties. They have found a wide use as models in different fields such as silicate/zeolite chemistry, catalytic chemistry[28,29] and also as scaffolds for the development of liquid crystals[30,31], biocompatible materials[32] and dendrimers[33]. Such important applications in surface and materials chemistry have led, in the last decades, to intense investigation for a high yielding and selective synthetic route to prepare them.

1.3.1 Synthesis of Spherosilicate Silsesquioxanes Cages

As noted previously, depending on the nature of the starting materials, two types of reaction for the synthesis of the polyhedral silsesquioxane cages have been developed. The first group of reactions involves only the variations in the structure and composition of the substituents at the silicon atom without modification of the silsesquioxane skeleton of the molecule. The second group involving the reactions giving rise to new Si-O-Si bonds and leading to the formation of the polyhedral silsesquioxane framework $(SiO_{3/2})_n$ by hydrolytic polycondensation of trifunctional monomers of the $XSiY_3$ type (with X being a chemically stable substituent and Y a highly reactive substituent).

Octahydrosilsesquioxane $H_8Si_8O_{12}$ was first prepared fortuitously in about 0.1% yield in 1959 by Muller and co-workers[34] in 1959, while studying the preparation of polyhydrydosilsesquioxanes. In 1970, Frye and Collins[35], reported the synthesis of the octahydrooctasilsesquioxane cage in about 13% yield by careful hydrolysis of trichlorosilane in a benzene-concentrated H_2SO_4 mixture, as shown in Figure 5.

Figure 5 Frye and Collins' route to the synthesis of octahydrooctasilsesquioxane cage

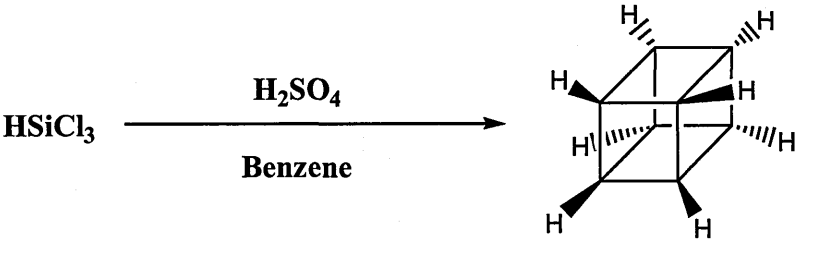

Yield = 13%

A further improvement was made by Agaskar[36] in 1991 who developed a new synthetic route which gave a mixture of T_8, $H_8Si_8O_{12}$ and T_{10}, $H_{10}Si_{10}O_{15}$ in 27% yield by using

partially hydrated $FeCl_3$ as the source of water for the hydrolysis of $HSiCl_3$, as shown in Figure 6.

Figure 6 Agaskar's route to the synthesis of octahydrooctasilsesquioxane cage

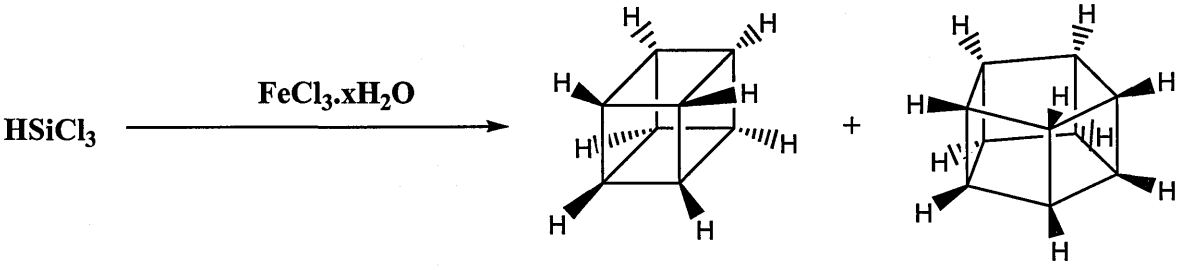

Yield = 27%

Initial routes[33] to functionalized T_8 cages focused on the hydrosilylation of alkenes with Si-H groups of these octahydrosilsesquioxane cages, $H_8Si_8O_{12}$, but have been limited by the low yield of the preparation of the $H_8Si_8O_{12}$ from the hydrolysis of trichlorosilane[36,22].

The second route for the synthesis of the polyhedral silsesquioxane cages involves the formation of the polyhedral silsesquioxane framework.

Scott[37] reported in 1946 the first octasilsesquioxane, $(CH_3SiO_{3/2})_8$, which was isolated along with other volatile compounds through thermolysis of the polymeric products of methyltrichlorosilane and dimethyldichlorosilane co-hydrolysis. However, this method has not been popular and the most common process now used to obtain oligosilsesquioxanes, where R is an organyl group, involves the controlled hydrolytic condensation of trifunctional monomers, $RSiX_3$, where R is a chemically stable organyl substituent and X is a highly reactive substituent, such as chloro or alkoxy. The yield obtained for the synthesis of octasilsesquioxane cages using this route are again low and not suitable to promote and extend the use of such interesting compounds.

The first report on the synthesis of octasilsesquioxane using the hydrolytic condensation route was by Sprung and Guenther[38,39] in 1955. Octamethyl and octaethyl silsesquioxane cages were found as by-products when the corresponding alkyltriethoxysilane was hydrolyzed in benzene with hydrochloric acid.

In the same year, Barry and co-workers[40] reported the synthesis of few octaalkyloctasilsesquioxane cages (R = propyl, *n*-propyl, *n*-butyl, *cyclo*-hexyl) by the hydrolysis of the corresponding $RSiCl_3$ compound with sodium hydroxide or potassium hydroxide as the catalyst.

It was only in 1958, that a major improvement in the yield of the synthesis of silsesquioxane cages was reported by Olsson[41]. Different octasilsesquioxane cages, $(RSiO_{3/2})_8$, were obtained in up to 44% yield by controlling the amount of water added to the hydrolysis of $RSiCl_3$ (R = methyl, ethyl, *n*-propyl, *n*-butyl, *iso*-butyl, phenyl), as shown in Figure 7.

Figure 7 Olsson's route to the synthesis of octaoctasilsesquioxane cage

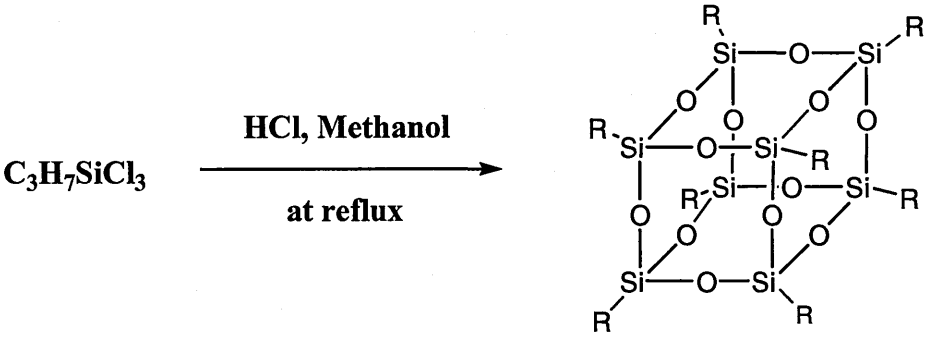

Larsson reported in 1960 the first investigation of these octasilsesquioxane cages using single crystal X-ray crystallography[42].

In 1963, Vogt and Brown[43] reported the synthesis of hexa, octa, deca and dodecasilsesquioxane cages by hydrolysis of methyltriethoxysilane with potassium hydroxide as the catalyst and methanol as the solvent, as shown in Figure 8.

Figure 8 Vogt and Brown's route to the synthesis of octaoctasilsesquioxane cage

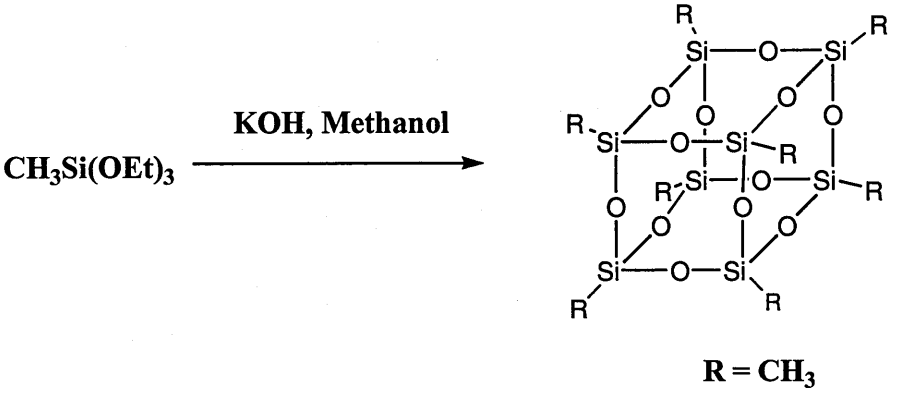

Brown and co-workers[44] also reported the synthesis of the octaphenyloctasilsesquioxane cage by the condensation of phenyltrichlorosilane.

Martynova and co-workers[45] reported the preparation of the octaallyloctasilsesquioxane cage from the hydrolysis of allyltrichlorosilane in ethanol at -40°C. After purification by sublimation, the structure was confirmed by single crystal X-ray crystallography. However, the yield (13%) of this reaction similarly remained low.

In 1989, Feher and Budzichowski[46] reported the synthesis of the octabenzyl, octa-*m*-tolyl and octa-3,5-dimethyloctasilsesquioxane cages by careful addition of the corresponding $RSiCl_3$ to well-stirred ethanol at room temperature and refluxing for 2 days. The same authors[47] synthesized the octa-(*p*-chloromethyl)phenyloctasilsesquioxane cage by hydrolyzing *p*-chloromethylphenyltrichlorosilane in an acetone-water solution. Voronkov[48] and later, Harrison and Hall[49], synthesized the octavinyloctasilsesquioxane cage by the hydrolytic condensation of vinyltrichlorosilane and reported higher yields (30-40%).

All these synthesis routes suffer from yields of no more than 40%. The increasing industrial interest for such compounds required the invention and investigation of novel and high yielding routes of synthesis.

In 2003, Unno and co-workers[50] reported the synthesis of the octa-*t*-butyldimethylsilyloctasilsesquioxane by the oxidation of the octa-*t*-butyldimethylsilyloctasilacubane in 98% yield, as shown in Figure 9. The reaction occurs in benzene at room temperature and addition of *m*-chloroperbenzoic acid as the oxidizing agent whilst stirring for 7 days.

Figure 9 Unno's synthesis route to octasilsesquioxane

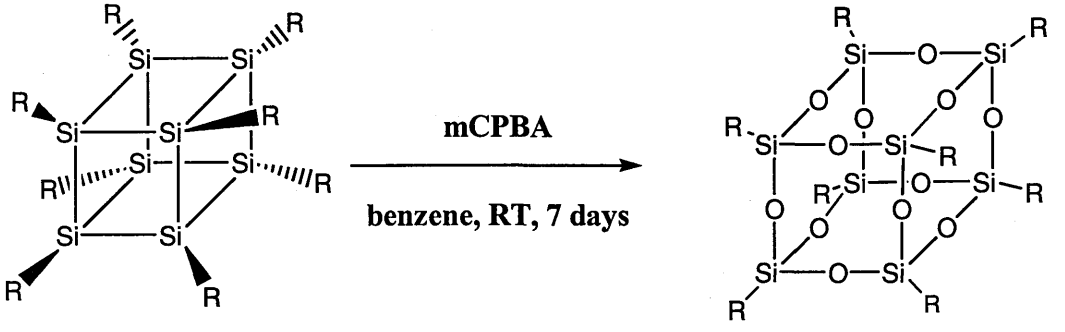

R = *t*-BuMe$_2$Si

Recently, Bassindale, Taylor and co-workers[51] have developed a novel and quicker route of synthesis that leads to T_8 silsesquioxane cages in much greater yields than previously reported.

1.3.2 The TBAF route synthesis

Sprung and Guenther[52] improved the yield for the synthesis of the octaphenyloctasilsesquioxane cage using tetrabutylammonium hydroxide in a base catalysis process. As tetrabutylammonium fluoride (TBAF) was a good base in aldol condensations[53], Bassindale, Taylor and co-workers[51] decided to investigate the use of TBAF to catalyze the hydrolysis of trialkoxysilanes, as shown in Figure 10. They reported very good yields of T_8 cages, up to 95% for the octa-*cyclo*-pentyloctasilsesquioxane cage, and reasonable yields were obtained with a large range of substituents on the silicon from primary alkyl and secondary alkyl to phenyl. The precise yield of T_8 cage depended upon the nature of the carbon adjacent to the silicon with bulky groups leading to higher T_8 cage yields.

Figure 10 TBAF synthesis route to octasilsesquioxane

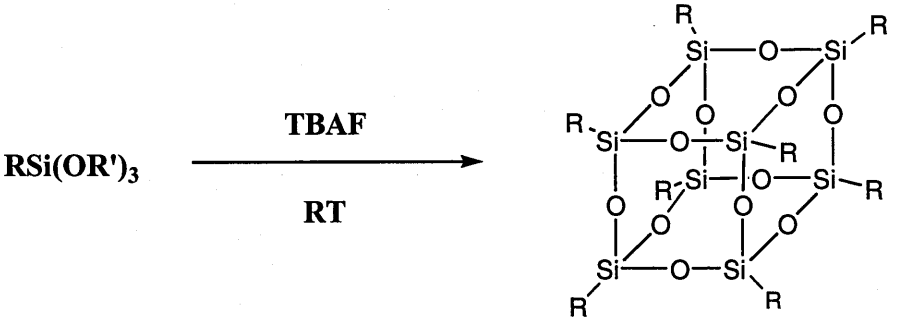

Since commercially available tetra-*n*-butylammonium fluoride contains 5% water, this amount was used as the source of water in the hydrolysis. After further investigation into the mechanism of cage formation[54], it appeared that the formation of the cage occurred by incorporation of the oxygen atoms from the water contained in the TBAF solution and that by optimising the water concentration improved yields of T_8 cages could be obtained. These

investigations also revealed that fluoride ion is a critical component of the reaction mechanism.

1.4 Mechanism of Formation of silsesquioxane cages by hydrolytic condensation

The formation of oliogosilsesquioxanes by hydrolytic polycondensation of $XSiY_3$ monomers in dilute solvents can be presented by the overall equation:

$$n\ XSiY_3 + 1.5\ n\ H_2O \rightarrow (XSiO_{1.5})_n + 3\ n\ HY$$

However, it is in reality a multistep and complicated process. The different hypotheses explaining the mechanism of this process are based on the nature of the identified intermediates formed in the course of hydrolytic polycondensation of the initial monomers. These intermediates have been isolated and identified by fractionation, GLC, chromatography-mass spectrometry, NMR, IR and UV spectrometry. Among these intermediates, linear oligosilsesquioxanes containing two to four silicon atoms, oligocyclosilsesquioxanes, as well as polycyclosilsesquioxanes have been isolated[25,38,39,55,56]. Sprung and Guenther[39] were the first to postulate that the hydrolysis of organonyltrifunctional monomers $XSiY_3$ involves the formation of linear, cyclic, polycyclic and finally polyhedral silsesquioxanes and assumed that the chain growth occurred randomly.

This hypothesis was further developed by Brown and co-workers, who studied the hydrolysis of cyclohexyl-[57] and phenyltrichlorosilane[55] and suggested the formation of polyhedral silsesquioxanes and their homoderivatives occurred as a result of consecutive stepwise polycondensation of cyclic macromolecules as shown in Figure 11.

Figure 11 Polycondensation of cyclic macromolecules

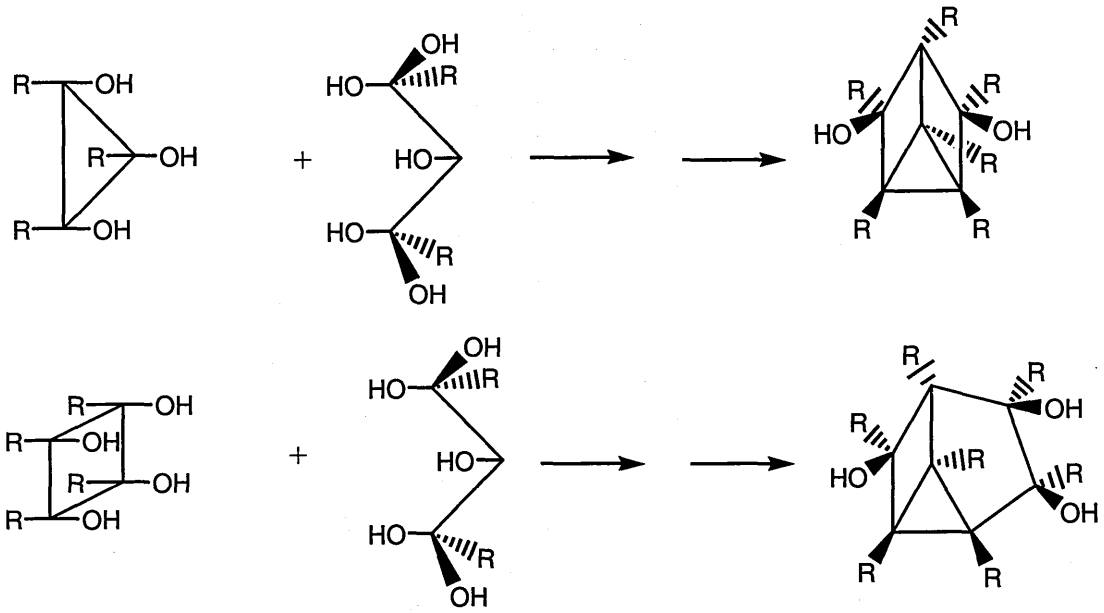
R
OH
HO
OH
R
R
OH
HO
OH
R
R
OH
HO
R
R
R

Figure 12 Co-condensation of cyclic oligosilsesquioxanes

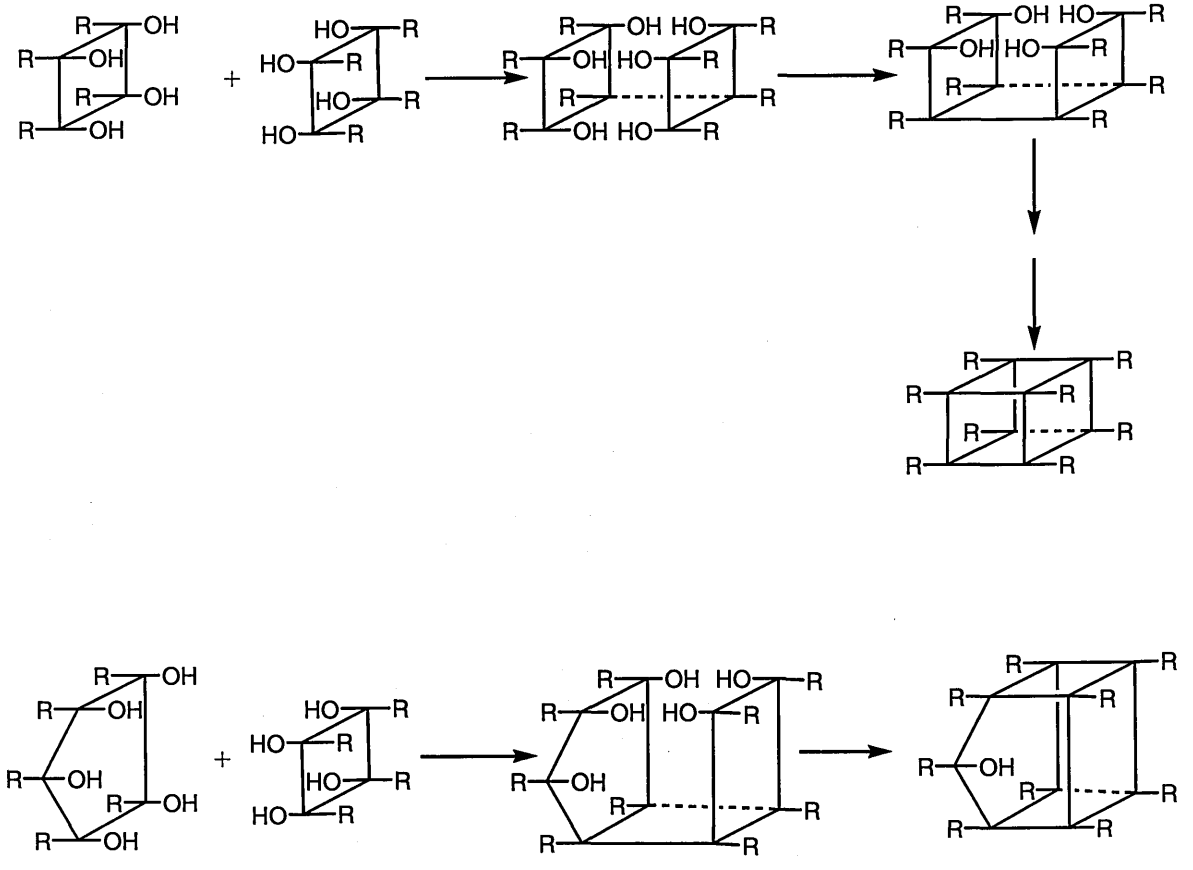

Korrigin and Lavrent'yev[58] have investigated the hydrolysis of vinyltrichlorosilane in aqueous butanol by GC-mass spectrometry. They proposed a consecutive stepwise polycondensation scheme as shown in Figure 13.

Figure 13 Korrigin and Lavrent'yev's stepwise polycondensation

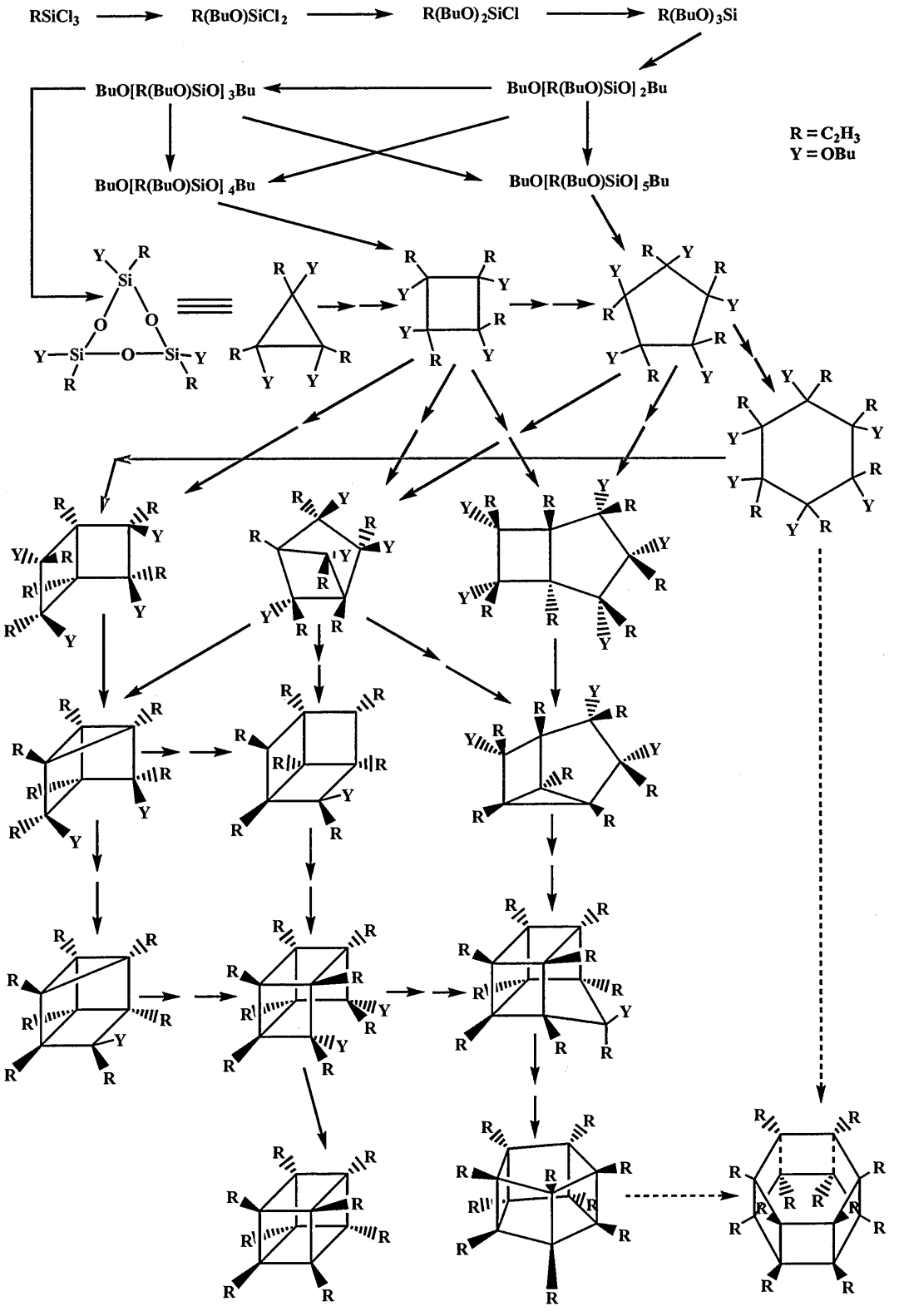

Bassindale, Taylor and co-workers[54] have investigated the synthesis and mechanism of formation of silsesquioxane cages using the tetra-*n*-butylammonium fluoride (TBAF) as the catalyst. Efficient yields of pure silsesquioxane cages have been obtained from the reaction of a various range of alkyltrialkoxysilanes with TBAF. It showed that TBAF is an excellent catalyst for the condensation reaction of silsesquioxanes. They also proved that water contained in the TBAF solution was involved in forming the cages and proposed a mechanism for the condensation of alkyltrialkoxysilane and the formation of the silsesquioxane cages, as shown in Figure 14. The hydrogen bonding of the fluoride ion and the water produces a nucleophile, which subsequently attacks the silicon atom with loss of EtO^-. It eventually led to the formation of high molecular weight cages. The different yields and structure of the silsesquioxane cages obtained were dependent upon the nature of the substituent group on the silicon atom and the solvent employed.

Figure 14 Proposed mechanism of the formation of the silsesquioxane cage

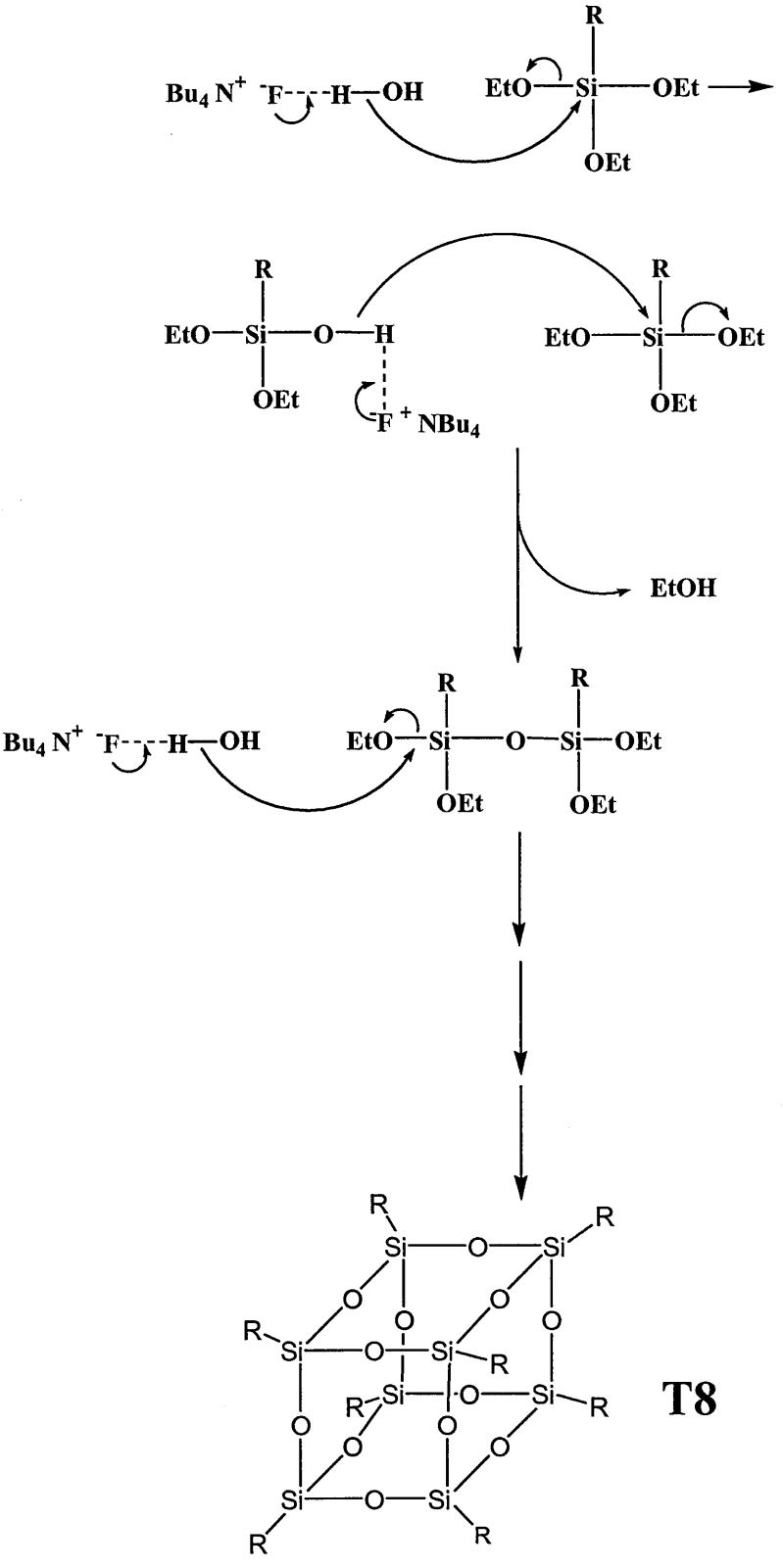

They also showed that the formation of silsesquioxane is taking place using the trace water present in the TBAF solution until its supply is exhausted, then, under anhydrous conditions, the fluoride ion attacks the silicon atom directly to lead to the formation of the pentacoordinated species $[NBu_4]^+[RSiF_4]^-$, as shown in Figure 14 . The pentacoordinated product was observed in the ^{29}Si NMR spectrum as a quintet.

Figure 15 The proposed mechanism for the formation of the pentacoordinated species $[NBu_4]^+[RSiF_4]^-$ from trialkoxysilane and TBAF in the absence of water

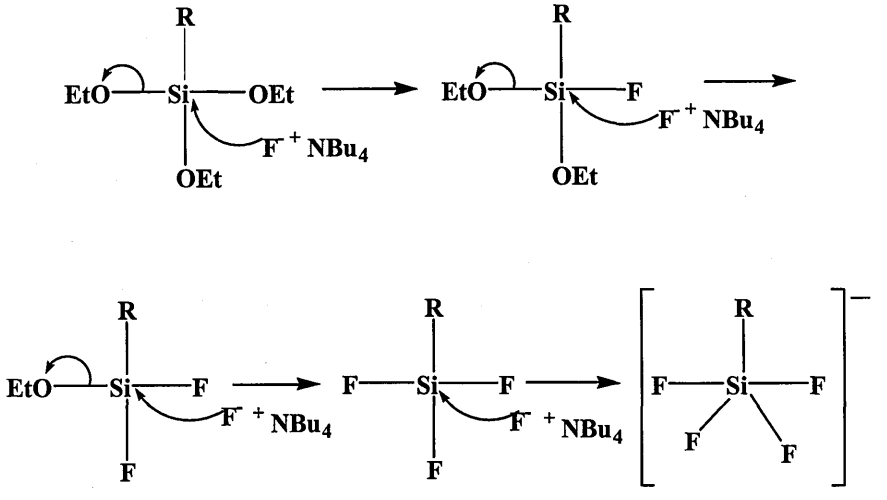

These conclusions of the catalytic role of the fluoride ion in the formation of silsesquioxane cage structure are highly relevant to the numerous reports in the literature about the use of the fluoride ion in the synthesis of microporous material such as the zeolites. Additionally, the $\{Si_8O_{12}\}$ framework of the polyhedral octasilsesquioxane cages is very similar to the double four-ring found in Linde Type A and other zeolites. This similarity shows the importance of a better understanding of the mechanism of formation of such compounds as they are the building blocks in the preparation of organosiliceous polymers and microporous crystalline material such as zeolites.

1.5 Zeolites

Zeolites are microporous crystalline aluminosilicates, composed of TO_4 tetrahedra (T = Si or Al) with the oxygen atoms connecting neighboring tetrahedra. For a completely siliceous structure, a combination of TO_4 (T = Si) units in this fashion leads to silica (SiO_2), which is an uncharged solid. Liebau and co-workers[59] have proposed a classification for porous tectosilicates (zeolites and zeolite-like materials) that distinguishes between aluminous (porolites) and siliceous (porosils) frameworks as well as frameworks that do (zeolites/zeosils) and do not (clathralites/clathrasils) allow exchange of guest species.

The access to the intracrystalline void of zeolites occurs through rings composed of T and O atoms. For rings that contain 6 T atoms (six-membered rings or 6 MR) or less, the size of the window is ~2 Å, and movement of species through these rings is restricted. Ions or molecules can be trapped in cages bound by rings of this size or smaller (5 MR, 4 MR, 3 MR). For zeolites containing larger rings, ions and molecules can enter the intracrystalline space. The internal volume of zeolites consists of interconnected cages or channels, which can have dimensionalities of one to three, as shown for the Fe-MCM22[60] in Figure 16. Pore sizes can vary from 0.2 to 0.8 nm.

Figure 16 Framework structure of the Fe-MCM22 zeolite[60]

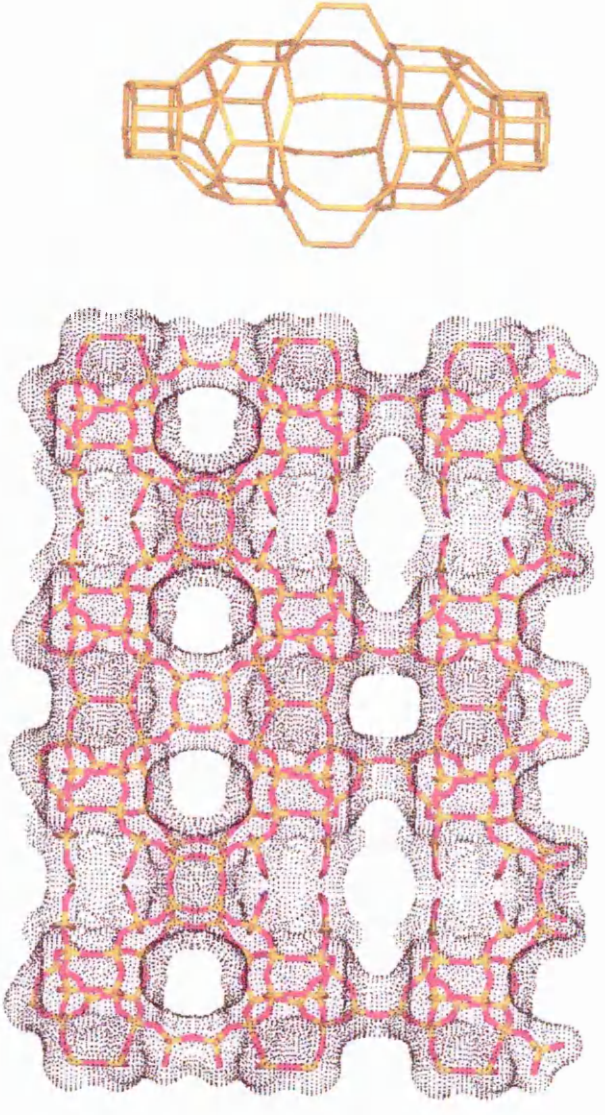

Zeolite synthesis occurs by a hydrothermal process with reagents being a silica source, an alumina source, a mineralizing agent such as OH^- or F^-, and, for higher Si/Al ratio zeolites, organic molecules as structure-directing agents. The nature of the counter cation is also determinant for the internal structure of the zeolite and it is interesting to notice that the nucleation can be disrupted by altering the length of the alkyl chain in a tetraalkylammonium cation for example.

In the last decade, the replacement of the hydroxide ion by the fluoride ion has made it possible to obtain zeolites at pH values lower than 10-11. During the synthesis, fluoride anions have been described playing several roles, acting as mineralizers, templates or structure directing agents[61].

More interesting are several reports of fluoride anions being clearly located in the double four-ring (D4R) units of the framework as for the octadecasil synthesis[62], in some aluminosilicates such as $AlPO_4$[63,64,65], in some gallophosphates such as $GaPO_4$[66,67] and more recently Morris and others obtained evidence of a fluoride-containing GeO_2 analogue of zeolite D4R building unit[68]. These observations of occluded fluoride ions in double four-ring cages demonstrates that, besides its mineralizing role, the fluoride ion has also a structure directing and templating effect.

Catlow and George[69] have investigated the behavior of the fluoride ion within the D4R by computational methods and examined the energetics of migration of this ion out of the D4R site. The results of these calculations show the fluoride anion to be stable within the D4R and that, once incorporated, the fluoride ion will be immobilized in the D4R cage due to the large energy barrier for its migration out of the ring. They concluded that the fluoride ion acts as an "anionic template" whose role is to promote D4R formation in the synthesis gel and that the ion size of F^- is such that monomer condensation around it would lead to D4R formation.

All these observations show that the fluoride ion can be entrapped in D4R structures which are analogous to a polyhedral silsesquioxane cage (T_8) structure. A fundamental question is thus to ask: could a fluoride ion be hosted in a single polyhedral silsesquioxane cage ? And if it is possible, what would be the conditions of the reaction and the substituent groups on the silicon atoms favoring such an encapsulation ?

Partial answers to these questions have been reported by Pach and Stosser[70]. They showed the entrapment of hydrogen atoms, derived from the organic substituents of the cages, after γ-irradiation treatment. It was investigated by means of electron spin resonance (ESR). Obviously this result shows the possibility of hosting atoms in T_8 cage structure, but fluoride ions are bigger than hydrogen atoms and they are also negatively charged. So are the dimensions of the polyhedral silsesquioxane cages large enough to host such an ion ?

1.6 Cage Structure and Dimension

By definition, a cage structure involves the presence of a space inside it. In fact, the polyhedral silsesquioxane cage contains an empty space in the middle of the core, but will it be large enough to host an isolated ion ?

Bassindale, Taylor and co-workers[54] have analysed a range of single crystal X-ray crystallography data obtained with different substituent groups on the silicon atom. The data showed that the variation in cage geometry is very limited and the mean of *ortho*, *meta* and *para* inter-silicon distances remain closely linked. They concluded from their studies that the structural differences between the different cores of the silsesquioxane cages are mainly influenced by the molecule's crystal lattice. They also stated that a secondary factor for influencing the cage geometry is the presence of sterically bulky groups on the silicon which has a determining influence on the size of silsesquioxane cages. As shown in Figure 17, the dimension of the "empty" space inside the core of the cages are consistent with the possibility of hosting an ion and with the fact that fluoride ions have been entrapped in very similar structure from polyhedral silsesquioxane cages, as in D4R units in zeolites structure[69,62]. Each ring in the cage defines a window, which is almost circular in the crown arrangement (of dimensions 3.8 × 3.8 Å) and rectangular in the hexagonal arrangement (of

dimensions 4.2 × 3.1 Å). We will investigate in this thesis the possibility of such encapsulation.

Figure 17 A schematic outline of an octasilsesquioxane cage to show the mean of three internal Si-Si cage distances measured in X-ray crystal structures of different octasilsesquioxane cages.

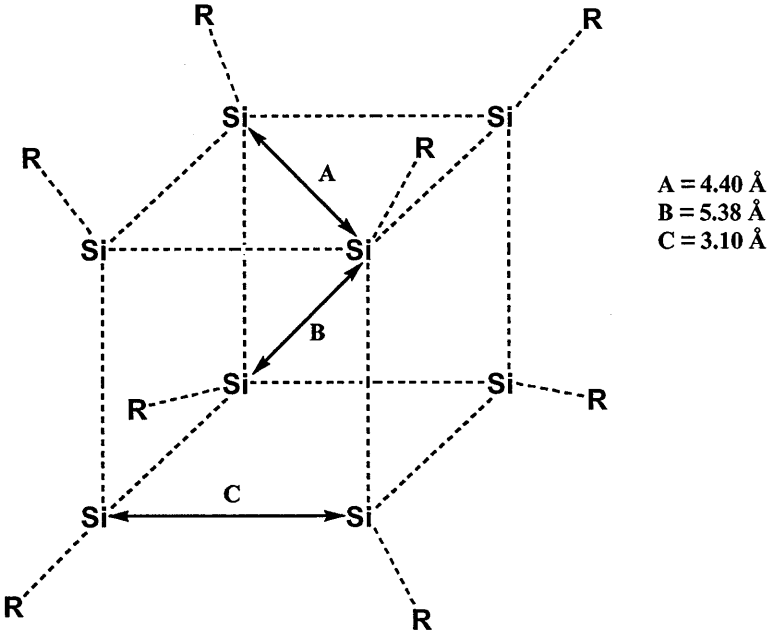

1.7 Analysis and characterization of polyhedral silsesquioxane cages

In recent years, reliable methods for isolating and characterizing polyhedral silsesquioxane cages and their homoderivatives have been developed. This, together with the large number of investigations in the literature suggests that the unambiguous assessment of novel product structures should be feasible. The methods available in our laboratories for product analysis include ^{1}H, ^{13}C, ^{29}Si and ^{19}F NMR, MALDI-TOF mass spectrometry, X-ray crystallography (Southampton) and elemental analysis. Recent work on polyhedral silsesquioxane cage synthesis has meant that a large library of spectral information for their identification is available. We will also use solid state ^{29}Si and ^{19}F NMR.

Chapter 2: Synthesis of tetra-*n*-butylammonium octaphenyloctasilsesquioxane fluoride

2.1 Introduction

In the first part of this work, we studied the influence of the solvent and the nature of the alkoxy group in the trialkoxysilane starting material, on the synthesis of octacyclopentyloctasilsesquioxane and octaphenyloctasilsesquioxane. We shall start with a review of the method of synthesis.

A great number of reactions leading to the formation of polyhedral silsesquioxanes are known. Depending on the nature of the starting material, these reactions can be divided into two groups. The first group involves the construction of Si-O-Si bonds with subsequent formation of polyhedral silsesquioxanes. These reactions are complex and multistep processes that lead to polymers and oligomers, which may include polyhedral silsesquioxanes and some homo derivatives[18,20]. These homo derivatives have a non regular structure with T silicons and one D silicon. The second group of reactions is based on the modification of a pre-existing silicon-oxygen framework. In other words, this second type of synthesis involves variation of the structure and composition of substituents on the silicon without affecting the Si-O-Si skeleton of the molecule.

The first part of our study focused on the former strategy, which allows the synthesis of polyhedral silsesquioxanes from monomers of the type $XSiY_3$ (where X is a chemically stable substituent and Y is a highly reactive substituent or good leaving group). These

reactions are commonly referred to as a hydrolytic condensation of trifunctional monomers, $XSiY_3$. As stated before, these reactions are complex and multistep processes and as a consequence, various factors influence the outcome of the reaction. We can predict that the rate of reaction, the degree of oligomerisation and the yield of the polyhedral silsesquioxanes will be dependent on the following factors:

- the concentration of the starting monomer in the solution
- the nature of the solvent
- the character of the substituent X in the initial monomer
- the nature of the functional group Y in the initial monomer
- the type of catalyst
- the temperature
- the concentration of water in the reaction mixture
- the solubility of the polyhedral silsesquioxanes formed

A large and detailed study of all these factors has been presented in the literature by M.G. Voronkov[18]. All these factors and their mutual effects influence the outcome of the reaction and help us to understand the complex processes of polycondensation. Our initial interest was focused on the synthesis of octacyclopentyloctasilsesquioxanes in which the substituent at the silicon, cyclopentyl, is a relatively bulky and stable group.

2.2 Influence of solvent and nature of the alkoxy group in the starting material on the synthesis of octacyclopentyloctasilsesquioxane

Sprung and co-workers[52] first reported the synthesis of octacyclopentyloctasilsesquioxanes in 1958. They used an ethoxy group as a leaving group in the initial monomer and carried out the reaction using 4-methylpentanone as the solvent. The catalyst that they utilised was tetraethyl ammonium hydroxide, and they obtained the silsesquioxane in a yield of 20 %.

We used a different catalyst, tetra-*n*-butylammonium fluoride, a system largely studied by Yuxing Yang[71] in her work at the Open University. We first synthesized a range of trialkoxysilanes from cyclopentyltrichlorosilane. The alcohol and cyclopentyltrichlorosilane were first dissolved in dried THF (exp. MP02); afterwards a solution of triethylamine in dry THF was added very slowly to the mixture. This was then stirred for a further 1.5 h during which time a white solid precipitated. The mixture was filtered under vacuum and the filtrate collected. A brown liquid was obtained after distillation. At this point we confirmed the purity of our product by ^{29}Si, ^{1}H and ^{13}C NMR. Using this procedure, we synthesized trimethoxy-(MP05), triethoxy-(MP02), tripropoxy-(MP07) and tributoxy-(MP09) silanes. Once we had obtained the different cyclopentyltrialkoxysilanes, the next step was to synthesise the corresponding octasilsesquioxane. The starting material, cyclopentyltrialkoxysilane, was dissolved in dried acetone. Tetra-*n*-butylammonium fluoride in THF was then added to the mixture and stirred at room temperature. A white solid precipitated. After 24 h we obtained a liquid that after filtration gave a white powder which dissolved in chloroform. The ^{29}Si NMR revealed a single sharp peak at -66.6 ppm,

which agreed with the expected ^{29}Si NMR chemical shift of octacyclopentyloctasilsesquioxane[72] (Cp_8T_8). The yields of each reaction with different starting materials are shown in Table 1.

Table 1

Starting material	Solvent	Time	Yield
cyclo-pentyltrimethoxysilane (MP06)	Acetone	24 h	69%
cyclo-pentyltriethoxysilane (MP04)	Acetone	24 h	96%
cyclo-pentyltripropoxysilane (MP08)	Acetone	24 h	95%
(MP62)	Pyridine	24 h	68%
cyclo-pentyltributoxysilane (MP10)	Acetone	24 h	93%

All the yields were quite high, and those involving the larger and less reactive leaving groups were the highest. In addition, we carried out the reaction of the tripropoxysilane in dry pyridine. The yield was lower than for the reaction carried out in acetone. Moreover, after filtration of the solid white powder, for which the ^{29}Si NMR displayed the same single peak at -66.6 ppm, we obtained a red filtrate which gave two ^{29}Si NMR peaks at -66.6 and δ -69.3 ppm in a ratio of 2:1. After one week the ^{29}Si NMR of the same red liquid was obtained, which showed the same two peaks, but in a different ratio of 1:2. This suggests that there is equilibrium between the two compounds, presumably between a Cp_8T_8 cage and a more stable compound that displays a ^{29}Si NMR chemical shift at -69.3 ppm. The

literature[72] suggests that this compound is a *cyclo*-pentyl-T_{10} cage. In fact, Yuxing Yang concluded that TBAF acted as an efficient catalyst for the rearrangement reactions of octasilsesquioxane cages, such as octaheptyl, octaoctyl, octanonyl, octadecyl, octadodecyl and octa-cyclo-hexyl octasilsesquioxane cages into larger cages as deca and dodecasilsesquioxane cages. Thus, the rearrangement of the *cyclo*-pentyl-T_8 cage into the *cyclo*-pentyl-T_{10} cage in the reaction solution, where TBAF is still present, is not surprising and is in agreement with Yuxing Yang's conclusions. The solid state ^{29}Si NMR of the white powder, obtained from reaction MP04 (Figure 18), shows a single sharp peak at -65.8 ppm as shown below.

Figure 18 ^{29}Si Solid State NMR of Cp_8T_8 (MP04)

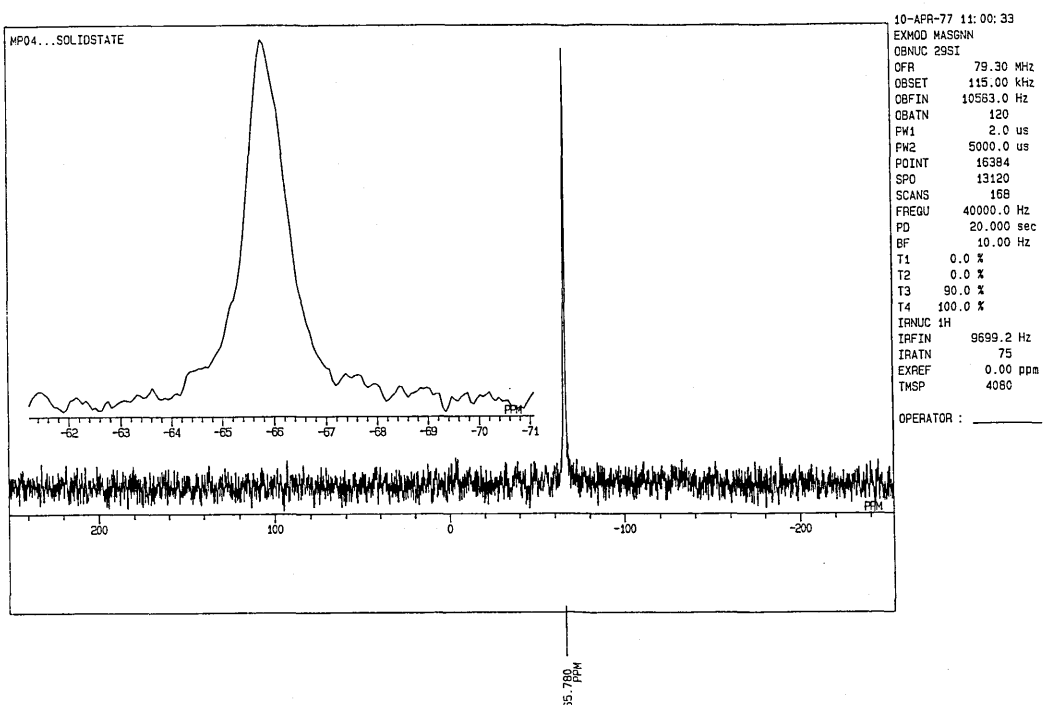

The explanations for this sharp peak signal in the solid state ^{29}Si NMR is that the eight silicon atoms of the *cyclo*-pentyl-T_8 cage are all equivalent and thus show only one silicon environment.

The XRD of the white powder (Figure 19) shows sharp peaks, which indicates a high degree of crystallinity. It is possible to obtain a crystal structure from the Rietfeld calculations but, as the *cyclo*-pentyl-T_8 cage has been already fully characterised[72], we decided that this was not our priority.

Figure 19 X-ray powder diffraction of Cp_8T_8 (MP04)

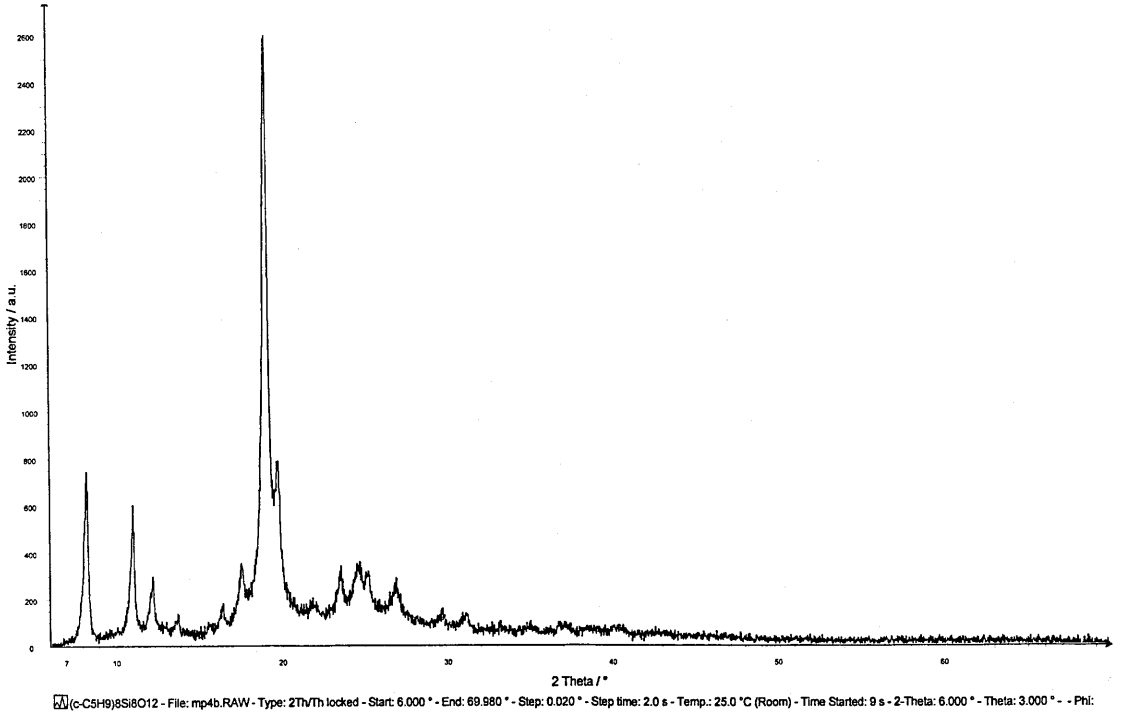

MP04: (c-C5H9)8Si8O12

Our second series of experiments involved the preparation of a cage with a phenyl substituent on the silicon atom. The octaphenyloctasilsesquioxane (Ph_8T_8) has been previously studied and reported in the literature. Brown and co-workers[73,74] used an equilibration method involving potassium hydroxide and phenyltrichlorosilane to obtain small amounts of Ph_8T_8 and dodecaphenyldodecasilsesquioxane ($Ph_{12}T_{12}$) crystals which are

formed along with prepolymer and the polymer polyphenylsilsesquioxane. Brown[7] also obtained some phenyl-T8 by condensation of phenylsilanetriol, although the major product is the *cis*, *cis*, *cis*-cyclotetrasiloxanetetrol (Figure 20). They also noticed that the Ph_8T_8, unlike most of the octasilsesquioxane cages, is insoluble in most solvents. This characteristic of the octaphenyloctasilsesquioxane cage makes it difficult to characterize using liquid NMR and we thus are expecting to use solid state NMR for characterization of our sample.

Figure 20 *cis*, *cis*, *cis*-cyclotetrasiloxanetetrol

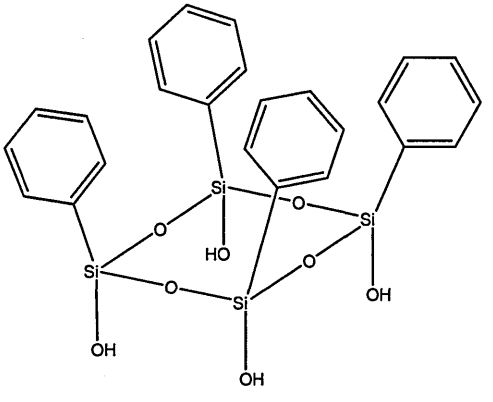

For the synthesis of octaphenyloctasilsesquioxane, we used the same method and catalyst as we used to synthesise the Cp_8T_8.

2.3 Influence of solvent and nature of the alkoxy group in the starting material on the synthesis of octaphenyloctasilsesquioxane

Here, we used a larger range of solvents such as chloroform, tetrahydrofuran, *n*-hexane, toluene, pyridine and acetone. The yields of T_8 are shown in Table 2.

Table 2 Yields of T_8 cages from different trialkoxysilanes in a range of solvents

Starting material	Solvent	Time	Yield
Phenyltrimethoxysilane			
(MP12)	acetone	24 h	6.5 %
(MP17)	chloroform	24 h	0 %
(MP31)	tetrahydrofuran	24 h	32.5 %
(MP35)	chloroform	48 h	81 %
Phenyltriethoxysilane			
(MP14)	acetone	24 h	3.5 %
(MP18)	chloroform	24 h	2 %
(MP19)	tetrahydrofuran	24 h	45.5 %
(MP20)	*n*-hexane	24 h	2 %
(MP27)	pyridine	24 h	38.5 %
(MP34)	chloroform	48 h	12.5 %
Phenyltripropoxysilane			
(MP23)	chloroform	24 h	0 %
(MP21)	*n*-hexane	24 h	2 %
(MP25)	toluene	24 h	12 %
(MP26)	pyridine	24 h	61 %
(MP30)	tetrahydrofuran	24 h	20 %
(MP33)	chloroform	48 h	18.5 %
Phenyltributoxysilane			
(MP24)	chloroform	24 h	0 %
(MP29)	tetrahydrofuran	24 h	0 %
(MP28)	pyridine	24 h	38%
(MP32)	chloroform	48 h	81%

The first observation of note is that the yields of Phenyl-T_8 are significantly lower than in the case of the cyclopentyl group. The reactions, which were carried out in tetrahydrofuran and pyridine, gave higher yields than those in acetone, toluene and chloroform. A particularly interesting set of results was obtained with chloroform. After a reaction time of 24 h, we did not observe the formation of a white powder. However, after 48 h the yield of white powder was quite high, but the powder that was obtained did not dissolve in chloroform, acetone or other solvents as expected. The insolubility of this product agrees with the behaviour of Ph_8T_8 reported in the literature[41,75]. The infrared spectrum of MP35 shows a broad peak in the 1100-1130 cm^{-1} region, which corresponds to an anti-symmetric stretch of the Si-O-Si bond, ν_{as}(Si-O-Si). We also observed sharp peaks at 3000 cm^{-1} which correspond to the stretching of the =C-H bond, ν(C=C) at 1600 cm^{-1} and γ(-HC=CH-) at 700 cm^{-1} for the out-of-plane bending of the C-H bond. These spectroscopic data are in agreement with those measured by Brown and co-workers[55,73]. The solid state ^{29}Si NMR revealed peaks at δ -76.4 ppm, δ -79.6 ppm and δ -81.2 ppm for MP32, and δ -76.3 ppm, δ -77.0 ppm and δ -79.7 ppm for MP35. Although, these two sets of shifts differ, they are both in the same ratio 2:4:2, suggesting a cage with a plane of symmetry through the atoms marked X shown in the Figure 21. However, the presence of different silicon environment is difficult to explain in an octasilsesquioxane cage with all the same organyl groups attached to each silicon atoms. In fact, as we have seen in the solid state ^{29}Si NMR of the *cyclo*-pentyl-T_8 cage, the silicon atoms look all equivalent and thus show only one silicon environment. An hypothesis can be discussed about the difference between these two octasilsesquioxane cages: in the case of the *cyclo*-pentyl-T_8 cage, the *cyclo*-pentyl groups may have more flexibility and freedom of motion in the long range packing resulting in making the eight silicon atoms of the cage effectively equivalent. The phenyl groups are

more bulky groups than *cyclo*-pentyl groups and thus may have less freedom of motion around the Si-C bond in the crystal structure packing. So we could suggest that the phenyl groups, in contrast to the *cyclo*-pentyl groups, could also adopt one of three different orientations resulting in three different silicon environments. This will result in showing three different peaks in the solid state ^{29}Si NMR of the Ph_8T_8 cage. This is our best explanation for such a difference in the solid state ^{29}Si NMR between the *cyclo*-pentyl-T_8 and the Ph_8T_8 cage. Further investigations will be needed to fully understand these three different silicon environments in the Ph_8T_8 cage.

Figure 21 There are two possibilities that lead to three peaks in a ratio of 2:4:2 in the solid state ^{29}Si NMR

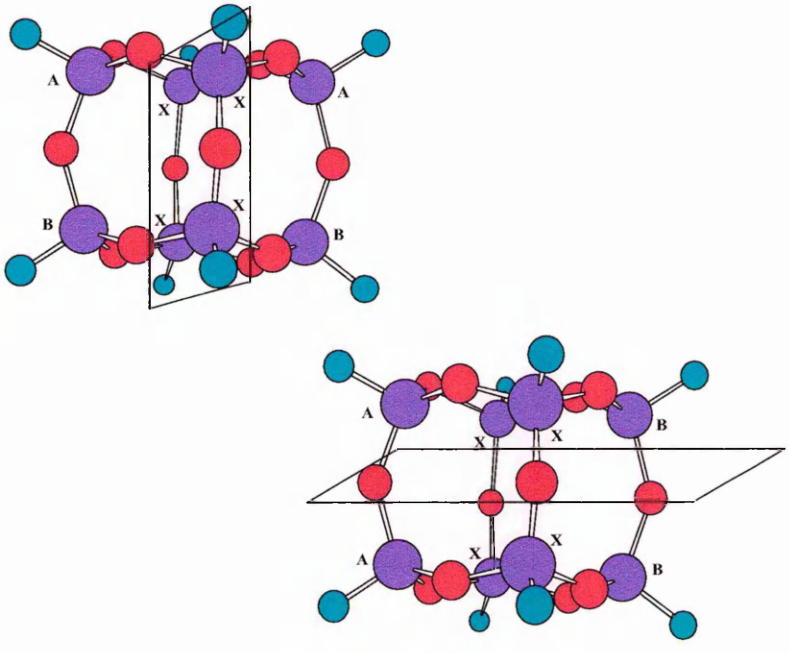

The differences in the chemical shifts between these two samples can be explained by the difference in the environments of the cages in each solid. This was confirmed by XRD measurements, which show a higher degree of crystallinity for the compound MP35. This

could indicate the presence of impurity, such as solvent, in the sample MP32 even if the cage itself has the same structure.

All the shifts are in agreement with those of an octaphenyloctasilsesquioxane. Thus we can say with confidence that the product, MP32 and MP35, obtained from chloroform and insoluble in any solvent, is phenyl-T_8, even if we were not able to obtain a single crystal X-ray structure.

In all other circumstances, we obtained a white powder, but this proved to be a different compound because it was soluble in acetone which is not expected for the Ph_8T_8 cage. The infrared spectrum of this product, obtained from reactions carried out in all solvents, except chloroform, showed all the same pattern with an additional sharp peak at 600 cm^{-1}, which is in the region for the vibrational mode of the Si-O-Si framework. The XRD measurements show sharp peaks, which indicate a high degree of crystallinity, but a different pattern was obtained than in the case of MP35 and MP32, which reinforced the idea that it was a different product. The ^{29}Si NMR (Figure 23) of every sample displayed a single sharp peak at -80.6 ppm in d_6 acetone, which is in the T-Si region but -1 ppm higher than expected for the ^{29}Si NMR chemical shift of the phenyloctasilsesquioxane (-79.6 ppm). We tried to "spike" this sample with some pure Ph_8T_8 cage to show the chemical shift were different but unfortunately the insolubility of the Ph_8T_8 cage made it impossible. The ^1H NMR (Figure 22) shows two multiplets at 7.17 and 7.68 ppm with an integration of 3:2, which indicates the presence of a phenyl group. In addition, the spectrum shows a triplet at 0.85 ppm (integration: 12 H), a multiplet at 1.30 ppm (8 H), another multiplet at 1.68 ppm (8 H) and a triplet at 3.30 ppm (8 H). This corresponds to the CH_3-CH_2-CH_2-CH_2-X system, which is part of the tetra-*n*-butylammonium fluoride that was used as a catalyst. This was confirmed by the ^{13}C NMR spectrum, which exhibits peaks at δ 13.81 ppm (s, CH_3); δ 20.35 ppm (s,

-CH_2-); δ 24.35 ppm (s, -CH_2-); δ 49.84 ppm (s, -CH_2-) and δ 128.06 ppm (2 C), δ 129.69 ppm (1 C), δ 134.90 ppm (2 C), δ 138.33 ppm (1 C) for the six carbons of the aromatic ring.

Figure 22 ^{1}H NMR and assignments of Ph_8T_8-TBAF

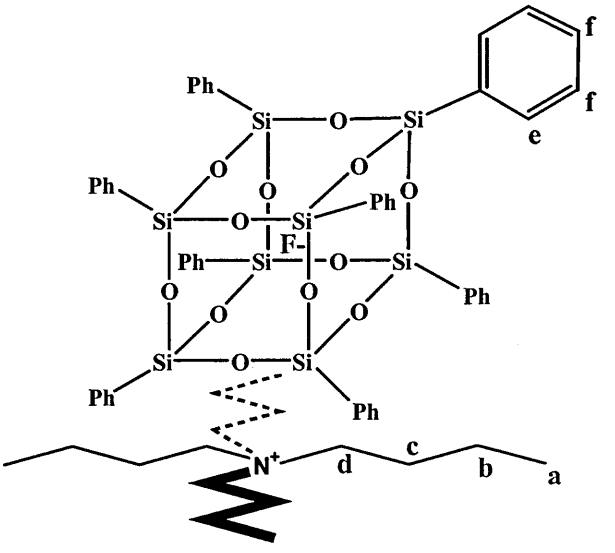

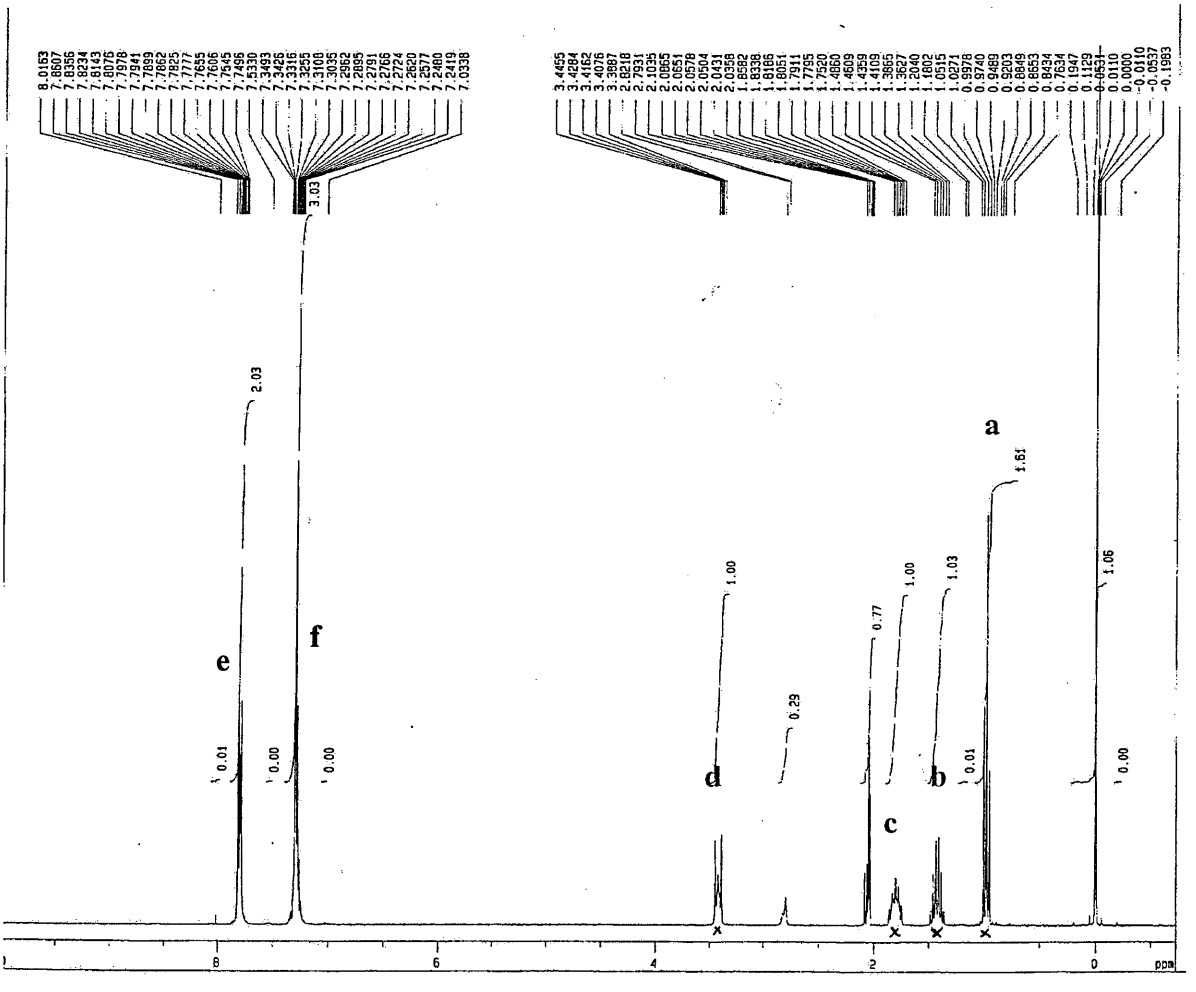

Figure 23 ^{29}Si NMR and assignments of Ph_8T_8-TBAF

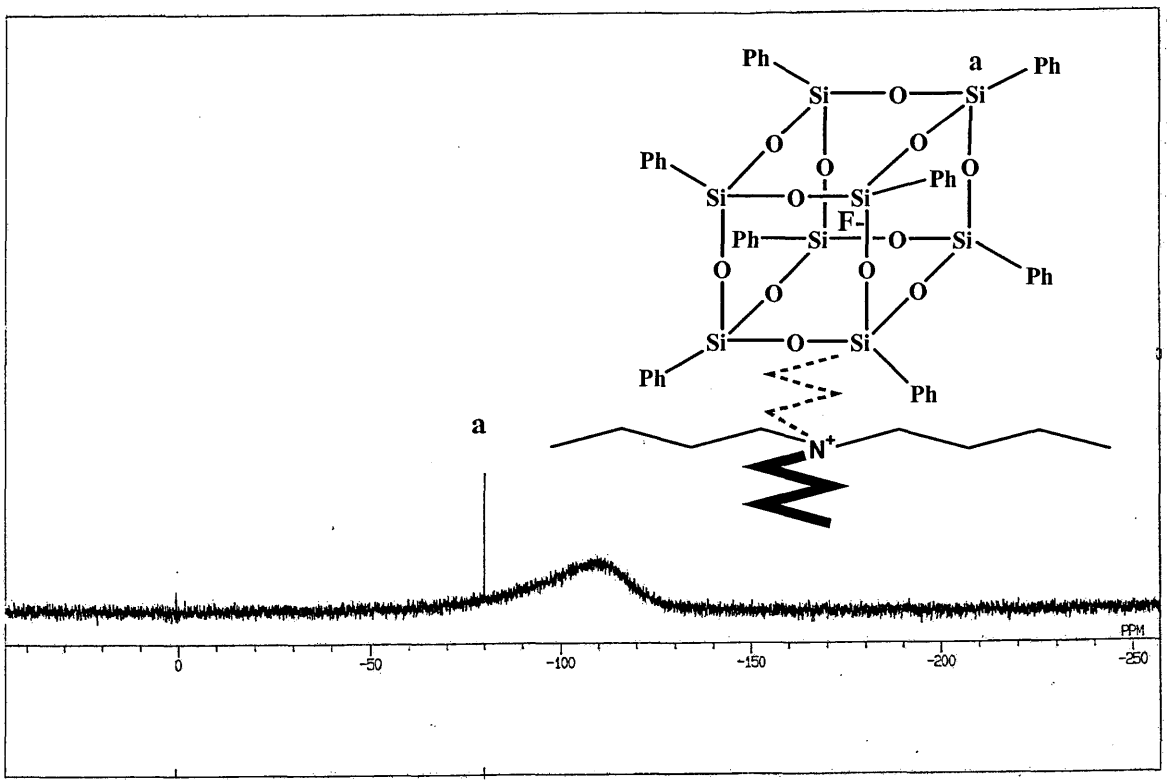

Additionally, we recorded the ^{19}F NMR spectrum (in d_6 acetone) which shows a single peak at -26.4 ppm. Similarly, the solid state ^{19}F NMR of Ph_8T_8-TBAF shows a single peak at -25.8 ppm for the encapsulated fluoride anion. The range of this chemical shift is in agreement with that observed for a fluoride ion encapsulated within the double D4R rings in a zeolite structure as reported by Caullet and co-workers[62] and independently predicted for a naked fluoride anion. We will discuss furthermore the "naked" character of the fluoride ion later in this thesis.

Figure 24 Solid State 19F NMR of Ph_8T_8-TBAF

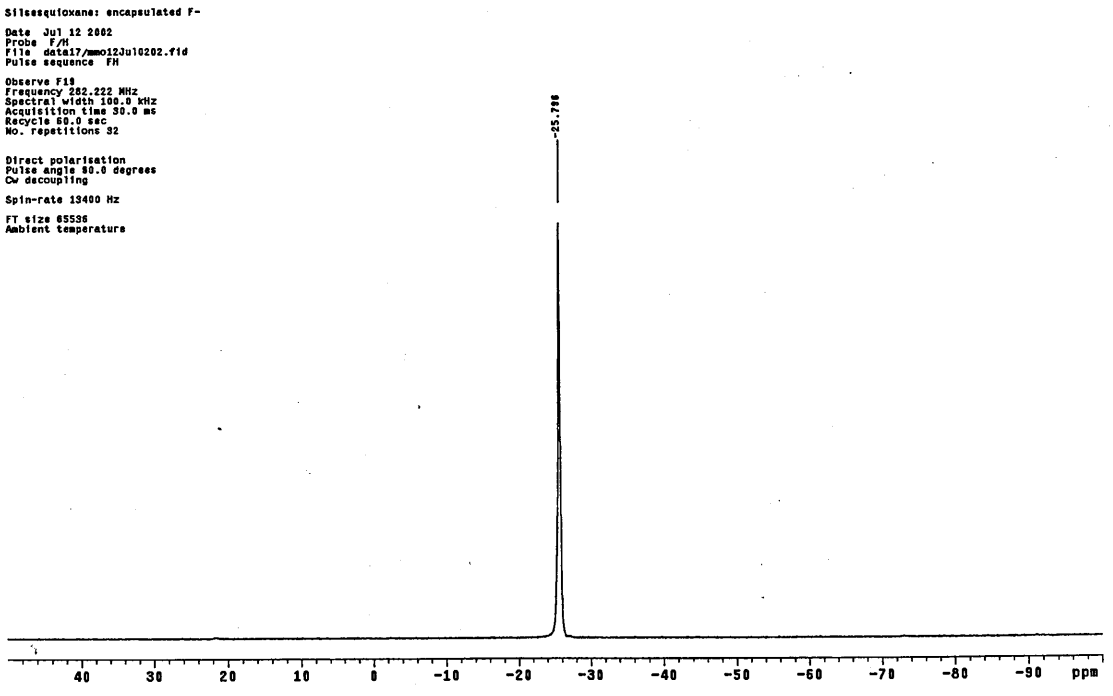

The integration of the peaks in the ^1H NMR shows a total of 36 for peaks due to the tetra-*n*-butylammonium fluoride and 40 for the protons of the phenyl groups. This corresponds to a ratio of 10:9, which is in complete agreement with the theorical ratio of one Ph_8T_8 cage (8 × 5H = 40H) for each molecule of tetra-*n*-butylammonium fluoride (4 × 9H = 36H). We obtained small crystals from the white powder (MP26) by the vapour diffusion method[76]. A small amount of a saturated solution (powder + acetone) was placed in a narrow tube, which was itself placed in a wider tube which contained a solution of a precipitant ($CHCl_3$), the precipitant is thus allowed to diffuse into the solution. After five days we observed the formation of small crystals at the bottom of the tube with the acetone. We obtained a single crystal X-ray structure, which is in agreement with all the data collected on this product: a Ph_8T_8 cage associated with one molecule of tetra-*n*-butylammonium fluoride. Unexpectedly,

the fluoride anion was centred perfectly in the middle of the cage (Figure 25), this suggests that the distances between the fluoride anion and the oxygen atoms, which are part of the framework of the cage, are surprisingly close.

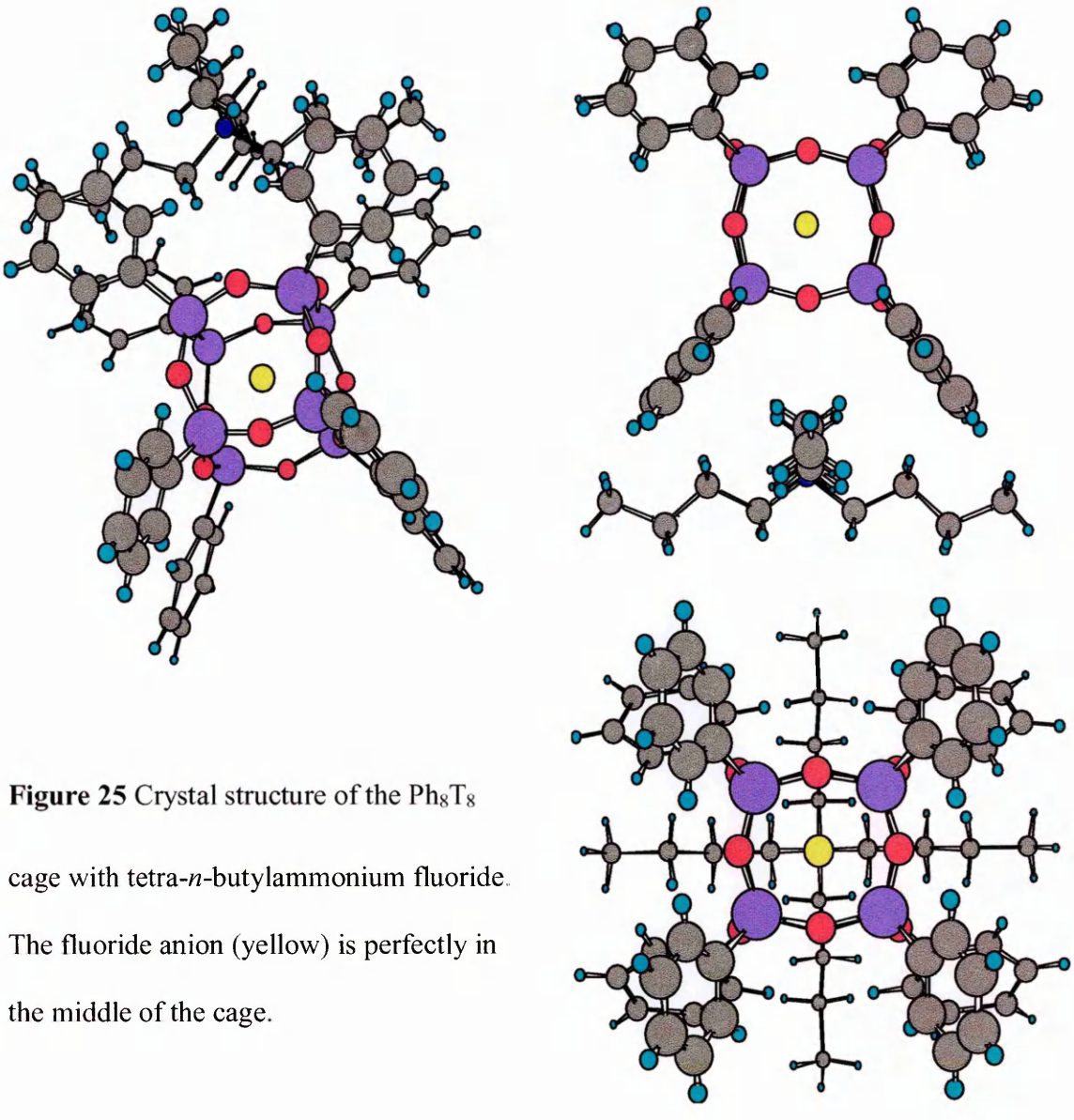

Figure 25 Crystal structure of the Ph_8T_8 cage with tetra-*n*-butylammonium fluoride. The fluoride anion (yellow) is perfectly in the middle of the cage.

We were interested in the interactions and the distances between the fluoride anion and the twelve oxygen atoms of the cage. We thus compared the F-O and F-N distances within our cage and the F-O and F-N distances of other cage encapsulated fluoride (Figure 26 and Figure 27) and chloride anions from the literature[77, 78].

Figure 26 Chen Q., Z. J.: Control of aggregation through Anion Encapsulation in Clusters of the V/O/$(RPO_3)_2$: $[NBu_4][VV_4O_6F(PhPO_3)_4]$

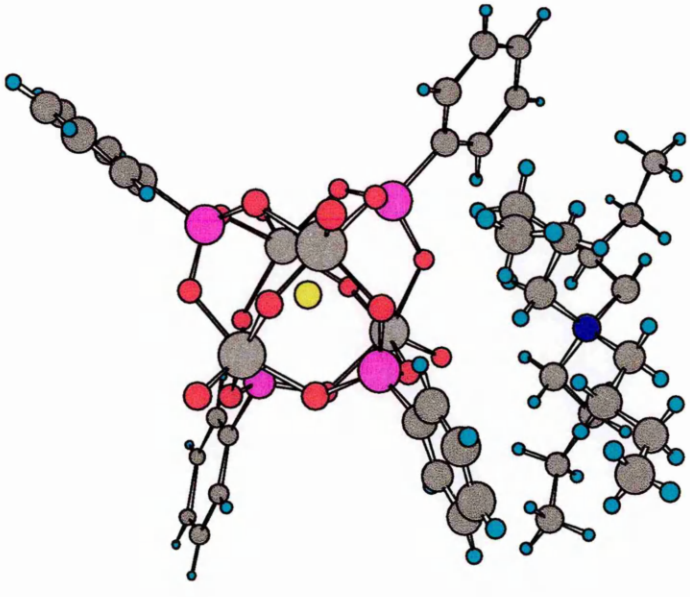

Figure 27 Chen Q., Z. J.: Control of aggregation through Anion Encapsulation in Clusters of the V/O/$(RPO_3)_2$: $[NBu_4]_2[VV_3VVIO_6F(PhPO_3)_4$

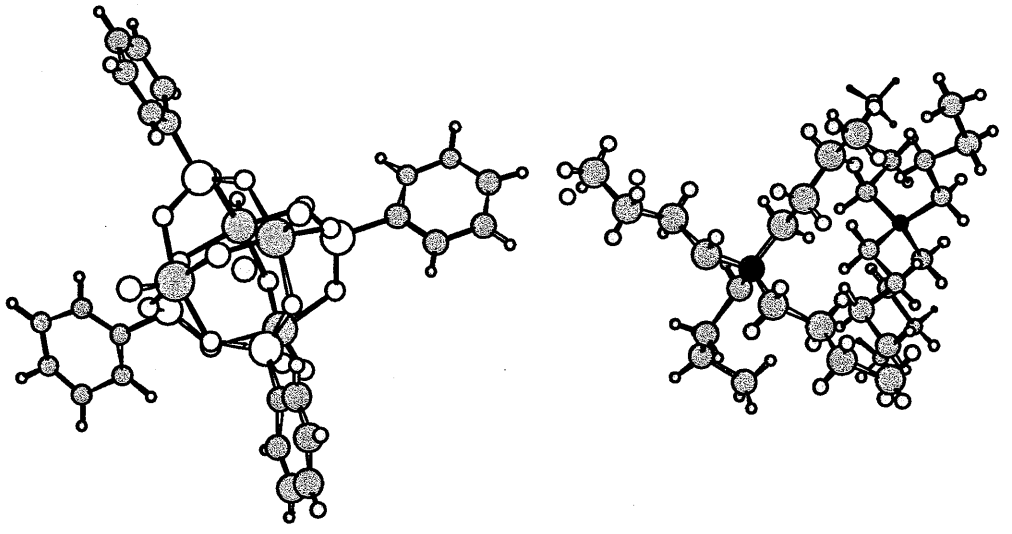

Table 3 lists all the F-O and F-N distances. We can see that the F-O distances in the Ph_8T_8 cage are shorter than those in the two other cages. The average is 2.7 Å in the Ph_8T_8 cage and 2.8 Å in the other cages. We compared the Ph_8T_8 cage symmetry with the symmetry of the Ph_8T_8 cage without a fluoride ion inside that we also synthesized and obtained a single X-ray crystal structure. In fact, we compared the Si-Si and O-O distances between opposite corners and faces within the same cage. We observed that the distances were more regular in the Ph_8T_8-TBAF cage than in the conventional Ph_8T_8 cage which shows a higher symmetry of the cage when the fluoride ion was present due to the weak interactions between the fluoride and silicon atoms.

Table 3

F-O distances in Ph_8T_8-TBAF (Å)		F-O distances in Chen Cage 1 (Å)		F-O distances in Chen Cage 2 (Å)	
F-O127	2.71	F-O14	2.74	F-O14	2.85
F-O128	2.67	F-O15	2.78	F-O15	2.81
F-O130	2.70	F-O19	2.75	F-O19	2.84
F-O131	2.75	F-O16	2.77	F-O16	2.80
F-O46	2.67	F-O17	2.78	F-O17	2.83
F-O47	2.74	F-O24	2.77	F-O24	2.77
F-O129	2.74	F-O20	2.77	F-O20	2.78
F-O49	2.75	F-O25	2.86	F-O25	2.81
F-O132	2.66	F-O26	2.80	F-O26	2.83
F-O50	2.66	F-O18	2.82	F-O18	2.80
F-O48	2.70	F-O22	2.85	F-O22	2.88
F-O45	2.71	F-O23	2.80	F-O23	2.80
		F-O21	2.87	F-O21	2.86
		F-O27	2.76	F-O27	2.80
F-N distances in Ph_8T_8-TBAF (Å)		**F-N distances in Chen Cage 1 (Å)**		**F-N distances in Chen Cage 2 (Å)**	
F-N	6.46	F-N	6.39	F-N	13.33

From the crystallographic data, the tetra-*n*-butylammonium octaphenyloctasilsesquioxane fluoride T_8 cage had crystallised with a monoclinic crystal system with a C2/c space group. The conventional Ph_8T_8 cage crystal structure without encapsulated fluoride ion had crystallised with a tetragonal crystal system with a P4/n space group. Water molecules were present in the packing of the conventional Ph_8T_8 cage. The presence of the tetra-*n*-butylammonium ion in the packing of our encapsulated fluoride cage causes a much more ordered packing than in the conventional case. In fact, the tetra-*n*-butyl arms fit nicely in the "valley" formed by the phenyl groups leading to higher order and closer packing as shown in Figure 28. The long range packing revealed to be even more interesting as it is surprisingly highly ordered. This can be explained by the fact that the tetrabutyl arms are completely stretched in a cross form which present Van der Waals interactions with phenyl groups of different cages. In fact, two opposite tetrabutyl arms fit on the top of a cage in the valley formed by its 4 phenyl groups with an average close contact distance of 3.8 Å. The other two opposite tetrabutyl arms fit also in the valley formed by the 4 phenyl groups but of a different cage placed on top of the first cage. The average close contact distances of the tetrabutyl arms with the phenyl groups of the second cage is again around 3.8 Å. We can also notice that the last carbon atoms of each tetrabutyl arms has close contact (average distance of 4.0 Å) with the phenyl groups of other surrounding cages. So the tetrabutyl of the tetrabutyl ammonium cation seemed to be the Van der Waals "glue" between the Ph_8T_8-TBAF cages and make it a very ordered long range packing.

Figure 28 Packing and unit cell of Ph_8T_8-TBAF

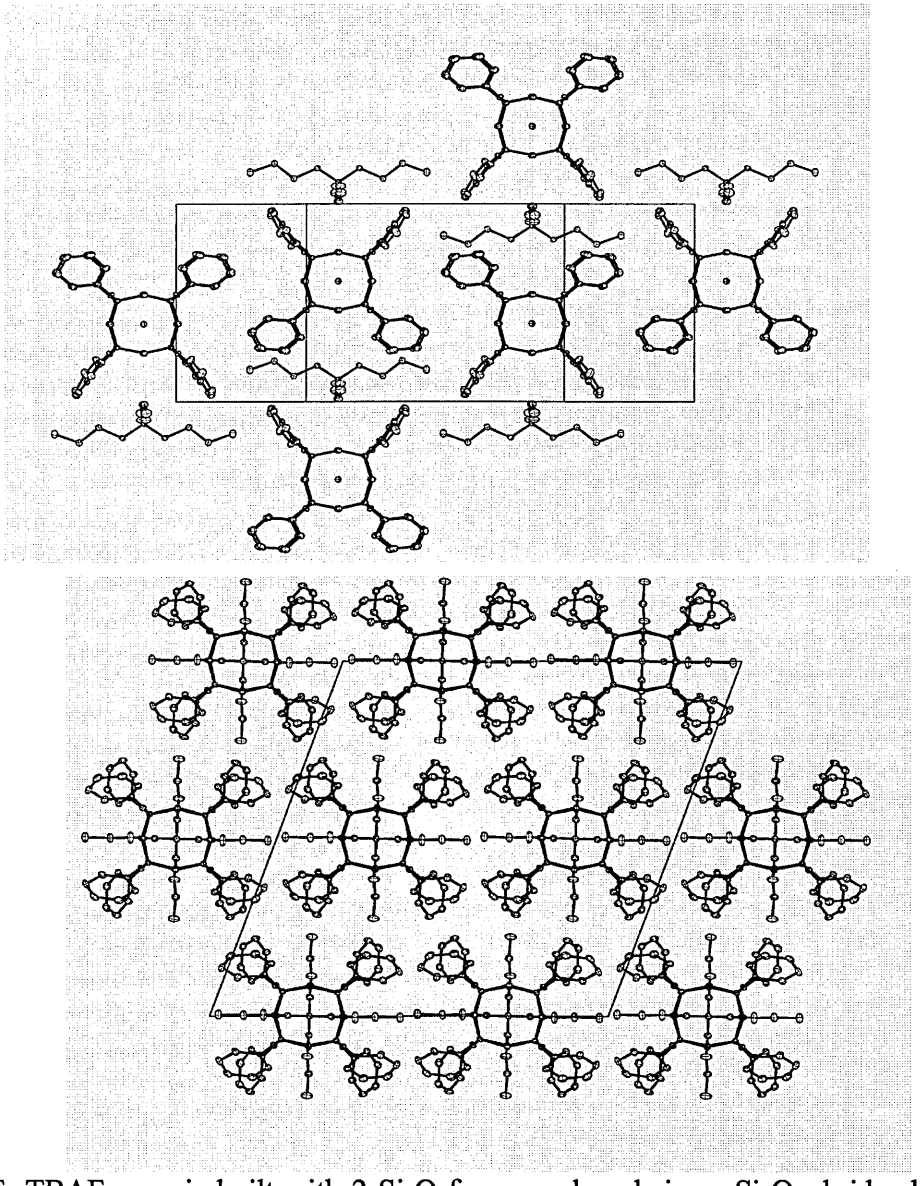

The Ph_8T_8-TBAF cage is built with 2 Si-O four membered rings, Si_4O_4, bridged with Si-O-Si linkages. The average Si-O bond length, Si-C bond length and Si-O-Si bond angle for the Si_4O_4 ring are similar to that of Si_4O_4 ring in the conventional Ph_8T_8 cage as we can see in Table 4. Nevertheless, we can observe a slight contraction of the Si_8O_{12} framework in the encapsulated fluoride cage due to a small interaction of the fluoride ion with its surrounding silicon atoms. This weak silicon-fluoride ion interaction also causes a slight lengthening of the Si-C bond length. We can also identify a decrease in the mean Si-O-Si bond angle,

which may due to the proximity and, thus, repulsion, between the encapsulated fluoride ion and the surrounding oxygen atoms of the Si_8O_{12} framework.

Table 4 NMR details and Selected bond distances and angles for Ph_8T_8-TBAF and Ph_8T_8 cages

Compound	Solution NMR		Crystal structure		
	δ ^{29}Si (/ppm)	δ ^{19}F (/ppm)	Mean Si-R(C_{sp2}) (/Å)	Mean trans Si-Si (*a*) (/Å)	Mean Si-O-Si (/°)
Ph_8T_8-TBAF cage	-80.6	-26.4	1.86	5.31	141.2
Ph_8T_8 cage	-79.7		1.83	5.38	149.2

The product was also analysed by MALDI-TOF mass spectroscopy. This confirms that a tetra-*n*-butylammonium octaphenyloctasilsesquioxane fluoride cage was obtained with a fragment at *m/z* 1294.5 corresponding to the Ph_8T_8-TBAF cage ($C_{64}H_{76}FNO_{12}Si_8$) [M^-], a fragment at *m/z* 1052.5 corresponding to the Ph_8T_8-F^- ($C_{48}H_{40}FO_{12}Si_8$) [M^--$C_{16}H_{36}N$], a fragment at *m/z* 1034 corresponding to the Ph_8T_8 ($C_{48}H_{40}O_{12}Si_8$) [M^--$C_{16}H_{36}NF$], a fragment at *m/z* 242.3 corresponding to the tetra-*n*-butylammonium cation ($C_{16}H_{36}N^+$) and a fragment at *m/z* 19 corresponding to the fluoride anion (F^-). The elemental analysis of the sample ($C_{64}H_{76}FNO_{12}Si_8$) with a theoretical molecular weight of 1294.98 g.mol^{-1} also confirmed the formula of this sample.

($C_{64}H_{76}FNO_{12}Si_8$) with a theoretical molecular weight of 1294.98 g.mol^{-1} also confirmed the formula of this sample.

To understand the mechanism of the reaction we measured the ^{19}F NMR (MP73) and ^{29}Si NMR (MP112) spectra at regular intervals during the reaction. Shibato and co-workers[79, 80] have reported that bis(allyl)silanes of the type A (Figure 29) were highly effective for generating allyl anion species via chelate formation of type B with tetra-*n*-butylammonium fluoride.

They reported a ^{19}F NMR chemical shift of -77.7 ppm for the fluoride anion in the chelate complex B (Figure 29) using ethyl trifluoroacetate ($\delta = 0$) as an external standard.

Figure 29

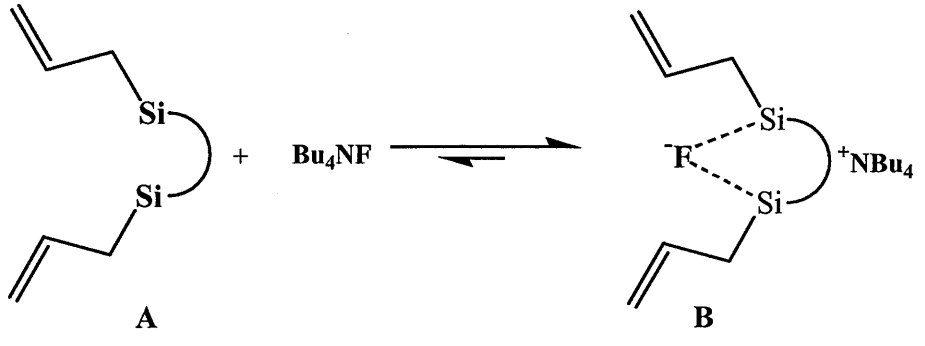

For our part, we used trifluoromethane as the external standard. We also looked for peaks other than the one which corresponds to the fluoride ion in the cage (-26.4 ppm). We observed other peaks at δ = -81.9 ppm, δ = -115.5 ppm, δ = -120.5 ppm, and δ = -135.5 ppm. After 1.5 hours of reaction time, the peak at -81.9 ppm appeared, but we were not able to assign this peak with any certainty to an intermediate structure. Nevertheless, we can

suggest a similar structure for such intermediate in the reaction for the fluoride encapsulation within an octasilsesquioxane cage, as shown in Figure 30.

Figure 30

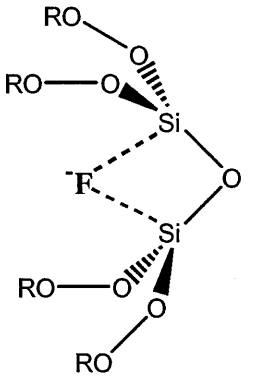

We also followed the reaction by ^{29}Si NMR which gave more useful information about the mechanism. The starting material, phenyltripropoxysilane, had a chemical shift of -57.9 ppm. We took the first measurement just after the starting material had been added and we observed three significant peaks at δ = -68.2 ppm, δ = -77.0 ppm, and δ = -77.8 ppm. The peak at -68.2 ppm corresponds to the shift of the T6 compound, which was synthesized by Marina Maesano[81] at the Open University during her PhD studies. This suggests that the first intermediate could be a phenyl-T6. For simplicity, the chemical shifts, the times and the intensities are reported in the Table 5.

Table 5

Time	$\delta^{29}Si$ (ppm)	Relative Intensity
0 hour	-68.16	1
	-77.01	1
	-77.77	1
10 hours	-68.88	2
	-71.93	1
	-77.75	1
	-78.51	4
	-79.71	1
	-80.65	2
24 hours	-68.88	2
	-71.93	1
	-77.73	1
	-78.51	4
	-79.71	1
	-80.65	4
48 hours	-68.92	1
	-71.93	0.5
	-77.73	1
	-78.53	2
	-79.71	1
	-80.65	4
after removal of the solvent without heating	-68.98	1
	-77.66	1
	-78.55	1
	-79.67	1
	-80.63	4
after removal of the solvent with heating	-78.55	1
	-80.63	4

Analysis of the NMR data with time suggests that our product, the Ph_8T_8 cage with a fluoride anion inside δ ^{29}Si = -80.6 ppm, is formed quite rapidly after 10 hours. However, the intensity of all the peaks increases with the time of reaction. Two other ^{29}Si NMR peaks attracted our attention, at -78.5 and -79.7 ppm, which fall within the range of the Ph_8T_8 cage without the fluoride anion inside. This could provide an insight into the mechanism of the reaction, suggesting the cage structure is formed in an initial step followed by the insertion of the fluoride into the cage. The diameter of the portal of the cage is 3.229 × 3.11 Å, which could possibly allow a fluoride anion (diameter 1.17-1.19 Å) to enter. The peak at -71.9 ppm is in the range of a silanol shift, suggesting a partial cage structure. Unfortunately, it was not possible to obtain a crystal structure of this intermediate.

Voronkov and Lavrent'yev[18] have reported a stepwise polycondensation of alkyltrichlorosilanes, which goes via linear, cyclic and polycyclic siloxanes as intermediates. One interesting step, in agreement with our ideas, is the formation of a T_6 intermediate. They have reported as a final step the formation of T_{10}. In our case, we observed a peak at -81.4 ppm in the ^{29}Si NMR spectra of the crude mixture and the red-brown liquid after filtration. This could be indicative of the formation of a phenyl-T_{10} but, unfortunately, we were unable to obtain a crystal structure. However, based on Marsmann's equation[72] (δ T_{10} = 1.028 × δ T_8), the peak at -81.4 ppm is arising from the phenyl-T_{10}.
Nevertheless, we did obtain some large crystals from our red-brown liquid and the X-Ray crystal structure shows a phenyl-T_{12} cage structure (Figure 31). Based on Marsmann's equation (δ_a T_{12} = 1.025 × δ T_8 and (δ_b T_{12} = 1.064 × δ T_8), the phenyl-T_{12} cage should show two peaks in the ^{29}Si NMR at -81.2 and -84.3 ppm. Unfortunately, we could not dissolve the phenyl-T_{12} cage crystals to verify these chemical shifts.

Figure 31 $Ph_{12}T_{12}$ X-ray crystal structure and packing

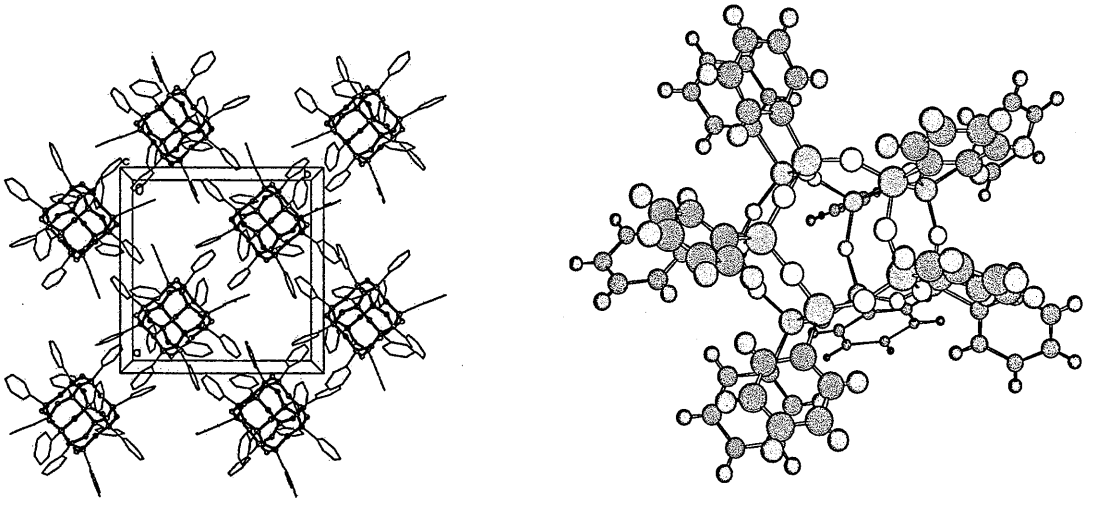

It would be interesting to look at the outcome of the reaction using other sources of fluoride ion as the catalyst and also investigate the possibility of encapsulating other anions than fluoride using salts with other anions with suitable counterions.

2.4 A problem with a high energy barrier to surmount: was it a temperamental reaction ?

As we decided to look in more detail at the parameters that affect the entrapment of the fluoride anion reaction and their optimization, we encountered a problem with the reaction itself. In fact, we were suddenly unable to obtain and produce the tetra-*n*-butylammonium octaphenyloctasilsesquioxane fluoride in anything like our previous yields. This was the beginning of a lengthy inquiry about the source of the problem!

We identified a number of key parameters to study:

- the purity of the starting material
- the reproducibility of the catalyst from the supplier
- the amount of water in the reaction mixture
- the concentration of catalyst
- the conditions used for removing the solvent

2.4.1 The purity of the starting material and the reliability of the catalyst supplier

First of all, we examined the purity of the starting material, phenyltrialkoxysilane, that was used in all of the experiments which did not work and compared it with the purity of the starting material used in our model experiment that did work. In none of the experiments that did not work would the starting material be considered as having a lower degree of purity than with the experiments that worked.

Since we had changed the supplier during the work, we checked to see if the reaction was working for both a 1M tetra-*n*-butylammonium fluoride solution in THF with 5% of water supplied from Accros and with one supplied from Aldrich. In both reactions no formation of the Ph_8T_8-TBAF was observed. This suggested that the problem may not be down to the supplier. At this stage we turned our attention to the amount of water in the reaction mixture.

2.4.2 The control of the amount of water in the reaction mixture

One interesting observation was that when we used a wet solvent, we did not obtain a pure product, but our cage dissolved in the resin by-product. This suggests that the amount of water present in the solvent is very important and has a big influence on the nature of the final product. The tetra-*n*-butylammonium fluoride (TBAF), which we used, is a solution of TBAF with a concentration of 1M but also contains 5% water.

The importance of the presence of water for the TBAF catalysed formation of the silicon-oxygen bond has been studied by Yuxing Yang[51] who reported an interesting experiment using oxygen 18. This work showed that cage formation only occurred by incorporation of the oxygen atoms from the water contained in the TBAF solution. In fact, the amount of ^{18}O from the catalyst solution, which was incorporated into the cage framework, was quantified in terms of the average number of ^{18}O atoms per cage. In the case of high ^{18}O water content, the average number of ^{18}O per cage ranged between 6 and 7 for T8 cages, accounting for at least 50% of the oxygen atoms of the octasilsesquioxane framework (Si_8O_{12}). This work concluded with the observation that the ^{18}O inclusion in the cage is proportional to the ^{18}O content of the water which demonstrated that the oxygen atoms forming the cage framework are solely derived from the water of the TBAF catalyst solution and not from the alkoxy-groups of the trialkoxysilane. So we might expect that a variation in the amount of water in the reaction mixture would have a large effect on the outcome of the reaction. We, thus, decided to do a series of experiments using phenyltrialkoxysilane and varying the amount of water from 0 to 10% in the reaction mixture.

In these series of experiments, we used solid TBAF. xH_2O. Some of this catalyst, TBAF. xH_2O, was dried overnight under high vacuum. A similar amount of catalyst was then placed in four sealed round bottom flasks that have been previously dried in an oven. Air was immediately replaced by nitrogen gas in all the flasks. 2.5ml of dried THF was added with a syringe to each flask to obtain 2.5ml of an anhydrous TBAF solution (1M) in THF. A different amount of water was added to each flask with a syringe to obtain four solution MP176, MP177, MP178 and MP179 with respectively 0, 2.5, 5 and 7.5% of water to the four different solutions. 20ml of dried toluene was then added to each flask before adding an equivalent of the starting material, phenyltripropoxysilane. All reaction mixtures were stirred at room temperature. After 24 hours the solvent was removed using a rotary

evaporator. All residues obtained were analysed using ^{29}Si NMR, ^{19}F NMR, ^{1}H NMR and ^{13}C NMR. The results obtained were very interesting:

- There was no reaction at all when no water was present (MP176), in fact, only the unchanged starting material was observed. We were not surprised at such a result as we knew water molecules would be needed for the formation of the Si-O-Si bond. However, we would have expected the formation of a fluoro silane.
- For the solution with 2.5 and 7.5% of water (MP177 and MP179), we observed a complex pattern in the ^{29}Si NMR spectra in the region of the octaphenyloctasilsesquioxane cage. Thus, we concluded that not enough or too much water in the medium led to the formation of a random ladder-like resin.
- The reaction with 5% water (MP178) led to an interesting result: the ^{29}Si NMR spectra showed the main peak at -79 ppm (-79.6 ppm in $CDCl_3$) corresponding to the Ph_8T_8 cage and a small one at -80.6 ppm corresponding to the Ph_8T_8-TBAF cage. This was confirmed by the presence of a small sharp peak at -26.4 ppm in the ^{19}F NMR spectrum corresponding to the fluoride anion encapsulated in the middle of the silsesquioxane cage. This suggests that the optimum amount of water for obtaining a pure fluoride encapsulated product is 5%.

Even though Ph_8T_8-TBAF was not the main product of this reaction (MP178), with a yield far lower than first obtained (MP19), we concluded that the presence of 5% of water in the

catalyst solution was required to obtain our tetra-*n*-butylammonium octaphenyloctasilsesquioxane fluoride cage.

At this point, we only had two more parameters to consider to find out the optimum parameters for the formation of Ph_8T_8-TBAF cage: the concentration of the catalyst and the conditions for removing the solvent.

2.4.3 The concentration of the catalyst

The concentration of the catalyst was an easy parameter to vary, however, we were already using the optimal ratio that had been determined by Yuxing Yang[71], that is a catalyst in a 1:2 ratio with the trialkoxysilane. Nevertheless, we tried different ratios, 1:1, 1:2 and 1:4, and controlled the amount of water as described previously, adding 5% water with a syringe in each sealed flask. The 1:1 and 1:4 ratios of siloxane to TBAF resulted in the formation of a resin-like product and we observed a complex pattern in the ^{29}Si NMR spectra in the region of the octaphenyloctasilsesquioxane cage. The 1:2 ratio was the only experiment to show a specific pattern with a main peak at -79 ppm corresponding at the Ph_8T_8 and a small peak at -80.6 ppm corresponding at the Ph_8T_8-TBAF. This was confirmed by the presence of a peak at -26.4 ppm in the ^{19}F NMR spectra. Thus, these experiments did not give any indication as to why we could not obtain the tetra-*n*-butylammonium octaphenyloctasilsesquioxane fluoride cage in the same yield as before.

To sum up, the optimum conditions for the synthesis of the tetra-*n*-butylammonium octaphenyloctasilsesquioxane fluoride cage were:

- A catalyst ratio of 1:2 with respect to the trialkoxysilane
- 5% of water in the catalyst solution

2.4.4 A study of the conditions used for removing the solvent

By this stage, we had decided that the solvent removing step must be the key determinant for this reaction. In fact, after careful consideration of all the facts we remembered that, after the last reaction which worked, we had to replace a joint in the condensor of the rotary evaporator because of a problem in maintaining the vacuum. This suggested that since then we had been removing the solvent too quickly and at too low a temperature, such that the conditions were no longer optimal for the fluoride encapsulation to occur. In fact on further consideration, we might well expect that the encapsulation of the fluoride anion in the middle of the cage is enhanced by the concentration process on removal of the solvent which in turn are affected by three parameters: temperature, vacuum and rate of concentration. The rate of concentration of the solution was determined by a careful combination of the other two parameters. This was then the subject of a detailed investigation during which we carried out seven important experiments to aid our understanding of the optimum conditions and the mechanism of the formation of the tetra-*n*-butylammonium octaphenyloctasilsesquioxane fluoride cage. In all of these experiments, we used a catalyst ratio of 1:2 with respect to the trialkoxysilane and a controlled amount of water (5%) in the reaction mixture.

MP154 experiment:

This first experiment was conducted using acetone as the solvent of the reaction. After 24 hours, the reaction was stopped and the solvent (b.p. of acetone: 56°C) removed at 50°C and 400 mbar on a rotary evaporator. A yellow solid gel was obtained. The ^{29}Si NMR spectrum of this mixture showed a peak in the T_8-Si region at -79.7 ppm which, based on Marsmann's equation, arises from octaphenyloctasilsesquioxane.

MP168 experiment:

We repeated the previous experiment (MP154) using THF as the solvent. After 24 hours, the reaction was stopped and the solvent (b.p. of THF: 66°C) removed at 55°C and 375 mbar on a rotary evaporator. A yellow solid gel was obtained. The ^{29}Si NMR spectrum of the mixture showed four peaks in the T_8-Si region at -78.4, -79.5, -79.6, and -81.4 ppm in a ratio 1:2:8:4. Thus, based on Marsmann's equation, the single peak at -78.4 ppm arises from octaphenyloctasilsesquioxane, phenylT_8, the single peak at -79.6 ppm arises from decaphenyldecasilsesquioxane, phenylT_{10}, and the peaks at -79.5 and -81.4 ppm from a dodecaphenyldodecasilsesquioxanes cage, phenylT_{12}, with two different silicon environments.

MP153 experiment:

This experiment was conducted in toluene as the solvent. After 24 hours, the reaction was stopped and the solvent (b.p. of toluene: 110.6°C) removed at 90°C and 200 mbar on a rotary evaporator. A yellow solid gel was obtained. The ^{29}Si NMR spectrum of the mixture showed a quintet at -122.1, -124.7, -127.3, -129.9 and -132.5 ppm which may be SiF_4, which is a gas at room temperature but does dissolve in some organic solvents. However, this should have been removed when the solvent was evaporated using a rotary evaporator at

40°C. Thus, this SiF_4 species is probably the pentacoordinate silicon compound, $PhSiF_4^-$, formed from the reaction of the phenytriethoxysilane with the fluoride. This could be due to the high temperature used to remove the solvent. Thus, we need to remove the toluene at a lower temperature and higher vacuum.

MP187 experiment:

We repeated the previous experiment (MP153) using acetone as the solvent of the reaction. After 24 hours, the reaction was stopped and the solvent removed at 50°C and 400 mbar for about 10 minutes. A yellow solid gel, **A**, was obtained. Analysis of the ^{29}Si NMR spectrum showed a very small peak at -80.6 ppm and a ^{19}F NMR chemical shift at -26.6 ppm which was also very small. These data confirm the presence, in a very low yield , of the tetra-*n*-butylammonium octaphenyloctasilsesquioxane fluoride cage. Thus, we redissolved the gel A in toluene and stirred it for 10 minutes. Then we removed the toluene at 73 mbar and 85°C for 10 minutes. A yellow solid gel, **B**, was obtained. We observed a stronger peak in the ^{19}F NMR spectrum at -26.6 ppm. Analysis of the ^{29}Si NMR spectrum shows a small peak at -79.4, but the main peak was at -80.6 ppm with a triplet at -125.4, -128 and -130.6 ppm. The triplet at -128 ppm indicates Si-F coupling corresponding to a R_2SiF_2 fragment. However, the chemical shift at -128 ppm is at too high a field for an R_2SiF_2 species which should be further downfield at -70 ppm. On the other hand, a chemical shift at -128 ppm suggests an $RSiF_4^-$ species. Although the NMR spectrum showed as a triplet, it could be part of a quintet where the two outer peaks are lost in the noise of the base line. However, the analysis of the gel **B** confirmed the presence of the fluoride cage in higher yield than before retreatment at higher temperature. We obtained a precipitate of a white and fine powder after redissolving the gel B in chloroform. After filtration, analysis of the fine and white powder shows a peak at -80.6 ppm in the ^{29}Si NMR and a peak at -26.6 ppm in the ^{19}F NMR

which are characteristic of a pure Ph_8T_8-TBAF cage. The ^{29}Si NMR analysis of the filtrate shows a broad peak in the T-Si region with a sharp peak inside this region with a ^{29}Si NMR chemical shift of -79.4 ppm but no peaks in the ^{19}F NMR spectrum. This is characteristic of a Ph_8T_8 cage incorporated in a resin.

MP189 experiment:

We repeated the previous experiment (MP187) using toluene as the solvent of the reaction. After 24 hours, the reaction was stopped and the solvent (b.p. of toluene: 110.6°C) removed at 73 mbar and at 60°C to 90°C over 25 minutes. A yellow solid gel, **A**, was obtained. Analysis of the ^{29}Si NMR spectrum (Figure 32 and Figure 33) shows a peak at -80.6 ppm which, together with the presence of a ^{19}F NMR peak at -26.6 ppm, demonstrates the presence of the Ph_8T_8-TBAF cage. However, this was not the main product of this reaction at this stage. In fact, the ^{29}Si NMR spectrum displays three more peaks at -68.9, -77.7 and -78.5 ppm with relative ratio of 3:1:3. As opposed to the two sharp peaks at -77.7 and -78.5 ppm, the peak at -68.9 ppm seemed to have a more complicated pattern. This pattern of three peaks is reported in literature to be associated to an open cage $Ph_7T_7(OH)_3$. We also observed two little peaks in the ^{19}F NMR spectrum (Figure 34) at -26.8 and -28.1 ppm which we will discuss later. These data confirm the presence, in a very low yield, of the tetra-*n*-butylammonium octaphenyloctasilsesquioxane fluoride cage in the presence of a $Ph_7T_7(OH)_3$ open cage.

Figure 32 ^{29}Si NMR of gel A

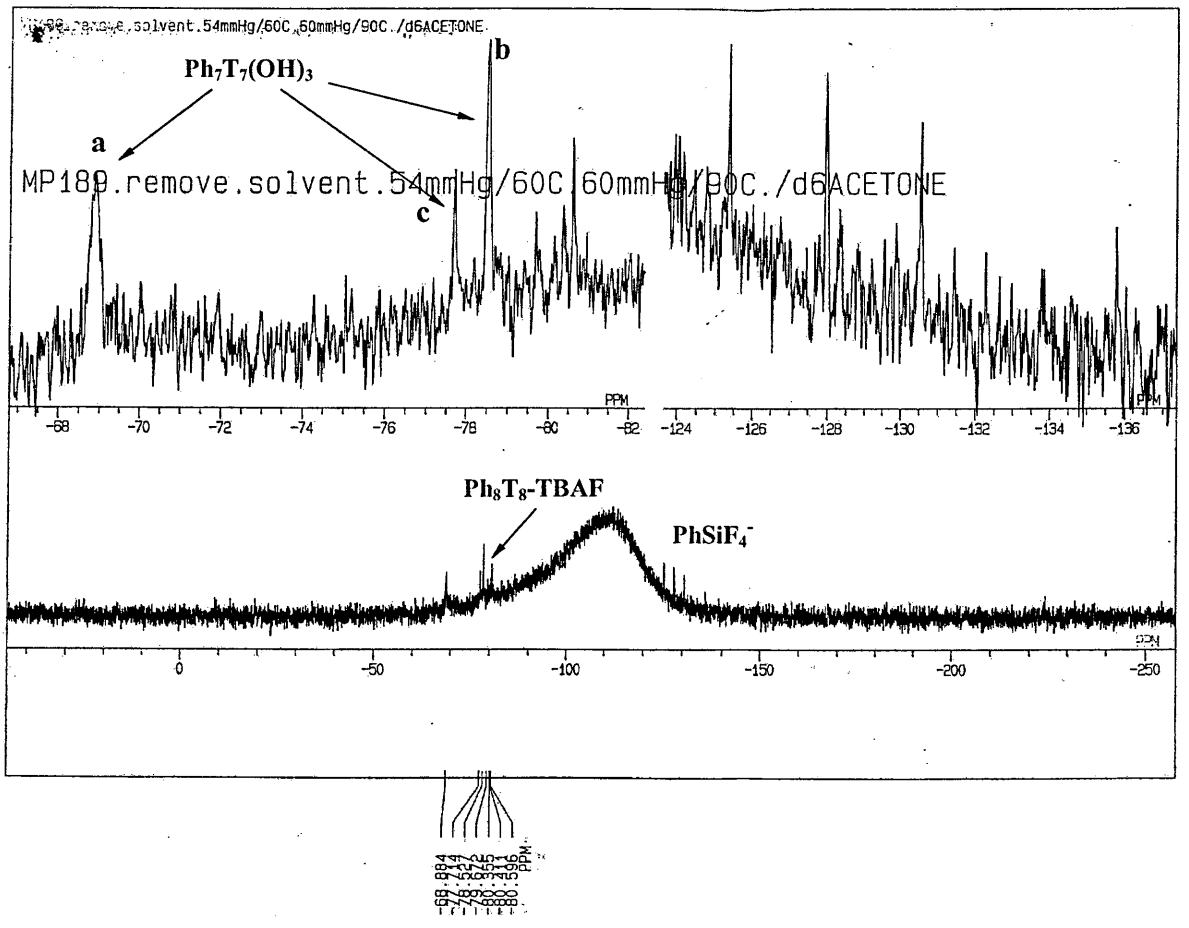

Figure 33 Assignment for $Ph_7T_7(OH)_3$

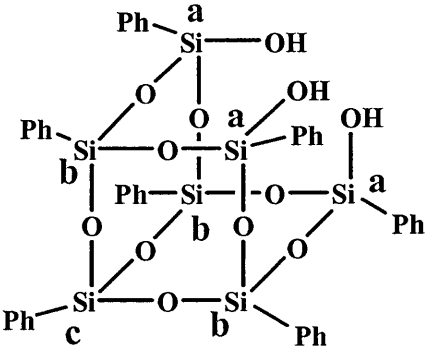

Figure 34 ^{19}F NMR of gel A

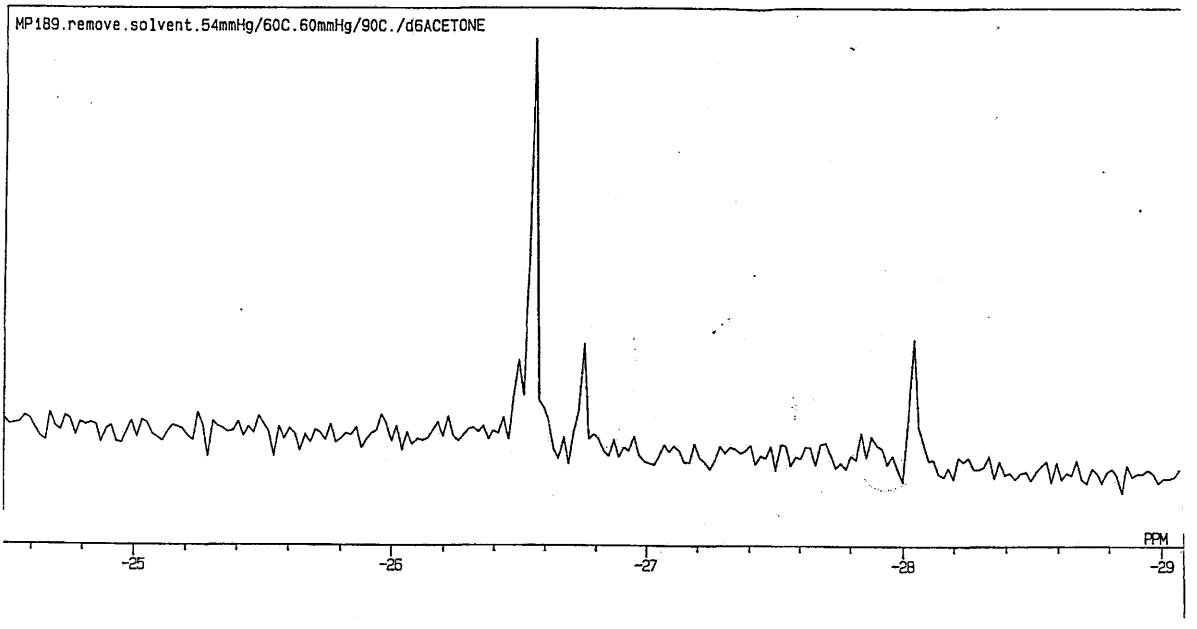

As in the previous experiment, we redissolved the gel **A** in toluene and stirred it for 10 minutes. We removed the toluene at 79 mbar and 60°C over 15 minutes and carry on heating at 70°C and at 79 mbar for a further 15 minutes. A yellow solid gel **B** was obtained. We observed only one strong peak in the ^{19}F NMR with a chemical shift of -26.6 ppm. Analysis of the ^{29}Si NMR spectrum shows a main peak at -80.6 ppm and a quintet at -122.1, -124.7, -127.3, -129.9 and -132.5 ppm which is thought to be the pentacoordinate silicon compound, $PhSiF_4^-$, formed from the reaction of the phenytriethoxysilane with the fluoride. This analysis of the gel **B** confirmed the presence of the fluoride cage in higher yield than before retreatment in toluene. The yellow solid gel **B** was then extracted with chloroform to give a white solid. After filtration, the analysis of the fine and white powder showed a peak at -80.6 ppm in the ^{29}Si NMR and a peak at -26.6 ppm in the ^{19}F NMR, which confirmed the presence of a pure Ph_8T_8-TBAF cage (Figure 35).

Figure 35 ^{29}Si NMR and ^{19}F NMR of white powder from gel B

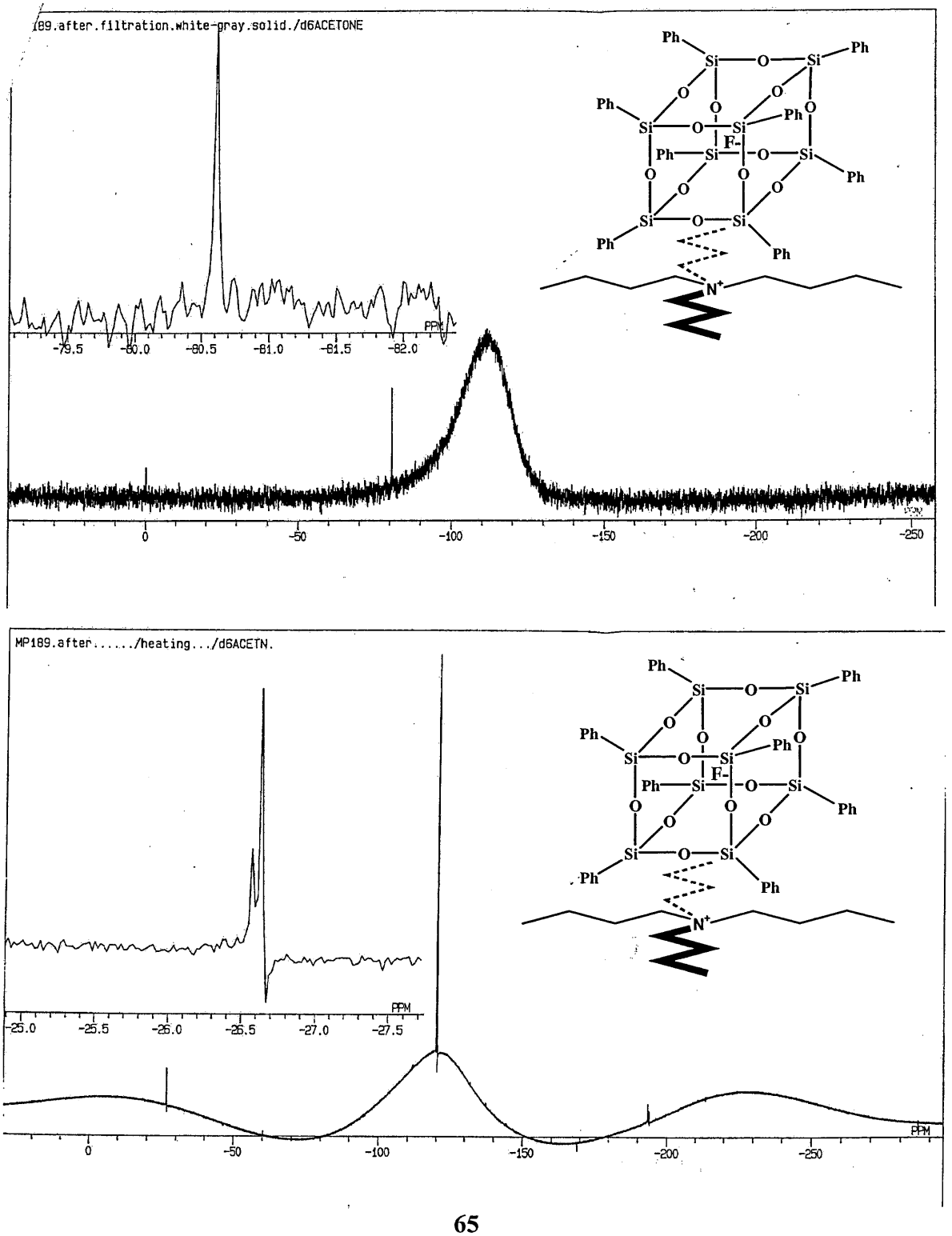

At this point, it was clear that the use of a high boiling solvent such as toluene favoured the formation of the Ph_8T_8-TBAF cage. Based on this conclusion, we started to use only toluene as the solvent which allowed us to use higher temperatures and higher vacuums to remove the solvent.

MP192 experiment:

This experiment was conducted using toluene as the solvent of the reaction. After 24 hours, the reaction was stopped and the solvent removed at 80°C and 73 mbar for 15 minutes using a rotary evaporator. A yellow solid gel was obtained which was then extracted with chloroform to give a white solid. After filtration, analysis of the powder showed a peak at -80.6 ppm in the ^{29}Si NMR and a peak at -26.6 ppm in the ^{19}F NMR which again indicated the synthesis of a pure Ph_8T_8-TBAF cage in very good yield.

Thus, these experiments demonstrated the complexity of setting up the optimum parameters for the synthesis of a pure Ph_8T_8-TBAF cage in very good yield. So for our experiments suggest the following parameters for this reaction:

- A catalyst ratio of 1:2 with respect to the trialkoxysilane.
- 5% of water in the catalyst solution.
- A temperature of about 80°C is required during the removal of the solvent.
- Toluene is the favoured solvent as it has a fairly high boiling temperature.
- A high vacuum (about 70 mbar) is also required during the removal of the solvent.

In order to check these parameters, we carried out a reaction (MP237) which separated the warming up step and the removal of the solvent step. This experiment was conducted in toluene. The mixture reaction was stirred and heated at 80°C for an hour before removing the solvent under vacuum distillation. A white solid gel was obtained. Analysis of the mixture showed a single peak at -80.6 ppm in the ^{29}Si NMR and a single peak at -26.6 ppm in the ^{19}F NMR which again indicated the synthesis of the Ph_8T_8-TBAF cage. Thus, all the parameters and conditions of the reaction were confirmed.

Chapter 3: Synthesis of tetra-*n*-butylammonium octavinyl, octa-*para*-tolyl and octa-*para*-chloromethylphenyl octasilsesquioxane fluoride

3.1 Introduction

In the first part of this work, we have shown that the high-yielding route for the synthesis of T_8-cages based on the reaction of tetra-*n*-butylammonium fluoride with trialkoxyphenylsilane can lead to a new class of octasilsesquioxane cage compound, Ph_8T_8-TBAF, whereby a fluoride ion becomes encapsulated and perfectly centered within the cage. This has been achieved by removing the solvent and concentrating the tetra-*n*-butylammonium fluoride with the cage or cage precursors instead of precipitating the cage by the addition of acetone. As we successfully optimised the parameters for the synthesis of this new class of octasilsesquioxane cage compound, we wanted to look at the possibility of reproducing this result with different substituent groups on the silicon atom. The cage may be formed as a result of the complementary interactions between the phenyl groups and the tetra-*n*-butylammonium cation where the phenyl groups form a valley within which the tetrabutyl arms fit perfectly. We thus decided to choose a vinyl group as the substituent where this interaction is not possible. We also focussed on other aromatic substituents such as *para*-tolyl and *para*-chloromethylphenyl.

3.2 Synthesis of tetra-*n*-butylammonium octavinyloctasilsesquioxane fluoride

3.2.1 Introduction

As we stated earlier, one of the aims is to investigate the "how" and "why" of the encapsulation of a fluoride anion in an octasilsesquioxane cage. The first substituent group we looked at was the vinyl group as it is the simplest group with an sp^2 carbon atom on the silicon atom.

3.2.2 Experiments

The first experiment (MP205) was conducted in toluene as the solvent. After 24 hours, the reaction was stopped and the solvent (b.p. of toluene: 110.6°C) removed on a rotary evaporator with a temperature gradient from 30°C to 80°C over 10 minutes, then leaving at 80°C and a vacuum of 70 mbar for 15 minutes. A yellow solid gel was obtained. The ^{29}Si NMR spectrum (in d_6 acetone) confirmed the presence of the T_8 cage and that the signal is shifted upfield by about 2 ppm from octavinyloctasilsesquioxane to a chemical shift of -82.89 ppm as shown in Figure 36. This suggests that a cage has been synthesized but that it is modified in some way from the vinylT_8.

Figure 36 ^{29}Si NMR spectrum of MP205

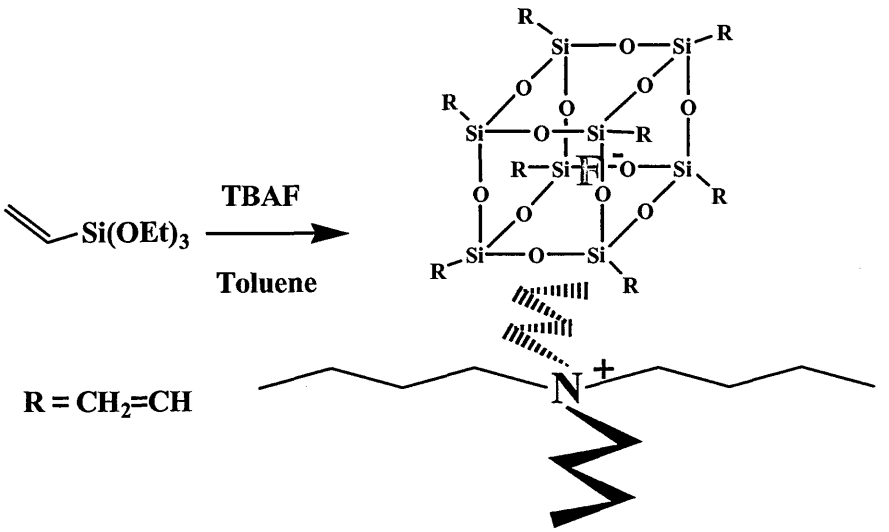

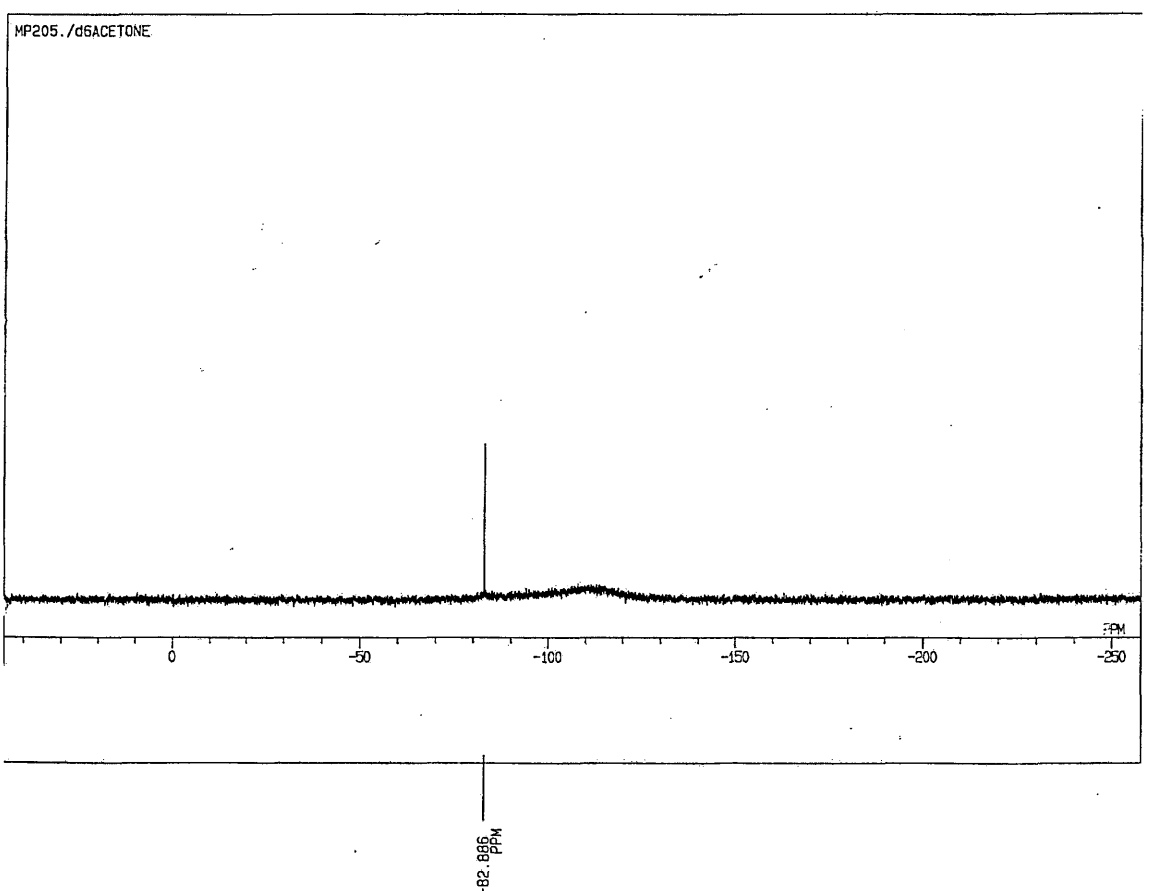

Based on what we had seen before in the case of the Ph_8T_8-TBAF cage, this was an encouraging result which suggested we should check the ^{19}F NMR spectrum. In fact, the ^{19}F NMR spectrum, shown in Figure 37, displays a sharp and intense peak with a chemical shift of -25.4 ppm which is consistent with the formation of the tetra-*n*-butylammonium octavinyloctasilsesquioxane fluoride cage, vinylT_8-TBAF. As with the Ph_8T_8-TBAF cage, a range of other peaks can be observed ranging from δ = -61 to -150 ppm depending upon the solvent coordination and hydrogen bonding which can be particularly important when moisture is present in the solvent.

Figure 37 ^{19}F NMR spectrum of MP205

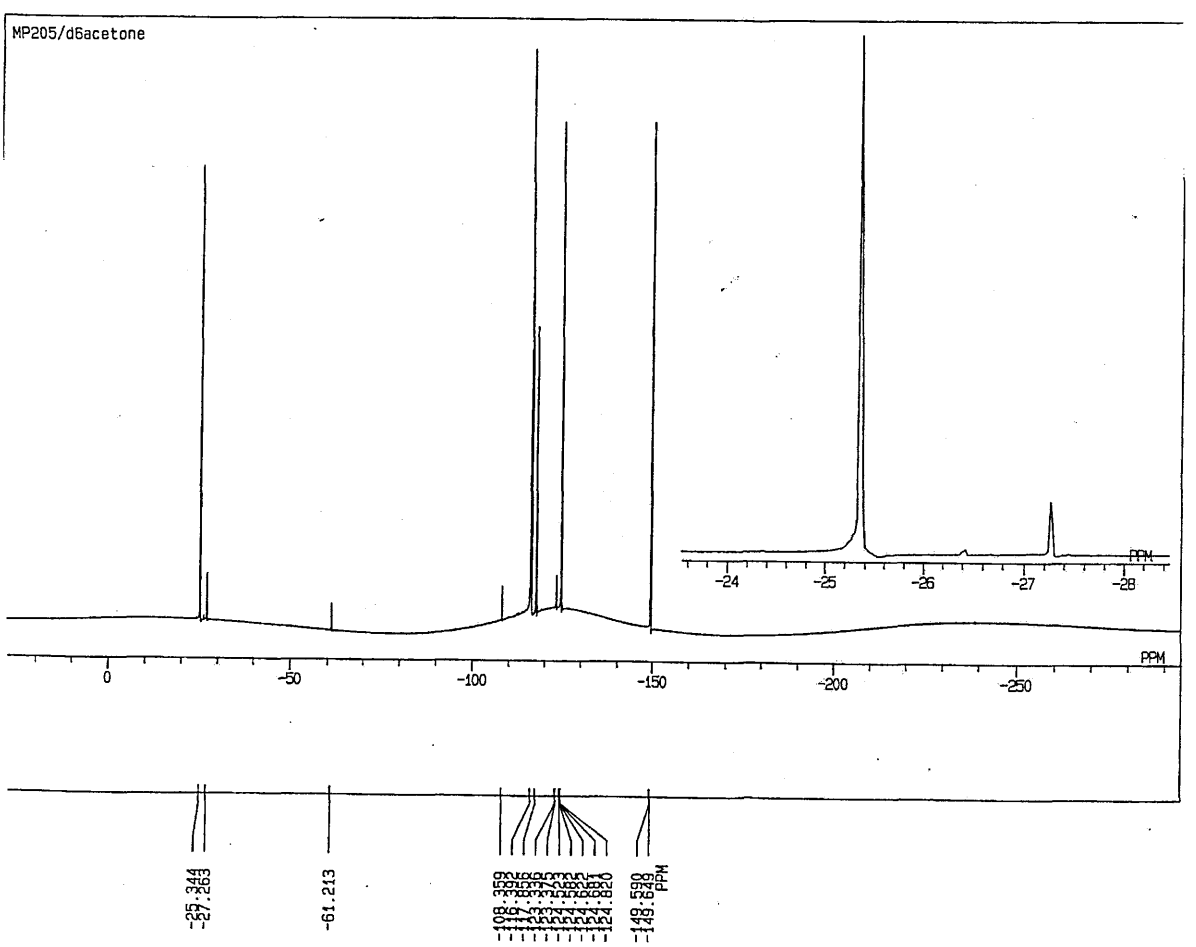

Additionally, we performed solid state ^{19}F NMR spectroscopy which revealed a single sharp peak with a chemical shift of -23.0 ppm, as shown in Figure 38. This value again suggests an isolated fluoride anion with little interaction with its near neighbours.

Figure 38 Solid state ^{19}F NMR spectrum of MP205

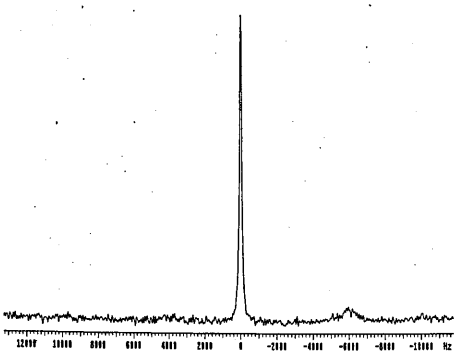

Furthermore, the ^{1}H NMR shows a multiplet with a chemical shift at 5.98 ppm (integration: 24H) which indicates the presence of a vinyl group (Figure 39). In addition, the spectrum displays a triplet at 0.98 ppm (integration: 12H), a multiplet at 1.42 ppm (8 H), another multiplet at 1.75 ppm (8 H) and a triplet at 3.44 ppm (8 H). The peaks at 0.98, 1.40, 1.75 and 3.40 ppm are associated with the CH_3-CH_2-CH_2-CH_2-X system, which is part of the tetra-*n*-butylammonium fluoride that was used as the catalyst. The integration confirms the 1:1 ratio between a cage and a tetra-*n*-butylammonium fluoride. This was confirmed by the ^{13}C NMR spectrum (Figure 40), which exhibits peaks at δ 13.80 ppm (s, CH_3); δ 20.32 ppm (s, -CH_2-); δ 24.37 ppm (s, -CH_2-); δ 59.33 ppm (s, -CH_2-) for the four carbon atoms of the tetra-*n*-butylammonium group and δ 131.89 ppm (C=C), δ 136.77 ppm (C=C) for the two carbon atoms of the vinyl group.

Figure 39 ^{1}H NMR spectrum of MP205

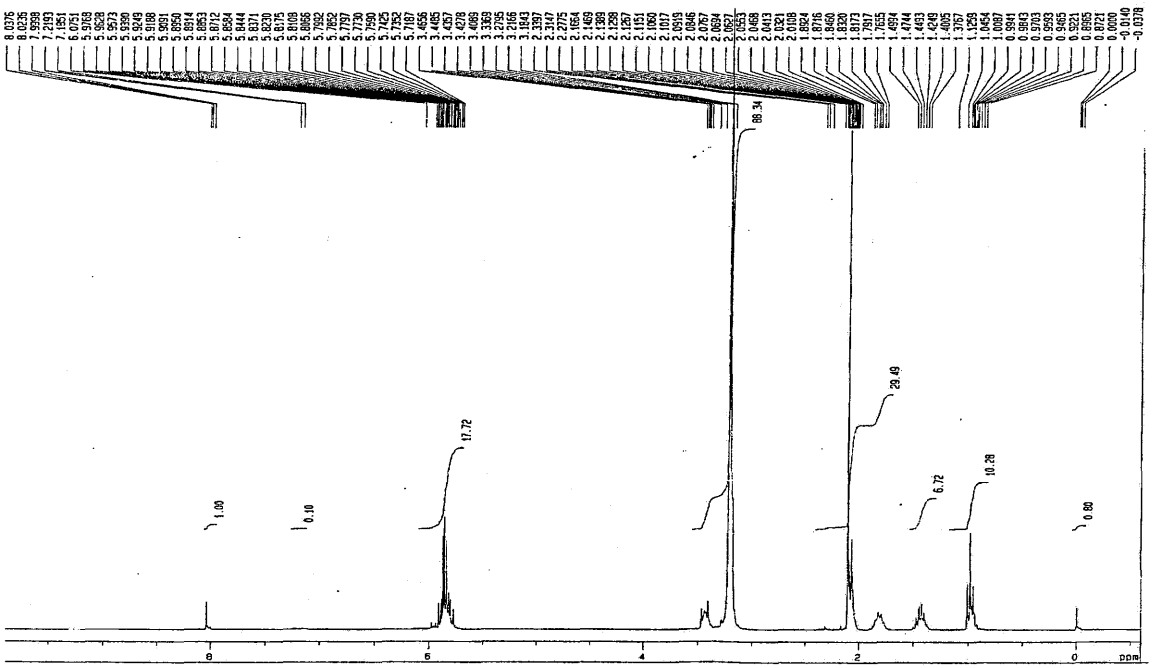

Figure 40 ^{13}C NMR spectrum of MP205

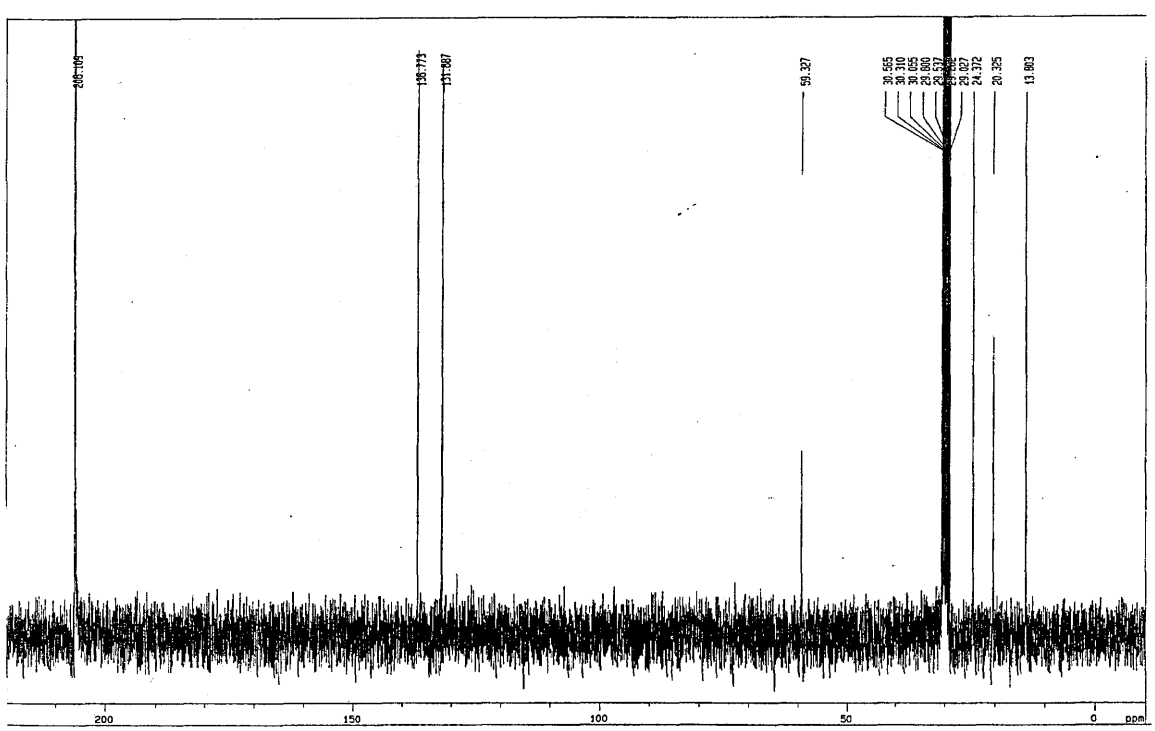

The product was also analysed by ESI mass spectroscopy. The analysis is shown in Figure 41 and confirms that the tetra-*n*-butylammonium octaphenyloctasilsesquioxane fluoride cage was obtained with a fragment at *m/z* 651.0 (100%) corresponding to the vinylT_8 cage with the fluoride anion ($C_{16}H_{24}FO_{12}Si_8^-$) [$M^-$] and a fragment at *m/z* 242.3 (100%) corresponding to the tetra-*n*-butylammonium cation ($C_{16}H_{36}N^+$) [M^+]. The elemental analysis of the sample ($C_{32}H_{60}FNO_{12}Si_8$) with a theoretical molecular weight of 894.53 $g.mol^{-1}$ also confirmed the high purity of this sample: calculated %C = 42.97, %H = 6.76, %N = 1.57, %F = 2.12; found: %C = 43.19, %H = 6.70, %N = 0.86, %F = 1.54

Figure 41 ESI mass spectroscopy of MP205

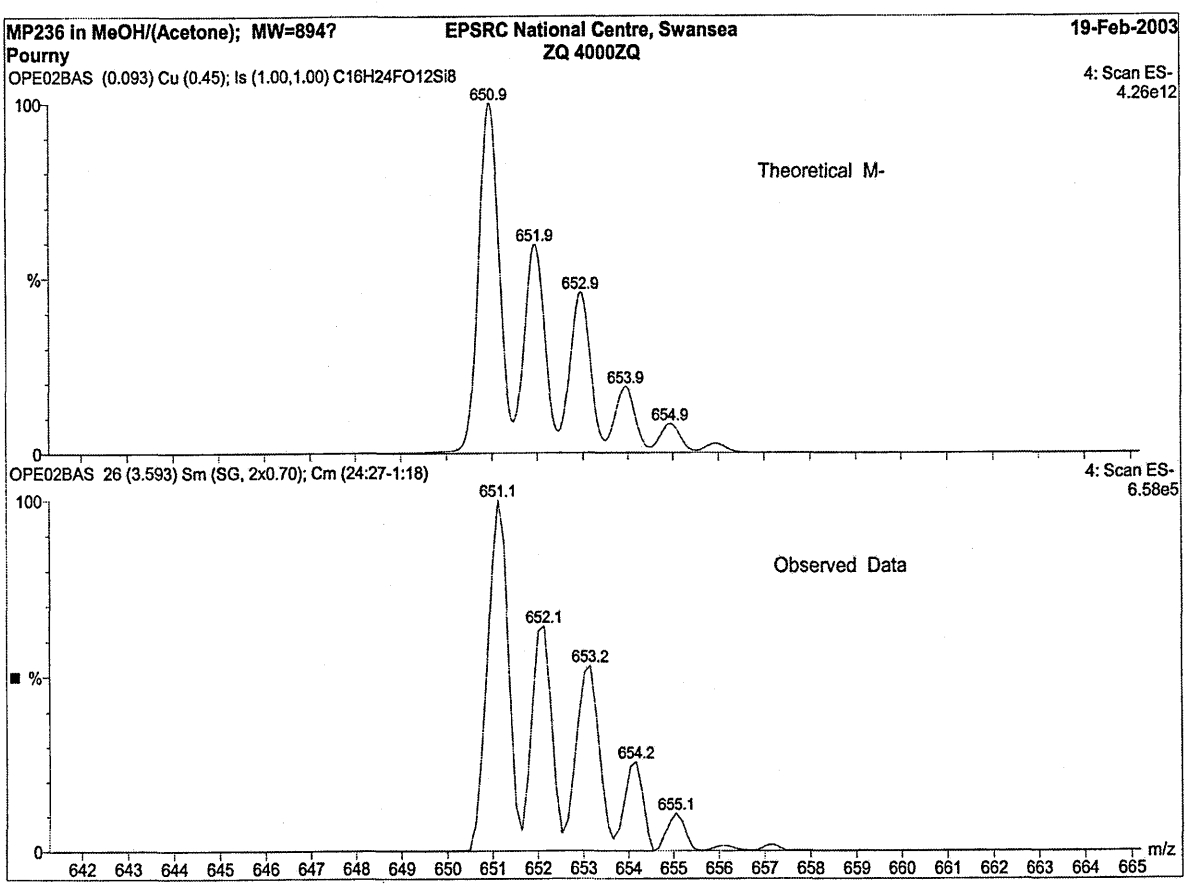

We obtained small crystals from our sample by the vapour diffusion method. A small amount of a saturated solution in acetone was placed in a narrow tube, which was itself placed in a wider tube which contained a solution of a precipitant ($CHCl_3$), the precipitant is thus allowed to diffuse into the solution. After five days we observed the formation of small crystals at the bottom of the tube containing acetone. We obtained 0.46g of colourless crystals which represent an isolated yield of 60%. The proposed structure of the tetra-*n*-butylammonium octavinyloctasilsesquioxane fluoride T_8 cage was confirmed by single-crystal X-ray crystallography as shown in Figure 42 and in agreement with all the data previously presented. In this new structure the fluoride ion is perfectly centred inside the silsesquioxane cage.

Figure 42 Structure of tetra-*n*-butylammonium octavinyloctasilsesquioxane fluoride

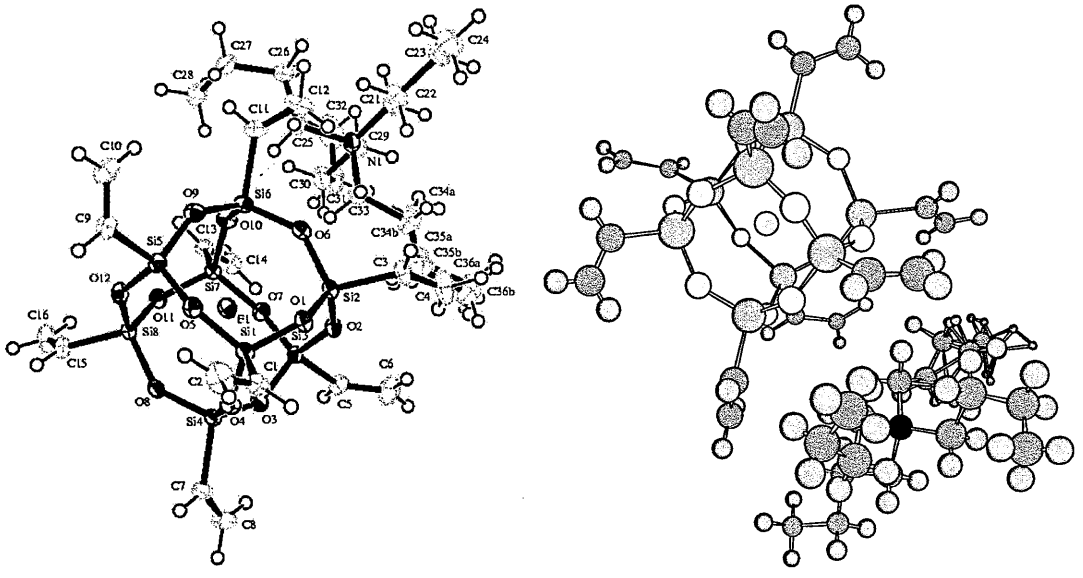

The crystallographic data revealed that the tetra-*n*-butylammonium octavinyloctasilsesquioxane fluoride T_8 cage had crystallised with a monoclinic crystal system with $P2_1/n$ space group. The silicon fluoride distance is 2.65 Å, which is similar to

that in the Ph_8T_8-TBAF cage. This size of the distance indicates that the interaction of each fluoride ion with its surrounding silicon atoms can be described as electrostatic at best. These weak fluoride silicon interactions were confirmed by the presence in the ^{29}Si NMR spectrum of a sharp singlet, as previously observed in the Ph_8T_8-TBAF cage. A comparison of the crystal structure data of the vinylT_8-TBAF cage with its nonencapsulated analogue shows how the fluoride ion entrapment inside the octasilsesquioxane cage causes the Si_8O_{12} cage framework to contract slightly in the fluoride-containing cage. This slight contraction of the framework is illustrated by the shrinkage of the mean Si-O-Si bond angle, as shown in Table 6, which may also be due to the repulsion of the oxygen and fluoride atoms. The sum of the O-Si-O bond angles also increases and there is a slight lengthening of the Si-C_{sp2} bond length, which is consistent with a weak silicon-fluoride ion interaction.

Table 6

Compound	Solution NMR		Crystal structure		
	$\delta\ ^{29}Si$ (/ppm)	$\delta\ ^{19}F$ (/ppm)	Mean Si-R(C_{sp2}) (/Å)	Mean O-Si-O (/°)	Mean Si-O-Si (/°)
Vy_8T_8-TBAF cage	-82.9	-25.3	1.85	338.5	141.1
Vy_8T_8 cage	-80.2		1.82	325.6	150.3

The arrangement of the tetra-*n*-butylammonium cation, with respect to the cage, is more complex where the shortest distance between the nitrogen and the fluoride ion is 6.68 Å. This is an increase, albeit small, compared to the nitrogen-fluoride distance in the

Ph_8T_8-TBAF cage, which is 6.465 Å. There are also three other N-F contacts of less than 10 Å. This arrangement causes a more complex packing than observed in the Ph_8T_8-TBAF cage where the tetrabutyl arms fitted nicely in the "valley" formed by the phenyl group which, in turn, was responsible of the highly ordered packing of the Ph_8T_8-TBAF cage.

The ^{29}Si NMR spectrum of our sample after leaving for a few days in a bottle revealed a slight change which is probably explained by a rearrangement of the vinylT_8-TBAF cage. In fact, the spectrum displays four peaks in the T_8-Si region at -81.85, -82.06, -83.64 and -83.79 ppm (in $CDCl_3$), as shown in Figure 43, still indicating the presence of high molecular weight silsesquioxanes.

Figure 43 ^{29}Si NMR spectrum of MP205 after few days

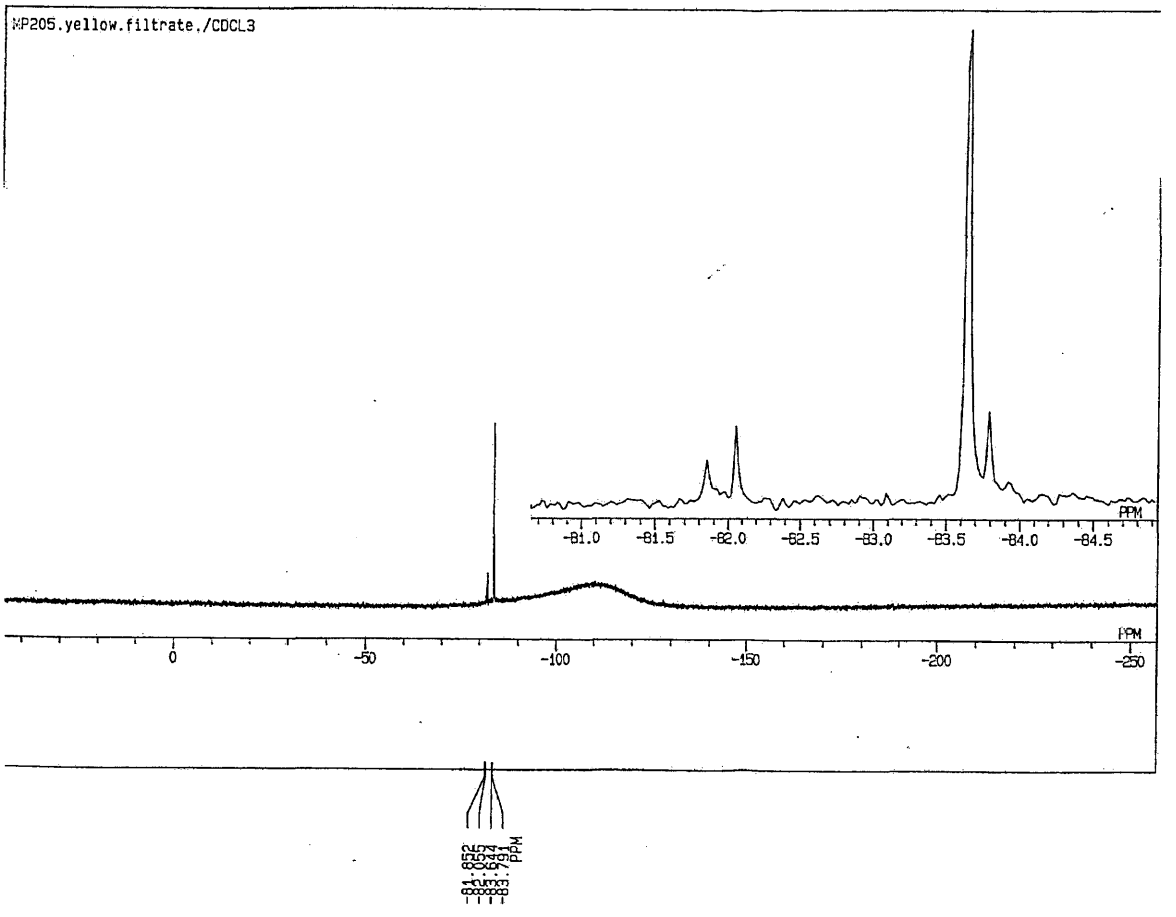

The ^{29}Si NMR chemical shift values were obviously slightly different to the values of the previous spectra which were measured in d_6 acetone giving, on average, a 0.758 ppm upfield shift. The calculated ^{29}Si NMR chemical shifts in acetone are -81.09, -81.30, -82.88 and -83.03 ppm. The peak at -82.88 ppm is our vinylT_8-TBAF cage which is confirmed by the presence of a peak at -26.83 ppm in the ^{19}F NMR spectrum. Based on the Marsmann's equation[72] ($\delta T_{10}R_{10} = 1.028 \times \delta T_8R_8$, $\delta T_{12}R_{12}A = 1.025 \times \delta T_8R_8$ and $\delta T_{12}R_{12}B = 1.064 \times \delta T_8R_8$) and Yuxing Yang's work[71], the peak at -81.30 ppm is thought to arise from the decavinyldecasilsesquioxane, vinylT_{10}, and the peaks at -81.09 and -83.03 ppm from the

dodecavinylsilsesquioxanes, vinylT_{12}, cage with two different silicon environments (Figure 44).

Figure 44

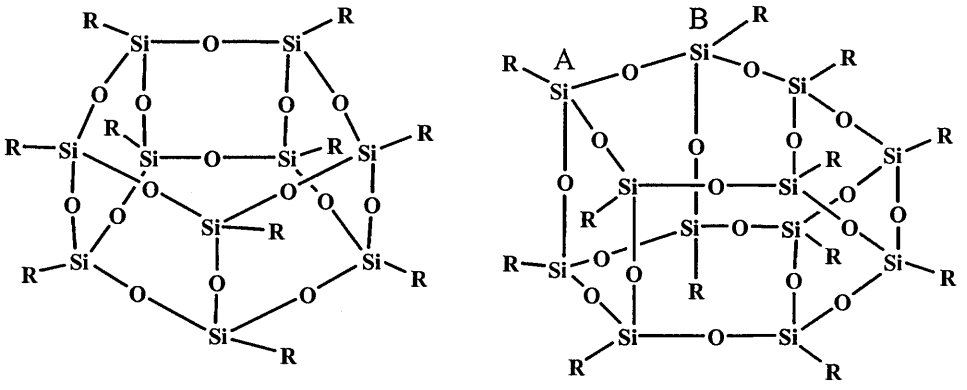

R= -C_2H_5

This result suggests that the tetra-*n*-butylammonium octavinyloctasilsesquioxane fluoride cage is reasonably stable but that, in the same way as its nonencapsulated analogue, eventually undergoes a few rearrangements leading to a conventional vinylT_{10} and vinylT_{12}, as discovered by Zhihua Liu and Yuxing Yang in their octasilsesquioxane cage rearrangement work[71, 82].

The encapsulation of the fluoride ion in the vinylT_8-TBAF cage confirms that our first result, the synthesis of the phenylT_8-TBAF cage, was not the consequence of an isolated chemical reaction but is a reproducible reaction albeit via a complex mechanism. We then looked at the effect of changing various reaction parameters during the removal of the solvent with the aim of understanding the fluoride entrapment mechanism.

A second experiment (MP209) was conducted in toluene as the solvent. After 24 hours, the reaction was stopped and the solvent (b.p. of toluene: 110.6°C) removed at room

temperature and 95 mbar on a rotary evaporator. A yellow solid gel **A** was obtained. As expected, the ^{29}Si NMR spectrum of this gel shows peaks at -63.6, -71, -74.2, -79.8, -80.7, -81.6, -82.3, -82.4 and -82.8 ppm, as shown in Figure 45. Whilst this looks like a very complex pattern, we will nevertheless attempt to associate each of the peaks to a corresponding compound.

Figure 45 ^{29}Si NMR spectrum of gel A (MP209)

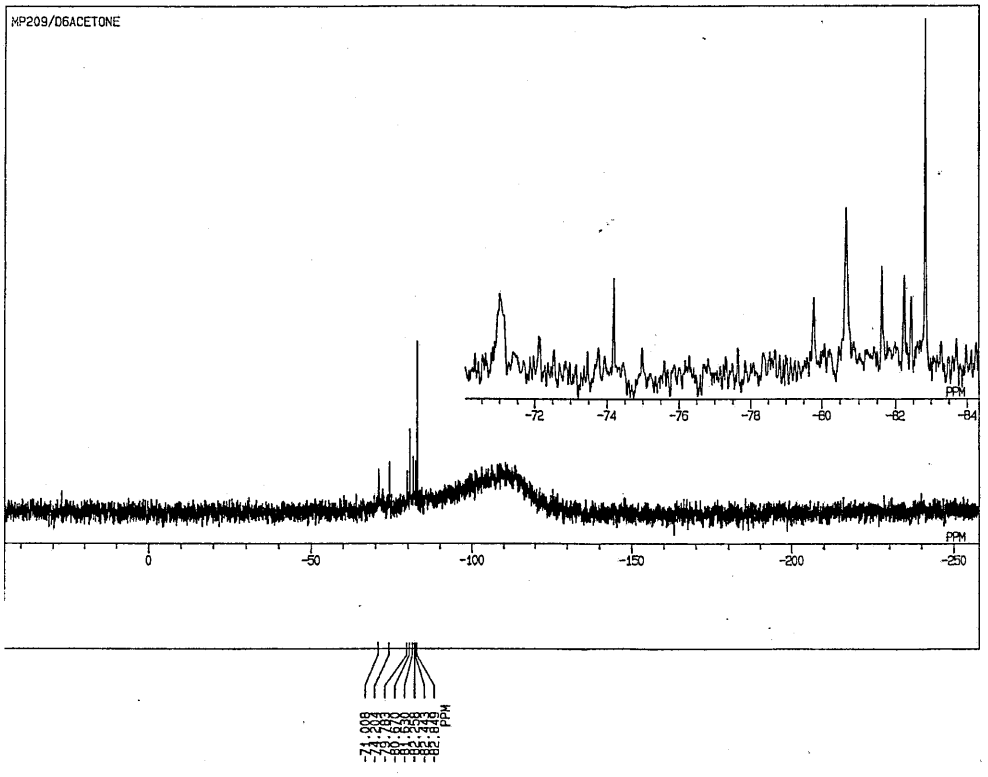

We redissolved the gel A in toluene, stirred it for ten minutes and removed the solvent using a temperature gradient from 30°C to 80°C in 10 minutes, then leaving at 80°C and a vacuum of 70 mbar for 15 minutes. A yellow solid, gel B, was obtained. The ^{29}Si NMR spectrum (in d_6 acetone) confirms the presence of the vinylT_8-TBAF cage and it revealed a spectacular decline in all the peaks except the peak with a chemical shift of -82.89 ppm, as shown in Figure 46.

Figure 46 ^{29}Si NMR spectrum of gel B (MP209)

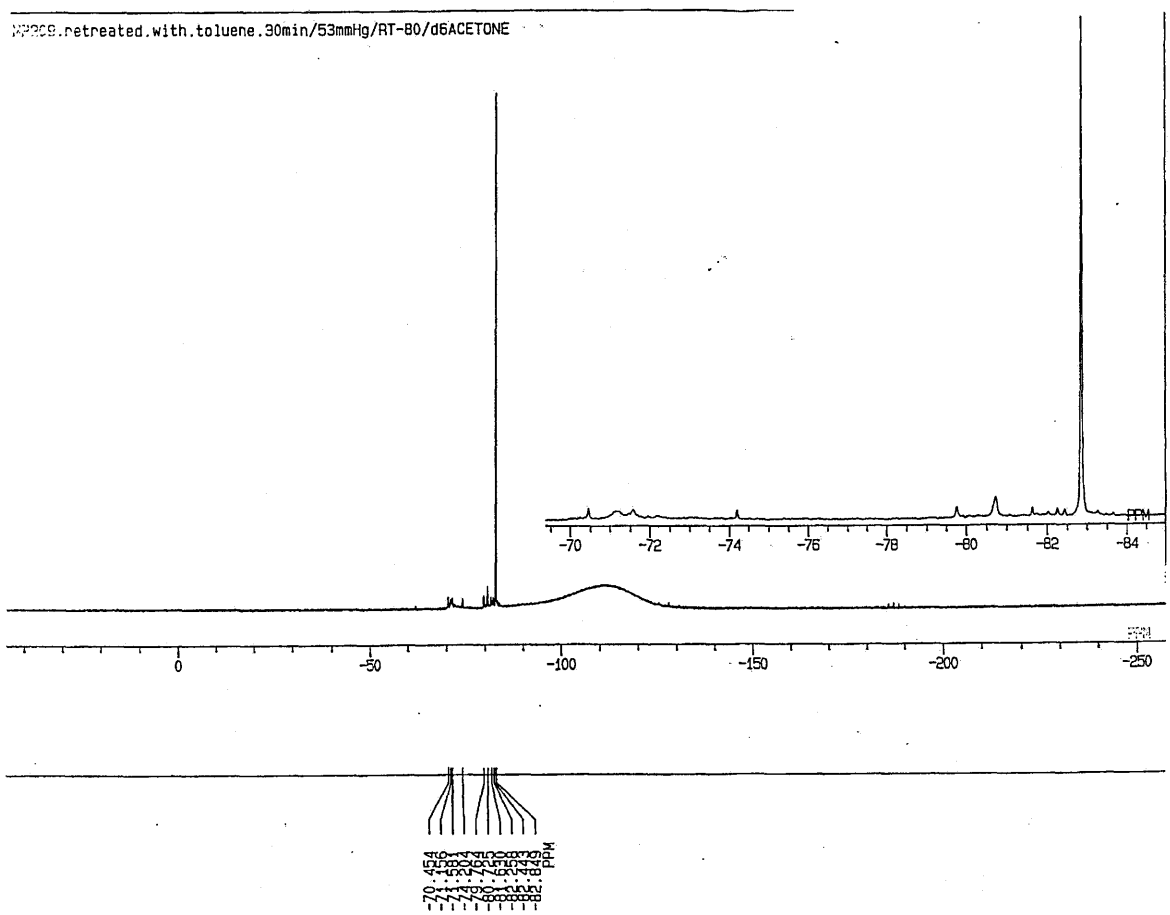

Additionally we compared the ^{19}F NMR spectrum of both gels (Figure 47). We were also able to obtain pure crystals from gel B whose NMR data confirmed the synthesis of the vinylT_8-TBAF cage.

Figure 47 ^{19}F NMR spectrum of gel A and B (MP209)

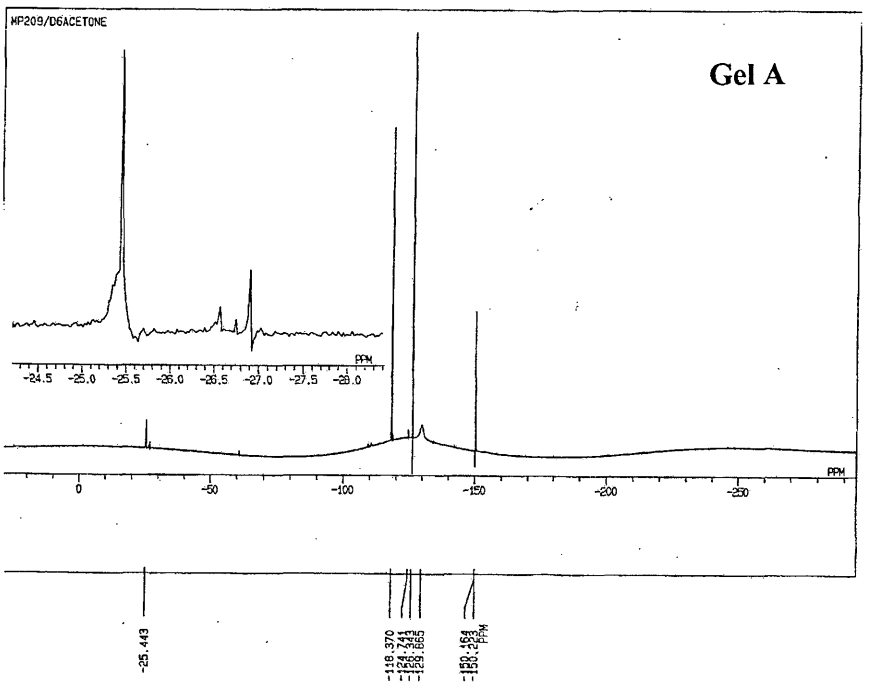

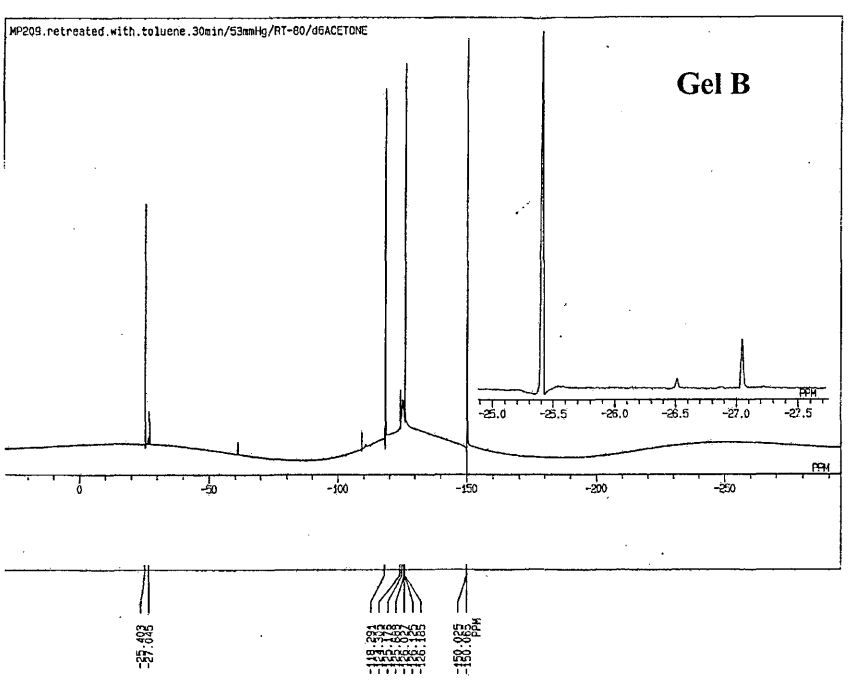

This result suggests that the peaks which were responsible for the complex pattern in the first step are mainly intermediates that lead to the encapsulated fluoride cages. We will now aim to identify the nature of these intermediates.

We first looked at which peaks (and associated compound) we would expect to see in this sort of reaction. Yuxing Yang, in her work[71] on octasilsesquioxane cage synthesis, demonstrated that the products of the reaction of vinyltriethoxysilane with tetra-*n*-butylammonium fluoride were vinylT_8, vinylT_{10} and vinyl T_{12} with yields of 1%, 46% and 53% respectively. As discussed previously and based on Marsmann's equations for calculating the T_{10} and T_{12} chemical shifts (-80.96 ppm for the vinylT_8, -82.24 for the vinylT_{10}, and -82.09 and -84.10 ppm for the vinylT_{12}), we proposed to assign the peaks as follows. We already know that the peak at -82.85 ppm corresponds to the vinylT_8-TBAF and we have obtained an X-ray crystal structure of this new compound. We do not observe a pair of peaks which can be assigned to the conventional vinylT_{12}. According to the work of Marina Maesano[81], the peak at -63.6 ppm arises from vinylT_6. The broad peak at -71 ppm with the peaks at -79.78 and -80.67 ppm in a ratio 3:1:3 can be linked with the uncondensed heptavinyl$T_7(OH)_3$ cage. We can also observe a peak at -82.26 ppm which can be assigned as the conventional vinylT_{10}. At this point, three peaks at -74.20, -81.63 and -82.44 ppm cannot be explained.

The ^{19}F NMR spectrum of both gels A and B (after retreatment) show two peaks at -25.4 and -27.0 ppm, as shown in Figure 47. We can see that the ratio between these two peaks changes from 4:1 in the ^{19}F NMR spectrum of gel A to a ratio of 11:2 in the ^{19}F NMR spectrum of gel B. The change in the ratio together with the fact that the solid state ^{19}F NMR spectrum showed only one single sharp peak at 23.0 ppm leads us to the conclusion that the peak at -25.4 ppm arises from the encapsulated fluoride ion inside the vinylT_8-TBAF. The second peak at -27.0 ppm suggests that another fluoride ion with a very similar

environment is present. This could be interpreted as an indication of the existence of an intermediate in the encapsulation reaction in which the fluoride ion could be already described as an isolated or "naked" fluoride ion. We will discuss of the nature of this encapsulated fluoride ion intermediate and its role in the synthesis later in this chapter.

At this point, we carried out four more experiments (MP236, MP277B, MP271 and MP293). MP271, MP277B and MP293 were carried out in toluene and stirred for 24 hours. The solvent was then removed on the rotary evaporator at 90°C at 100, 90 and 80 mbar respectively. MP236 was carried out in toluene and heated at 95°C for 1 hour, the solvent was then removed by distillation under vacuum. All these experiments gave very similar results based on the ^{19}F NMR and ^{29}Si NMR spectra, as shown in **Figure 48**. The ^{29}Si NMR spectra for all experiments show a major peak with a chemical shift of -82.9 which arises from the vinylT_8-TBAF cage as we concluded previously. Additionally, a series of minor peaks are present in all the spectra with chemical shifts of -84.4, -84.0, -82.5, -82.1, -81.7, -81.1, -79.6, -79.4 ppm. Based on Marsmann's equation and Yuxing Yang's work, the peaks at -82.1 and -84.4 ppm suggest the presence of the fluoride nonencapsulated vinylT_{12} cage, with the conventional vinylT_{10} cage with a peak at -82.5 ppm. The ^{19}F NMR spectra show three peaks with chemical shifts of -25.3, -26.4 and -27.1 ppm. The peak at -25.3 ppm arises from the vinylT_8-TBAF cage as we have seen previously. It is clear that the ratio between the peaks at -25.3 ppm and -27.1 ppm changes; in fact the decreasing of the peak at -27.1 ppm comes with the decreasing of the minor peaks in the ^{29}Si NMR spectra which may arise from some intermediates of the fluoride encapsulation reaction.

Figure 48 ^{29}Si NMR and ^{19}F NMR spectra of MP271, MP277B, MP293 and MP236

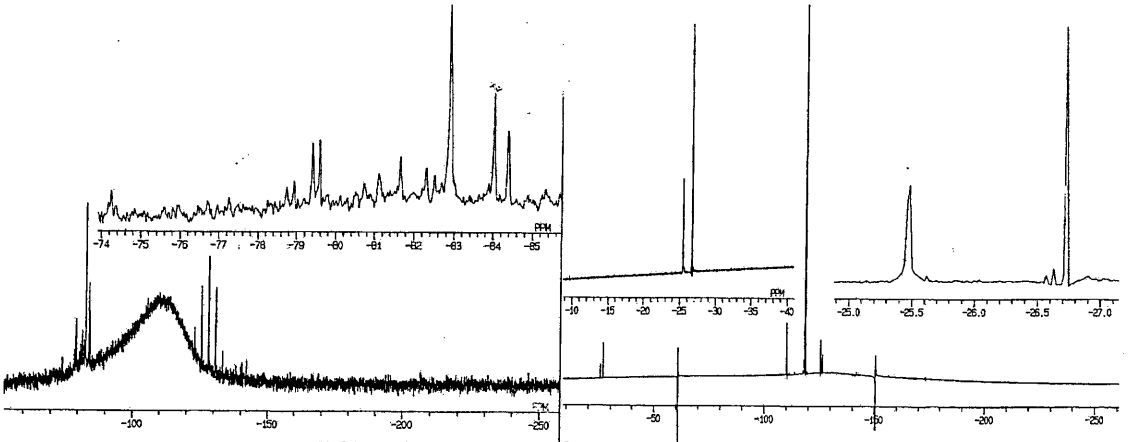

MP271 Removal of the solvent at 100

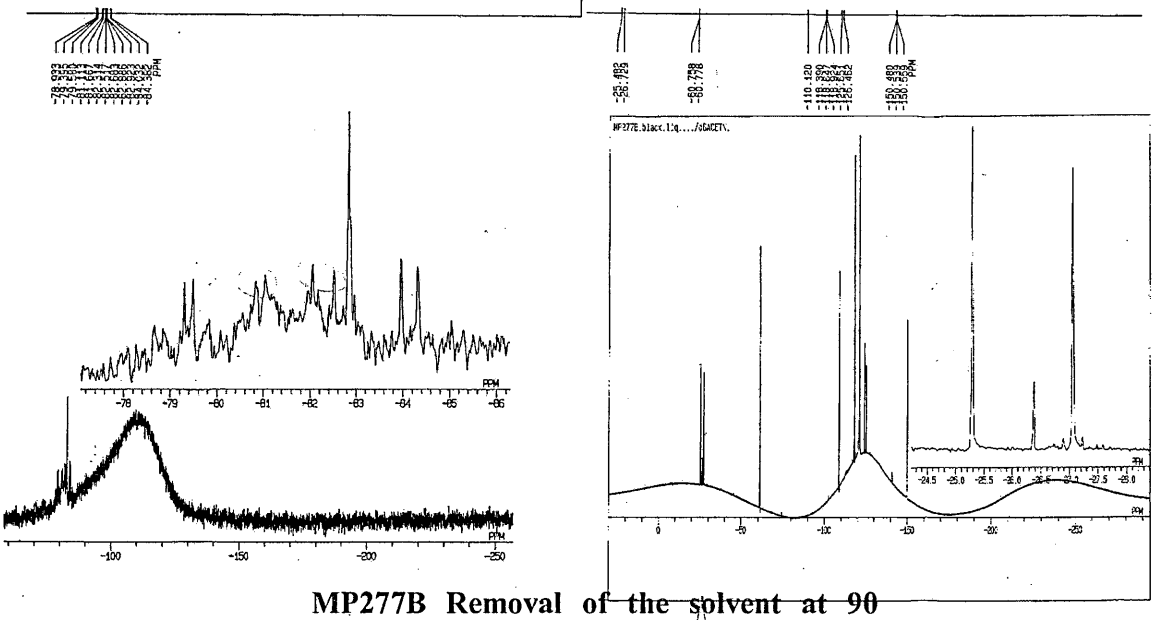

MP277B Removal of the solvent at 90

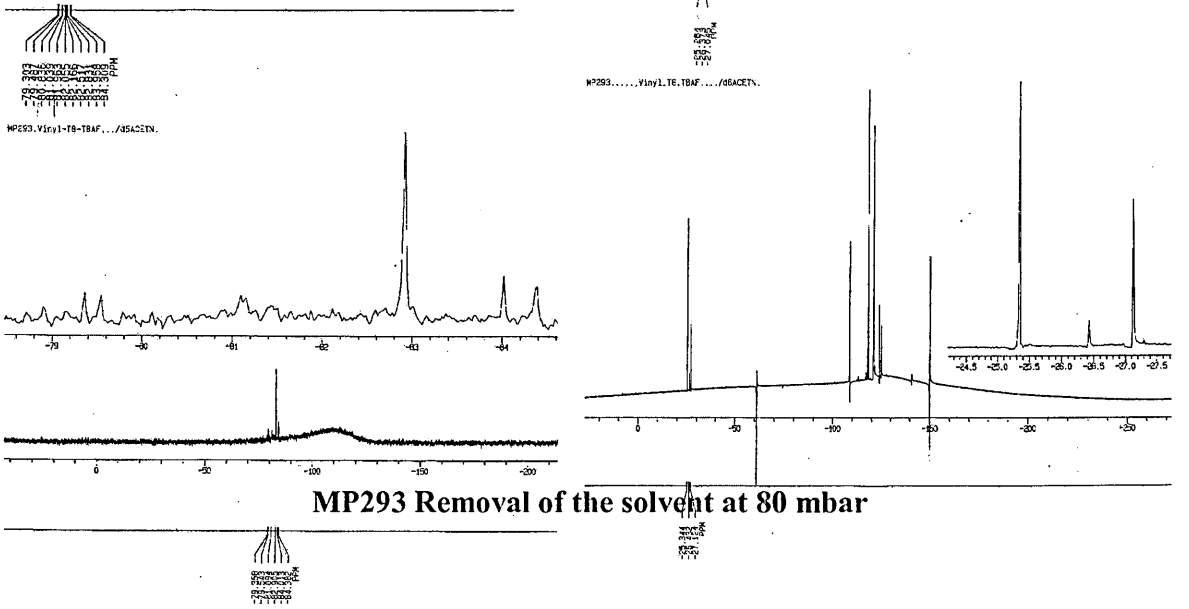

MP293 Removal of the solvent at 80 mbar

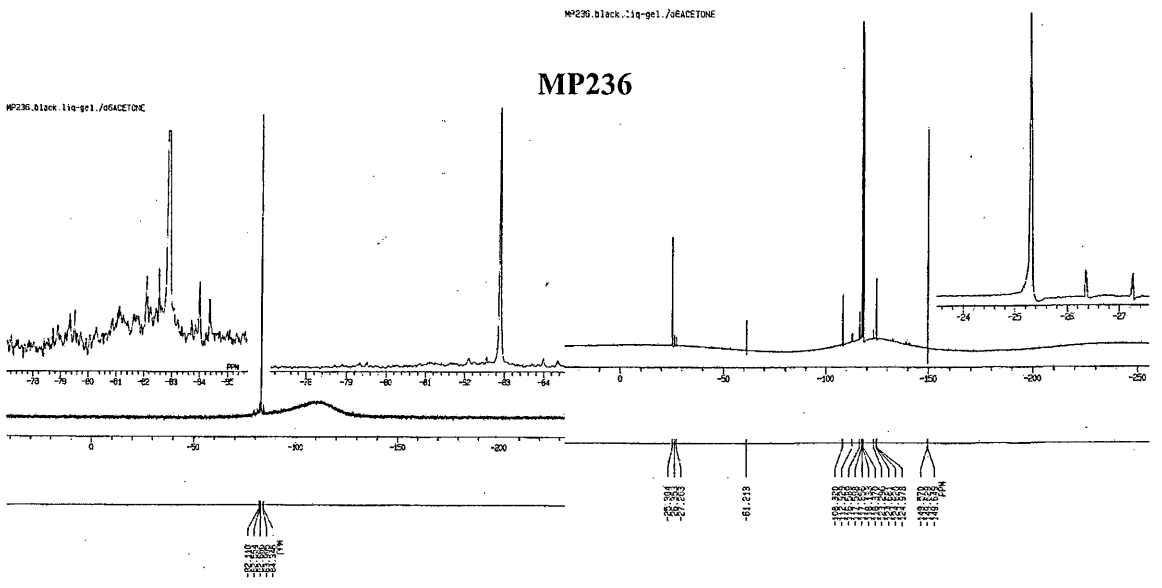

The ^{19}F NMR spectra seemed to provide information for understanding the nature of the intermediates in this encapsulated fluoride ion reaction. We thus carried out an experiment (MP333) in which we followed the reaction by ^{19}F NMR spectroscopy during the removal of the solvent.

The experiment was carried out in toluene and we repeated the procedures that led to the synthesis of a pure vinylT_8-TBAF cage (as seen in experiment MP205). We then performed six ^{19}F NMR spectroscopy measurements at different time for the same reaction: at time t = 0 and at time t = 24h after 10 minutes on the rotary evaporator at 70°C, and then after removal of 25%, 50% and 75% of the solvent, and finally after complete removal of the solvent. As shown in Figure 49, the ^{19}F NMR spectra of the crude mixture at t = 0 displays a very small peak at -26.8 ppm. This peak increases after 24 hours stirring at RT and ten minutes at 70°C. During the removal of the solvent, we notice the decrease of this peak at -26.8 ppm together with the increase of the peak at -25.1 ppm which arises from the

vinylT_8-TBAF cage. When 100% of the solvent has been removed, the ^{19}F NMR spectrum displays only the peak with a chemical shift at -25.1 ppm. This result reinforces the suggestion of the existence of an intermediate in the fluoride ion encapsulation mechanism in which the fluoride ion could be already encapsulated with weak interactions with its neighbouring atoms.

Figure 49 Removal of the solvent followed by ^{19}F NMR spectrum (MP333)

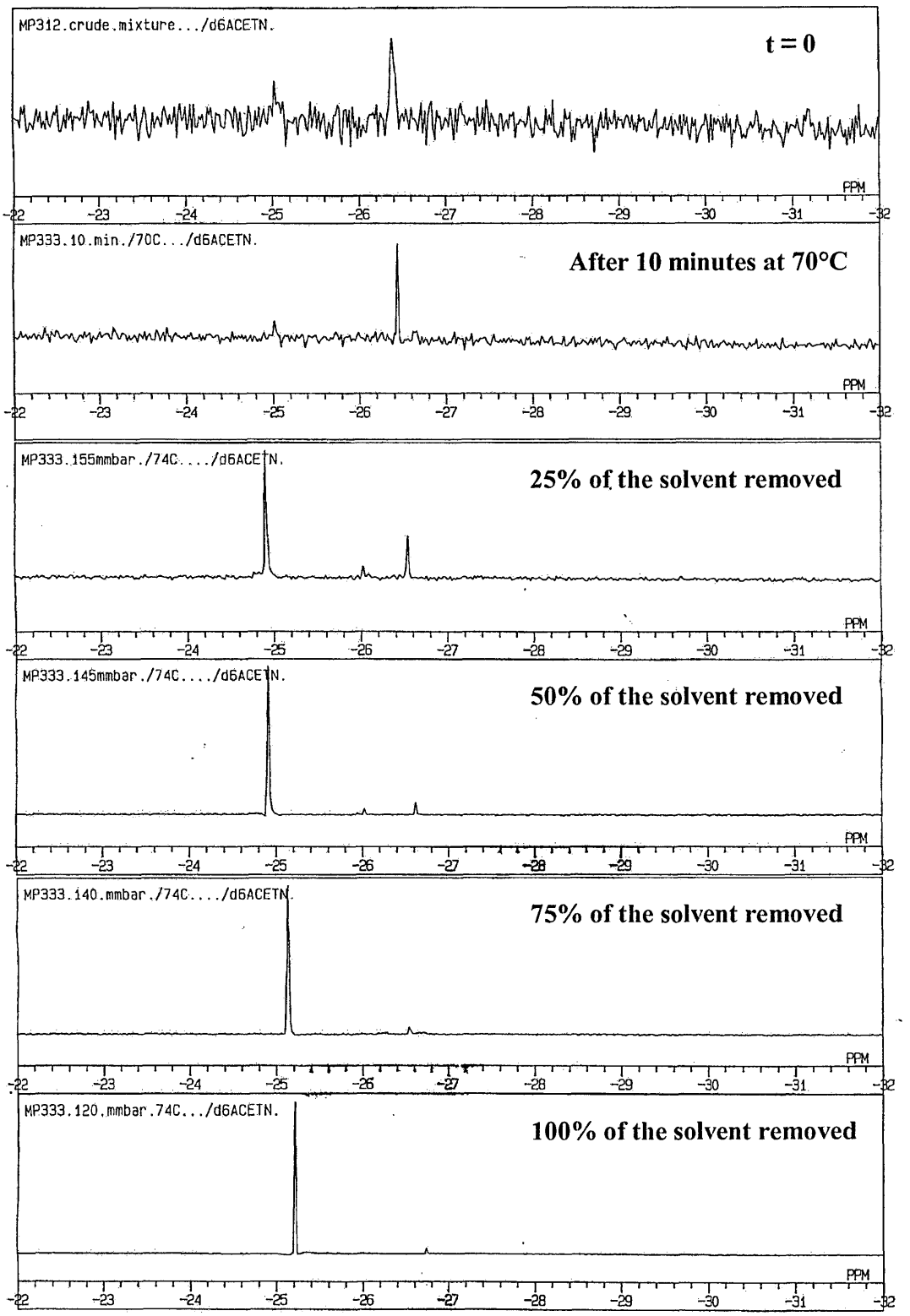

Additionally, the ^{29}Si NMR spectra (Figure 50) at when 25% and 75% of the solvent had been removed show a major peak at -82.7 which arises from the vinylT_8-TBAF cage and three other peaks at -70.7, -79.5 and -80.3 ppm in a ratio 3:1:3 which arise from the uncondensed heptavinyl$T_7(OH)_3$ cage. The proportion of the heptavinyl$T_7(OH)_3$ cage decreases with the ongoing removal of the solvent.

Figure 50 ^{29}Si NMR spectra of MP333

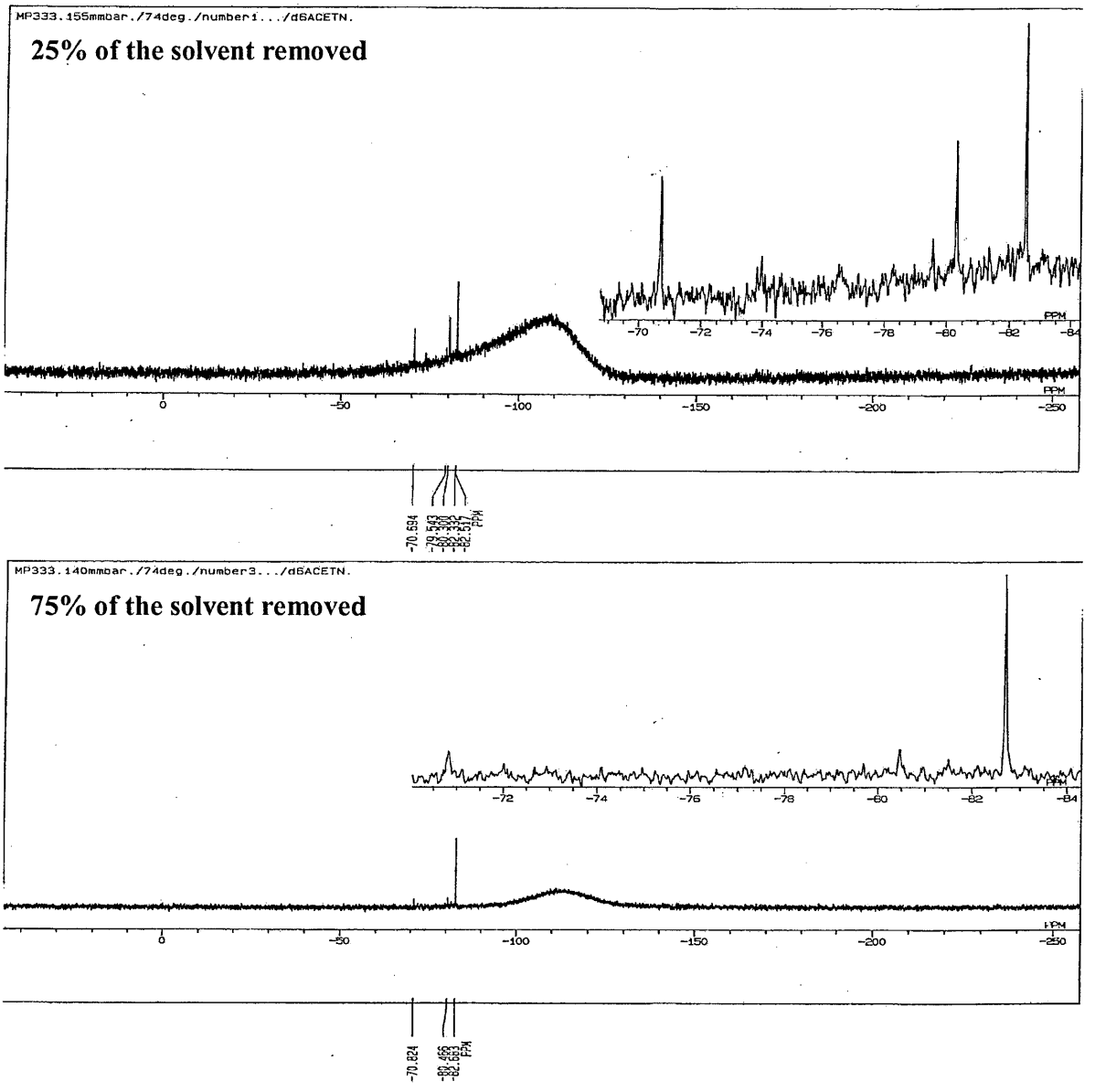

This result suggests the involvement of the heptavinyl$T_7(OH)_3$ cage as a possible intermediate in the fluoride ion entrapment reaction even though no further evidence has been found. We will later discuss in more detail the structure of the possible intermediates.

3.2.3 Conclusion

We have synthesized a second encapsulated fluoride ion octasilsesquioxane cage, the vinylT_8-TBAF cage, and thus demonstrated that the phenylT_8-TBAF cage was not an isolated result. In consequence, we can say that a new class of cage compound has been formed. We have also identified the presence of probable intermediates in this fluoride ion encapsulation reaction and provided some evidence that these intermediates already contain isolated fluoride ion.

3.3 Synthesis of tetra-*n*-butylammonium octa-*para*-tolyloctasilsesquioxane fluoride

3.3.1 Introduction

As we have shown previously, the encapsulation of a fluoride ion in an octaphenyloctasilsesquioxane cage was not a random event but represents a new class of octasilsesquioxane cage compound. Even though this result was encouraging and provided a glimpse of the possible intermediates, we still hope to obtain a better understanding of how this fluoride ion encapsulation occurs and gain more evidence about the nature of its intermediates. We, thus, decided to synthesize a fluoride octasilsesquioxane cage with a pendant group at the silicon atom which was very similar to a phenyl group, such as a *para*-tolyl group.

3.3.2 Experiments

The first experiment (MP252) was conducted using chloroform as the solvent. In this experiment we dissolved 1.06 g of *para*-tolyltripropoxysilane (3.57 mmol) in chloroform. Then we added 2.5 ml of tetra-*n*-butylammonium fluoride (1M solution in THF, 2.5mmol). After 24 hours, the reaction was stopped and the solvent removed on a rotary evaporator with a temperature gradient from 30°C to 50°C over 10 minutes and a vacuum of 500 mbar for 15 minutes. A yellow solid gel was obtained. The ^{29}Si NMR spectrum (in $CDCl_3$) displayed three single sharp peaks in the T-Si area. The main peak has a chemical shift of -

79.5 ppm and the two smaller peaks have chemical shifts of -78.1 and -81.0 ppm (Figure 51).

Figure 51 ^{29}Si NMR spectrum of MP252

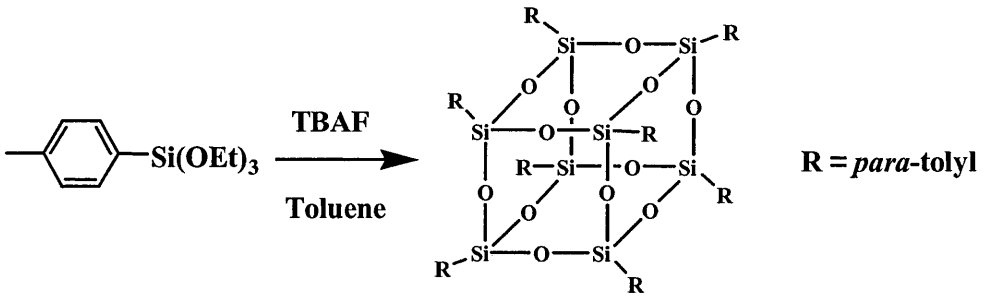

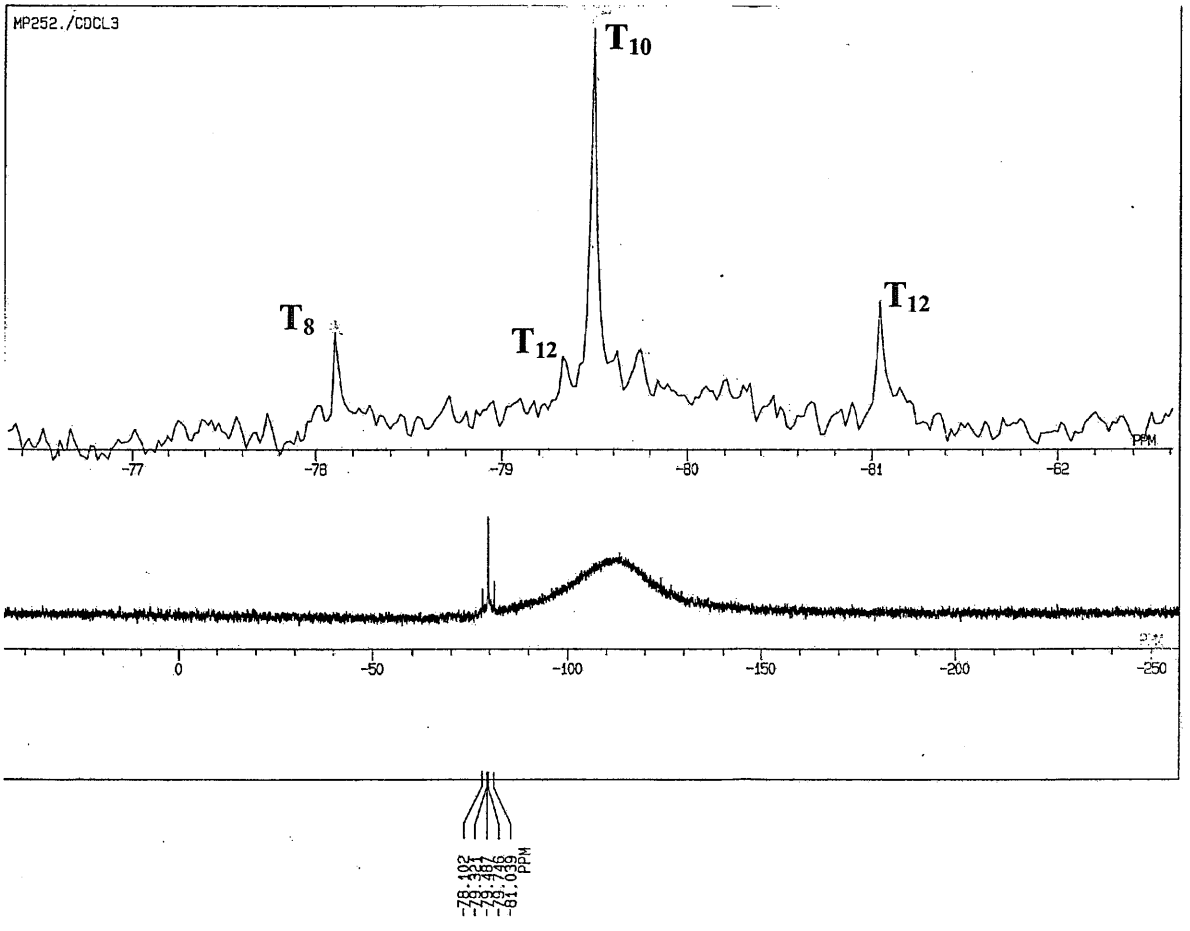

Based on what we had seen in the case of the Ph_8T_8-TBAF and $Vinyl_8T_8$-TBAF cages, we measured the ^{19}F NMR spectrum. The ^{19}F NMR spectrum did not show any peaks in the region previously designated for the encapsulated fluoride anion chemical shift. This

demonstrated that the fluoride anion was not incorporated in the cage during this reaction and that the conventional cage was synthesized. In fact, based on Marsmann's Equation, if the peak at -78.1 ppm arises from octa-*para*-tolyloctasilsesquioxane, then the peak at -79.6 ppm arises from deca-*para*-tolyldecasilsesquioxane and the peak at -79.5 and -81.1 ppm arise from dodeca-*para*-tolyldodecasilsesquioxane.

As we discussed previously for the phenyl and vinyl cages, the conditions used to remove the solvent are of crucial importance in order to ensure the fluoride anion encapsulation. Thus, as for the two previous cases, we looked at optimising these parameters to achieve the synthesis of the octa-*para*-tolyloctasilsesquioxane cage.

One experiment (MP265) was conducted in toluene which, from the previous results, looked to be the optimum solvent in which the fluoride anion encapsulation reaction occurs. In this experiment we dissolved 1.05 g of *para*-tolyltrimethoxysilane (4.95 mmol) in toluene, and we then added 2.5 ml of tetra-*n*-butylammonium fluoride 1M solution in THF (2.5mmol) so we had a 1: 1.9 ratio. After 24 hours, the reaction was stopped and the solvent (b.p. of toluene: 110.6°C) removed on a rotary evaporator with a temperature gradient from 25°C to 87°C over 10 minutes and a vacuum of 100 mbar for 15 minutes. A brown gel was obtained. The ^{29}Si NMR spectrum (in d_6 acetone) was a completly different and more complex than that observed for the first experiment, as shown in Figure 52. Indeed, we can observe 7 single peaks all occuring in the T-Si area. The main peak has a chemical shift of -80.4 ppm with all the other peaks being smaller, at -68.5, -71.6, -77.4, -78.1, -79.4 and -80.0 ppm.

Figure 52 ^{29}Si NMR spectrum of MP265

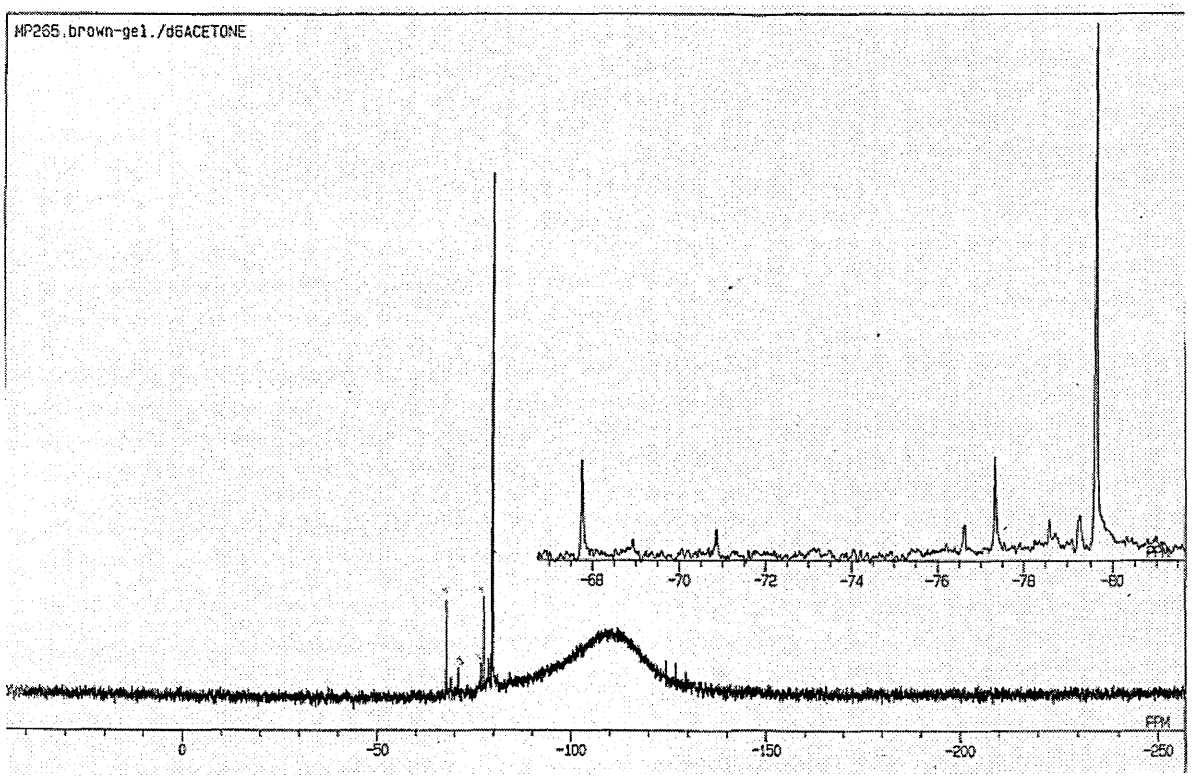

The ^{19}F NMR spectrum (in d_6 acetone) displayed a single sharp peak in the chemical shift region expected for a fluoride anion encapsulated in a octasilsesquioxane cage. This main peak was at -26.8 ppm (Figure 53), together with very small peaks with chemical shifts of -26.0, -26.5 and -27.8 ppm. The peak in the ^{19}F NMR spectrum together with the chemical shift of -80.4 ppm in the ^{29}Si NMR spectrum, is consistent with the main product being a tetra-*n*-butylammonium octa-*para*-tolyloctasilsesquioxane fluoride cage. The three very small peaks in the ^{19}F NMR spectrum will be discussed later.

Figure 53 ^{19}F NMR spectrum of MP265

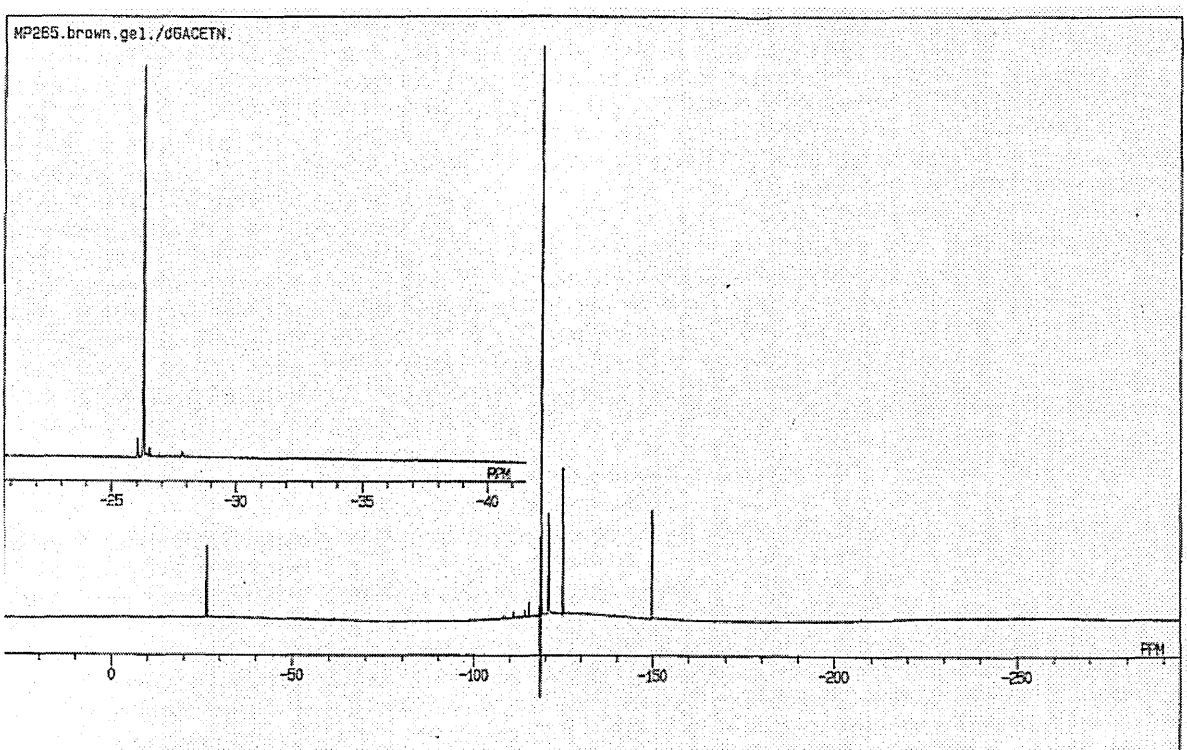

While we are confident we can associate the -80.4 ppm in the ^{29}Si NMR spectrum with the eight silicon atoms in the tetra-*n*-butylammonium octa-*para*-tolyloctasilsesquioxane fluoride cage, the other peaks are more difficult to assign. The -68.5, -77.4 and -78.1 ppm peaks are present in a ratio of 3:1:3, which is characteristic of a $T_7(OH)_3$ open cage, and thus is

probably associated with a hepta-*para*-tolyl-$T_7(OH)_3$ cage. The peak with a ^{29}Si NMR chemical shift of -79.4 ppm can be attributed to the conventional octa-*para*-tolyloctasilsesquioxane cage. The peak at -71.6 ppm is more difficult to assign as no reference compounds have been found to give peaks in this area. However, based on the work on hexasilsesquioxane cages of Marina Maesano[81] and extension of the Marsmann's equation for the T_6 cages, we propose that the -71.6 ppm peak arises from a hexa-*para*-tolyl-T_6 but whilst this is our most probable hypothesis, no other evidence has been found for this at the moment.

We have been able to obtain single crystals of this product (0.56g of colourless crystals which represent an isolated yield of 55%) and ^{1}H, ^{13}C, ^{19}F and ^{29}Si NMR spectroscopy gave more evidence consistent with the tetra-*n*-butylammonium octa-*para*-tolyloctasilsesquioxane fluoride cage. In fact, the ^{19}F and ^{29}Si NMR spectrum displayed a single sharp peak with a chemical shift at respectevely -26.8 and -80.4 ppm. As suggested earlier these values again suggest the successful synthesis of a *p*-tolyl-T_8-TBAF cage with an isolated fluoride anion with little interaction with its near neighbours.

Figure 54 ^{29}Si and ^{19}F NMR spectrum of a single crystal from MP265

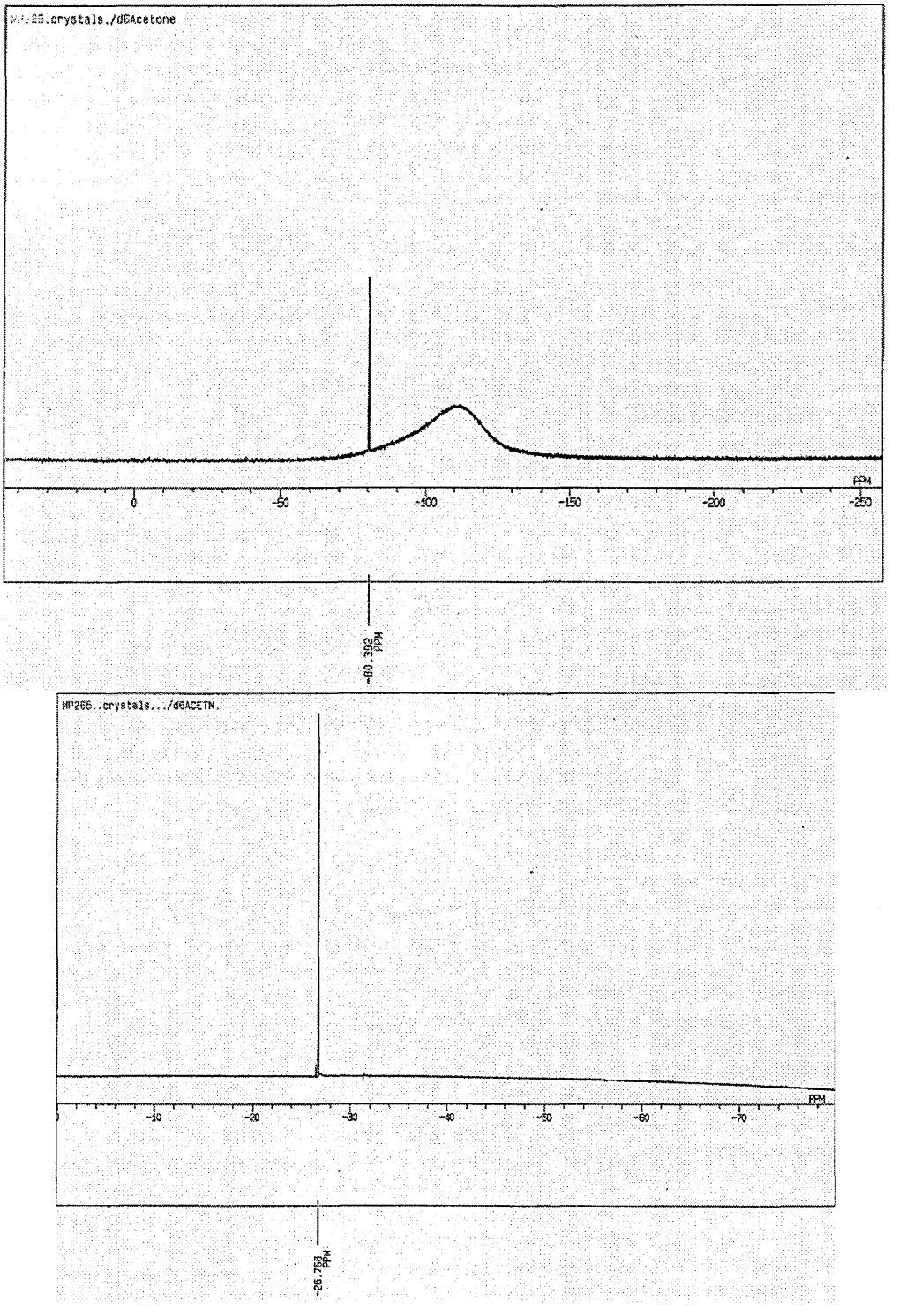

Furthermore, the ^{1}H NMR shows two doublets with chemical shifts of 7.60 (integration: 2H) and 7.20 ppm (integration: 2H) and a singlet with a chemical shift at 2.20 ppm (integration: 3H) which is consistent with the presence of a *para*-tolyl group. In addition, the spectrum displays a triplet at 0.90 ppm (integration: 1.5 H), a multiplet at 1.33 ppm (integration: 1 H), another multiplet at 1.71 ppm (1 H) and a triplet at 3.33 ppm (1 H). The peaks at 0.90, 1.33, 1.71 and 3.33 ppm are associated with the CH_3-CH_2-CH_2-CH_2-X system, which is part of the tetra-*n*-butylammonium fluoride that was used as the catalyst. If we measure the ratio of the integration of the hydrogen atoms for both systems (*para*-tolyl and tetrabutyl group), we obtain an integration of 7H for the *para*-tolyl group and 4.5H for the tetrabutyl group. This 7:4.5 ratio is exactly the ratio for a octa-*para*-tolyloctasilsesquioxane cage (56H) with one tetra-*n*-butylammonium group (36H) which again is consistent for the tetra-*n*-butylammonium octa-*para*-tolyloctasilsesquioxane fluoride cage. The ^{13}C NMR spectrum is also in complete agreement with this assumption: it exhibits peaks at δ 13.8 ppm (CH_3); δ 20.3 ppm (-CH_2-); δ 24.4 ppm (-CH_2-); δ 59.3 ppm (N-CH_2-) for the four carbon atoms of the tetra-*n*-butylammonium group and δ 128.7 ppm (*o*-CH), δ 135.0 ppm (*m*-CH), δ 135.2 ppm (*i*-C), δ 139.0 ppm (*p*-C) and δ 21.5 ppm (Ar-CH_3) for the carbon atoms of the *para*-tolyl group. The product was also analysed by MALDI-TOF mass spectroscopy. The theoretical (top) and observed (bottom) data are shown in Figure 55 and confirms that the tetra-*n*-butylammonium octa-*para*-tolyloctasilsesquioxane fluoride cage was obtained with a fragment at *m/z* 1164.4 (100%) corresponding to the *p*-tolyl-T8 cage with the encapsulated fluoride anion ($C_{56}H_{56}FO_{12}Si_8^-$) [$M^-$] (calculated: 1164.2) and a fragment at *m/z* 242.3 (100%) corresponding to the tetra-*n*-butylammonium cation ($C_{16}H_{36}N^+$) [M^+] (calculated: 242.3).

Figure 55 Theorical and observed MS data for the *para*-tolyl-T_8-TBAF cage

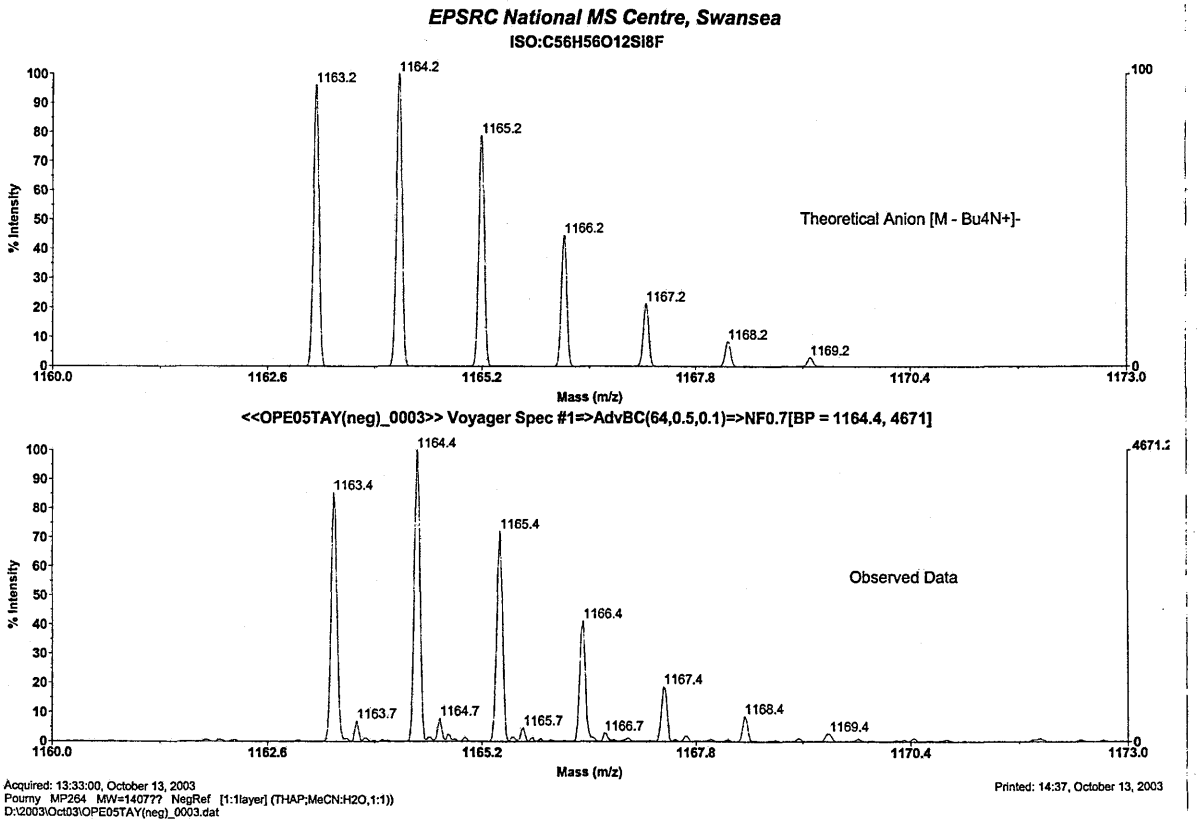

The elemental analysis of the sample ($C_{72}H_{92}FNO_{12}Si_8$) with a theoretical molecular weight of 1407.2 g.mol^{-1} also confirmed the high purity of this sample: calculated %C = 61.45, %H = 6.59, %N = 1.00, %F = 1.35; found: % C = 61.75, %H = 6.83, %N = 0.86.

The proposed structure of a tetra-*n*-butylammonium octa-*para*-tolyloctasilsesquioxane fluoride T_8 cage was confirmed by single-crystal X-ray crystallography as shown in Figure 56, in agreement with all the data previously presented. In this new structure the fluoride ion is perfectly centered inside the silsesquioxane cage.

Figure 56 Structure of tetra-*n*-butylammonium octa-*para*-tolyloctasilsesquioxane fluoride

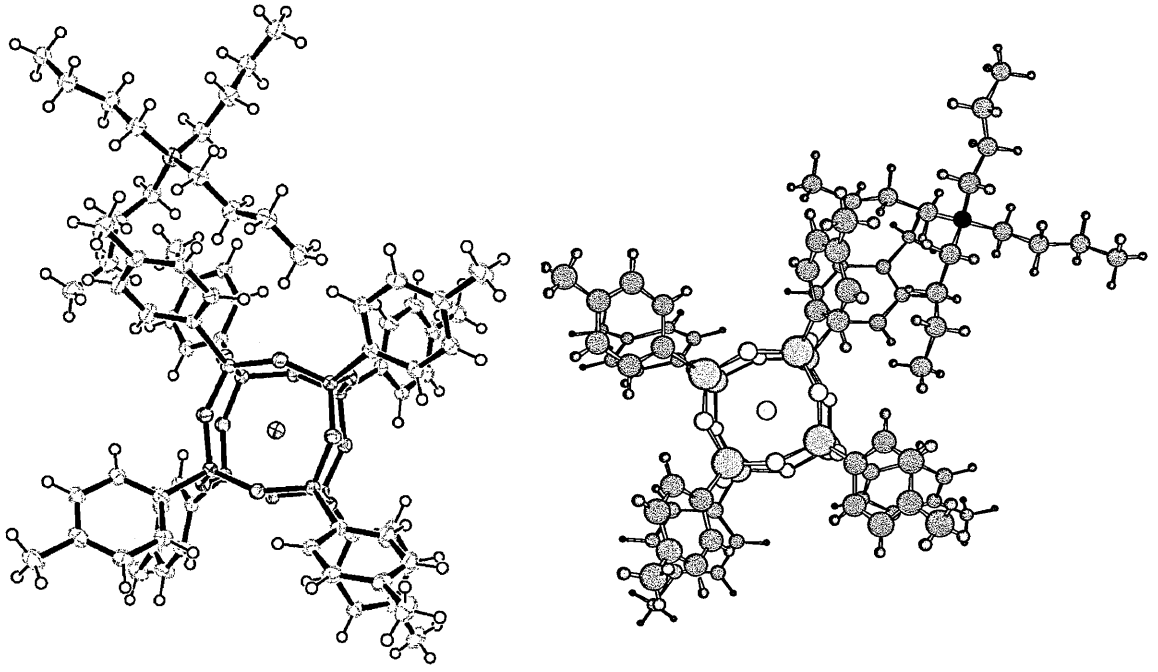

The crystallographic data revealed that the tetra-*n*-butylammonium octa-*para*-tolyloctasilsesquioxane fluoride T_8 cage had crystallised with a tetragonal crystal system with *I*-4 space group. The silicon fluoride distance is 2.66 Å which is similar to that in the Ph_8T_8-TBAF (2.65 Å) and vinyl-T8-TBAF (2.65 Å) cages. This confirms that the interaction of each fluoride ion with its surrounding silicon atoms can be described as electrostatic at best. These weak fluoride silicon interactions were again confirmed by the presence in the ^{29}Si NMR spectra of a sharp singlet, as previously observed in the Ph_8T_8-TBAF and vinyl-T_8-TBAF cage. A comparison of the crystal structure data of the octa-*para*-tolyloctasilsesquioxane fluoride T_8 cage with its nonencapsulated analogue is not possible as no crystal structure of the conventional T_8 cage has been reported in literature at this date.

The arrangement of the tetra-*n*-butylammonium cation, with respect to the cage, is complex with the shortest distance between the nitrogen and the fluoride atom being 8.95 Å, representing a major increase with respect to the nitrogen-fluoride distance in the Ph_8T_8-TBAF cage (6.46 Å) and vinyl-T_8-TBAF cage (6.68 Å). The tetra-*n*-butylammonium groups sit slightly skewed over one face of the cage above a cleft formed by the *para*-tolyl groups in a manner reminiscent of that seen in the crystal structure of the Ph_8T_8-TBAF cage. However, this arrangement causes a more complex packing than that observed in the Ph_8T_8-TBAF cage where the tetra-*n*-butyl arms fitted perfectly on one face of the cage in a cleft formed by the phenyl group.

The encapsulation of the fluoride ion in the octa-*para*-tolyloctasilsesquioxane fluoride T8 cage confirms our earlier results and claims for the discovery of a completely new class of cage compound whereby a fluoride anion becomes encapsulated within the cage. We suggested, in the previous discussion of the vinyl-T_8-TBAF cage, the possible existence of some intermediates wherein a fluoride anion would be already encapsulated with weak interactions with its neighboaring atoms. In fact, some of the results suggested the involvement of the heptavinyl-$T_7(OH)_3$ cage as a possible intermediate in the fluoride entrapment reaction. To add weight to this assumption, the ^{29}Si NMR spectrum of the experiment MP265 showed a main peak for the product, the *p*-tolyl-T_8-TBAF cage, but also peaks associated with a hepta-*para*-tolyl-$T_7(OH)_3$ cage. So one question is: could the uncondensed T_7 cage be considered as a possible intermediate ? The catalyst ratio to the starting material, was 1.98:1, so we repeated the experiment with a ratio over 2:1 (MP266) and using exactly the same condition to see if this would vary the T_7:T_8 ratio.

In this experiment we dissolved 1.43 g of *para*-tolyltrimethoxysilane (6.73 mmol) in toluene. Then we added 2.5 ml of tetra-*n*-butylammonium fluoride 1M solution in THF (2.5mmol) so we had a 1: 2.7 ratio of siloxane to TBAF. After 24 hours, the reaction was stopped and the solvent removed on a rotary evaporator with a temperature gradient from 25°C to 87°C over 10 minutes and a vacuum of 100 mbar for 15 minutes. A brown gel was obtained. The ^{29}Si NMR spectrum (in d_6 acetone) displayed a single sharp peak with a chemical shift at -80.4 ppm which arises from the octa-*para*-tolyloctasilsesquioxane fluoride T8 cage. The ^{19}F NMR spectrum (in d_6 acetone) also confirmed this result with a single sharp peak with a chemical shift at -26.3 ppm. It shows that the reaction had gone to completion and the absence of hepta-*para*-tolyl-$T_7(OH)_3$ cage emphasizes this result. We concluded that, for the *para*-tolyl-trialkoxysilane reaction, a bigger catalyst ratio was needed to have the reaction to go to completion. Furthermore, we decided to undertake more studies on the nature of the possible intermediates by using lower ratios of siloxane to TBAF to try to stop the reaction before completion.

We conducted two other experiments (MP239) and (MP267). In the first experiment (MP239), we dissolved 1.22 g of *para*-tolyltripropoxysilane (4.11 mmol) in toluene. Then we added 2.5 ml of tetra-*n*-butylammonium fluoride (1M solution in THF, 2.5mmol) so we had a 1:1.6 ratio of siloxane to TBAF. After 24 hours, the reaction was stopped and the solvent removed on a rotary evaporator with a temperature gradient from 25°C to 87°C over 10 minutes and a vacuum of 100 mbar for 15 minutes. A brown gel was obtained. The ^{29}Si NMR spectrum (in d_6 acetone) displayed three single peaks all in the T-Si area with chemical shifts at -68.5, -77.4 and -78.1 ppm with a ratio of 3:1:3 as shown in Figure 57. This pattern and chemical shifts are characteristic of a hepta-*para*-tolyl-$T_7(OH)_3$ cage. Nervertheless, a very small peak can be seen with a chemical shift of -80.4 ppm.

Figure 57 ^{29}Si NMR spectrum of MP239

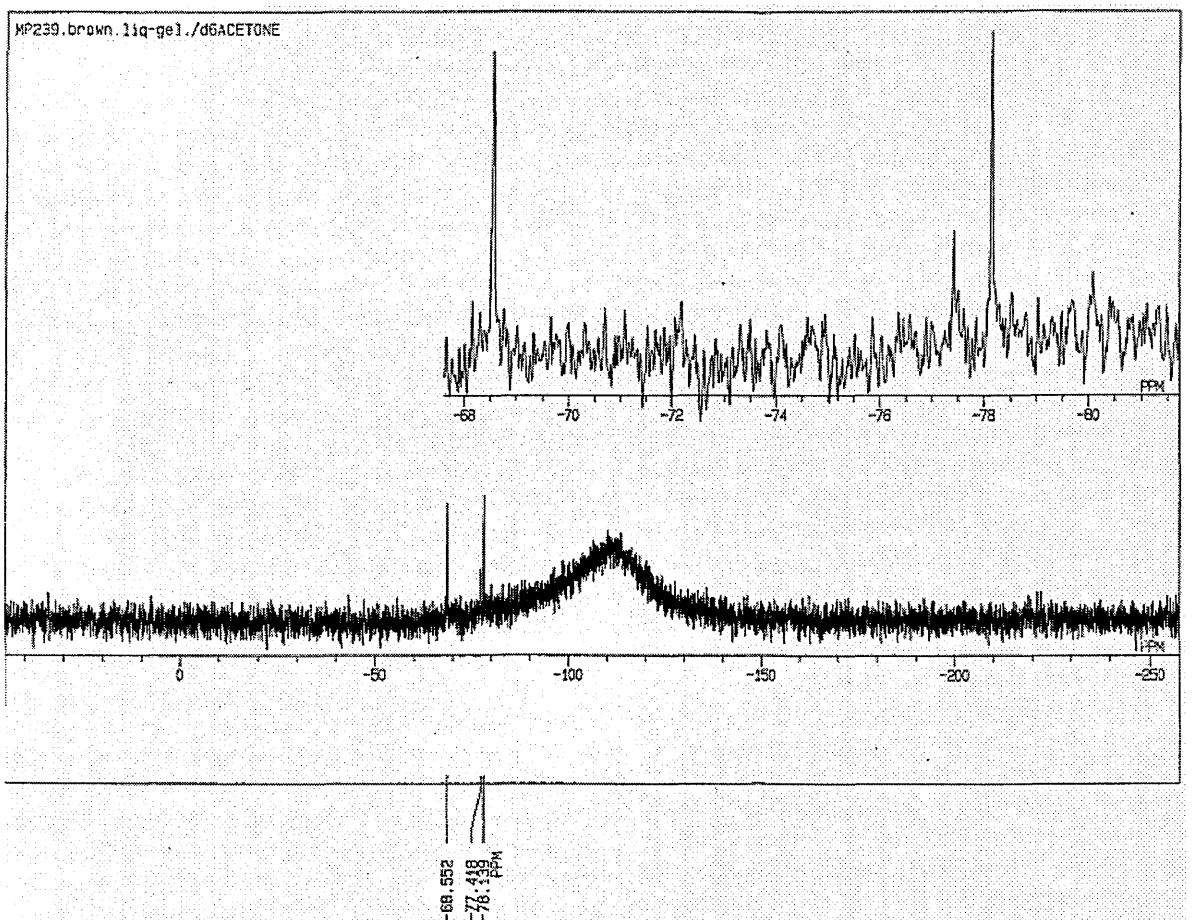

The ^{19}F NMR spectrum (in d_6 acetone) displayed two very small sharp peaks with chemical shifts at -26.4 and -27.7 ppm with a approximate ratio of 1:2 (Figure 58). We can associate the peak at -26.4 ppm with the small amount of octa-*para*-tolyloctasilsesquioxane fluoride T_8 cage. The designation of the -27.7 ppm peak is far more complicated as we have never observed it before and it has not been reported in the literature. Nevertheless, the predominance of the hepta-*para*-tolyl-$T_7(OH)_3$ cage in this sample suggests the existence of an isolated fluoride anion which is partially encapsulated in the hepta-*para*-tolyl-$T_7(OH)_3$ cage, as shown in Figure 58.

Figure 58 ^{19}F NMR spectrum of MP239

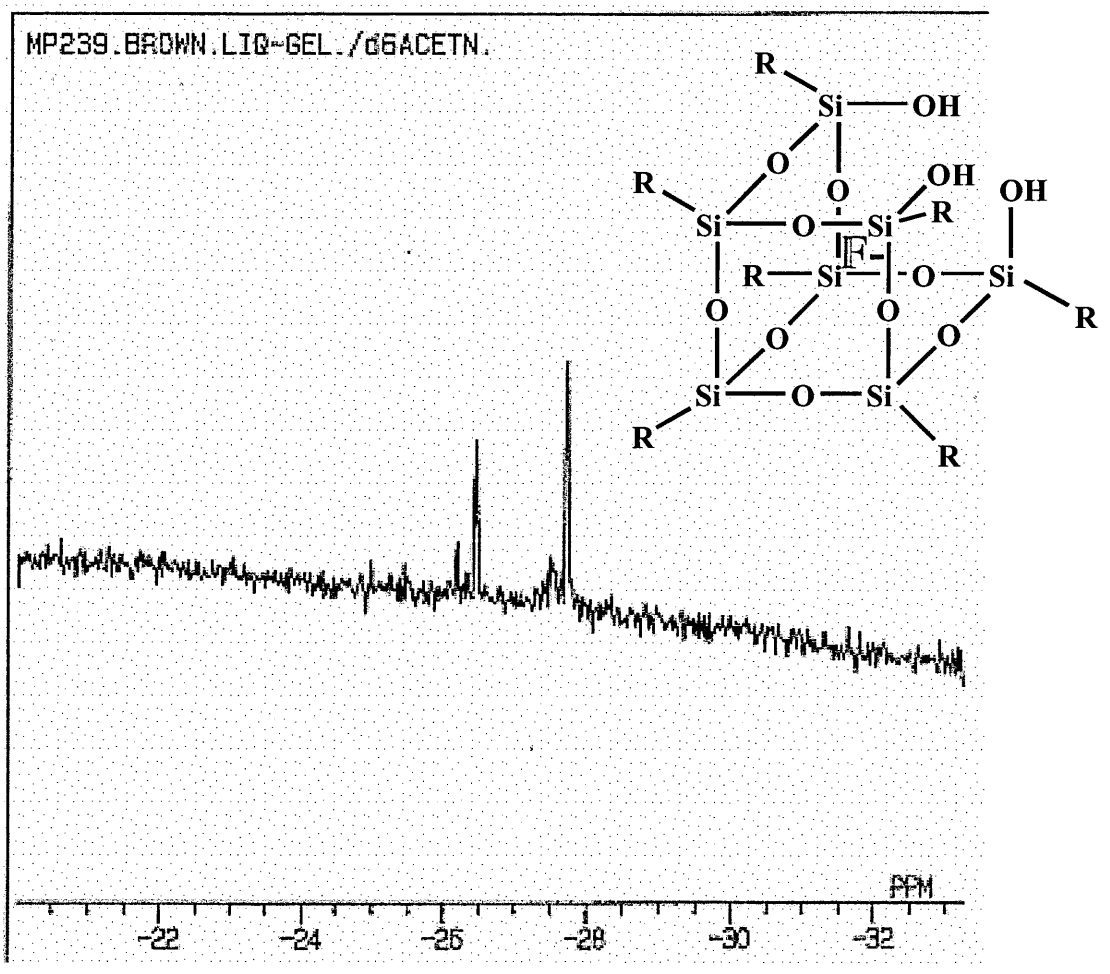

A second experiment was conducted (MP267) using the same conditions with a ratio of siloxane to TBAF of 1:1.9. We dissolved 1.41 g of *para*-tolyltripropoxysilane (4.76 mmol) in toluene, we then added 2.5 ml of tetra-*n*-butylammonium fluoride (1M solution in THF, 2.5mmol). After 24 hours, the reaction was stopped and the solvent removed on a rotary evaporator with a temperature gradient from 25°C to 87°C over 10 minutes and a vacuum of 100 mbar for 15 minutes. A brown gel was obtained. The ^{29}Si NMR spectrum (in d_6 acetone) displayed a major sharp peak with a chemical shift of -80.4 ppm and three single peaks with chemical shifts of -68.5, -77.4 and -78.1 ppm with a ratio of 3:1:3 as observed previously (Figure 59).

Figure 59 ^{29}Si NMR spectrum of MP267

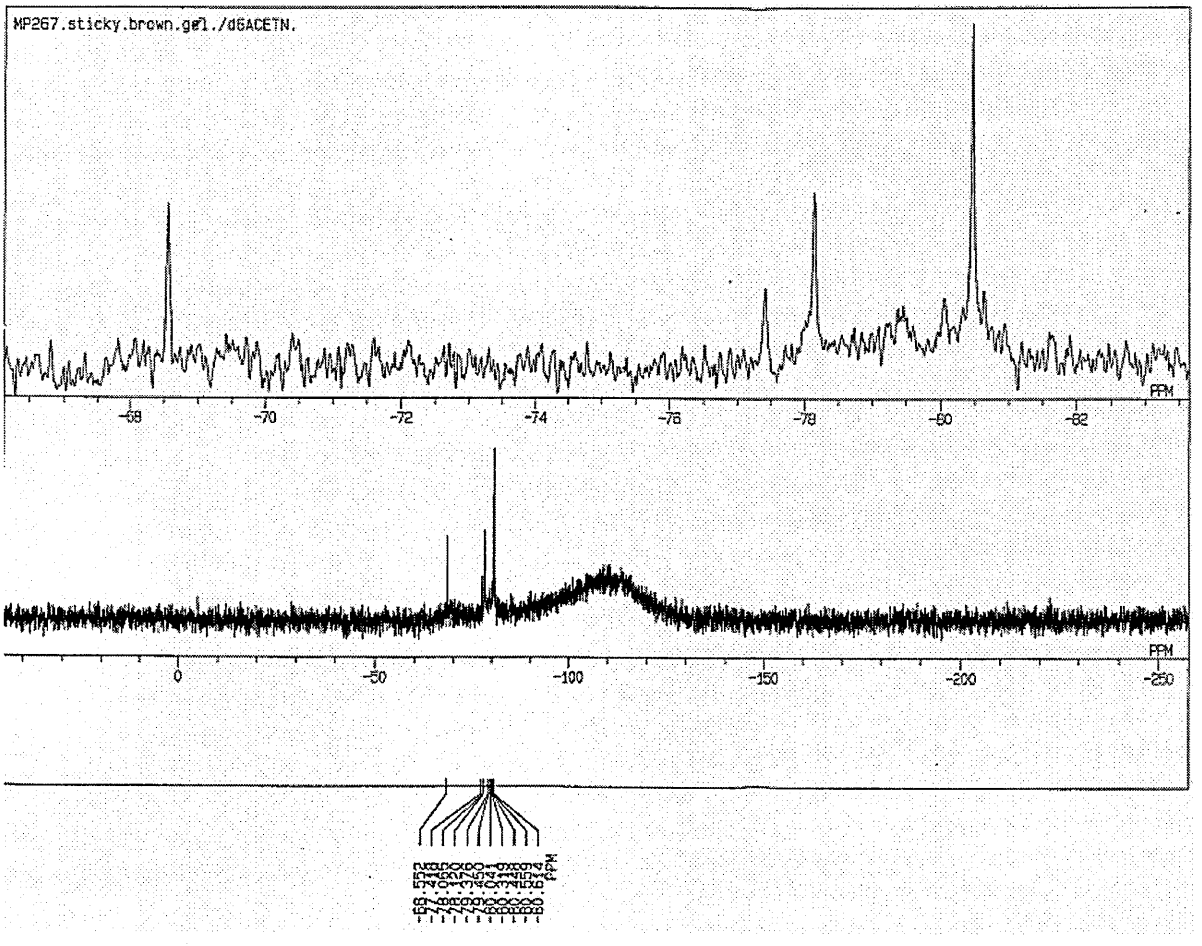

This pattern and chemical shifts are again associated with a hepta-*para*-tolyl-$T_7(OH)_3$ cage. The ^{19}F NMR spectrum (in d_6 acetone) displayed two very small sharp peaks with chemical shifts at -26.0 and -26.3 ppm with an approximate ratio of 1:3 (Figure 60). We can associate the peak at -26.3 ppm with the small amount of octa-*para*-tolyloctasilsesquioxane fluoride T_8 cage. The designation of the -26.0 ppm peak is again more complicated. Nevertheless, the persistent presence of the hepta-*para*-tolyl-$T_7(OH)_3$ cage in this sample reinforces our proposal of the existence of an isolated fluoride anion which would be partially encapsulated in the hepta-*para*-tolyl-$T_7(OH)_3$ cage.

Figure 60 ^{19}F NMR spectrum of MP267

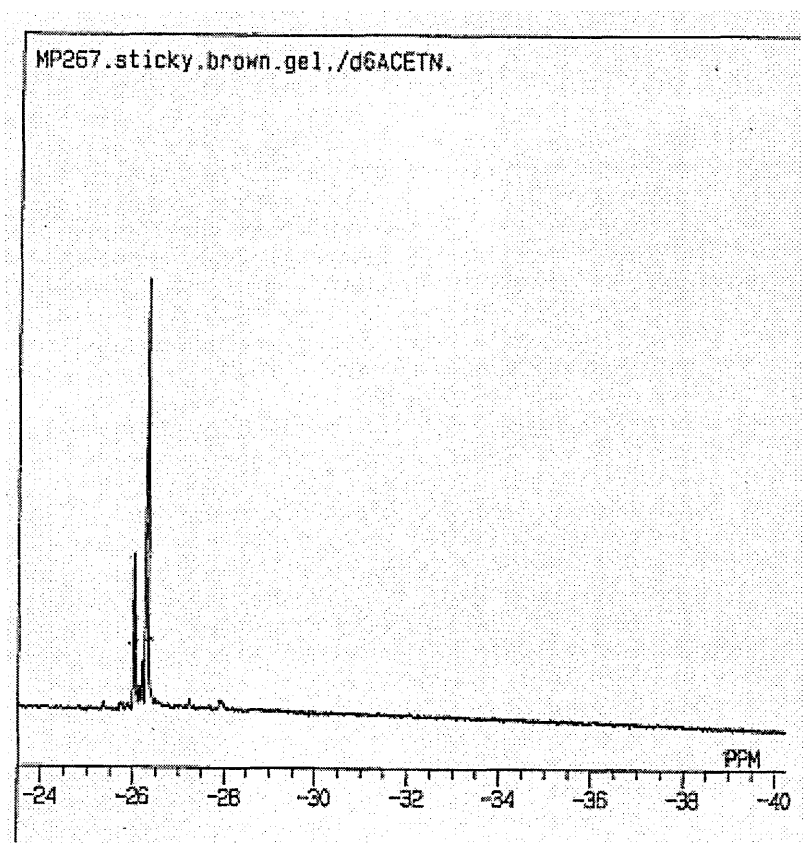

We were able to obtain single crystals from this experiment. Unfortunately, the ^{19}F, ^{1}H, ^{13}C and ^{29}Si NMR spectroscopy data and the single-crystal X-ray crystallography only confirmed the synthesis of the octa-*para*-tolyloctasilsesquioxane fluoride T8 cage. These

results are interesting because whilst they do not tell us the exact nature of the intermediates but they give glimpses of its structure. Nevertheless, our evidence points to the presence of the hepta-*para*-tolyl-$T_7(OH)_3$ cage when the reaction did not go to completion because of the deficiency of the trialkoxysilane. In this case we also observed, in the ^{19}F NMR spectrum, another single peak in the area of an isolated fluoride anion with a chemical shift very close to that of the encapsulated fluoride anion. This suggests the presence of a "naked" fluoride ion with again very little interactions with its surrounding environment. As we did not obtain more evidence for this assumption, we first propose the most probable nature for us of this intermediate for which some indications have been seen in the case of the vinyl-T8-TBAF and *para*-tolyl-T8-TBAF cage: a hepta-*para*-tolyl-$T_7(OH)_3$ cage with a fluoride sitting on the edge of the open face near the centre of the future octasilsesquioxane cage. The three hydroxy groups can have an important role in closing up the fluoride anion within the structure by interacting between each other with hydrogen bonds. In this case though, we should have observed F-H coupling which we did not see in the NMR spectra. Thus, we concluded that the fluoride ion must be encapsulated and already sitting in the middle of the open cage, the hepta-*para*-tolyl-$T_7(OH)_3$ cage, as shown in Figure 61.

Figure 61 Proposal for a possible intermediate

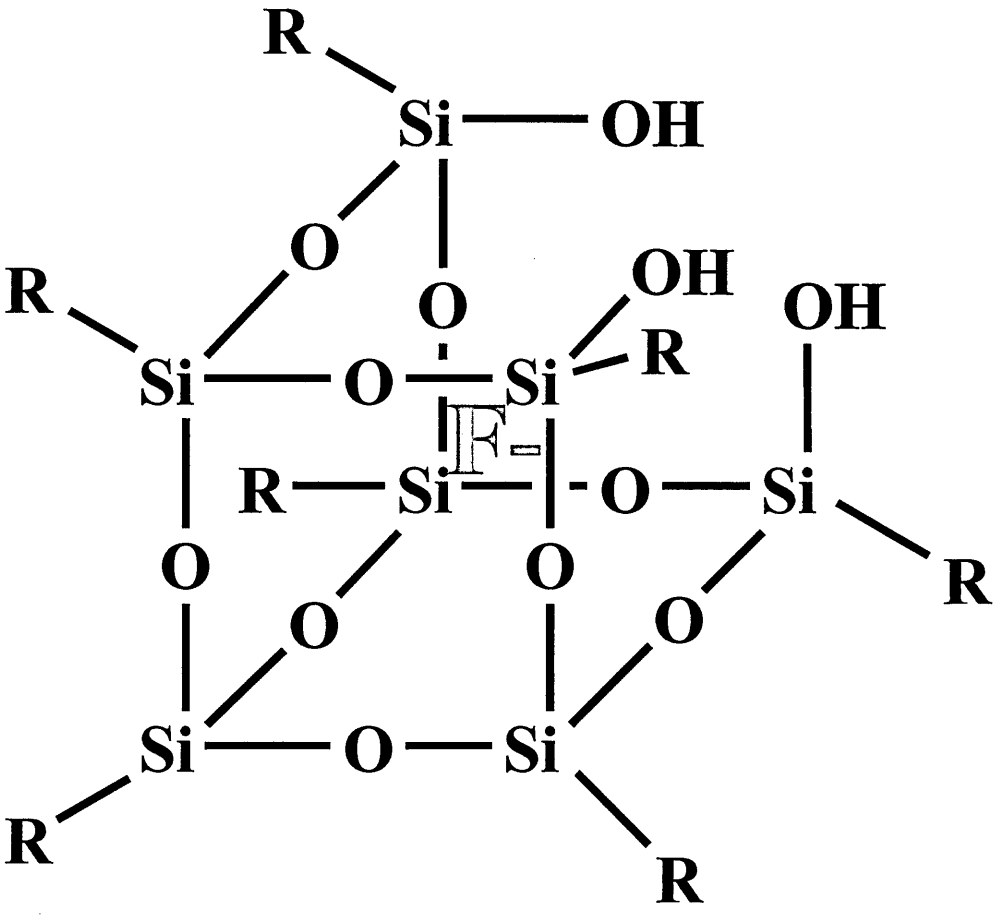

3.3.3 Conclusion

We have been able to synthesize another example of encapsulated fluoride anion within a octa-*para*-tolyloctasilsesquioxane fluoride T8 cage using the same TBAF and scarce water-catalyzed route. The ^{19}F and ^{29}Si NMR spectroscopy data and the X-ray crystal structure confirm the isolated environment of this fluoride anion perfectly centered within the cage. The nature of the R group at the silicon atoms in the new compound is still C_{sp}^2 and we believe that the hybridisation is highly important to the fluoride ion's stability at the centre of the cage and could be one of the drivers to the encapsulation, under the right conditions, together with the template and catalytic role of the fluoride anion. This matter will be the subject of other inquiries discussed later in this thesis.

We also observed the presence of what we suggest to be an intermediate in the synthesis of our encapsulated fluoride ion cages where we obtained on indications of its nature and have proposed a possible structure.

3.4 Synthesis of tetra-*n*-butylammonium octa-*para*-chloromethylphenyloctasilsesquioxane fluoride

3.4.1 Introduction

By using the TBAF synthetic route and refining the parameters of the reaction by careful control of temperature, pressure and TBAF concentration, we have synthesized a new class of compound whereby a fluoride ion becomes encapsulated within the octasilsesquioxane cage. We have been able to synthesize three different compounds, as examples of this new class of compounds but only one has arms that can be functionalised further, the tetra-*n*-butylammonium octavinyloctasilsesquioxane fluoride cage. Thus, we wanted to synthesize another compound with functionalised arms that would enable us to elaborate the cage further. The *para*-chloromethylphenyl group looked interesting as it is not too different from the *para*-tolyl and phenyl groups which have both worked previously. This may provide another example of an encapsulated fluoride ion within a functionalised cage which will give a platform for future development.

3.4.2 Experiments

The first experiment (MP201) was conducted in acetone as the solvent. In this experiment we dissolved 1.03 g of *para*-chloromethylphenyltrimethoxysilane (4.17 mmol) in acetone. Then we added 2.5 ml of tetra-*n*-butylammonium fluoride 1M solution in THF (2.5mmol) so we had a 1:1.7 ratio of siloxane to TBAF. After 24 hours, the reaction was stopped and

the solvent removed on a rotary evaporator at a temperature of 40°C and a vacuum of 80 mbar over 15 minutes. A pink-red gel was obtained.

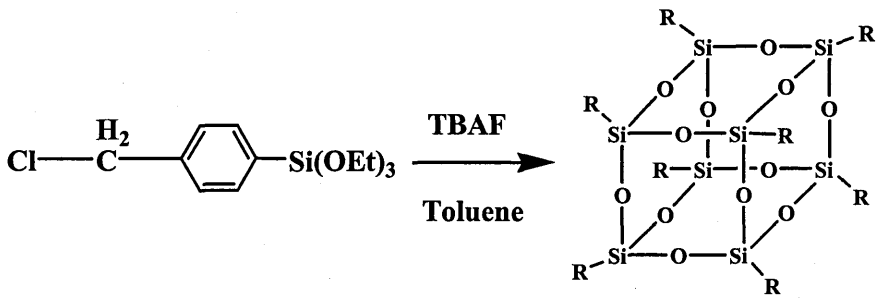

R = *para*-chloromethylphenyl

The ^{29}Si NMR spectrum (in d_6 acetone) displayed two single sharp peaks in the T-Si area. The main peak had a chemical shift of -80.8 ppm and the smaller peak had a chemical shift of -78.7 (Figure 62).

Figure 62 ^{29}Si NMR spectrum of MP201

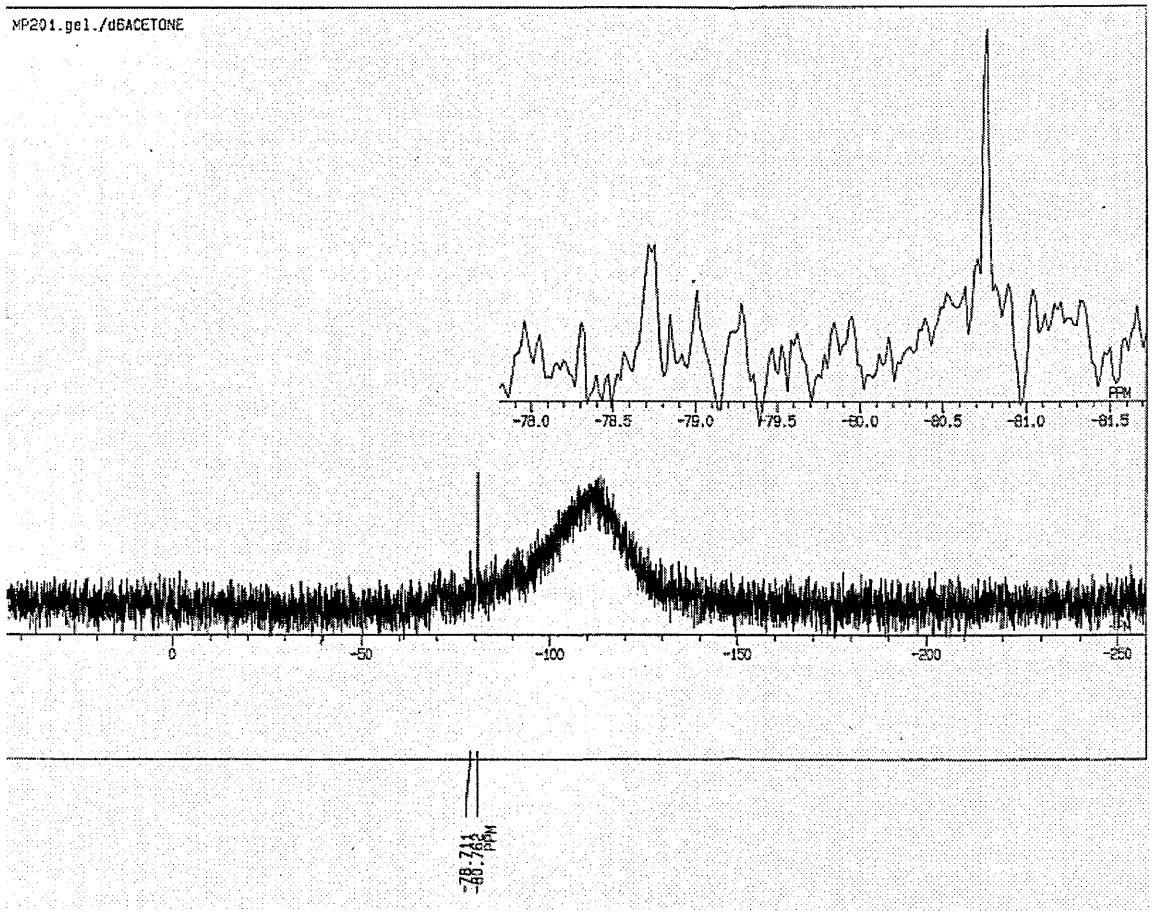

The ^{19}F NMR spectrum displayed one single sharp peak with a chemical shift at -26.5 ppm. This is again in the area previously seen for the incapsulated fluoride anion chemical shift. This demonstrates that a fluoride ion had been incorporated in the cage during this reaction and that we can confirm we had synthesized a tetra-*n*-butylammonium octa-*para*-chloromethylphenyloctasilsesquioxane fluoride cage. Based on our previous studies, we can confirm that the peak with a ^{29}Si NMR chemical shift at -78.7 ppm arises from the octa-*para*- chloromethylphenyloctasilsesquioxane conventional cage and the peak with a ^{29}Si NMR chemical shift at -80.8 ppm arises from the tetra-*n*-butylammonium octa-*para*-

chloromethylphenyloctasilsesquioxane fluoride cage. However, these remain as suggestions as we did not obtain any further evidences in this experiment.

The fact that only a small quantity of octa-*para*-chloromethylphenyloctasilsesquioxane cage was found suggests that the optimum conditions were not met during the reaction workup. As we have demonstrated in the previous phenyl, vinyl and *para*-tolyl cage discussions, the conditions which we used to remove the solvent were of great importance to cause the reaction to lead to fluoride anion encapsulation. Thus, as we did in the previous cases, we looked for the optimum conditions to synthesize the tetra-*n*-butylammonium octa-*para*-chloromethylphenyloctasilsesquioxane fluoride cage.

A second experiment (MP227) was conducted in toluene, which the previous results suggested was the optimum solvent in which the fluoride anion encapsulation reaction would occur. In this experiment we dissolved 1.30 g of *para*-chloromethylphenyltrimethoxysilane (5.28 mmol) in toluene. Then we added 2.5 ml of tetra-*n*-butylammonium fluoride (1M solution in THF, 2.5mmol) so that we had a 1: 2.1 ratio of siloxane to TBAF. After 24 hours, the reaction was stopped and the solvent removed on a rotary evaporator with a temperature of 80°C and a vacuum of 70 mbar for 20 minutes. A yellow gel was obtained. The ^{29}Si NMR spectrum (in d_6 acetone) displayed a single peak with a chemical shift of -80.8 ppm. The ^{19}F NMR spectrum (in d_6 acetone) gave a single sharp peak at -26.3 ppm in the chemical shift area expected for a fluoride anion encapsulated in a octasilsesquioxane cage. This peak in the ^{19}F NMR spectrum associated with a peak with a chemical shift at -80.4 ppm in the ^{29}Si NMR spectrum confirms our previous suggestion that the main product is a tetra-*n*-butylammonium octa-*para*-chloromethylphenyloctasilsesquioxane fluoride cage.

Using this reaction (MP227) we obtained some crystals (0.48g of colourless crystals which represent an isolated yield of 35%). The ^{29}Si NMR spectrum showed a peak with a chemical shift at -80.4 ppm (Figure 63) and the ^{19}F NMR spectrum displayed a single sharp peak with a chemical shift at -26.5 ppm (Figure 64). Both results again provide evidence for the tetra-*n*-butylammonium octa-*para*-chloromethylphenyloctasilsesquioxane fluoride cage with an isolated fluoride anion with little interaction with its nearest neighbours.

Figure 63 ^{29}Si NMR spectrum of MP227

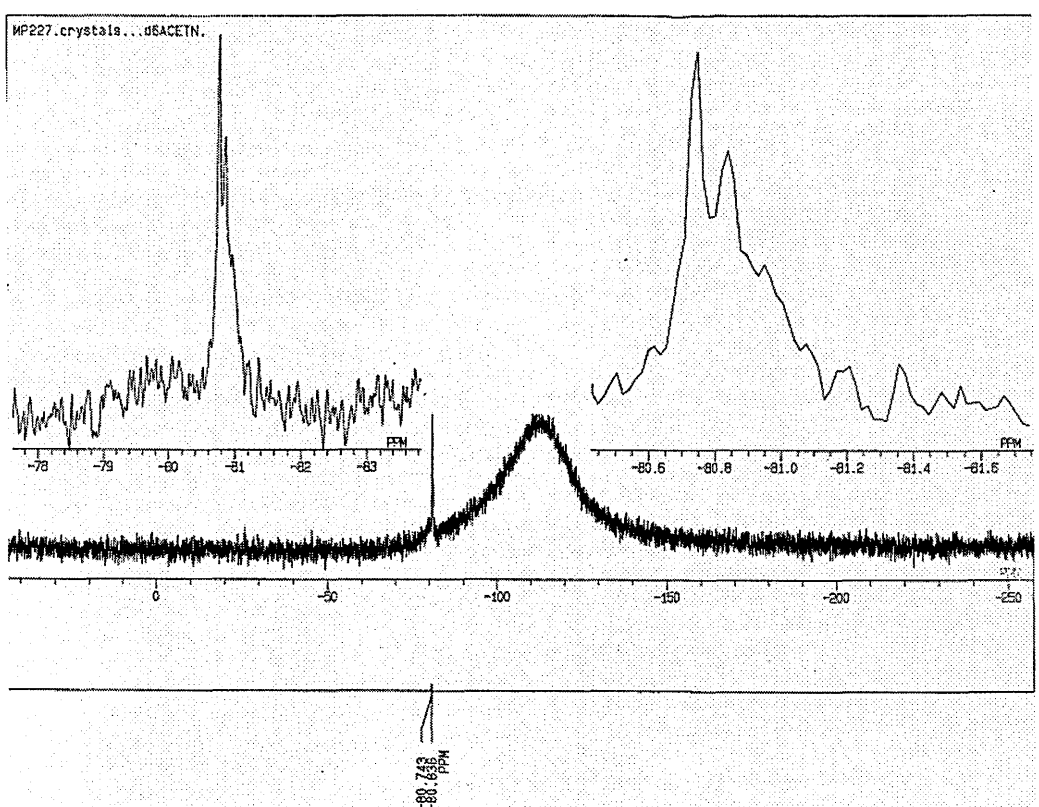

Figure 64 ^{19}F NMR spectrum of MP227

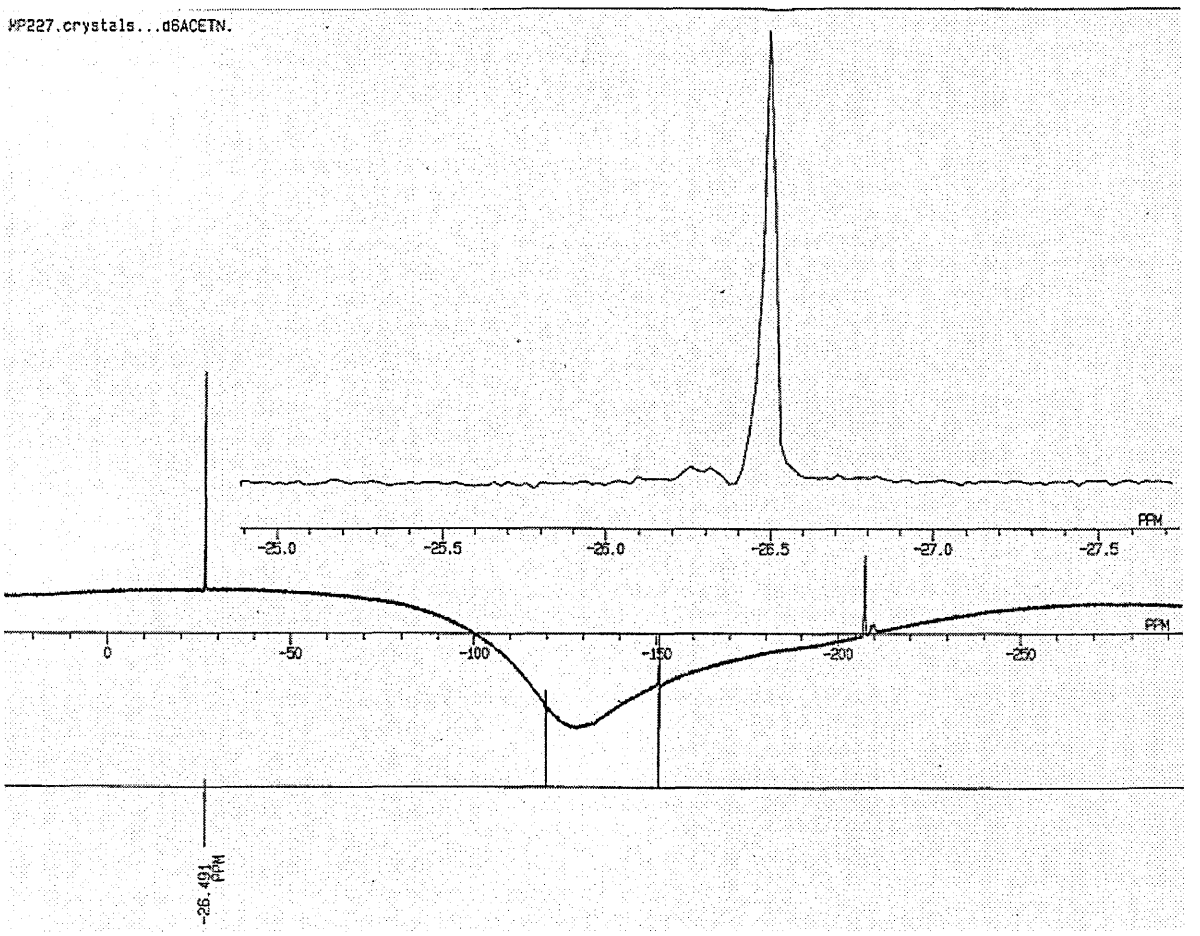

However, as shown in Figure 63, we noticed that the peak with a chemical shift of -80.4 ppm thought arise from the tetra-*n*-butylammonium octa-*para*-chloromethylphenyloctasilsesquioxane fluoride cage is not as sharp as expected. We expected a single sharp peak in the ^{29}Si NMR spectrum because all the silicon atoms of the cage have the same organic subsituents and environments. The peak in the ^{19}F NMR with a chemical shift at -26.5 ppm leaves no other alternative to a "naked" fluoride ion with weak interactions with its near neighbours which can only be encapsulated in the octa-*para*-chloromethylphenyloctasilsesquioxane cage. Thus, the ^{29}Si NMR spectrum is telling us that the environments of these silicon atoms are not so different because they are so close. We

suggest that the similar environment which leads to the multiple peaks may be explained by the conversion of some of the chlorine atoms in the CH_2Cl group to some hydroxyl groups during the workup of the reaction. In fact, even using controlled conditions during the reaction, water molecules are still present in the air when we remove the solvent on the rotary evaporator. Unfortunately we have been unable to obtain an X-ray single crystal structure from this sample to confirm this suggestion.

Furthermore, the ^1H NMR shows two doublets with a chemical shift at 7.82 (integration: 2H) and 7.75 ppm (integration: 2H) and a singlet with a chemical shift at 4.63 ppm (integration: 2H) which indicate the presence of a *para*-chloromethylphenyl group. In addition, the spectrum displays a triplet at 0.93 ppm (integration: 1.5 H), a multiplet at 1.36 ppm (integration: 1 H), another multiplet at 1.68 ppm (1 H) and a triplet at 3.38 ppm (1 H). The peaks at 0.93, 1.36, 1.68 and 3.38 ppm are associated with the CH_3-CH_2-CH_2-CH_2-X system, which is part of the tetra-*n*-butylammonium fluoride that was used as the catalyst. If we compare the sum of the integration of the hydrogen atoms for both systems (*para*-chloromethylphenyl and tetrabutyl group), we obtain an integration of 6H for the *para*-chloromethylphenyl group and 4.5H for the tetrabutyl group. This 7:4.5 ratio is precisely the ratio for a octa-*para*-chloromethylphenyloctasilsesquioxane cage (48H) with one tetra-*n*-butylammonium group (36H) which again is evidence of the tetra-*n*-butylammonium octa-*para*-chloromethylphenyloctasilsesquioxane fluoride cage. The ^{13}C NMR spectrum is in complete agreement with this assumption: it exhibits peaks at δ 13.9 ppm (CH_3); δ 20.3 ppm (-CH_2-); δ 24.4 ppm (-CH_2-); δ 59.1 ppm (N-CH_2-) for the four carbon atoms of the tetra-*n*-butylammonium group and δ 126.0 ppm (*o*-CH), δ 128.9 ppm (*m*-CH), δ 129.6 ppm (*i*-C), δ 139.2 ppm (*p*-C) and δ 46.9 ppm (Cl-CH_2-) for the carbon atom of the *para*-chloromethylphenyl group. There is an additional peak at 54.5 ppm in the ^{13}C NMR

spectrum that is evidence for the conversion of some of the chlorine atoms in the CH_2Cl group to some hydroxyl groups during the workup of the reaction.

We did a third experiment (MP314) which was conducted in toluene with the aim of trying to define more precisely the structure of this new compound. In this experiment we dissolved 1.57 g of *para*-chloromethylphenyltrimethoxysilane (6.36 mmol) in toluene. Then we added 2.5 ml of tetra-*n*-butylammonium fluoride (1M solution in THF, 2.5mmol) so we had a 1: 2.5 ratio of siloxane to TBAF. After 24 hours, the reaction was stopped and the solvent removed on a rotary evaporator at a temperature of 76°C and a vacuum of 170 mbar for 20 minutes. A yellow gel was obtained. The ^{29}Si NMR spectrum (in d_6 acetone) displayed a peak with a chemical shift of -80.8 ppm. As we observed in the previous experiment, the peak is not sharp but is more like a multiplet with a small coupling costant (Figure 65). This again implies the presence of silicon atoms with slightly different environments and we again suggest the possibility of the conversion of some chlorine atom of the CH_2Cl group to hydroxide groups from the water molecule during the workup of the reaction. The ^{19}F NMR spectrum (in d_6 acetone) displayed a single sharp peak at -26.2 ppm in the chemical shift area expected for a fluoride anion encapsulated in a octasilsesquioxane cage.

Figure 65 ^{29}Si NMR spectrum of MP314

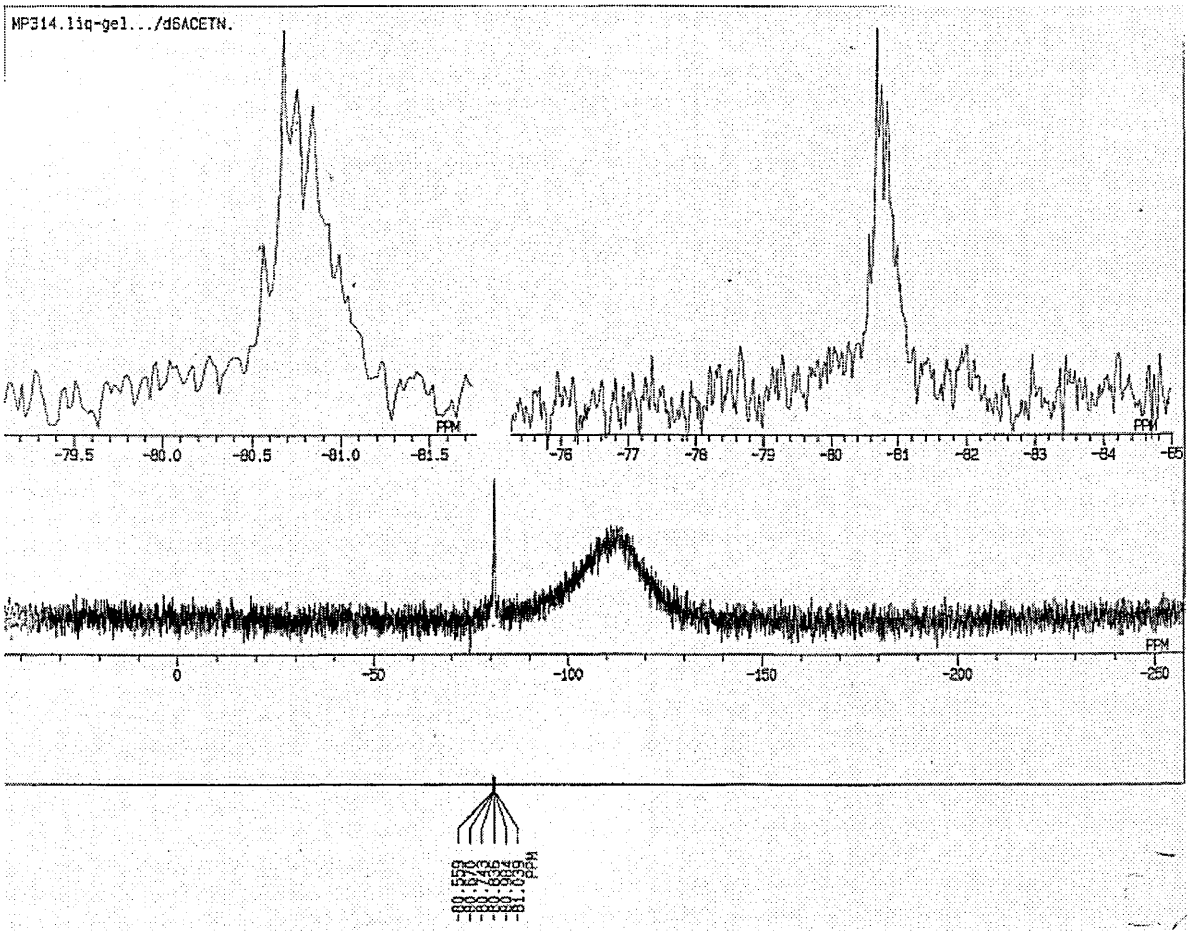

Unfortunately the same problem occurs: we were unable to obtain an X-ray single crystal structure from this sample to confirm our suggestion. However, the mass spectrometric analysis gave some interesting results. The product was analysed by both MALDI-TOF and negative ion FAB mass spectroscopy. The MALDI-TOF analysis confirms that the tetra-*n*-butylammonium octa-*para*-chloromethylphenyloctasilsesquioxane fluoride cage was obtained with a fragment at *m/z* 1440.1 (80%) corresponding to the *p*-chloromethylphenyl-T8 cage with the fluoride anion ($C_{56}H_{48}FCl_8O_{12}Si_8^-$) [$M^-$] (calculated: 1440.3) and a fragment at *m/z* 242.3 (100%) corresponding to the tetra-*n*-butylammonium cation

($C_{16}H_{36}N^+$) [M^+] (calculated: 242.3). Additionally, the analysis revealed the presence of further fragments that can be assigned as follows:

- a fragment at *m/z* 1421.2 (70%) corresponding to the *p*-chloromethylphenyl-T8 cage with the fluoride anion and the substitution of one chlorine atom with an hydroxyl group ($C_{56}H_{49}FCl_7O_{13}Si_8^-$) [$M^-$] (calculated: 1421.8)
- a fragment at *m/z* 1403.2 (70%) corresponding to the *p*-chloromethylphenyl-T8 cage with the fluoride anion and substitution of two chlorine atoms with hydroxyl groups ($C_{56}H_{50}FCl_6O_{14}Si_8^-$) [$M^-$] (calculated: 1403.4)
- a fragment at *m/z* 1385.2 (35%) corresponding to the *p*-chloromethylphenyl-T8 cage with the fluoride anion and substitution of three chlorine atoms with hydroxyl groups ($C_{56}H_{51}FCl_5O_{15}Si_8^-$) [$M^-$] (calculated: 1385.0)
- a fragment at *m/z* 1366.2 (25%) corresponding to the *p*-chloromethylphenyl-T8 cage with the fluoride anion and substitution of four chlorine atoms with hydroxyl groups ($C_{56}H_{52}FCl_4O_{16}Si_8^-$) [$M^-$] (calculated: 1366.5)

These results, together with the presence of a peak at 54.5 ppm in the ^{13}C NMR spectrum, support our proposal for the substitution of some chlorine atoms with hydroxy groups during the reaction. The substition of the organic groups on the silicon of the octasilsesquioxane cage is thus responsible for the broad peak in the ^{29}Si NMR spectrum. We conclude that the conditions required for the encapsulation of the fluoride ion in the

cage were not compatible with the *para*-chloromethylphenyl group and that under these conditions a mixture of cages is obtained. At this point we carried out the same experiment but instead of removing the solvent on the rotary evaporator, we decided to carry out a distillation under vacuum (MP242). We dissolved 1.09 g of *para*-chloromethylphenyltrimethoxysilane (4.42 mmol) in toluene. Then we added 2.5 ml of tetra-*n*-butylammonium fluoride (1M solution in THF, 2.5mmol) so we had a 1: 1.8 ratio of siloxane to TBAF. The reaction mixture was stirred and heated at 95 °C under nitrogen. After 1 hour, the reaction was stopped and the solvent removed by distillation under vacuum at 95°C and a vacuum of 120 mbar. A yellow gel was obtained. The ^{29}Si NMR spectrum (in d_6 acetone) displayed a single peak with a chemical shift of -80.8 ppm, as shown in Figure 66. This peak is a bit sharper than that in the previous experiment which is explained by a lower extent of substitution of the chlorine atoms. Nevertheless, the peak is not sharp enough for the silicon atoms to all have the same environment and we conclude again that one or two chlorine atoms may have been substituted with hydroxy groups during the workup of the reaction. The ^{19}F NMR spectrum (in d_6 acetone) displayed a single sharp peak at -26.2 ppm in the expected chemical shift region for a fluoride anion encapsulated in a octasilsesquioxane cage which again confirms the "naked" nature of the fluoride ion within the cage (Figure 67).

Figure 66 ^{29}Si NMR spectrum of MP242

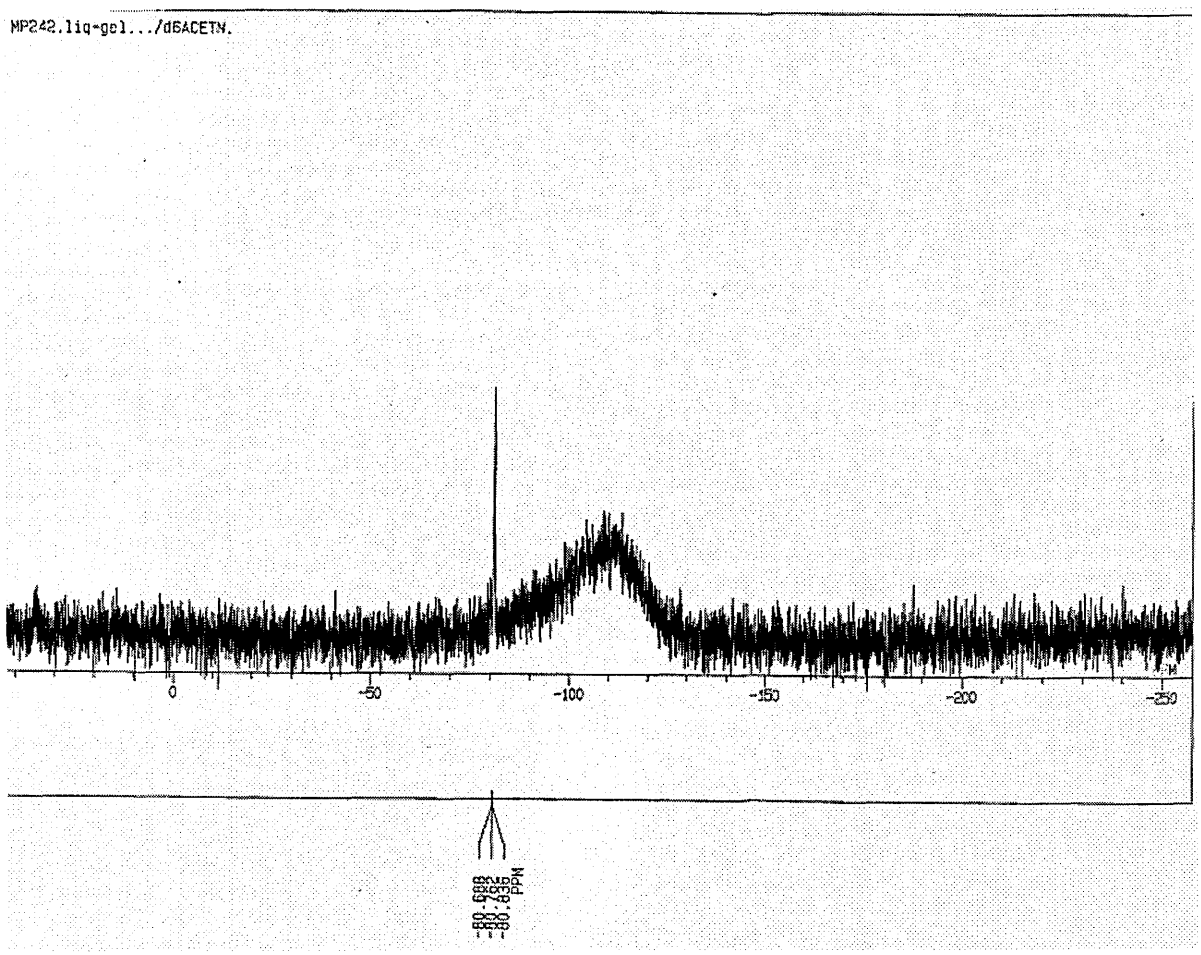

Furthermore, the ^{1}H NMR shows two doublets with a chemical shift at 7.82 (integration: 2H) and 7.75 ppm (integration: 2H) and a singlet with a chemical shift at 4.63 ppm (integration: 2H) which indicate the presence of a *para*-chloromethylphenyl group. In addition, the spectrum displays a triplet at 0.93 ppm (integration: 1.5 H), a multiplet at 1.36 ppm (integration: 1 H), another multiplet at 1.68 ppm (1 H) and a triplet at 3.38 ppm (1 H). The peaks at 0.93, 1.36, 1.68 and 3.38 ppm are associated with the CH_3-CH_2-CH_2-CH_2-X system, which is part of the tetra-*n*-butylammonium fluoride that was used as the catalyst. The integration confirms again a ratio of one molecule of TBAF for one cage. The ^{13}C NMR spectrum is in complete agreement with this assumption: it exhibits peaks at δ 13.9 ppm

(CH_3); δ 20.3 ppm (-CH_2-); δ 24.4 ppm (-CH_2-); δ 59.1 ppm (N-CH_2-) for the four carbon atoms of the tetra-*n*-butylammonium group and δ 126.0 ppm (*o*-CH), δ 128.9 ppm (*m*-CH), δ 129.6 ppm (*i*-C), δ 139.2 ppm (*p*-C), δ 46.9 ppm (Cl-CH_2-) for the carbon atom of the *para*-chloromethylphenyl group. There is an additional peak at 54.5 ppm in the ^{13}C NMR spectrum that is evidence for the conversion of some of the chlorine atoms in the CH_2Cl group to some hydroxyl groups during the workup of the reaction.

Figure 67 ^{19}F NMR spectrum of MP242

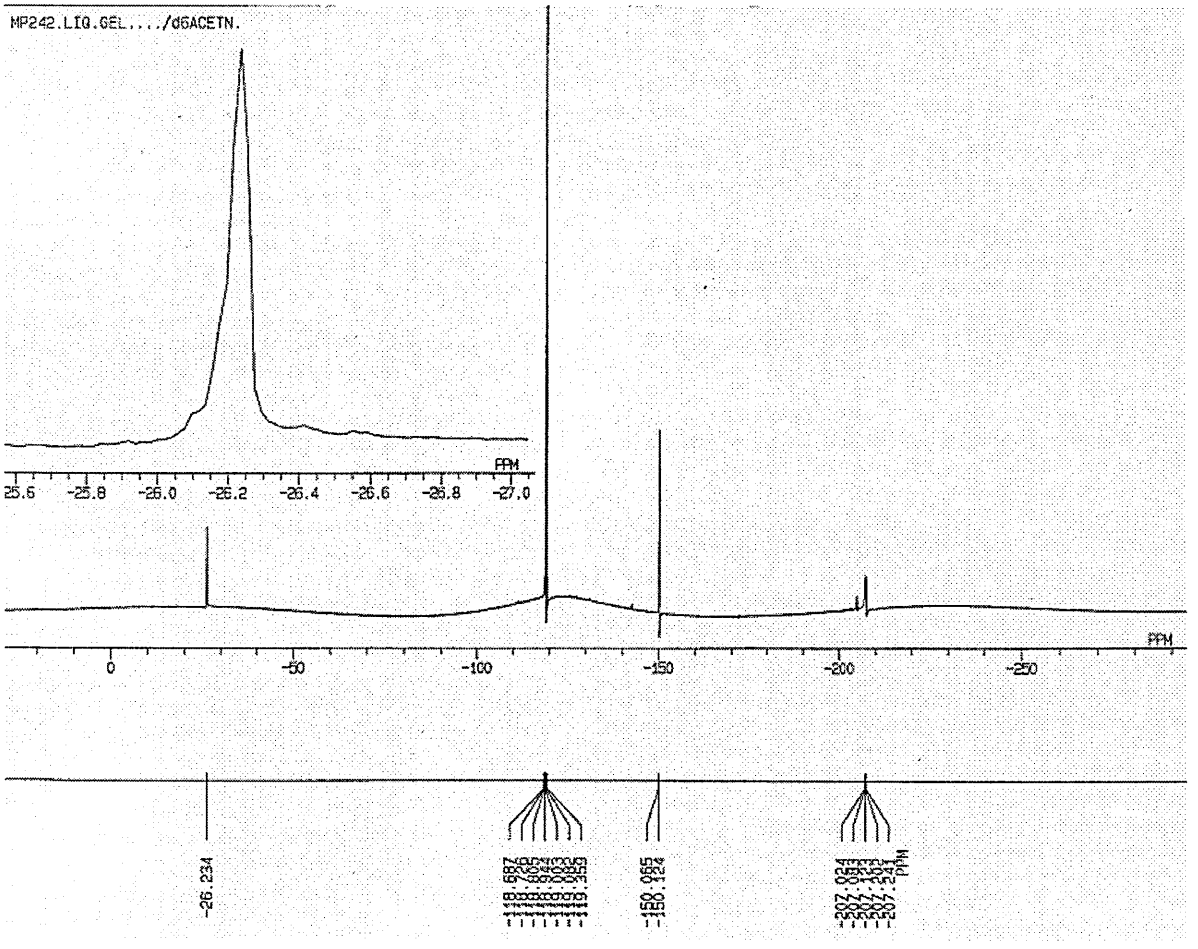

3.4.3 Conclusion

We have demonstrated the existence of a new class of compound wherby a fluoride ion is encapsulated in the cage, by synthesizing a fourth tetra-*n*-butylammonium octasilsesquioxane fluoride cage: a tetra-*n*-butylammonium octa-*para*-chloromethylphenyloctasilsesquioxane fluoride cage. We have shown that the conditions for the encapsulation of the fluoride ion were not well suited to this organic substituent because of the random substitution of the chlorine atoms with hydroxy groups. Nevertheless, the ^{19}F NMR spectrum confirmed the encapsulation of the fluoride within the cage with weak interactions with its neighboring environment. MALDI-TOF mass spectrometric analysis also confirmed the synthesis of the tetra-*n*-butylammonium octa-*para*-chloromethylphenyloctasilsesquioxane fluoride cage together with some tetra-*n*-butylammonium octa-*para*-$(chloro)_{8-n}(hydroxy)_n$ methylphenyloctasilsesquioxane fluoride cages.

Chapter 4: What about the encapsulation of different anions using other catalysts ?

4.1 Introduction

Our success in the synthesis of this new class of compound whereby a fluoride ion is encapsulated within the cage has led us to try other sources of fluoride ion and other anions. In order to understand better the mechanism of the encapsulation of the fluoride anion within the octaphenyloctasilsesquioxane cage, we examined different anion catalysts and other sources of the fluoride anion. In fact, numerous anion catalysts analogues of TBAF have been reported in the literature, such as tetra-*n*-butylammonium iodide (TBAI), tetra-*n*-butylammonium chloride (TBACl) and tetra-*n*-butylammonium bromide (TBABr). Other sources of fluoride anion are caesium fluoride (CeF), lithium fluoride (LiF) and tris(dimethylamino)sulfonium difluorotrimethylsilicate (TASF). An alternative strategy for a fluoride source is to change the length of the carbon skeleton on the ammonium salt, for example, tetraethylammonium fluoride (TEAF), which is commercially available.

4.2 Utilisation of other anion catalysts

4.2.1 tetra-*n*-butylammonium bromide

In an initial experiment (MP64), tetra-*n*-butylammonium bromide was added with phenyltripropoxysilane (in a ratio of 1:2) to 20 ml of dried pyridine. After stirring for 24 hours, the reaction was stopped and the solvent removed at 80°C and under a vacuum of 70

mbar. Analysis of the ^{29}Si NMR spectrum shows a peak at -58.7 ppm which arises from the phenyltripropoxysilane. We, thus, concluded that under these conditions tetra-*n*-butylammonium bromide was not a good catalyst for this reaction. Nevertheless, we decided to carry out a second experiment (MP65) with tetra-*n*-butylammonium bromide. We thus repeated the previous reaction but used a 1:1 mixture of tetra-*n*-butylammonium bromide and tetra-*n*-butylammonium fluoride as the catalyst. The solvent was removed at the same temperature and pressure and a gel was obtained. Analysis of the mixture showed a single peak at a -80.6 ppm in the ^{29}Si NMR and a single peak at a -26.6 ppm in the ^{19}F NMR which indicated the synthesis of the Ph_8T_8-TBAF cage. We obtained no evidence that the bromide ion had a role in this synthesis.

4.2.2 Tetra-*n*-butylammonium chloride

In an initial experiment (MP66), tetra-*n*-butylammonium chloride was added with phenyltripropoxysilane (in a ratio of 1:2) to 20 ml of dried pyridine. After stirring for 24 hours, the reaction was stopped and the solvent removed at 80°C and under a vacuum of 70 mbar. Analysis of the ^{29}Si NMR spectrum shows a peak at -58.7 ppm which arises from the phenyltripropoxysilane. We, thus, concluded that under these conditions tetra-*n*-butylammonium chloride was not a good catalyst for this reaction. Nevertheless, as in the case of tetra-*n*-butylammonium bromide, we decided to carry out a second experiment (MP72) using a 1:1 mixture of tetra-*n*-butylammonium chloride and tetra-*n*-butylammonium fluoride as catalyst. The solvent was removed at the same temperature and pressure and a gel was obtained. This gel was then extracted with chloroform and a white solid precipitated out. After filtration, analysis of the fine white powder shows a single peak at -80.6 ppm in the ^{29}Si NMR and a single peak at -26.6 ppm in the ^{19}F NMR which again indicated the

synthesis of the Ph_8T_8-TBAF cage. The ^{29}Si NMR spectrum of the filtrate displayed a single peak at -81.4 ppm which, based on Marsmann's equations, arises from the $Ph_{10}T_{10}$. We obtained no evidence that the chloride ion had a role in this synthesis.

4.2.3 Tetra-*n*-butylammonium iodide

In an initial experiment (MP71), tetra-*n*-butylammonium iodide was added with phenyltripropoxysilane (in a ratio of 1:2) to 20 ml of dried pyridine. After stirring for 24 hours, the reaction was stopped and the solvent removed at 80°C and under a vacuum of 70 mbar. Analysis of the ^{29}Si NMR spectrum shows a peak at -58.7 ppm which arises from the phenyltripropoxysilane. We, thus, concluded that under these conditions tetra-*n*-butylammonium iodide was not a good catalyst for this reaction. Nevertheless, as in the case of tetra-*n*-butylammonium bromide, we decided to carry out a second experiment (MP78) using a 1:1 mixture of tetra-*n*-butylammonium iodide and tetra-*n*-butylammonium fluoride as catalyst. The solvent was removed at the same temperature and pressure and a gel was obtained. This gel was then extracted with chloroform and a white solid precipitated out. After filtration, analysis of the fine white powder shows a single peak at -80.6 ppm in the ^{29}Si NMR and a single peak at -26.6 ppm in the ^{19}F NMR which again indicated the synthesis of the Ph_8T_8-TBAF cage. We decide to compare the solid state ^{29}Si NMR spectrum of the powder obtained in this experiment with the spectrum of the powder of the Ph_8T_8-TBAF obtained using only TBAF as the catalyst. Both spectra (Figure 68) are very similar with a peak at -80.4 ppm. Thus we concluded that we had not obtained a new compound in this experiment (MP78) and that the iodide ion did not have a role in this synthesis.

Figure 68 MP61 and MP78 solid state ^{29}Si NMR

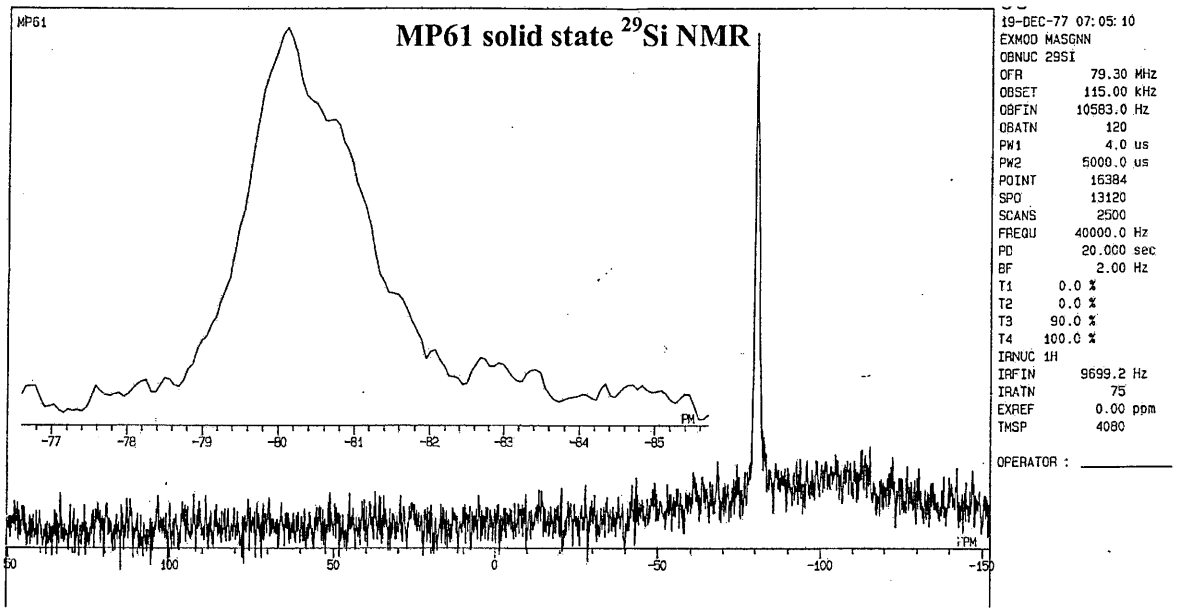

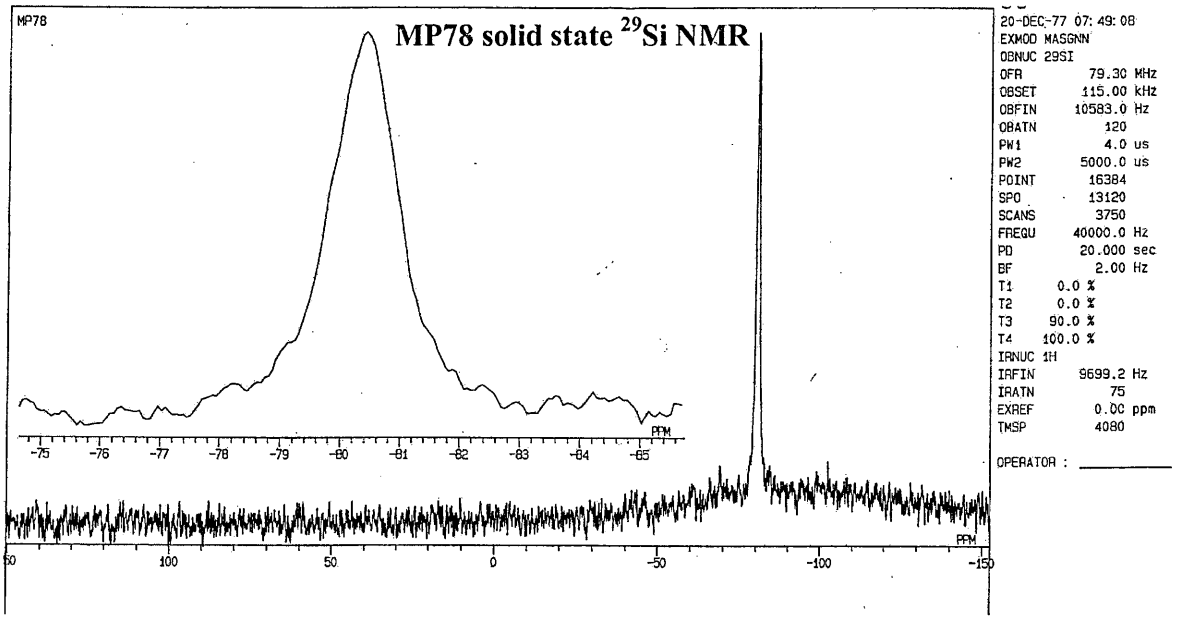

Figure 68 MP61 and MP78 solid state ^{29}Si NMR

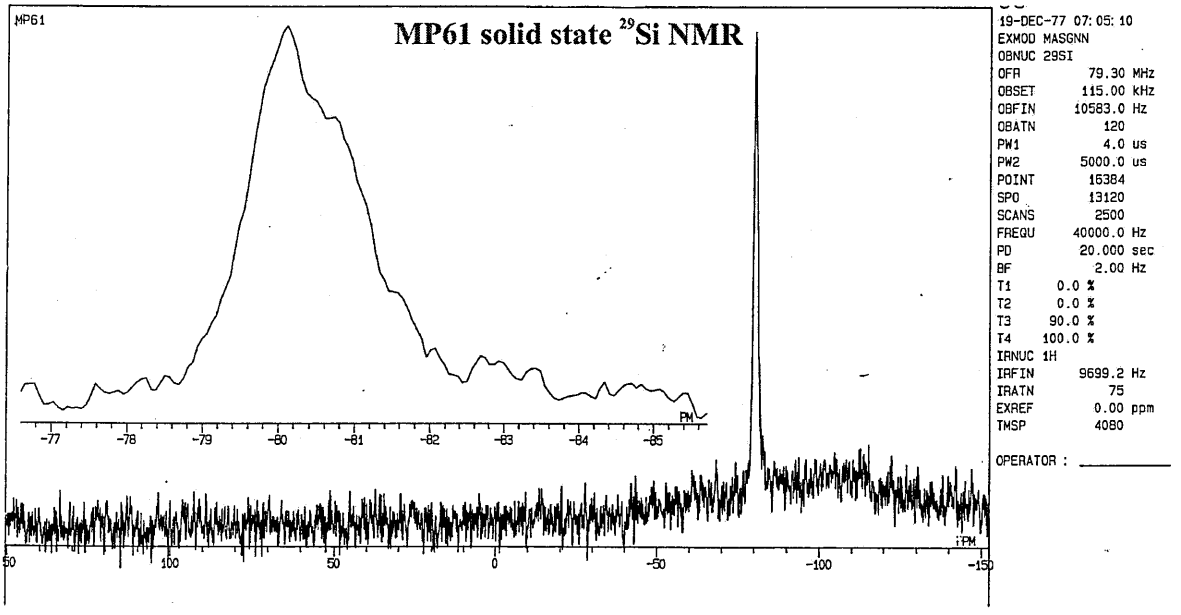

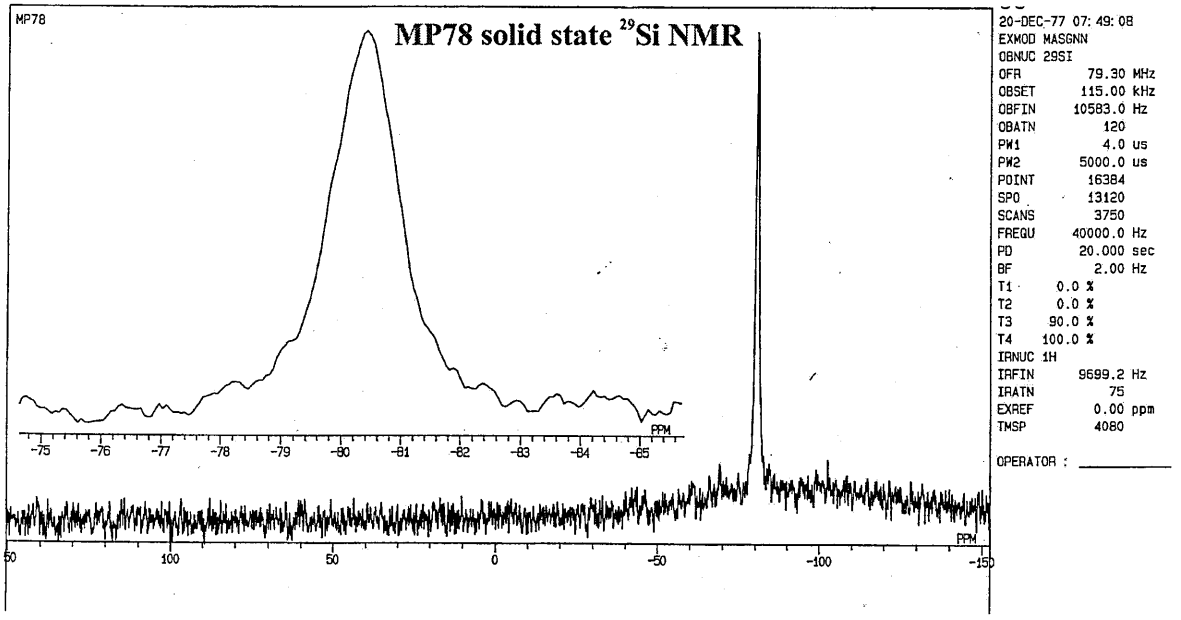

4.2.4 Tetra-*n*-butylammonium hydroxide

Catlow and George [69] have reported calculations of the structures and energetics of fluoride ions in the octadecasil zeolite structure. They calculated the energy required to introduce both a fluoride ion and a hydroxide ion into the double D four ring (D4R) cage. They proposed that there was a large difference between the relative energies of F^- and OH^- and the results suggested that the OH^- ion should be more thermodynamically stable within a D4R cage than the F^- ion. Obviously this result suggests the possibility of encapsulation of a hydroxide ion within the octasilsesquioxane cage. One suitable and commercially available catalyst for this reaction is tetraethylammonium hydroxide. The TEA hydroxide is available as a liquid with 35 % by weight of water. This might be a problem for our reaction as we had previously determined that the maximum amount of water is 5 %. Nevertheless, an experiment (MP389) was conducted in toluene. 0.86 g of tetraethylammonium hydroxide (3.8 mmol) was added to a solution of 1.44 g of vinyltriethoxysilane (7.6 mmol) in toluene. After stirring for 24 hours, the reaction was stopped and the solvent removed at 80°C and under a vacuum of 70 mbar. Analysis of the ^{29}Si NMR spectrum shows a great number of peaks in the Si-T region. However, there are three major peaks with chemical shifts at -72.0, -73.3 and -82.5 ppm in the ^{29}Si NMR. The assignment of these peaks is very difficult but the peak at -82.5 ppm is very close to the chemical shift of the vinylT_8-TBAF encapsulated cage and in this case we might expect the vinylT_8-TEAOH encapsulated cage to have a similar chemical shift. The ^1H and ^{13}C NMR did not provide any more evidence for the presence of the vinylT_8-TEAOH cage. Unfortunately we could not obtain a single crystal X-ray structure or MS data for this sample as we observed its quick degradation to resin like material.

Thus we have not been able to confirm the synthesis of the vinylT_8-TEAOH cage. However, the ^{29}Si NMR is encouraging which, together with Catlow's calculations, suggests we should carry out more research on the possibility of encapsulation of a hydroxide ion within the octavinylsilsesquioxane cage.

4.3 Other sources of fluoride anion

4.3.1 Caesium fluoride (MP152)

We thought that caesium fluoride would be an interesting catalyst to use for the synthesis of encapsulated fluoride octasilsesquioxane cages become it would lead to a large caesium cation outside the cage. In fact, caesium fluoride could be dissolved in acetone at 30°C and thus such a solution would be suitable for catalysing the reaction. As we have described in previous sections, the maximum amount of water allowable for obtaining a pure product is 5%. Thus, we first dried the caesium fluoride in an oven. Sufficient catalyst for a 1:2 ratio with phenyltripropoxysilane was then added to a solution of dried acetone and the trialkoxysilane with a controlled amount of water (5 %). After the reaction was stirred and heated under a nitrogen atmosphere for 24 hours, the solvent was removed and a liquid obtained. The ^{29}Si NMR spectrum shows a single peak at -58.7 ppm in the ^{29}Si NMR which arises from the phenyltripropoxysilane. We repeated this reaction but unfortunately no reaction was observed. Nevertheless, we obtained some crystals from the reaction mixture after 2 weeks from which we obtained a crystal structure (Figure 69) corresponding to a phenyl-T_8 with water molecules in the cells. We compared selected bond lengths and bond angles of this crystal structure of Ph_8T_8 cage with those of the published Ph_8T_8 cage from Hossain and co-workers [83]. The crystal structure of the latter revealed acetone molecules

trapped in the packing. Both structures are very similar as we would have expected and the presence of water or acetone molecules seems to make very little difference to the structure of the cage.

Figure 69 Ph_8T_8 X-ray crystal structure and packing

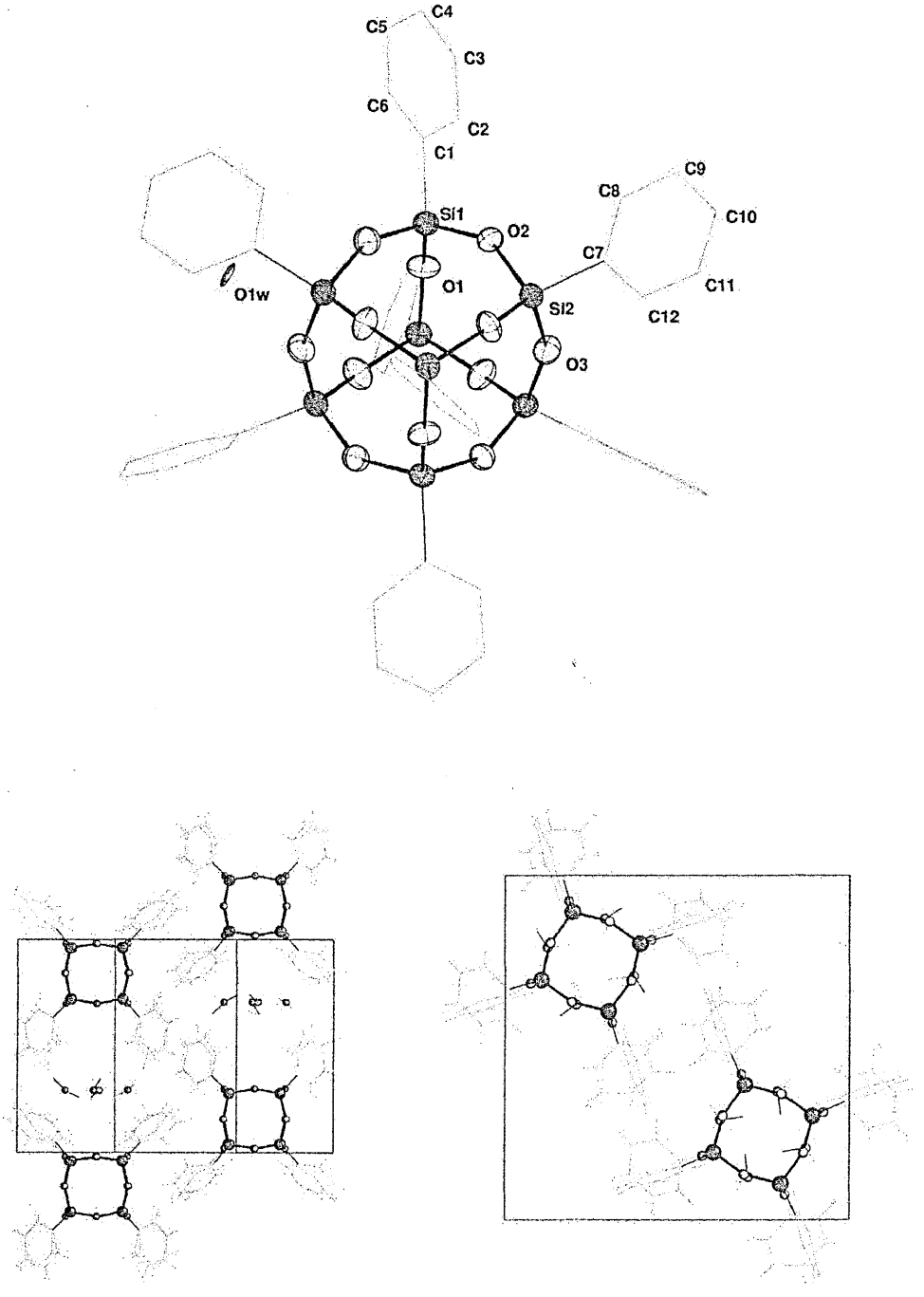

4.3.2 Lithium Fluoride (MP92)

Another source of fluoride ion which we could use as a catalyst for the synthesis of encapsulated fluoride octasilsesquioxane cages was lithium fluoride. This salt would lead to a lithium cation sitting outside the cage with a much smaller atomic radius (2.05 Å) than the caesium ion (3.34 Å). In fact, this atomic radius is sufficiently low to allow encapsulation of a lithium atom inside the cage. One of the problems encountered with this approach was that lithium fluoride does not have a good solubility in any organic solvent. However, an experiment was conducted in acetone at 30°C using the maximum amount of water allowable for obtaining a pure product (5 %) and the right amount of catalyst (ratio of 1:2 ratio with *para*-tolylalkoxysilane). 2.08g of p*ara*-tolyltrimethoxysilane were added to a solution of dried acetone with a controlled amount of water (5 %) containing 0.13g of LiF (5mmol). The reaction was stirred and heated under a nitrogen atmosphere for 24 hours, then the solvent was removed and a liquid obtained. The ^{29}Si NMR spectrum shows a single peak at -57.9 ppm in the ^{29}Si NMR which arises from the p*ara*-tolyltrimethoxysilane. This unsuccessful outcome was quite disappointing as Park and co-workers[84] have recently reported promising calculations that suggest that the inclusion of both a fluoride anion and a lithium cation in octasilsesquioxane cages was energetically favorable. Their work supports our idea that the inclusion of a lithium ion is possible and that perhaps the conditions of our synthesis have not been optimized for the encapsulation of a lithium ion. The search for such optimum conditions will be the subject of further investigations.

4.3.3 Tris(dimethylamino)sulfonium difluorotrimethylsilicate (TASF)

The use of tris(dimethylamino)sulfonium difluorotrimethylsilicate (TASF) as a catalyst for the condensation of Si-O-Si systems has been previously reported in the literature [85]. Thus

TASF is an obvious source of fluoride ion for the synthesis of our encapsulated systems. TASF has also been used as a method for the selective removal of silicon-containing protecting groups [86, 87]. It gives high yields of the desired products without disturbing other functional groups that previous deprotecting reagents (such as TBAF) would disrupt. Two experiments were conducted: the first as a control experiment in dry THF under N_2 (MP316) and the second in dry THF with 5 % water (MP317). 0.40 g of TASF (1.45 mmol) was added to a solution in THF containing 0.55 g of vinyltriethoxysilane (2.90 mmol) and the solution was stirred for 24 hours at room temperature. The solvent was removed at 375 mbar and at 55°C. In the first experiment (MP316), no reaction was observed as the ^{29}Si NMR spectrum revealed a single peak with a chemical shift of -59.1 ppm which arises from the vinyltriethoxysilane. However, the second experiment showed a different result. After removing the solvent, two liquid layers were obtained. One was the transparent upper layer for which the ^{29}Si NMR spectrum displayed a number of peaks: a single peak with a chemical shift of -59.1 ppm which arises from the vinyltriethoxysilane, two peaks in a ratio of 2:1 with chemical shifts of -66.5 and -66.6 ppm and two small peaks in a ratio of 1:1 with chemical shifts of -74.2 and -74.3 ppm. We have not been able to explain and assign the presence of these peaks. The lower layer, obtained after the removal of the solvent, was brown and showed a single peak at -82.87 ppm in the ^{29}Si NMR which is very closed to the ^{29}Si NMR chemical shift of our vinylT_8-TBAF cage at -82.89 ppm. Unfortunately, the ^{19}F NMR spectrum did not show any peak in the expected area for an encapsulated fluoride ion. No further evidence was obtained to characterize this compound. As with the LiF experiment, the TASF experiment should be the subject of further investigation and research.

4.3.4 Tetraethylammonium Fluoride (TEAF)

Another source of fluoride ion which is suitable for our cage synthesis and commercially available is tetraethylammonium fluoride (TEAF), we thus conducted an experiment in acetone (MP286), as shown in Figure 70. 0.50 g of TEAF (3.20 mmol) was added to a solution in acetone containing 1.20 g of vinyltriethoxysilane (6.30 mmol) and the solution was stirred for 24 hours at room temperature. The solvent was removed at 400 mbar and at 55°C. A yellow solid gel was obtained. The ^{29}Si NMR spectrum (in d_6 acetone) confirmed the presence of the vinylT_8-TEAF cage with a signal at -82.83 ppm (the vinylT_8-TBAF cage had a chemical shift at -82.89 ppm in the ^{29}Si NMR)

Figure 70 Reaction of vinyltriethoxysilane with tetraethylammonium fluoride

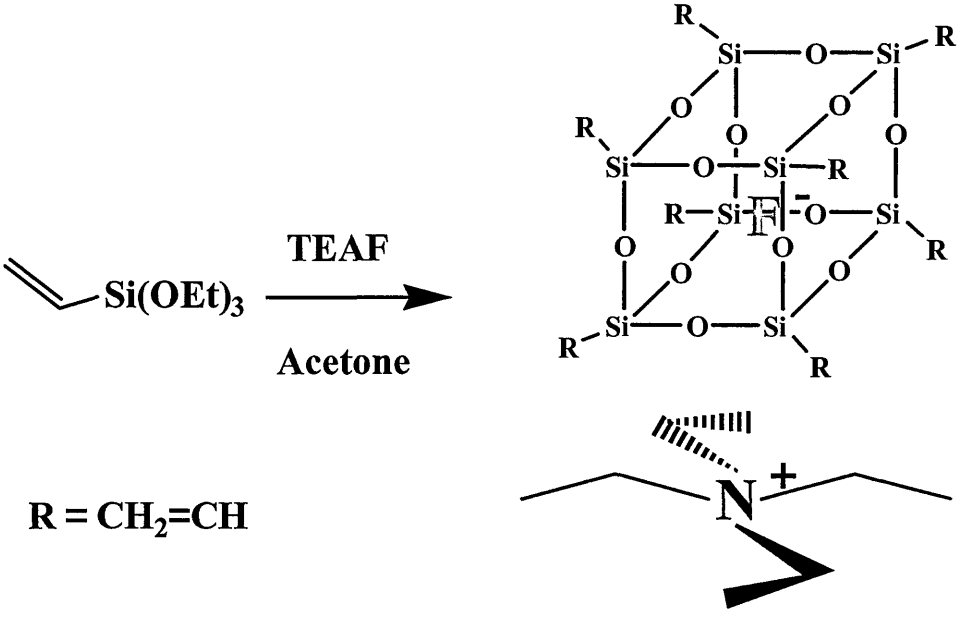

Additionally, the ^{19}F NMR spectrum displayed a sharp and intense peak with a chemical shift of -25.1 ppm which is consistent with the formation of the tetraethylammonium octavinyloctasilsesquioxane fluoride cage, vinylT_8-TEAF. The vinylT_8-TBAF cage showed

a signal with a chemical shift at -25.4 ppm in the ^{19}F NMR. This value again suggests an isolated fluoride anion with little interaction with its near neighbouring silicon atoms. Furthermore, the ^{1}H NMR shows a multiplet with a chemical shift of 5.85 ppm (integration: 24H) which indicates the presence of a vinyl group. In addition, the spectrum displays a triplet at 1.06 (integration: 12H) and a quartet at 3.50 ppm (8 H). The peaks at 1.06 and 3.50 ppm are associated with the CH_3-CH_2-X system, which is part of the tetraethylammonium fluoride that was used as the catalyst. The integration between the hydrogen atoms from the vinyl groups and the hydrogen atoms from the ethyl groups shows a ratio of 1:1 between the cage and the tetraethylammonium cation. This was confirmed by the ^{13}C NMR spectrum, which exhibits four peaks at δ 19.27 ppm (s, CH_3) and δ 56.99 ppm (s, -CH_2-) for the carbon atoms of the tetraethylammonium group and δ 132.50 ppm (C=C), δ 136.65 ppm (C=C) for the carbon atoms of the vinyl group. Unfortunately we could not obtain a single crystals X-ray structure of this sample.

4.4 Ion Exchange

4.4.1 Introduction

As encapsulation of other ions or other fluoride sources was not particularly successful in giving pure samples for X-ray crystallography, we decided to start with the encapsulated fluoride cage itself and try to exchange the TBA outside the cage for different cations. We used caesium Iodide (CeI), Lithium Iodide (LiI), Sodium Iodide (NaI) and Lithium Tetraphenylborate.

4.4.2 Ph_8T_8-TBAF reaction with CeI

We used caesium iodide as the exchange reagent in acetone (MP82). 0.3 g of Ph_8T_8-TBAF was dissolved in acetone and an excess of CeI was added to the solution. The reaction was stirred at room temperature for 12 hours. After removal of the solvent, the ^{29}Si NMR spectrum showed a peak with a chemical shift of -80.6 ppm and the ^{19}F NMR spectrum displayed a single sharp peak at -26.7 ppm. The two spectra suggest the presence of the unchanged Ph_8T_8-TBAF cage.

4.4.3 $VinylT_8$-TBAF reaction with LiI

We also used lithium iodide as the exchange reagent in acetone (MP291). 0.4 g of $vinylT_8$-TBAF was dissolved in acetone and 5 ml of a solution of acetone saturated with LiI was added to it. The reaction was stirred at room temperature for 12 hours. After removal of the solvent, the ^{29}Si NMR spectrum showed two peaks with chemical shifts of -79.8 and -81.2 ppm, which, based on the work of Yuxing Yang, arise respectively from $vinylT_8$ and $vinylT_{10}$ cages. Thus we concluded that instead of ion exchange, the fluoride cage rearranged to give the conventional $vinylT_8$ and $vinylT_{10}$ cages. This conclusion was confirmed by the absence of peaks in the ^{19}F NMR spectrum. This could be an evidence that the fluoride ion may get out through a face of the cage without breaking its structure as suggested by Pitmann and co-workers [84].

4.4.4 Ph_8T_8-TBAF reaction with NaI

We also used sodium iodide as the exchange reagent in acetone (MP249). 0.3 g of Ph_8T_8-TBAF was dissolved in acetone and an excess of NaI was added to the solution. The reaction was stirred and heated at reflux for 12 hours. After removal of the solvent, the ^{29}Si

NMR spectrum showed a peak with a chemical shift of -80.6 ppm and the ^{19}F NMR spectrum displayed a single sharp peak at -26.7 ppm. The two spectra suggest the presence of the unchanged Ph_8T_8-TBAF cage.

4.4.5 VinylT$_8$-TBAF reaction with Lithium Tetraphenylborate

We also used lithium tetraphenylborate ($LiPh_4B$) as the exchange reagent in acetone (MP298). 0.95 g of vinylT$_8$-TBAF was dissolved in acetone and 5 ml of a solution of acetone saturated with 0.6 g of $LiPh_4B$ was added to it. The reaction was stirred at room temperature for 12 hours. After removal of the solvent, the ^{29}Si NMR spectrum showed a peak with a chemical shift of -82.8 ppm and the ^{19}F NMR spectrum displayed a single sharp peak at -25.4 ppm. The two spectra suggest the presence of the unchanged vinylT$_8$-TBAF cage.

4.5 Experiments on vinylT$_8$-TBAF

4.5.1 NMR measurement of chemical shift versus temperature

An interesting aspect of our encapsulated fluoride ion cage is that the fluoride ion is entrapped in a closed environment and the NMR spectroscopy measurements obtained showed single and sharp peaks in the ^{19}F NMR and ^{29}Si NMR. These results, together with the downfield chemical shift value obtained in the ^{19}F NMR, demonstrate that the fluoride ion has only very weak interactions with its neighbouring silicon atoms and can be considered to be an isolated fluoride ion. In order to understand better the nature of the encapsulated fluoride ion, we examined how the chemical shift in the ^{19}F NMR changes with the temperature. The experiment was conducted using the vinylT$_8$-TBAF cage. The ^{19}F

NMR and ^{29}Si NMR spectra of the compound were checked before and after the experiment to make sure that the vinylT_8-TBAF cage structure was not affected by the temperature variations. We did the measurements every 10°C over a temperature range of 25°C to -70°C. At this point, we repeated the measurements but this time from -70°C to 50°C. We then went back to 25°C to do the final check. As seen in Figure 71, all the measurements could be fitted to a straight line with a formula: $y = 0.0314 \times -26.163$. Additionally, we did not observed a change in the shape of the peak which remained a single sharp peak for all the measurements. This demonstrates that the isolated nature of the encapsulated fluoride ion does not drastically change over a temperature range of -70°C to 50°C. It also shows that the ^{19}F NMR chemical shift decreases with a decrease in the temperature. This shift in the fluoride ion signal at lower temperature suggests the fluoride ion has stronger interactions with its neighbouring silicon atoms.

Figure 71 NMR measurement of chemical shift versus temperature

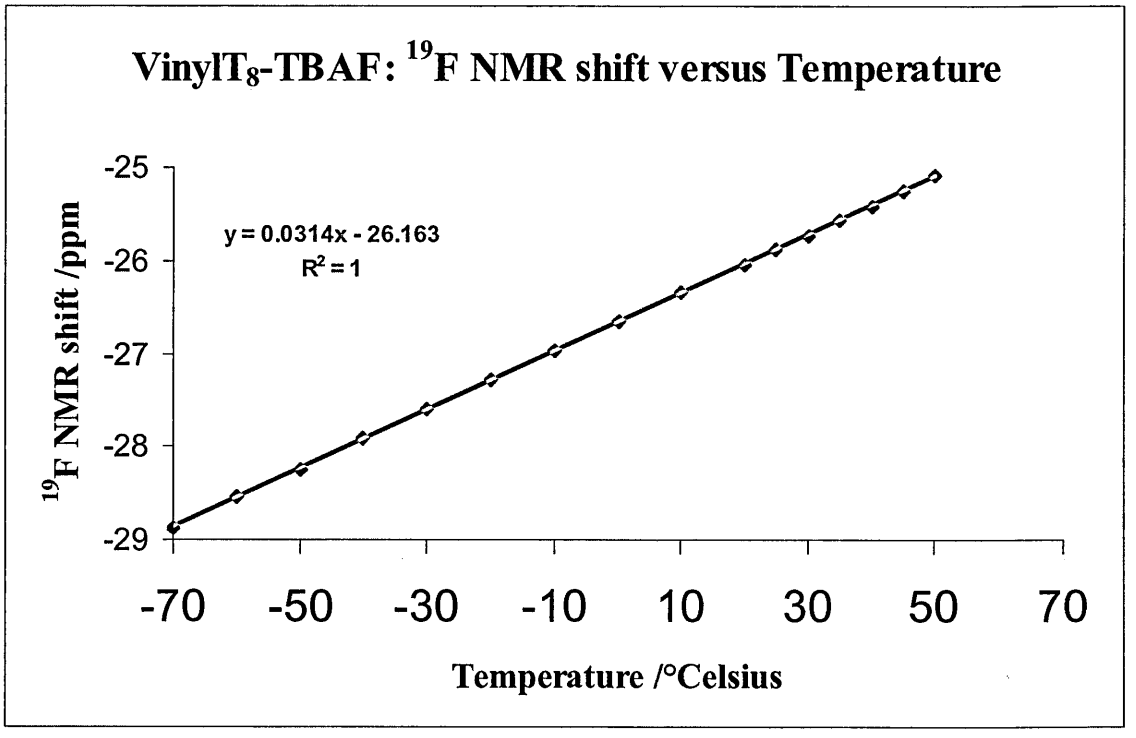

Catlow has suggested that the fluoride ion in the D4R cage of a zeolite is not centred in the cage but forms a pentacoordinate silicon species with one of the silicon atoms at the vertex of the cage. We have found the fluoride ion to be centred within our cages, however, the carbon substituent attached to the cage is not a good leaving group so pentacoordination will be less likely in our systems than in zeolites where all four atoms attached to the silicon are oxygens. However, Catlow's observations are supported by the fact that at lower temperatures there is greater Si-F bond formation in our systems and thus greater silicon pentacoordination.

4.6 Conclusion

In this work, the attempt to encapsulate ions other than fluoride, such as bromide, chloride and lithium, within an octasilsesquioxane cage failed. However, we did obtain some evidence for the encapsulation of hydroxide ion within the vinylT_8-TBAF cage using tetraethylammonium hydroxide as the catalyst.

We also failed to synthesize octasilsesquioxane fluoride cages with other source of fluoride ions except when we used tetraethylammonium fluoride as the catalyst. In this latter case, we obtained strong NMR evidence that the fluoride ion was encapsulated.

We were not able to achieve the exchange of TBA for different cations using salts such as LiI, NaI and $LiPh_4B$.

These results warrant further investigation, particularly the characterization of the encapsulated hydroxide ion.

We also confirmed through the variation of the ^{19}F NMR chemical shift with the temperature that the fluoride ion has very little interaction with the silicon atoms of the cage, such that the fluoride anion can be described essentially as a naked fluoride ion.

Chapter 5: Is the encapsulation of a fluoride anion possible when the R group on the silicon atom is attached by an sp^3 carbon atom ?

5.1 Introduction

The four new cages which we have fully characterised have been synthesized with sp^2 carbon attached to the silicon. Since the literature mainly reports the synthesis of octasilsesquioxanes with sp^3 carbon attached to the silicon, we wanted to carry out the reaction of trialkoxysilanes with sp^3 carbon attached to the silicon using the same TBAF synthetic route that we used previously. This part of our work has been driven by an interest in extending this new class of compound, the better comprehension of the fluoride encapsulation mechanism and to understand the significance of the nature of the organic group at the silicon.

5.2 Reaction with *cyclo*-hexyltrialkoxysilane

The first experiment (MP113) was conducted using pyridine as the solvent. In this experiment we dissolved 1.17 g of *cyclo*-hexyltripropoxysilane (4.06 mmol) in pyridine (b.p. of pyridine: 115°C). We then added 2.5 ml of tetra-*n*-butylammonium fluoride (1M solution in THF, 2.5mmol) so we had a 1:1.7 ratio of siloxane to TBAF. After 24 hours, the reaction was stopped and the solvent removed on a rotary evaporator at a temperature of 80°C and a vacuum of 80 mbar for 15 minutes. A brown-red gel was obtained.

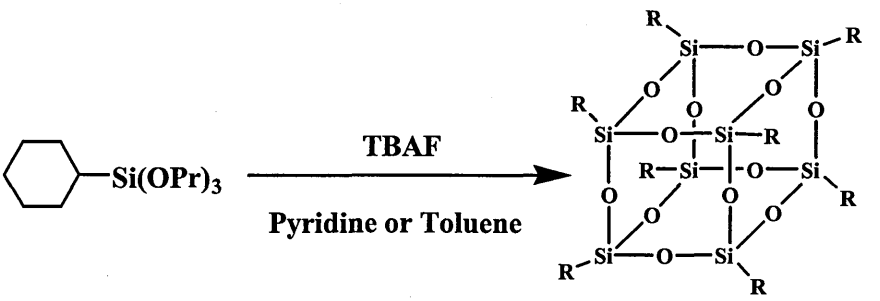

The ^{29}Si NMR spectrum (in $CDCl_3$) displayed a single sharp peak in the T-Si area with a chemical shift at -69.0 ppm. The ^{19}F NMR spectrum did not show any peaks with a chemical shift in the area described previously for an encapsulated fluoride ion (around -25ppm). This demonstrated that no fluoride ion had been incorporated in this reaction and that we are reasonably confident that we synthesized an octa-*cyclo*-hexyloctasilsesquioxane cage. In fact, Yuxing Yang and other publications have reported the synthesis of the octa-*cyclo*-hexyloctasilsesquioxane cage with a ^{29}Si NMR chemical shift of -68.7 ppm. The ^{1}H NMR shows three multiplets with chemical shifts of 1.70 ppm (40H, vbr, m, CH_2), 1.19 ppm (40H, vbr, m, CH_2) and one multiplet at 0.72 ppm (8H, vbr, m, CH) which indicates the presence of a *cyclo*-hexyl group. The ^{13}C NMR spectrum is in complete agreement with this assumption: it exhibited peaks at δ 23.2 ppm (CH); δ 26.7 ppm (-CH_2-); δ 27.5 ppm (-CH_2-).

A second experiment (MP216) was conducted using toluene as the solvent. In this experiment we dissolved 1.08 g of *cyclo*-hexyltripropoxysilane (3.7 mmol) in toluene (b.p. of toluene: 110.6°C). We then added 2.5 ml of tetra-*n*-butylammonium fluoride (1M solution in THF, 2.5mmol) so we had a 1:1.5 ratio of siloxane to TBAF. After 24 hours, the

reaction was stopped and the solvent removed by distillation under vacuum at a temperature of 80°C. A brown-red gel was obtained. The ^{29}Si NMR spectrum (in $CDCl_3$) displayed a single sharp peak in the T-Si area with a chemical shift of -68.7 ppm. The ^{19}F NMR spectrum did not show any peaks with a chemical shift around -25ppm. This demonstrates again that no fluoride ion had been incorporated in this reaction and that we had synthesized an octa-*cyclo*-hexyloctasilsesquioxane cage. The ^{1}H NMR shows three multiplets with chemical shifts of 1.70 ppm (40H, vbr, m, CH_2), 1.19 ppm (40H, vbr, m, CH_2) and one multiplet at 0.72 ppm (8H, vbr, m, CH) which indicates the presence of a *cyclo*-hexyl group. The ^{13}C NMR spectrum is in complete agreement with this assumption: it exhibited peaks at δ 23.2 ppm (CH); δ 26.7 ppm (-CH_2-); δ 27.5 ppm (-CH_2-).

We concluded that the reaction of *cyclo*-hexyltripropoxysilane using the same TBAF synthetic route did not give an encapsulated fluoride ion cage. The reaction only gave the conventional octa-*cyclo*-hexyloctasilsesquioxane cage.

5.3 Reaction with *cyclo*-pentyltrialkoxysilane

The first experiment (MP74) was conducted using pyridine as the solvent. In this experiment we dissolved 1.18 g of *cyclo*-pentyltripropoxysilane (4.3 mmol) in pyridine (b.p. of pyridine: 115°C). We then added 2.5 ml of tetra-*n*-butylammonium fluoride (1M solution in THF, 2.5mmol) so we had a 1:1.7 ratio of siloxane to TBAF. After 24 hours, the reaction was stopped and the solvent removed on a rotary evaporator at a temperature of 80°C and a vacuum of 80 mbar for 15 minutes. A brown-red gel was obtained.

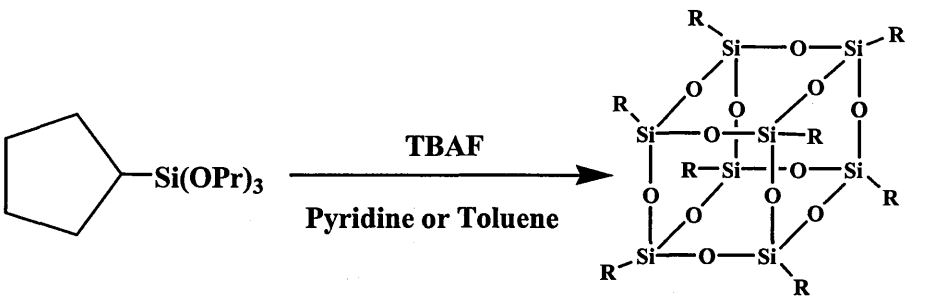

The ^{29}Si NMR spectrum (in $CDCl_3$) displayed a single sharp peak in the T-Si area with a chemical shift of -66.6 ppm. The ^{19}F NMR spectrum did not show any peaks with a chemical shift in the area described previously for an encapsulated fluoride ion (around -25 ppm). This demonstrated that no fluoride ion had been incorporated in this reaction and that we are reasonably confident that we had synthesized an octa-*cyclo*-pentyloctasilsesquioxane cage. In fact, Yuxing Yang and other publications have reported the synthesis of the octa-*cyclo*-pentyloctasilsesquioxane cage with a ^{29}Si NMR chemical shift at -66.6 ppm. The ^{1}H NMR shows three multiplets with chemical shifts of 1.70 ppm (16H, vbr, m, CH_2), 1.44 ppm (48H, vbr, m, CH_2) and one multiplet at 0.90 ppm (8H, vbr, m, CH) which indicates the presence of a *cyclo*-pentyl group. The ^{13}C NMR spectrum is in complete agreement with this assumption: it exhibited peaks at δ 22.3 ppm (CH); δ 27.0 ppm (-CH_2-); δ 27.3 ppm (-CH_2-).

A second experiment (MP196) was conducted using toluene as the solvent. In this experiment we dissolved 1.09 g of *cyclo*-pentyltripropoxysilane (4.0 mmol) in toluene (b.p. of toluene: 110.6°C). We then added 2.5 ml of tetra-*n*-butylammonium fluoride (1M solution in THF, 2.5mmol) so we had a 1:1.6 ratio of siloxane to TBAF. After 24 hours, the

reaction was stopped and the solvent removed on a rotary evaporator at a temperature of 80°C and a vacuum of 100 mbar for 15 minutes. A brown-red gel was obtained. The ^{29}Si NMR spectrum (in $CDCl_3$) displayed a single sharp peak in the T-Si area with a chemical shift of -66.6 ppm. The ^{19}F NMR spectrum did not show any peaks with a chemical shift around -25 ppm. This demonstrated again that no fluoride ion had been incorporated during this reaction and that we had synthesized an octa-*cyclo*-hexyloctasilsesquioxane cage. The ^{1}H NMR shows three multiplets with chemical shifts of 1.70 ppm (16H, vbr, m, CH_2), 1.44 ppm (48H, vbr, m, CH_2) and one multiplet at 0.90 ppm (8H, vbr, m, CH) which indicates the presence of a *cyclo*-pentyl group. The ^{13}C NMR spectrum is in complete agreement with this assumption: it exhibited peaks at δ 22.3 ppm (CH); δ 27.0 ppm (-CH_2-); δ 27.3 ppm (-CH_2-).

As with *cyclo*-hexyltripropoxysilane, we concluded that the reaction of *cyclo*-pentyltripropoxysilane using the same TBAF synthetic route did not give an encapsulated fluoride ion cage. The reaction only gave the conventional octa-*cyclo*-pentyloctasilsesquioxane cage.

5.4 Reaction with *iso*-butyltrialkoxysilane

An experiment (MP203) was conducted using toluene as the solvent. In this experiment we dissolved 1.02 g of *iso*-butyltrimethoxysilane (5.7 mmol) in toluene (b.p. of toluene: 110.6°C). We then added 2.5 ml of tetra-*n*-butylammonium fluoride (1M solution in THF, 2.5mmol) so we had a 1:2.3 ratio of siloxane to TBAF. After 24 hours, the reaction was stopped and the solvent removed on a rotary evaporator at a temperature of 80°C and a vacuum of 75 mbar for 15 minutes. A brown gel was obtained.

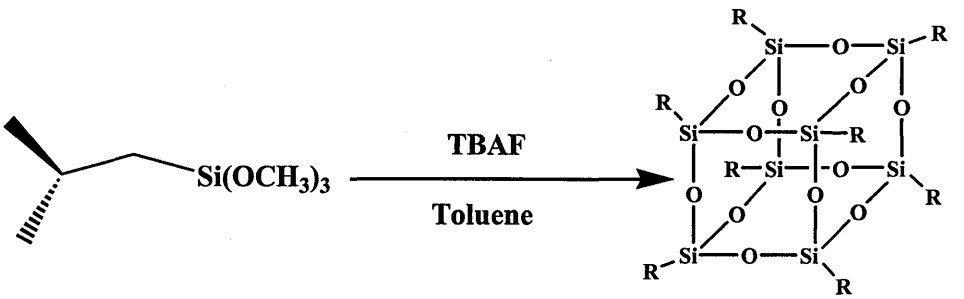

The ^{29}Si NMR spectrum (in $CDCl_3$) displayed a single sharp peak in the T-Si area with a chemical shift of -67.9 ppm. The ^{19}F NMR spectrum did not show any peaks with a chemical shift in the area described previously for an encapsulated fluoride ion (around -25 ppm). This demonstrated that no fluoride ion had been incorporated in this reaction and that we are reasonably confident that we had synthesized an octa-*iso*-butyloctasilsesquioxane cage. In fact, Yuxing Yang had reported the synthesis of the octa-*iso*-butyloctasilsesquioxane cage with a ^{29}Si NMR chemical shift of -67.9 ppm. The ^{1}H NMR shows two doublets with chemical shifts of 0.18 ppm (16H, d, $SiCH_2$), 0.54 ppm (48H, d, CH_3) and one multiplet at 1.35-1.53 ppm (8H, m, CH) which indicated the presence of a *iso*-butyl group. The ^{13}C NMR spectrum confirmed the synthesis of the octa-*iso*-butyloctasilsesquioxane cage: it exhibited peaks at δ 22.5 ppm ($SiCH_2$); δ 23.9 ppm (-CH-); δ 25.7 ppm ($-CH_3$).

We also obtained some crystals from our sample using the vapour diffusion method. A small amount of a saturated solution in toluene was placed in a narrow tube, which was itself placed in a wider tube which contained a solution of the precipitant (acetone). The precipitant was thus allowed to diffuse into the solution. After 7 days we observed the formation of small crystals at the bottom of the tube. We obtained 0.42g of colourless crystals which represent an isolated yield of 67%. The structure of the octa-*iso*-butyloctasilsesquioxane cage was confirmed by single-crystal X-ray crystallography as shown in Figure 72 and is in agreement with that obtained by ZhiHua Liu[82].

Figure 72 Octa-*iso*-butyloctasilsesquioxane cage

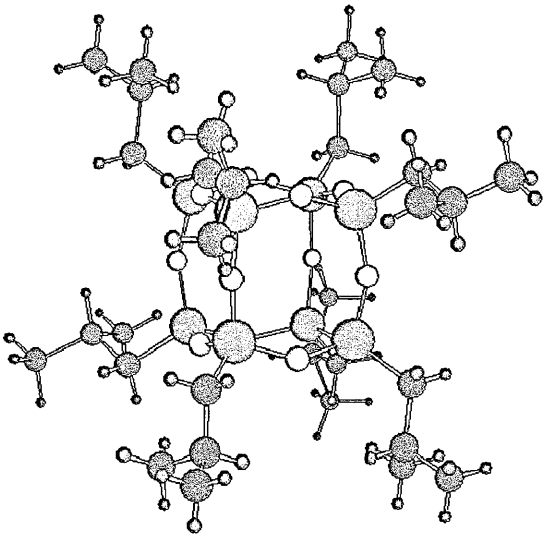

We concluded that the reaction with *iso*-butyltrimethoxysilane using the same TBAF synthetic route did not give us a new encapsulated fluoride ion cage. The reaction only gave the conventional octa-*iso*-butyloctasilsesquioxane cage.

5.5 Reaction with 5-*bicyclo*-heptenyltrialkoxysilane

The 5-*bicyclo*-heptenyltrichlorosilane was purchased as a mixture of *endo*-5-*bicyclo*-heptenyltrichlorosilane and *exo*-5-*bicyclo*-heptenyltrichlorosilane as shown in the Figure 73 below. The first experiment (MP54) was conducted using acetone as the solvent. In this experiment we dissolved 0.98 g of 5-*bicyclo*-heptenyltributoxysilane (2.9 mmol) in acetone. We then added 2.5 ml of tetra-*n*-butylammonium fluoride (1M solution in THF, 2.5mmol) so we had a 1:1.2 ratio of siloxane to TBAF. After 24 hours, the reaction was stopped. A white solid was obtained after removing the solvent on a rotary evaporator at a temperature of 40°C and a vacuum of 80 mbar for 15 minutes.

Figure 73 Reaction of 5-*bicyclo*-heptenyltripropoxysilane with TBAF

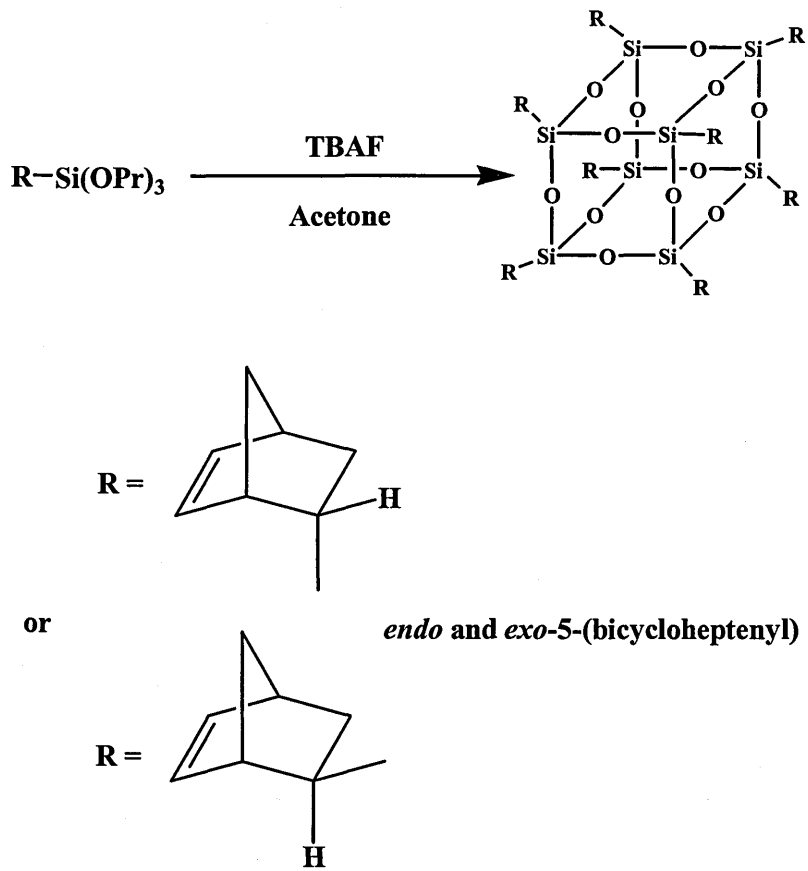

The ^{29}Si NMR spectrum (in $CDCl_3$) displayed two sets of three peaks in the T-Si region with chemical shifts of -68.4 and -67.6 ppm with a ratio of 2:1 respectively. Each set had a ratio of 1:3:1. The ^{19}F NMR spectrum did not show any peaks with a chemical shift in the area described previously for an encapsulated fluoride ion (around -25 ppm). This demonstrated that no fluoride ion had been incorporated in this reaction and that we are reasonably confident that we had synthesized an octa-5-*bicyclo*-heptenyloctasilsesquioxane cage. In fact, ZhiHua Liu has reported the synthesis of a pure octa-*endo*-5-*bicyclo*-heptenyloctasilsesquioxane cage with a ^{29}Si NMR chemical shift of -68.7 ppm and a pure octa-*exo*-5-*bicyclo*-heptenyloctasilsesquioxane cage with a ^{29}Si NMR chemical shift of -66.9

ppm. From our result we concluded that we had obtained a mixture of cages with *endo* and *exo* groups. The ^{1}H NMR displayed multiplets with chemical shifts of 0.40 ppm (1H, m, SiC**H**), 1.25 ppm (2H, m, SiCHC**H**$_2$), 1.70 ppm (1H, m, SiCHCH$_2$C**H**), 2.90 ppm (2H, m, SiCHCHC**H**$_2$), 5.95 ppm (1H, m, C**H**=C**H**) and one multiplet at 6.12 ppm (1H, m, C**H**=C**H**) which arose from the *exo*-5-*bicyclo*-heptenyl group. There were also multiplets with chemical shifts of 1.11 ppm (2H, m, SiCHC**H**$_2$), 1.29 ppm (1H, m, SiCHCH$_2$C**H**), 1.83 ppm (1H, m, SiC**H**), 2.90 ppm (1H, m, SiCHCHC**H**$_2$), 3.00 ppm (1H, m, SiCHCHC**H**$_2$) and one multiplet at 5.95 ppm (2H, m, C**H**=C**H**) which arose from the *endo*-5-*bicyclo*-heptenyl group. These two sets of multiplet gave a exo: endo ratio of 1:2. The ^{13}C NMR spectrum displayed peaks with chemical shifts of 21.4 ppm (Si**C**H), 26.8 ppm (SiCH**C**H$_2$), 42.5 ppm (SiCH**C**H), 44.3 ppm (SiCHCH$_2$**C**H), 50.7 ppm (SiCHCH**C**H$_2$), 133.8 ppm (**C**H=**C**H) and 135.6 ppm (**C**H=**C**H) which arose from the *endo*-5-*bicyclo*-heptenyl group. Additionally it showed peaks with chemical shifts of 21.3 ppm (Si**C**H), 26.4 ppm (SiCH**C**H$_2$), 42.3 ppm (SiCH**C**H), 42.8 ppm (SiCHCH$_2$**C**H), 46.9 ppm (SiCHCH**C**H$_2$), 133.9 ppm (**C**H=**C**H) and 137.6 ppm (**C**H=**C**H) which arose from the *exo*-5-*bicyclo*-heptenyl group.

A second experiment (MP57) was conducted using acetone as the solvent. In this experiment we dissolved 0.39 g of 5-*bicyclo*-heptenyltripropoxysilane (1.3 mmol) in acetone. We then added 2.5 ml of tetra-*n*-butylammonium fluoride (1M solution in THF, 2.5mmol) so we had a 1:0.5 ratio of siloxane to TBAF. After 24 hours, the reaction was stopped. A white solid was obtained after removing the solvent on a rotary evaporator at a temperature of 40°C and a vacuum of 80 mbar for 15 minutes.

The ^{29}Si NMR, ^{19}F NMR, ^{1}H NMR and ^{13}C NMR spectra (in $CDCl_3$) were identical to those obtained in the first experiment (MP54).

We concluded that the reaction with 5-*bicyclo*-heptenyltripropoxysilane and 5-*bicyclo*-heptenyltributoxysilane with TBAF did not give a new encapsulated fluoride ion cage. The reaction only gave the conventional octa-5-*bicyclo*-heptenyloctasilsesquioxane cage.

5.6 Reaction with 3-*para*-methoxyphenylpropyltrialkoxysilane

The first experiment (MP50) was conducted using THF as the solvent. In this experiment we dissolved 1.63 g of 3-*para*-methoxyphenylpropyltriethoxysilane (5.2 mmol) in THF (b.p. of THF: 66°C). We then added 2.5 ml of tetra-*n*-butylammonium fluoride (1M solution in THF, 2.5mmol) so we had a 1:2.1 ratio of siloxane to TBAF. After 24 hours, the reaction was stopped and the solvent removed on a rotary evaporator at a temperature of 80°C and a vacuum of 80 mbar for 15 minutes. A brown-red gel was obtained.

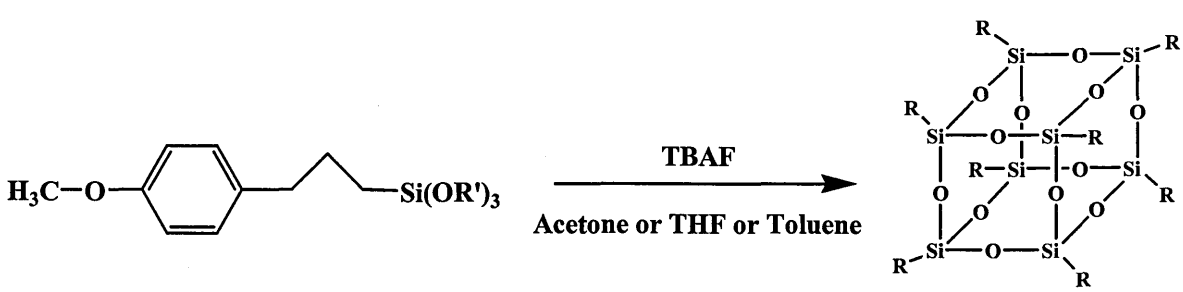

The ^{29}Si NMR spectrum (in $CDCl_3$) displayed a single sharp peak in the T-Si area with a chemical shift of -68.7 ppm. The ^{19}F NMR spectrum did not show any peaks with a chemical shift in the area described previously for an encapsulated fluoride ion (around -25 ppm). This demonstrated that no fluoride ion had been incorporated in this reaction. Yuxing Yang reported the synthesis of the octa-3-*para*-methoxyphenylpropyloctasilsesquioxane

cage with a ^{29}Si NMR chemical shift of -66.8 ppm. There is about a 2 ppm difference in between the ^{29}Si NMR chemical shift of the octa-3-*para*-methoxyphenylpropyloctasilsesquioxane cage and the compound we had synthesized. Based on Marsmann's equation ($\delta T_{10}R_{10} = 1.028 \times \delta T_8R_8$), the peak at -68.7 probably arose from the deca-3-*para*-methoxyphenylpropyldecasilsesquioxane cage. The ^1H NMR shows peaks with chemical shifts of 0.31 ppm (16H, t, $SiCH_2$), 1.10 ppm (16H, m, $SiCH2CH_2CH_2Ar$), 3.15 ppm (16H, t, $SiCH2CH_2CH_2Ar$), 3.17 ppm (24H, s, CH_3OAr), 6.17 ppm (16H, d, CH=CH) and at 6.50 ppm (16H, d, CH=CH) which indicated the presence of a 3-*para*-methoxyphenylpropyl group. The ^{13}C NMR spectrum is in complete agreement with this assumption: it exhibited peaks at δ 13.8 ppm ($SiCH_2$); δ 28.9 ppm ($SiCH_2CH_2$); δ 38.6 ppm ($ArCH_2$), δ 55.0 ppm (CH_3), δ 113.4 ppm (CH=CH), δ 129.1 ppm (CH=CH), δ 134.5 ppm (C of Ar) and δ 157.4 ppm (C of Ar).

A second experiment (MP80) was conducted using acetone as the solvent. In this experiment we dissolved 1.09 g of 3-*para*-methoxyphenylpropyltripropoxysilane (3.1 mmol) in acetone (b.p. of acetone: 56°C). We then added 2.5 ml of tetra-*n*-butylammonium fluoride (1M solution in THF, 2.5mmol) so we had a 1:0.4 ratio of siloxane to TBAF. After 24 hours, the reaction was stopped and the solvent removed on a rotary evaporator at a temperature of 40°C and a vacuum of 80 mbar for 15 minutes. A brown-red gel was obtained.

The ^{29}Si NMR spectrum (in $CDCl_3$) displayed two sharp peaks in the T-Si region with chemical shifts of -68.7 ppm and -66.9 ppm. The peak at -68.7 ppm arises from the deca-3-*para*-methoxyphenylpropyldecasilsesquioxane cage and the peak at -66.9 ppm from the octa-3-*para*-methoxyphenylpropyloctasilsesquioxane cage. We also distinguished two small

peaks with chemical shifts of -68.6 and -71.2 ppm in a ratio of 1:2 which fit perfectly with the dodeca-3-*para*-methoxyphenylpropyldodecasilsesquioxane cage according to Marsmann's equation ($\delta'T_{12}R_{12} = 1.025 \times \delta T_8R_8$ and $\delta''T_{12}R_{12} = 1.064 \times \delta T_8R_8$). The ^{19}F NMR spectrum did not show any peaks with a chemical shift in the area described previously for an encapsulated fluoride ion (around -25 ppm). This demonstrated that no fluoride ion had been incorporated in this reaction.

A third experiment (MP85) was conducted using toluene as the solvent. In this experiment we dissolved 1.11 g of 3-*para*-methoxyphenylpropyltripropoxysilane (3.1 mmol) in toluene (b.p. of toluene: 110.6°C). We then added 2.5 ml of tetra-*n*-butylammonium fluoride (1M solution in THF, 2.5mmol) so we had a 1:0.4 ratio of siloxane to TBAF. After 24 hours, the reaction was stopped and the solvent removed on a rotary evaporator at a temperature of 80°C and a vacuum of 80 mbar for 15 minutes. A brown-red gel was obtained.

The ^{29}Si NMR spectrum (in $CDCl_3$) displayed two sharp peaks in the T-Si region with chemical shifts of -68.7 ppm and -66.9 ppm which again, based on Marsmann's equation and Yuxing Yang's work, arise respectively from the octa-3-*para*-methoxyphenylpropyloctasilsesquioxane and deca-3-*para*-methoxyphenylpropyldecasilsesquioxane cages. The ^{19}F NMR spectrum did not show any peaks with a chemical shift in the encapsulated fluoride ion area (around -25 ppm). This confirmed that no fluoride ion had been incorporated in this reaction.

We concluded that the reaction with 3-*para*-methoxyphenylpropyltrialkoxysilane using the same TBAF synthetic route did not give a new encapsulated fluoride ion cage. The reaction

only gave the conventional octa, deca and dodeca-3-*para*-methoxyphenylpropyloctasilsesquioxane cages.

5.7 Reaction with methyltripropoxysilane

The experiment (MP243) was conducted using toluene as the solvent. In this experiment we dissolved 1.04 g of methyltripropoxysilane (4.7 mmol) in toluene (b.p. of toluene: 110.6°C). We then added 2.5 ml of tetra-*n*-butylammonium fluoride (1M solution in THF, 2.5mmol) so we had a 1:1.9 ratio of siloxane to TBAF. After 24 hours, the reaction was stopped and the solvent removed on a rotary evaporator at a temperature of 80°C and a vacuum of 80 mbar for 15 minutes. A gel was obtained.

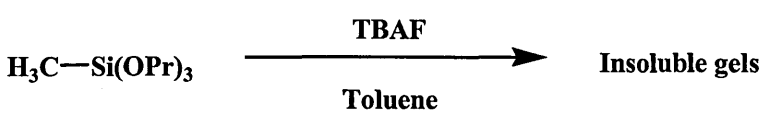

Although both structures of octamethyloctasilsesquioxane and decamethyldecasilsesquioxane have been reported in literature (ref) and confirmed by single crystal X-ray crystallography, we only obtained insoluble gels which we were not able to characterize.

5.8 Reaction with allyltriethoxysilane

The experiment (MP222) was conducted using toluene as the solvent. In this experiment we dissolved 1.04 g of allyltriethoxysilane (5.1 mmol) in toluene (b.p. of toluene: 110.6°C). We then added 2.5 ml of tetra-*n*-butylammonium fluoride (1M solution in THF, 2.5mmol) so we had a 1:2 ratio of siloxane to TBAF. After 24 hours, the reaction was stopped and the solvent removed on a rotary evaporator at a temperature of 80°C and a vacuum of 80 mbar for 15 minutes. A yellow gel was obtained.

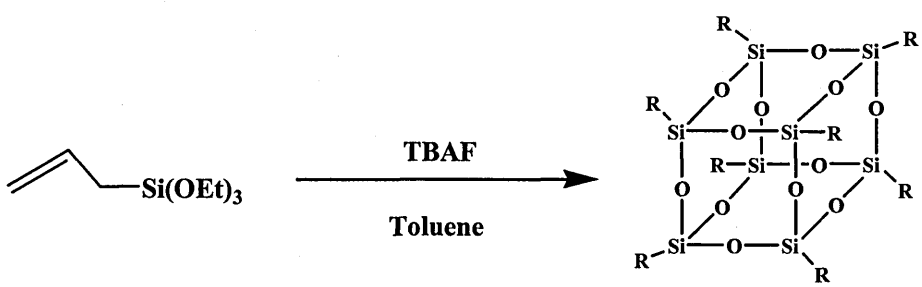

The ^{29}Si NMR spectrum (in $CDCl_3$) displayed sharp peaks in the T-Si region with chemical shifts of -71.5 ppm, -73.4 ppm, -73.6 ppm and -76.1 ppm. Based on Marsmann's equation and Yuxing Yang's work, the main peak at -73.6 ppm arises from the decaallyldecasilsesquioxane cage, the two peaks at -73.4 ppm and -76.1 ppm are associated with the dodecaallyldodecasilsesquioxane cage and the small peak at -71.5 ppm arises from the octaallyloctasilsesquioxane cage. The ^{19}F NMR spectrum did not show any peaks with a chemical shift in the area described previously for an encapsulated fluoride ion (around -25 ppm). This demonstrated that no fluoride ion had been incorporated in this reaction. The ^{1}H

NMR showed peaks with chemical shifts of 0.86-1.12 ppm (16H, m, $SiCH_2$), 4.26-4.55 ppm (16H, m, $SiCH_2CHCH_2$) and 5.07-5.12 ppm (8H, m, $SiCH_2CHCH_2$) which indicated the presence of an allyl group. The ^{13}C NMR spectrum is in complete agreement with this assumption: it exhibited peaks at δ 13.8 ppm ($SiCH_2$); δ 114.6 ppm ($SiCH_2CHCH_2$) and δ 131.7 ppm ($SiCH_2CHCH_2$).

We concluded that the reaction with allyltriethoxysilane using the same TBAF synthetic route did not give a new encapsulated fluoride ion cage. The reaction only gave the conventional octa, deca and dodecaallyltriethoxysilane cages.

5.9 Reaction with *n*-hexyltriethoxysilane

The experiment (MP229) was conducted using toluene as the solvent. In this experiment we dissolved 1.07 g of *n*-hexyltriethoxysilane (4.3 mmol) in toluene (b.p. of toluene: 110.6°C). We then added 2.5 ml of tetra-*n*-butylammonium fluoride (1M solution in THF, 2.5mmol) so we had a 1:1.7 ratio of siloxane to TBAF. After 24 hours, the reaction was stopped and the solvent removed on a rotary evaporator at a temperature of 80°C and a vacuum of 80 mbar for 15 minutes. A gel was obtained.

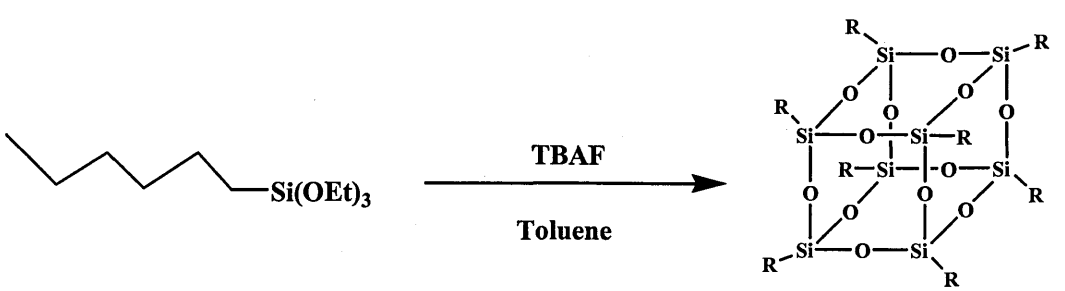

The ^{29}Si NMR spectrum (in $CDCl_3$) displayed one single sharp peak in the T-Si region with a chemical shift of -66.6 ppm. Based on Zhihua Liu's work[82], the peak at -66.6 ppm arises

from the octa-*n*-hexyloctasilsesquioxane cage. The ^{19}F NMR spectrum did not show any peaks with a chemical shift in the area described previously for an encapsulated fluoride ion (around -25 ppm). This demonstrated that no fluoride ion had been incorporated in this reaction. The ^{1}H NMR showed peaks with chemical shifts of 0.61 ppm (16H, t, $SiCH_2$ CH_2), 0.89 ppm (24H, t, CH_2CH_3) and 1.31 ppm (64H, m, $SiCH_2CH_2CH_2CH_2CH_2CH_3$) which indicated the presence of the *n*-hexyl group. The ^{13}C NMR spectrum is in complete agreement with this assumption: it exhibited peaks at δ 11.9 ppm ($SiCH_2$), δ 14.1 ppm (CH_2CH_3), δ 22.5 ppm ($SiCH_2CH_2CH_2CH_2CH_2CH_3$), δ 22.6 ppm ($SiCH_2CH_2CH_2CH_2CH_2CH_3$), δ 31.5 ppm ($SiCH_2CH_2CH_2CH_2CH_2CH_3$) and δ 32.4 ppm ($SiCH_2CH_2CH_2CH_2CH_2CH_3$).

We concluded that the reaction with *n*-hexyltriethoxysilane using the same TBAF synthetic route did not give a new encapsulated fluoride ion cage. The reaction only gave the conventional octa-*n*-hexyloctasilsesquioxane cage.

5.10 Reaction with 2-chloroethyltriethoxysilane

The experiment (MP230) was conducted using toluene as the solvent. In this experiment we dissolved 1.10 g of 2-chloroethyltriethoxysilane (4.9 mmol) in toluene (b.p. of toluene: 110.6°C). We then added 2.5 ml of tetra-*n*-butylammonium fluoride (1M solution in THF, 2.5mmol) so we had a 1:1.9 ratio of siloxane to TBAF. After 24 hours, the reaction was stopped and the solvent removed on a rotary evaporator at a temperature of 80°C and a vacuum of 80 mbar for 15 minutes. We only obtained an insoluble gel which we could not characterize, as shown in the Figure 74 below.

Figure 74 Reaction of 2-chloroethyltriethoxysilane with TBAF

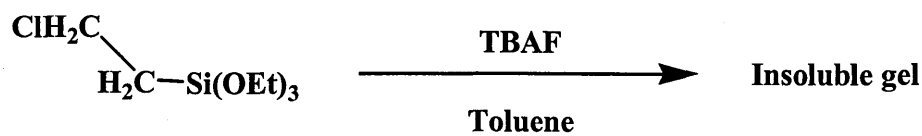

5.11 Reaction with benzyltrialkoxysilane

The first experiment (MP46) was conducted using chloroform as the solvent. In this experiment we dissolved 1.06 g of benzyltributoxysilane (3.1 mmol) in chloroform (b.p. of chloroform: 61°C). We then added 2.5 ml of tetra-*n*-butylammonium fluoride (1M solution in THF, 2.5mmol) so we had a 1:1.3 ratio of siloxane to TBAF. After 24 hours, the reaction was stopped and the solvent removed on a rotary evaporator at a temperature of 50°C and a vacuum of 80 mbar for 15 minutes. A yellow gel was obtained.

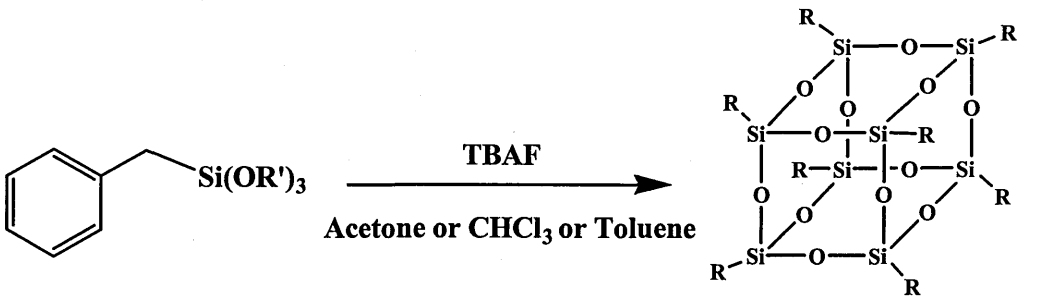

The ^{29}Si NMR spectrum (in $CDCl_3$) displayed sharp peaks in the T-Si region with chemical shifts of -71.3 ppm, -73.0 ppm, -73.1 ppm and -75.6 ppm. Based on Marsmann's equation and Yuxing Yang's work, we concluded that the main peak at -73.1 ppm arises from the decabenzyldecasilsesquioxane cage, the two small peaks at -73.0 ppm and -75.6 ppm are associated with the dodecabenzyldodecasilsesquioxane cage and the small peak at -71.3 ppm arises from the octabenzyloctasilsesquioxane cage. The ^{19}F NMR spectrum did not show any peaks with chemical shifts in the region previously described for the encapsulated fluoride ion (around -25 ppm). This demonstrated that no fluoride ion had been incorporated in this reaction. The ^{1}H NMR showed peaks with chemical shifts of 1.66 ppm (20H, s, $SiCH_2$), 6.21 ppm (20H, m, CH=CH) and 6.45 ppm (30H, m, CH=CH) which indicated the presence of benzyl group. The ^{13}C NMR spectrum is in complete agreement with this assumption: it exhibited peaks at δ 21.2 ppm ($SiCH_2$), δ 124.7 ppm (C of Ar), δ 128.2 ppm (CH=CH), δ 128.7 ppm (CH=CH) and δ 136.6 ppm (CH=CH).

A second experiment (MP84) was conducted using acetone as the solvent. In this experiment we dissolved 1.17 g of benzyltripropoxysilane (3.9 mmol) in acetone (b.p. of

acetone: 56°C). We then added 2.5 ml of tetra-*n*-butylammonium fluoride (1M solution in THF, 2.5mmol) so we had a 1:1.6 ratio of siloxane to TBAF. After 24 hours, the reaction was stopped and the solvent removed on a rotary evaporator at a temperature of 40°C and a vacuum of 80 mbar for 15 minutes. A yellow gel was obtained.

The ^{29}Si NMR spectrum (in $CDCl_3$) displayed one sharp peak in the T-Si region with a chemical shift of -73.2 ppm. The peak at -73.2 ppm arose from the decabenzyldecasilsesquioxane cage. The ^{19}F NMR spectrum did not show any peaks with chemical shifts in the region previously described for the encapsulated fluoride ion (around -25ppm). Thus, no fluoride ion had been incapsulated in this reaction.

A third experiment (MP275) was conducted using toluene as the solvent. In this experiment we dissolved 1.27 g of benzyltriethoxysilane (5.0 mmol) in toluene (b.p. of toluene: 110.6°C). We then added 2.5 ml of tetra-*n*-butylammonium fluoride (1M solution in THF, 2.5mmol) so we had a 1:2 ratio of siloxane to TBAF. After 24 hours, the reaction was stopped and the solvent removed on a rotary evaporator at a temperature of 70°C and a vacuum of 100 mbar for 15 minutes. A yellow gel was obtained.

The ^{29}Si NMR spectrum (in d_6 acetone) displayed one single peak, not in the T-Si region, but with a chemical shift of -99.8 ppm, as shown in Figure 75.

Figure 75 ^{29}Si NMR spectrum of MP275

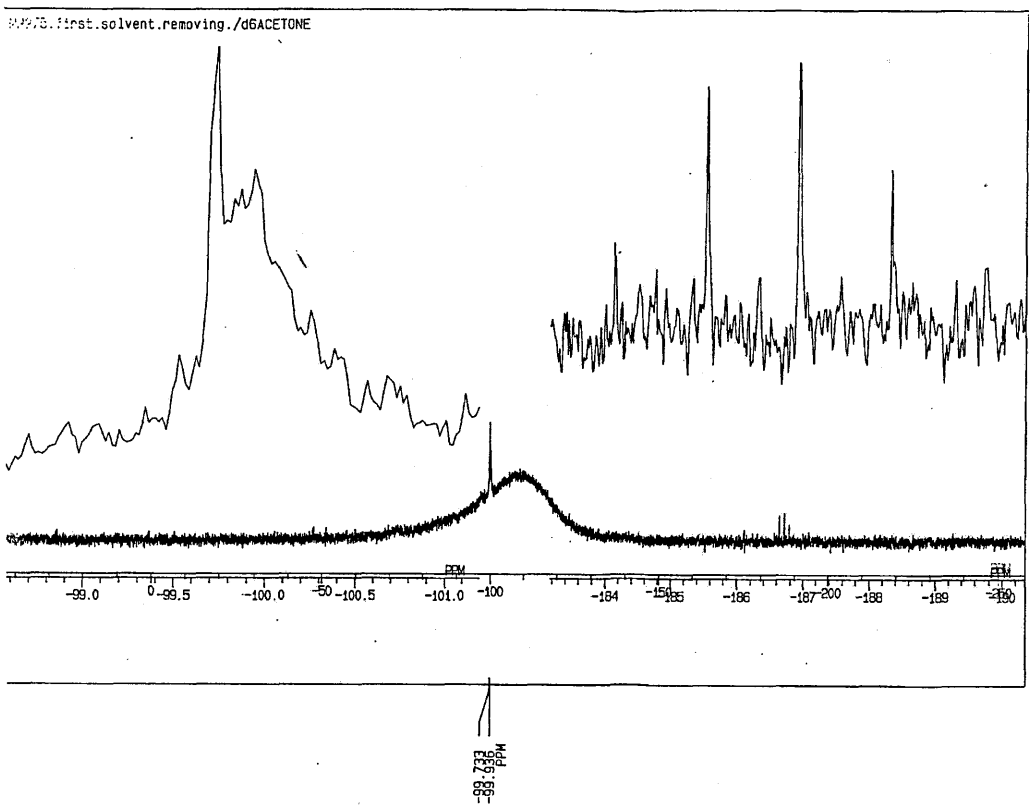

The ^{19}F NMR spectrum showed a series of small peaks with a remarkable pattern in the encapsulated fluoride ion region with chemical shifts of -28.2 ppm, -29.7 ppm, -31.1 ppm, -32.6 ppm, -34.1 ppm, -35.6 ppm and a broad peak at -36.0 ppm (Figure 76).

Figure 76 ^{19}F NMR spectrum of MP275

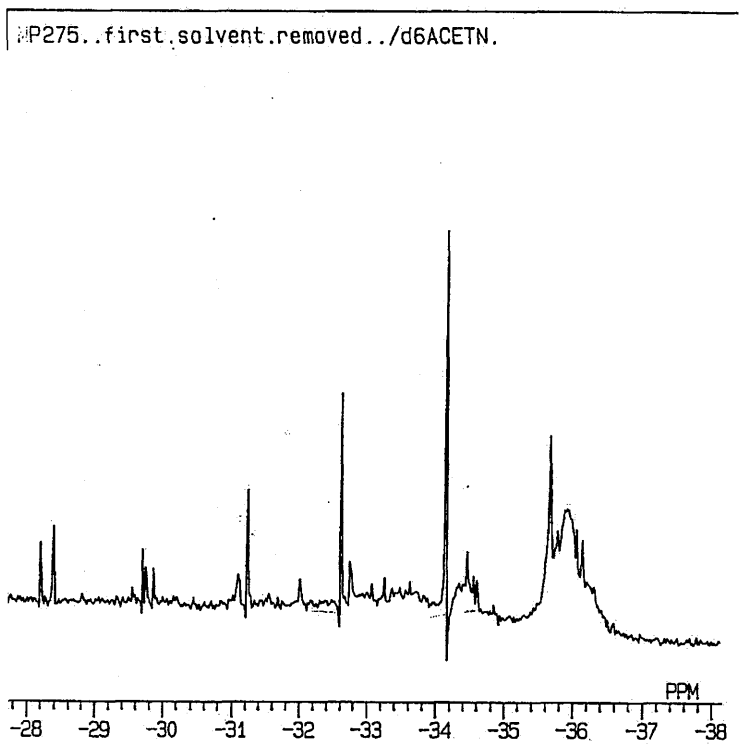

The ^{19}F NMR spectrum confirms the presence of an isolated fluoride ion with weak interactions with the neighbouring silicon atoms. Additionally, we did not observe the formation of any conventional benzyl-T_8 or T_{10} cages. Such peaks in the ^{29}Si NMR with chemical shifts around -99.8 ppm usually arise from spherosilicate cages where the silicon atom is linked with four oxygen atoms. We propose that since the benzyl anion is a better leaving group than an aryl or alkyl anion, under the conditions of the reaction workup a fluoride ion attacks the silicon atom leading to the scission of the carbon-silicon bond as shown in Figure 77. If water is present in a sufficient amount the reaction can go all the way to form the spherosilicate cage.

Figure 77 Mechanism proposal for scission of the carbon-silicon bond in benzyl-T_8 cage

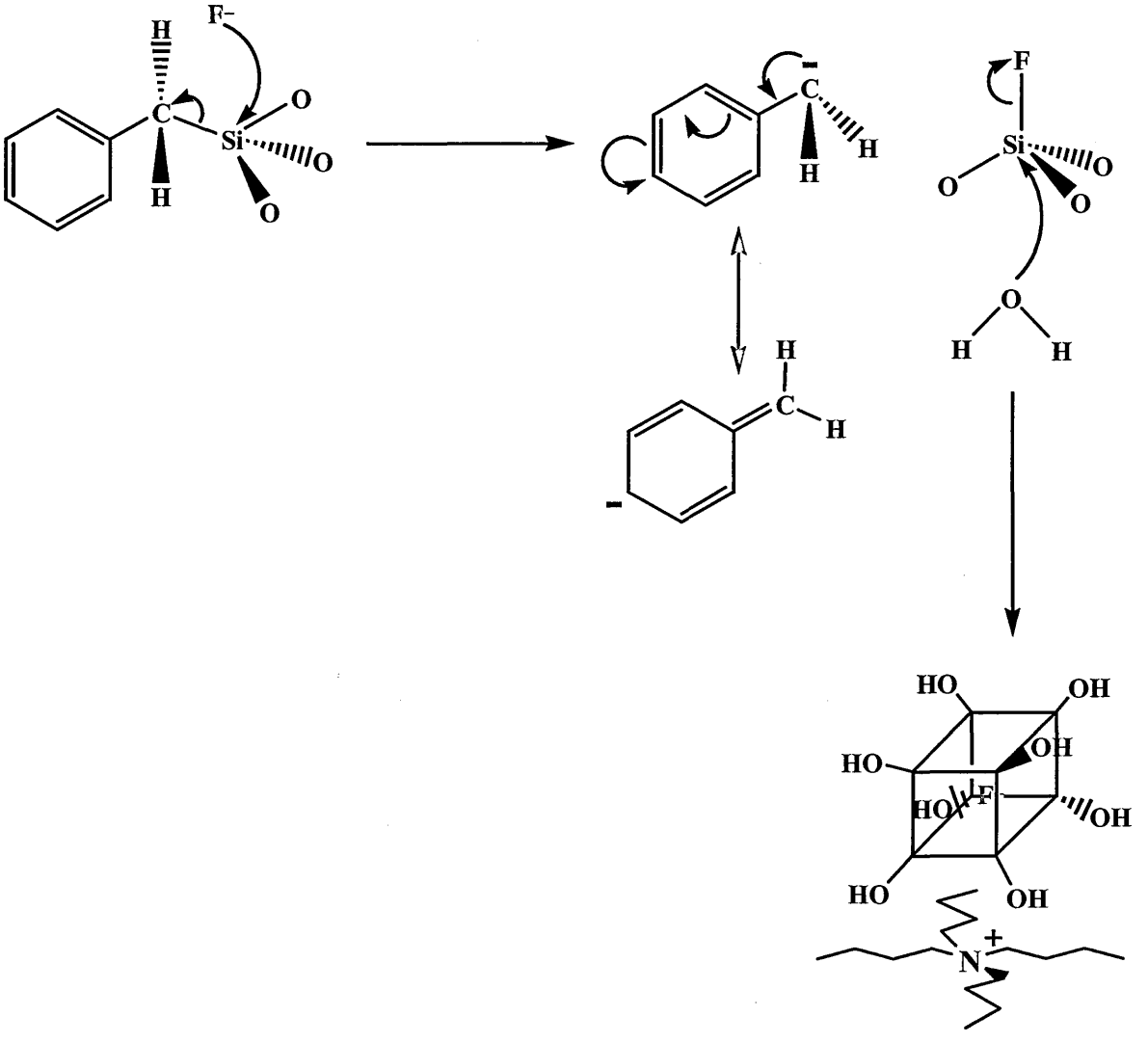

We would like to suggest that the fluoride ion is encapsulated within the spherosilicate cage, however we have not been able to obtain convincing evidence for such a suggestion other than the series of ^{19}F NMR peaks in the region -28 ppm to -38 ppm. Caullet[62] has shown that a fluoride ion encapsulated in the double D4R ring of a zeolite exhibits a ^{19}F NMR chemical shift of -38.2 ppm. The pattern we obtained between -28 ppm and -38 ppm is reminiscent of coupling, possibly with the eight hydrogens of the OH groups (J = 580 Hz). However we only see one arm of this splitting pattern and, apart from a slightly broadened ^{29}Si NMR peak, no Si-F coupling is observed in this region. We have not been able to send a sample for MS analysis because of the quick degradation of the gel to resin like material.

The last experiment (MP282) was conducted using chloroform as the solvent. In this experiment we dissolved 0.78 g of benzyltriethoxysilane (3.1 mmol) in chloroform (b.p. of chloroform: 61°C). We then added 2.5 ml of tetra-*n*-butylammonium fluoride (1M solution in THF, 2.5mmol) so we had a 1:1.3 ratio of siloxane to TBAF. After 24 hours, the reaction was stopped and the solvent removed on a rotary evaporator at a temperature of 40°C and a vacuum of 80 mbar for 15 minutes. A yellow gel was obtained.

The ^{29}Si NMR spectrum (in d_6 acetone) displayed sharp peaks in the T-Si region with chemical shifts of -70.5 ppm, -70.7 ppm, -70.9 ppm, -71.1 ppm, -73.0 ppm, -74.5 ppm, -75.5 ppm and -76.2 ppm, as shown in Figure 78.

Figure 78 ^{29}Si NMR spectrum of MP282

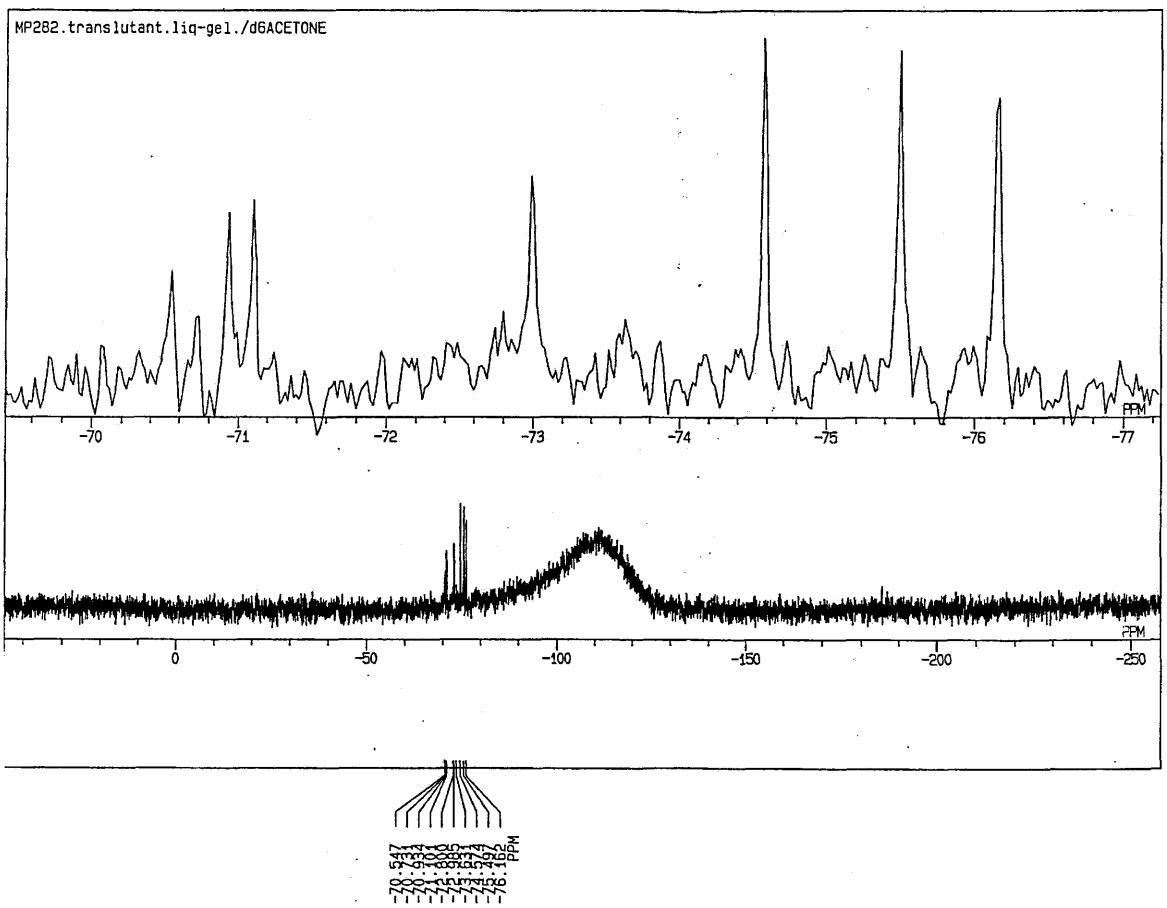

The ^{19}F NMR spectrum showed two small peaks in the encapsulated fluoride ion region with chemical shifts of -26.5 ppm and -29.0 ppm. The ^{19}F NMR spectrum confirmed the presence of two isolated fluoride ion species with weak interactions with their neighbouring silicon atoms. The ^{29}Si NMR chemical shift at -73.0 ppm usually arises from the decabenzyldecasilsesquioxane cage. The two doublets at -70.5 ppm/-70.7 ppm and -70.9 ppm/-71.1 ppm together with the three peaks at -74.5 ppm, -75.5 ppm and -76.2 ppm, suggest a fluoride ion encapsulated in a benzyl-$T_9(OH)_3$ species, as shown in the Figure 79 below.

Figure 79 Suggestion of structure for a fluoride ion encapsulated in a benzyl-$T_9(OH)_3$ species

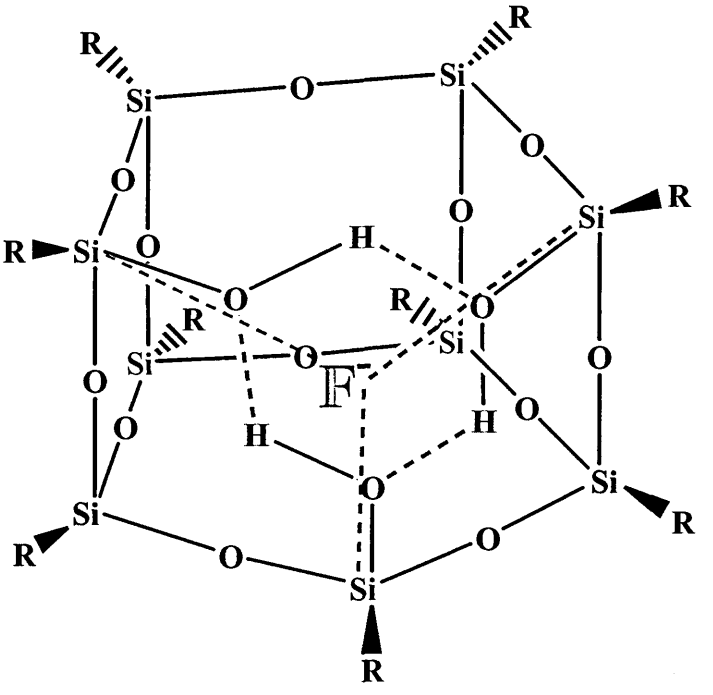

R = benzyl

The doublet in the region of -70.7 ppm arises from Si-OH centres where the better leaving group ability of OHs leads to increased Si-F interactions and thus coupling. The 2:1 ratio of the doublets is in agreement with this assignement. This then leaves four pairs of equivalent silicon atoms leading to the other four peaks.

We conclude that the reaction of TBAF with benzyltrialkoxysilane did not result in the encapsulation of the fluoride ion within the octasilsesquioxane cage, since we did not isolate and characterize such a species. However, the reaction with benzyltriethoxysilane did provide some interesting results based on the ^{29}Si NMR spectra and we suggest the formation of an open cage, benzyl-$T_9(OH)_3$, where the fluoride ion would be located towards the open edge of the cage, but closed in by the three OH groups. This fluoride is not

located in the centre of the cage but has weak interactions with the three silicon atoms attached to the hydroxyl groups (-SiOH), resulting in the presence of two pairs of doublets in the ^{29}Si NMR spectrum in a ratio 1:2. Unfortunately, we have not been able to confirm this suggestion as no further evidence has been obtained.

5.12 Is the encapsulation of a fluoride anion possible when the R group on the silicon atom is attached by an sp carbon atom ?

As we have investigated the synthesis of an encapsulated fluoride ion within an octasilsesquioxane cage with an of sp^3 carbon atom attached to the silicon atoms, we will examine the possible synthesis of trialkoxysilane with an sp carbon atom aatached to the silicon and its reaction with TBAF.

Sodium amide ($NaNH_2$) granular was weighed (2.6g, 67.5 mmol) and rapidly place in a mortar with dry toluene to be crushed into a fine suspension.The suspension liquid was added to 50 ml of dry toluene in a three neck flask with a condensator and under nitrogen. Phenylacetylene was then added slowly (4.6 g, 45 mmol). The reaction flask was placed in a ice bath and the reaction mixture stirred for 4 hours. $Si(OEt)_4$ was added (20.8 g, 0.1 mol), dropping slowly to react with phenylacetylene and neutralize the unreacted sodium amide. As it is an exothermic reaction, the flask was placed in an ice bath and the reaction mixture stirred overnight. After 12 hours, the reaction was stopped and the reaction mixture was brown. $Si(OEt)_4$ was added to neutralize the unreacted sodium amide. After filtration, the filtrate was then distilled under vacuum (b.p. of phenylacetylene = 143°C, b.p. of tetraethylorthosilicate = 168°C and b.p. of amidetriethoxysilane = 66°C at a pressure of 18

mbar). We would expect the phenylacetylenetriethoxysilane to be formed and collected after the distillation. Unfortunately, the ^{29}Si NMR spectrum did not show any peaks.

So the synthesis of a starting material, trialkoxysilane, with an sp carbon atom attached to the silicon atom failed. We decided not to carry on because acetylene is a better leaving than the benzyl group and our previous experience from the reaction of benzyltrilkoxysilane with TBAF had shown little success in the synthesis of an encapsulated fluoride ion in a benzyl cage.

5.13 Conclusion

We have not been able to synthesize an encapsulated fluoride ion within an octasilsesquioxane cage with an sp^3 carbon atom attached to the silicon atoms. As yet we do not have an explanation for the negative outcome of the reactions for the synthesis of these encapsulated fluoride ion cages. If we focus on the interactions and the distribution of partial charges in the cages we have synthesised, the fluoride anion has weak interactions with the silicon atoms which have a δ positive charge which will place a δ negative charge on the carbon atom attached to it. The stability of the fluorine-silicon-carbon arrangement will thus depend upon the carbon atom's capacity to stabilize this δ negative charge and we know that the greater the sp character the greater the ability to stabilize the negative charge. Thus, organic groups with sp^2 and sp carbon atoms at the silicon will result in the encapsulation of the fluoride ion, as we observed for the synthesis of tetra-*n*-butylammonium octaphenyl, octavinyl and octa-*para*-tolyl octasilsesquioxane fluoride cages. However, there is a delicate balance. Whilst sp^3 carbons do not stabilize the F-Si interaction sufficiently sp carbons may stabilize it too well leading to the formation of a F-Si

bond and cleavage of the Si-C_{sp} bond. For an octasilsesquioxane cage with an sp^3 carbon atom attached to the silicon atom which can stabilize a negative charge ocurring to the adjacent phenyl group, the silicon-carbon bond will be weakened by the presence of the fluoride ion within the cage and the Si-C bond will break followed by the destruction of the cage.

The explanation of why the fluoride ion sits perfectly in the middle of the cage is thought to be due to the presence of the LUMO of the silsesquioxane lying at the centre of the cage (Figure 80) as Pittman and co-workers have reported in there studies [84].

Figure 80 Isosurfaces for the HOMO (lower row) and LUMO (upper row) of the octahydrooctasilsesquioxane cage

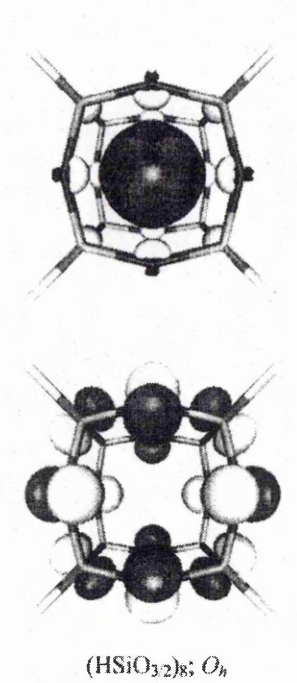

$(HSiO_{3/2})_8$; O_h

This may be the driving force for the fluoride ion to stay within the cage and this could be described as a metastable state where the fluoride ion is effectively isolated, as reflected by its peculiar ^{19}F NMR chemical shift (around -26 ppm).

The benzyl experiment (MP275) led to a peculiar result displaying a peak in the ^{29}Si NMR spectrum with a chemical shift of -99.8 ppm. This ^{29}Si NMR chemical shift is usually

reported to arise from a spherosilicate Q_8 and we suggest that such a species is formed here. There is also some ^{19}F NMR evidence of an encapsulated fluoride ion. In this case the oxygen atom is ideally suited to stabilize the δ negative charge formed due to the weak interaction between the fluoride ion and the silicon. This led us to try to synthesise spherosilicate Q_8 cages using the TBAF synthetic route that we have used for the tetra-*n*-butylammonium octasilsesquioxane cages.

Chapter 6: Synthesis of tetra-*n*-butylammonium octaethoxy- and octapropoxy-octasilsesquioxane fluoride

6.1 Introduction

Silsesquioxane and octasilsesquioxane cages are the building blocks for the synthesis of zeolites. Zeolites are synthesized by hydrothermal and sol-gel methods starting from silica with distilled water and an acid solution together with some structuring agent (template) which is removed by calcination. The literature reports some fluoride ion encapsulation within the double D4R structure when using an organic fluoride salt as the template. We have been able to synthesize a number of octasilsesquioxane T_8 cages with an encapsulated fluoride ion at the centre using the TBAF route. Although the nature of our cages is different from the spherosilicate Q_8 cages encountered in zeolite structures, we are in a position to predict the optimum parameters and conditions for such an encapsulation. It will be very interesting to see if the conditions of the workup of the TBAF synthetic route can be used for the synthesis of spherosilicate Q_8 cages with fluoride ion encapsulation.

6.2 Reaction of tetraethylorthosilicate with TBAF

6.2.1 Experiments

The first experiment (MP292) was conducted using toluene as the solvent. In this experiment we dissolved 2.11 g of tetraethylorthosilicate (10.1 mmol) in toluene. We then added 2.5 ml of tetra-*n*-butylammonium fluoride (1M solution in THF, 2.5mmol) so we had a 1:4 ratio of orthosilicate to TBAF. We removed some of the reaction mixture after 24 hours, 120 hours and 10 days, and in each we removed the solvent (b.p. of toluene: 110.6°C) on a rotary evaporator at a temperature of 50°C and a vacuum of 70 mbar for 15 minutes. A yellow gel was obtained for each sample.

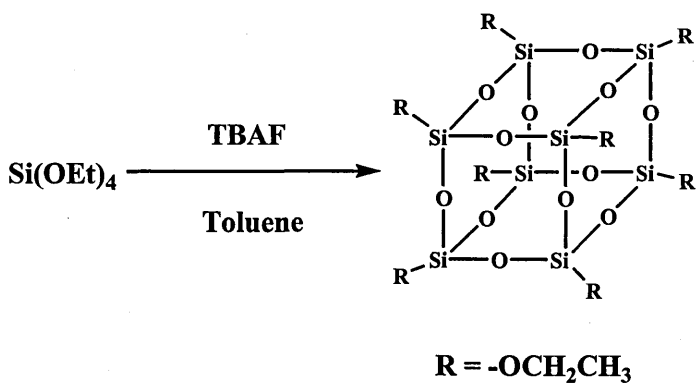

The ^{29}Si NMR spectrum (in d_6 acetone) of the sample after 24 and 120 hours of reaction time were similar and displayed a few peaks in the Q-Si region. The main peak is a doublet with chemical shifts of -99.7 and -99.9 ppm. A large single sharp peak is also present with a chemical shift of -81.9 ppm. Two other doublets can be seen at -88.65 and -88.8 ppm and at -106.7 and -106.9 ppm. The ^{29}Si NMR spectrum (in d_6 acetone) of the sample after 10 days (Figure 81) was similar to the previous samples although the two peripheral doublets with chemical shifts around -88.7 and -106.9 ppm were drastically diminished together with the

peak at -81.9 ppm. This latter peak arises from the starting material, the tetraethylorthosilicate.

Figure 81 ^{29}Si NMR spectrum of MP292

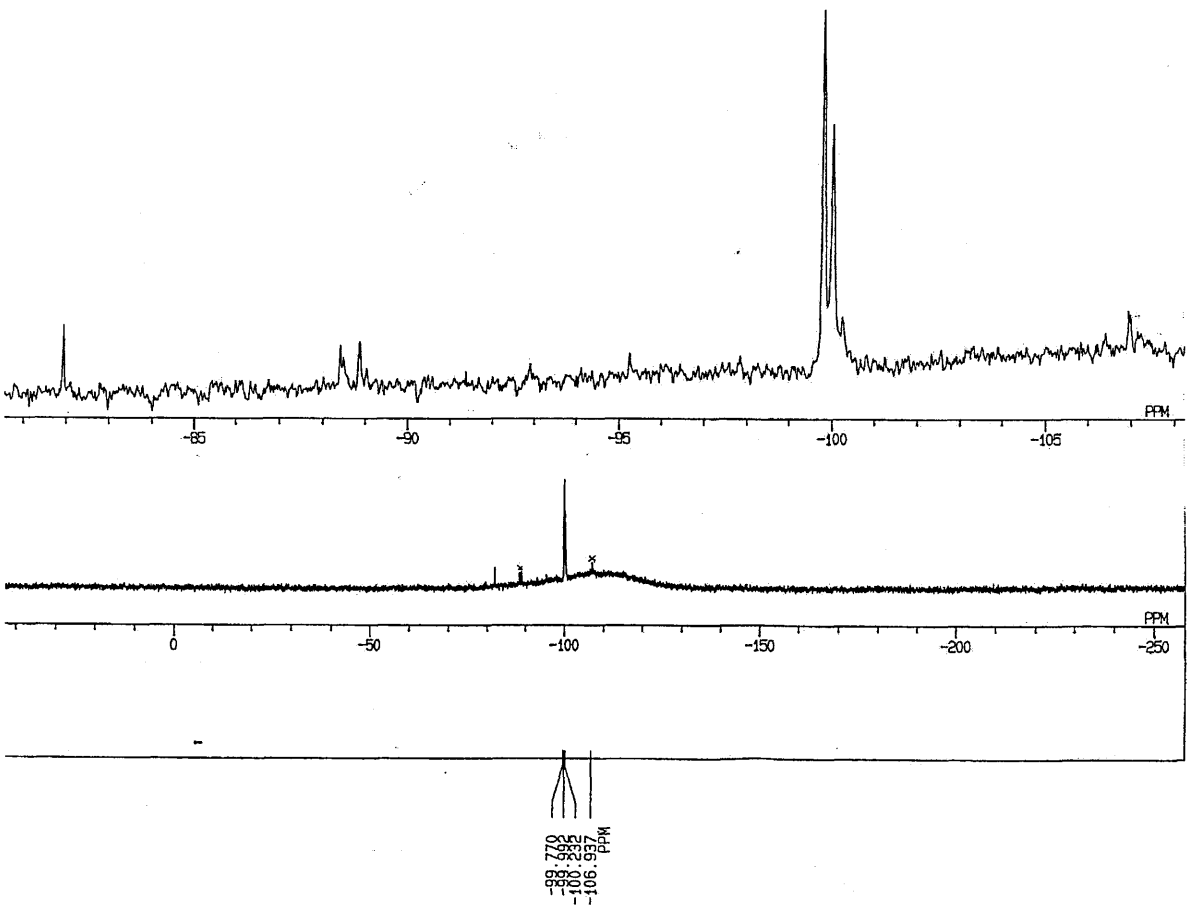

The ^{19}F NMR spectrum displayed three single sharp peaks with chemical shifts at -35.5 ppm, -36.0 ppm and -36.5 ppm, as shown in Figure 82. Such chemical shifts values are similar to that found previously for fluoride anions trapped in the double D4R cage of a zeolite (octadecasil) which has been reported in literature by Caullet and co-workers [62] to be -38.2 ppm. This demonstrates that a fluoride ion has been incorporated in this reaction within a Q_8 structure. However, the fact that we have three different ^{19}F NMR signals in this area suggests the presence of three isolated fluoride ions with three different environments.

Figure 82 ^{19}F NMR spectrum of MP292

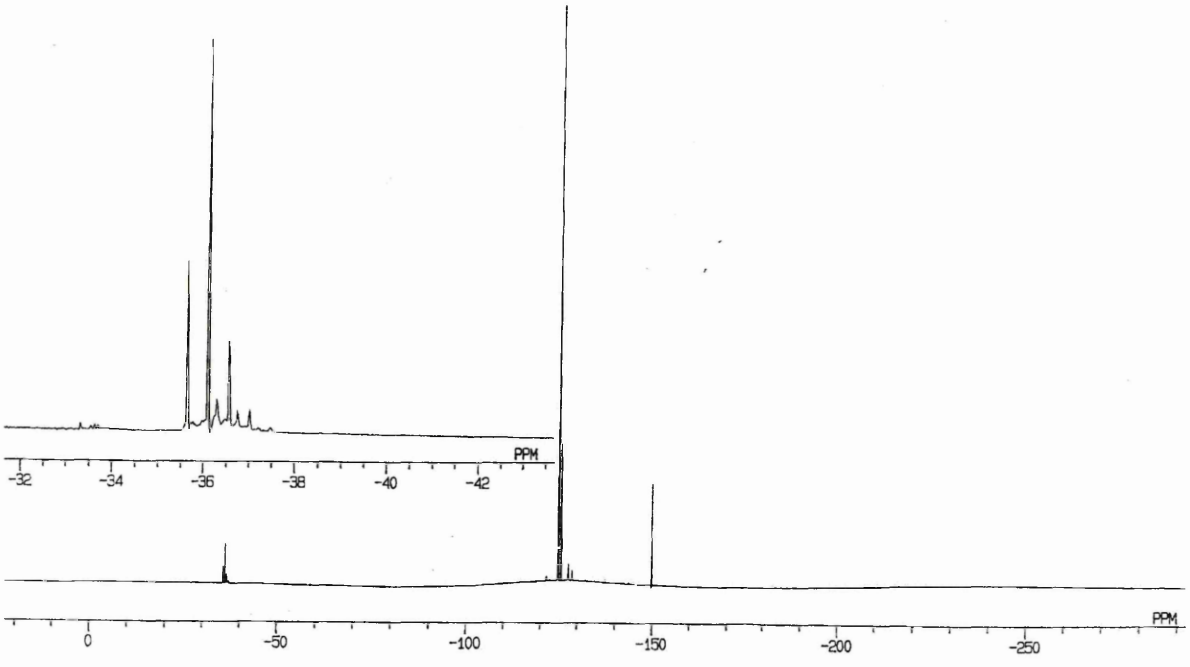

Returning to the ^{29}Si NMR spectrum, Caullet and others observed a doublet with chemical shifts of -106.8 and -107.8 ppm which they ascribed to the silicon atoms forming the double-4-ring within the octadecasil structure. These silicon atoms have a different environment to our Q_8 cage as they involve **Si**-O-Si linkages at the corners. Looking at the chemical shifts between the two species $(CH_3)_3SiOEt$ and $(CH_3)_3SiOSi(CH_3)_3$ with + 18 and + 8 ppm respectively[88], we would expect the silicon atoms of a Q_8 with ethoxy groups to be shifted downfield consistent with the main signal in our sample being a the doublet with ^{29}Si NMR chemical shifts of -99.7 and -99.9 ppm. This peak can reasonably be assigned to a tetra-*n*-butylammonium octaethoxyoctasilsesquioxane fluoride cage as the main product of this reaction.

A second experiment (MP299) was conducted under N_2 using THF as the solvent. In this experiment we dissolved 1.10 g of tetraethylorthosilicate (5.3 mmol) in dry THF. We then

added 1 ml of tetra-*n*-butylammonium fluoride (1M solution in THF, 1 mmol) so we had a 1:5.3 ratio of orthosilicate to TBAF. After 24 hours, the reaction was stopped and the solvent (b.p. of THF: 56°C) removed on a rotary evaporator at a temperature of 55°C and a vacuum of 95 mbar for 15 minutes. A yellow gel was obtained. The ^{29}Si NMR spectrum (in d_6 acetone) of the sample displayed a number of peaks in the Q-Si area. The main peak is a doublet with chemical shifts of -99.7 and -99.9 ppm. The peak assigned to the tetraethylorthosilicate is still present and was fairly large with a chemical shift of -81.9 ppm. Two other doublets of minor intensity can be seen at -88.3 and -88.7 ppm and at -106.9 and -107.1 ppm. The ^{19}F NMR spectrum displayed a major sharp peak with a chemical shift of -36.2 ppm and 5 minor peaks with chemical shifts of -35.7 ppm, -36.4 ppm, -36.6 ppm, -36.7 ppm and -37.1 ppm. Such chemical shifts values are again close to that found previously for fluoride anions trapped in the double D4R structure reported by Caullet and co-workers [62]. This experiment confirms that the signal of the fluoride ion we observe is a little downfield with respect to the encapsulated fluoride ion that Caullet has reported which could be explained by the difference in the environment between the **Si**-OR of this experiment and the **Si**-O-Si in the octadecasil structure. This result confirms that the main product of the tetraethylorthosilicate reaction with TBAF is likely to be the $(Ethoxy)_8Q_8$ compound with an encapsulated fluoride ion within the cage. We have been able to analyse this sample by ESI, MALDI-TOF and negative ion FAB mass spectroscopy. These analyses confirm that the tetra-*n*-butylammonium octaethoxyoctasilsesquioxane fluoride cage was obtained. The ESI mass spectroscopic analysis (Figure 83) shows a fragment at *m/z* 795.4 (100%) corresponding to the $(Ethoxy)_8Q_8$ cage with a fluoride anion ($C_{16}H_{40}FO_{20}Si_8^-$) [$M^-$] (calculated: 795.0) and a fragment at *m/z* 242.3 (100%) corresponding to the tetra-*n*-butylammonium cation ($C_{16}H_{36}N^+$) [M^+] (calculated: 242.3).

Figure 83 ESI mass spectroscopic analysis of MP299

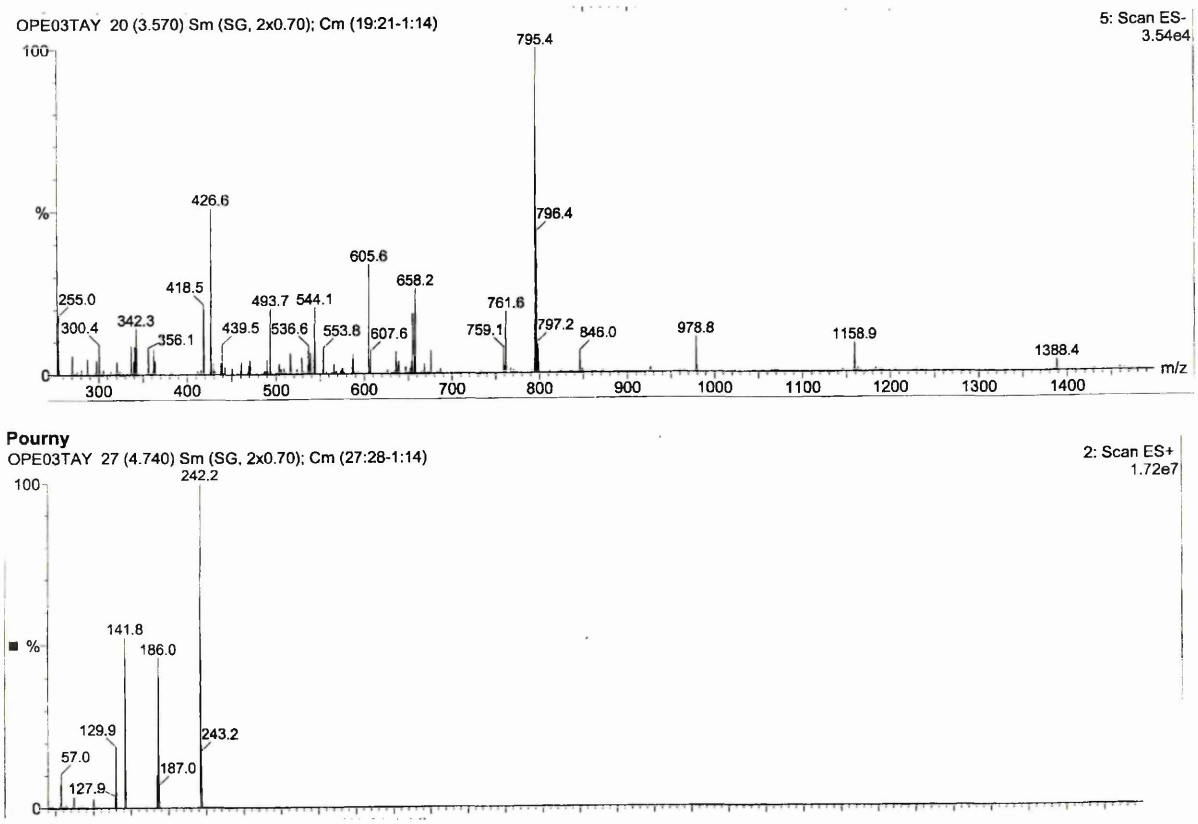

The MALDI-TOF analysis displayed a fragment at *m/z* 795.0 (70%) corresponding to the $(Ethoxy)_8Q_8$ cage with a fluoride anion ($C_{16}H_{40}FO_{20}Si_8^-$) [$M^-$] (calculated: 795.0) and a fragment at *m/z* 242.2 (100%) corresponding to the tetra-*n*-butylammonium cation ($C_{16}H_{36}N^+$) [M^+] (calculated: 242.3). The product was also analysed by negative ion FAB mass spectroscopy as shown in Figure 84.

Figure 84 FAB mass spectroscopic analysis of MP299

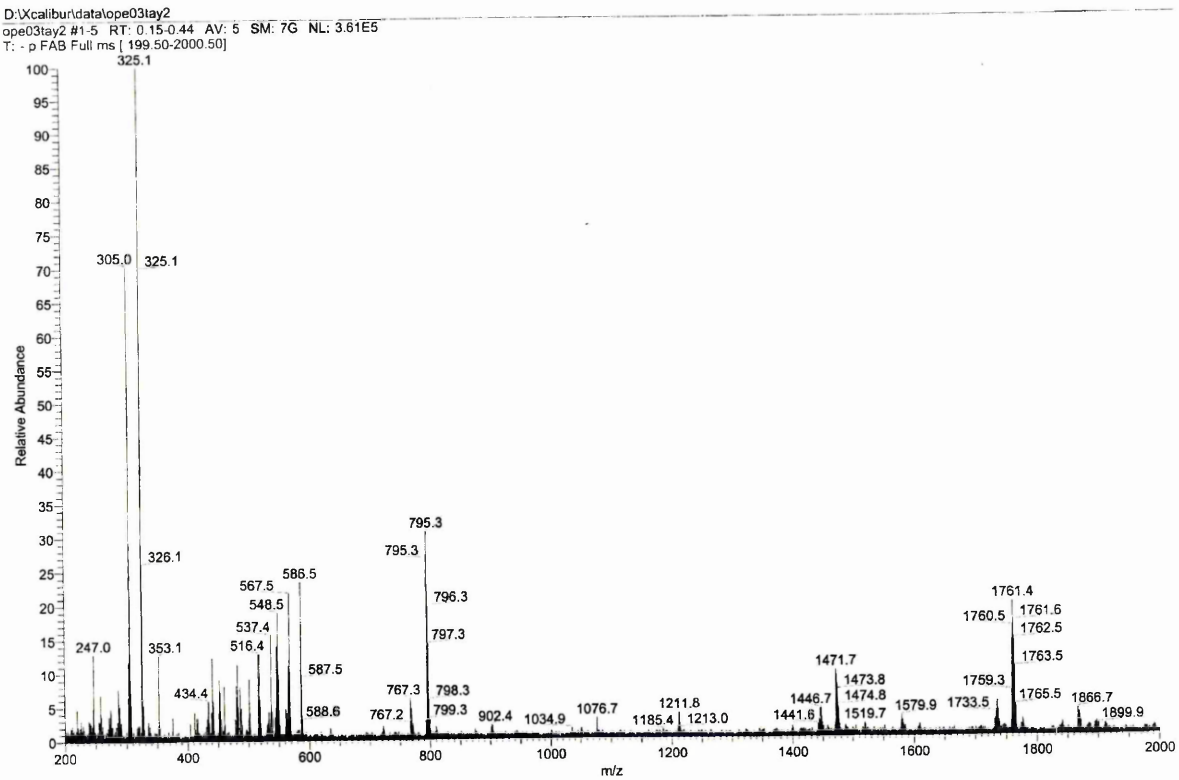

The analysis shows a fragment with a *m/z* of 795.3 corresponding to the $(Ethoxy)_8Q_8$ cage containing the fluoride anion ($C_{16}H_{40}FO_{20}Si_8^-$) but with a low percentage of 35%. This can be explained by the low stability of this compound when using this Mass Spectrometric method. Whilst mass spectroscopic analysis confirms the synthesis of the tetra-*n*-butylammonium octaethoxyoctasilsesquioxane fluoride cage, we still have no explanation for the three different isolated fluoride ion environments we observed using the ^{19}F NMR spectroscopy analysis.

We conducted the same experiment but with an orthosilicate: TBAF ratio of 1:2 under the same conditions: under N_2 and in dry THF (MP300). In this experiment we dissolved 1.10 g of tetraethylorthosilicate (5.3 mmol) in dried THF. We then added 2.5 ml of tetra-*n*-butylammonium fluoride (1M solution in THF, 2.5mmol). After 24 hours, the reaction was

stopped and the solvent (b.p. of THF: 56°C) removed on a rotary evaporator at a temperature of 55°C and a vacuum of 95 mbar for 15 minutes. A yellow gel was obtained. The ^{29}Si NMR spectrum (in d_6 acetone) displayed a major peak with a chemical shift of -99.8 ppm together with a large shoulder at -100.0 ppm. The peak assigned to the tetraethylorthosilicate with a chemical shift of -81.9 ppm had completely disappeared and showed that the reaction had gone to completion. The ^{19}F NMR spectrum displayed two single sharp peaks with chemical shifts of -35.7 ppm and -36.1 ppm which again demonstrates the presence of an entrapped fluoride anion in a double D4R like structure as seen in octadecasil. This result shows that the optimum conditions to obtain the $(Ethoxy)_8Q_8$ are a 1:2 ratio of tetraethylorthosilicate to TBAF and a temperature and pressure when removing the solvent of 55°C and 95 mbar respectively.

As the compound did not precipitate out and seemed to degrade quickly into a resin like gel, we decided to exchange the tetra-*n*-butylammonium cation for a lithium ion (MP303). We redissolved 1 g of the yellow gel previously obtained (MP300) in dried THF and we added 0.60 g of lithium tetraphenylborate, $LiPh_4B$. The reaction was stirred for 24 hours. After removing the solvent, a white solid was obtained. The ^{29}Si NMR spectrum (in d_6 acetone) displayed a single sharp peak with a chemical shift of -99.7 ppm, as shown in **Figure 85.**

Figure 85 ^{29}Si NMR spectrum of MP303

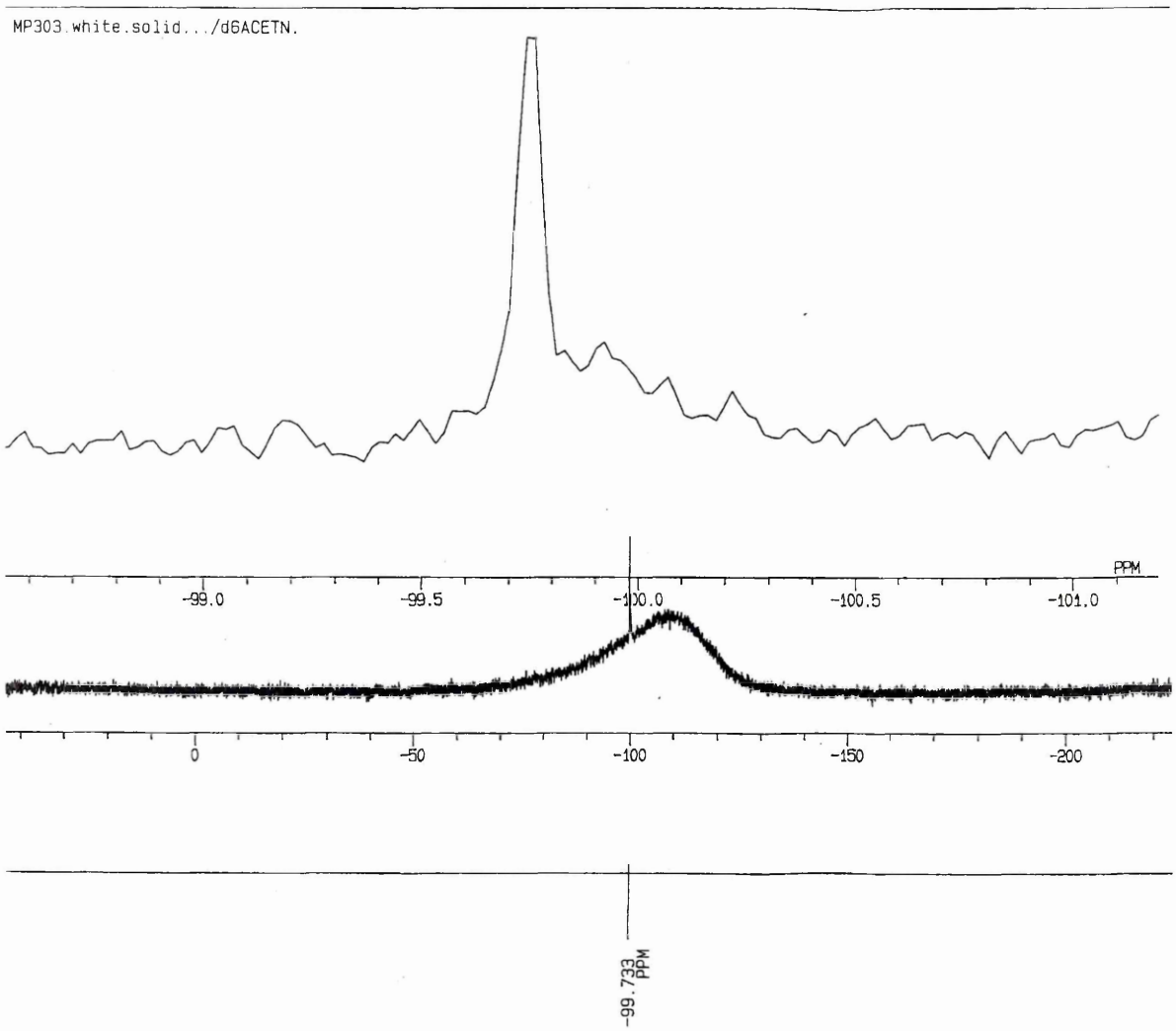

The ^{19}F NMR spectrum displayed a major sharp peak with a chemical shift of -35.8 ppm. A number of smaller signals were also observed with chemical shifts of -33.3 ppm, -35.85 ppm and -36.1 ppm. This result is remarkable as it provides clear evidence that the signal with a ^{19}F NMR chemical shift of -35.8 ppm can be assigned to an isolated fluoride ion encapsulated within a $(Ethoxy)_8Q_8$ cage. We were unable to obtain a single crystal from this compound so we were unable to obtain an X-ray crystal structure and thus we cannot be certain of the exchange of cation. Nevertheless, we are certain that the peak with a ^{29}Si NMR chemical shift of -99.7 ppm is a sharp singlet that can be associated with an

encapsulated fluoride $(Ethoxy)_8Q_8$ cage. Furthermore, the ^1H NMR shows a triplet with a chemical shift at 1.08 ppm (3H, t, CH_3) and a quadruplet at 3.48-3.55 ppm (2H, q, O-CH_2) which indicate the presence of an ethoxy group. In addition, the spectrum displays a triplet at 0.96 ppm (3H, t, CH_3), a multiplet at 1.10-1.19 ppm (2H, vbr, m, CH_2), another multiplet at 1.35-47 ppm (2H, vbr, m, CH_2) and a triplet at 3.34 ppm (2H, t, N-CH_2). The peaks at 0.96, 1.1, 1.4 and 3.3 ppm are associated with the CH_3-CH_2-CH_2-CH_2-X system, which is part of the tetra-*n*-butylammonium fluoride that was used as the catalyst. The integration shows a ratio of one molecule of TBAF for one ethoxy group which suggests the presence of 8 TBAF ions for 1 cage. So we have more TBAF ions than we would expect for a pure $(ethoxy)_8$-Q_8-TBAF. The ^{13}C NMR spectrum is in complete agreement with this assumption: it exhibits peaks at δ 14.1 ppm (CH_3); δ 19.2 ppm (-CH_2-); δ 24.5 ppm (-CH_2-); δ 57.1 ppm (N-CH_2-) for the four carbon atoms of the tetra-*n*-butylammonium group and δ 20.3 ppm (CH_3) and δ 68.2 ppm (O-CH_2-) for the carbon atoms of the ethoxy group.

We conducted a final experiment (MP295) in toluene on a bigger scale. In this experiment we dissolved 20 g of tetraethylorthosilicate (96 mmol) in toluene. We then added 25 ml of tetra-*n*-butylammonium fluoride (1M solution in THF, 2.5mmol) so we had a 1:3.8 ratio of orthosilicate to TBAF. After 24 hours, the reaction was stopped and the solvent (b.p. of toluene: 110.6°C) removed on a rotary evaporator at a temperature of 55°C and a vacuum of 95 mbar for 15 minutes. A yellow gel was obtained. The ^{29}Si NMR spectrum (in d_6 acetone) displayed a major large signal with a chemical shift of -99.7 ppm with a small peak at -99.9 ppm. The ^{19}F NMR spectrum displayed a large single sharp peak with a chemical shift at -35.9 ppm and two other small peaks at -36.3 and -36.8 ppm. Thus, the reaction can be carried out on a larger scale and the optimum conditions remain unchanged.

6.2.2 Conclusion

We have demonstrated that we can synthesize a tetra-*n*-butylammonium octaethoxyoctasilsesquioxane fluoride cage. The ^{19}F NMR spectrum confirmed the encapsulation of the fluoride within the cage by showing a peak at -35.8 ppm. This chemical shift has moved upfield with respect to that previously observed (around -26 ppm) for octa-phenyl-, vinyl- and *para*-tolyl- octasilsesquioxane cages. This upfield shift of the encapsulated fluoride ion signal is an indication of a minor "naked" character of the encapsulated fluoride ion. It thus shows the greater interaction of the fluoride ion with its neighbouring silicon atoms in the Q_8 cage than in the T_8 cages. The ESI, negative ion FAB and MALDI-TOF mass spectrometric analyses also confirmed the synthesis of the $(ethoxy)_8$-Q_8-TBAF. However, the ^{19}F NMR spectrum shows a number of smaller signals in the isolated fluoride ion chemical shift region which demonstrates the presence of more than one environment around the fluoride ions. Whilst we have shown that the main isolated fluoride environment is the $(ethoxy)_8$-Q_8-TBAF cage, we have not been able to describe the others environments.

6.3 Reaction of tetrapropylorthosilicate with TBAF

6.3.1 Experiment

The experiment (MP343) was conducted using toluene as the solvent. In this experiment we dissolved 1.38 g of tetrapropylorthosilicate (5.2 mmol) in toluene. We then added 2.5 ml of tetra-*n*-butylammonium fluoride (1M solution in THF, 2.5mmol) so we had a 1:2.1 ratio of orthosilicate to TBAF. After 24 hours, the reaction was stopped and the solvent (b.p. of

toluene: 110.6°C) removed on a rotary evaporator at a temperature of 55°C and a vacuum of 95 mbar for 15 minutes. A yellow gel was obtained.

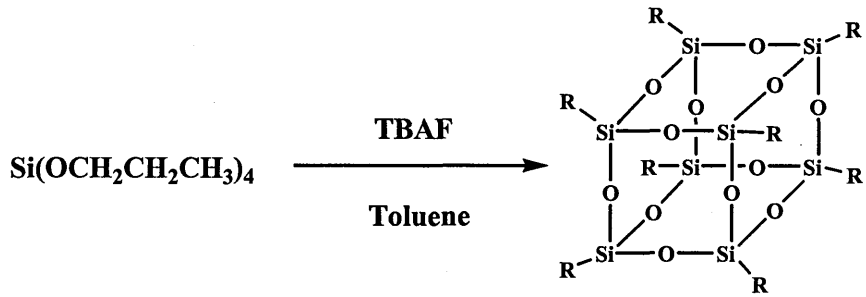

R = -$OCH_2CH_2CH_3$

The ^{29}Si NMR spectrum (in d_6 acetone) displayed a major sharp peak in the Q-Si region with a chemical shift of -99.7 ppm with a small peak at -99.8 ppm. The ^{19}F NMR spectrum displayed a large single sharp peak with a chemical shift of -35.5 ppm and two smaller peaks at -33.2 and -35.9 ppm. Such chemical shift values are again close to those found previously for fluoride anions trapped in the double D4R of a zeolite (octadecasil), and the results are similar to those obtained for the tetraethylorthosilicate reaction. Thus, the main signal in the ^{29}Si NMR spectrum at -99.7 can be reasonably assigned to a tetra-*n*-butylammonium octapropoxyoctasilsesquioxane fluoride cage which is the main product of this reaction. Nevertheless, we again observe the presence of other isolated fluoride ions with more than one environment. Unfortunately, we did not get a single crystal from this compound and so no more evidence could be obtained regarding the precise structure of this compound.

6.3.2 Conclusion

We are able to synthesize a tetra-*n*-butylammonium octapropoxyoctasilsesquioxane fluoride cage. The ^{19}F NMR spectrum confirmed the encapsulation of the fluoride within the cage with weak interactions with its neighbouring silicon atoms. However, the ^{19}F NMR spectrum shows other signals in the isolated fluoride ion chemical shift region which demonstrate, as seen previously in the tetraethylorthosilicate reaction, the presence of isolated fluoride ions with more than one neighbouring environment. Nevertheless, we have shown that the main isolated fluoride environment is the $(propoxy)_8$-Q_8-TBAF cage.

6.4 Conclusion

We have shown we are able to extend the new class of compound whereby a fluoride ion is encapsulated in a cage by synthesizing two Q_8-TBAF cages: the tetra-*n*-butylammonium octaethoxyoctasilsesquioxane fluoride and the tetra-*n*-butylammonium octapropoxyoctasilsesquioxane fluoride cages. We have shown that the conditions of reaction for the encapsulation of the fluoride ion were similar to those used for the synthesis of the tetra-*n*-butylammonium octaphenyloctasilsesquioxane fluoride, tetra-*n*-butylammonium octavinyloctasilsesquioxane fluoride and tetra-*n*-butylammonium octa-*para*-tolyloctasilsesquioxane fluoride cages. As expected, the oxygen atoms can stabilize the δ negative charge formed from the weak interaction between the fluoride ion and the silicon atoms and, unlike with sp^3 carbon atoms at the silicon atoms, the reaction leads to the encapsulation of the fluoride ion within a fairly stable octasilsesquioxane cage. As discussed previously, one explanation for the fluoride ion encapsulation within the octasilsesquioxane cage could be the presence of the LUMO of these compounds at the centre of the cage as Pittman and co-workers [84] have reported. In fact, their calculations identified two ions for

which inclusion within the cage was energetically favorable, the fluoride and the lithium ions. Obviously the encapsulation of the fluoride ion is helped by its dual function in this reaction as a template and a catalyst.

Chapter 7: Thermogravimetric Analysis of different silsesquioxane cages

7.1 Introduction

Thermogravimetric Analysis (TGA) and Differencial Thermal Analysis (DTA) are employed to study thermal degradation of compounds under air or nitrogen atmospheres. TGA studies of polysiloxanes and a few octa(alkyl)silsesquioxanes have been reported in literature. In order to evaluate and compare the thermal properties of our new class of compound with conventional octasilsesquioxane cages, thermogravimetric analysis (TGA) was performed using a Perkin-Elmer TGA thermal analyser under flowing air or nitrogen. The samples were placed under a gas flowing at 50ml/min and then heated at a fixed rate (20°C/min) from room temperature to 900°C.

7.2 TGA studies of tetra-*n*-butylammonium octasilsesquioxane fluoride cages

7.2.1 TGA of tetra-*n*-butylammonium octaphenyloctasilsesquioxane fluoride cage

The TGA plot (in pink) and the DTA curve (in blue) of the Ph_8T_8-TBAF under a nitrogen atmosphere are shown in Figure 86. The TGA curve shows no weight loss at around 100°C which demonstrates that the compound is anhydrous. The TGA/DTA plot shows two

distinctive mass-loss regions at 320-360°C and at 480-680°C which suggests a complicated degradation process.

The first mass loss step between 320-360°C represents a weight loss of 20 % and may be due to the loss of TBA (MW = 242 which represents 19 % of the total weight of the Ph_8T_8-TBAF cage, MW = 1295) with a corresponding endothermic peak at 350°C. The loss of TBA occurs through an Hoffmann's elimination, as shown in Scheme 1, wherein a base attacks the hydrogen in β to form HF, a molecule of butene and tributylamine. Butene (MW = 56.1, b.p. = -6.3°C) and tributylamine (MW = 185.4, b.p. = 216°C) are both volatile and represent 4.5 % and 14.5 % respectively of the total weight of the Ph_8T_8-TBAF cage. The base can come from trace of water present in the crystal structure or fluoride ion.

Scheme 1

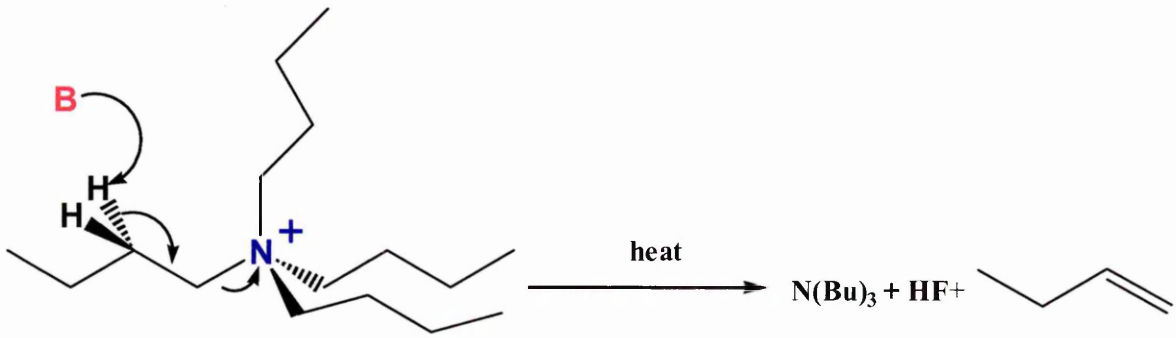

The mass loss between 480 and 680°C (20 %) exhibits a weak inflexion point at 570°C. The former rapid weight loss between 480 and 570°C does not present obvious endothermic peak in the DTA curve. The latter rapid weight loss between 570 and 680°C is associated to a broad weak endothermic peak at 610-660°C. This weight loss can be ascribed to the decomposition and loss of the organic phenyl groups followed by a subsequent cross-linking reactions that lead to the formation of a SiO_xC_y network. The total weight loss (45 % at 900°C) is thus lower than the organic fraction of the materials (68 %), indicative of the

incorporation of a small fraction of organic matter being trapped in the larger siloxane network. It should be noted that even at the highest temperature reached (900°C) the weight is still decreasing. On completion of the thermal analysis the residue was completely black. The conventional octaphenyloctasilsesquioxane cage has been described as a "rock" and the thermal stability of this compound is reported to be high[41, 44, 75]. We were expecting to see a reduction in the thermal stability of our new compound, the tetra-*n*-butylammonium octaphenyloctasilsesquioxane fluoride cage, because of the presence of the fluoride anion within the cage. This expectation turned out to be false as the TGA results demonstrate that it has a reasonable thermal stability until 320°C. This suggests that this new octasilsesquioxane cage compound has very interesting thermal properties.

Figure 86 TGA of the Ph_8T_8-TBAF cage under N_2 and air atmosphere

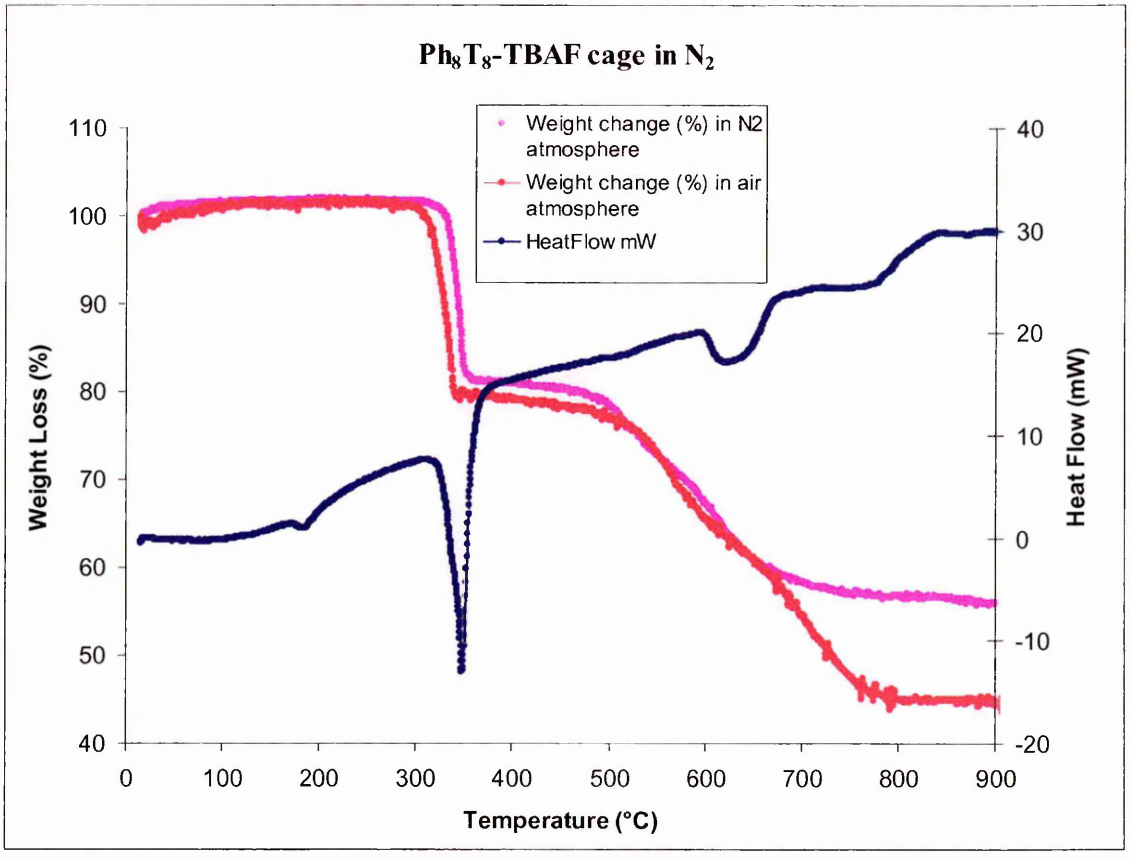

The same analysis was carried out under an air atmosphere (curve in red in Figure 86). The thermal behaviour seems to be very similar under an air or nitrogen atmosphere. No oxidation in air occured as no weight increase was observed in the first step. The decomposition and weight loss of the compound began at a lower temperature under an air atmosphere: 320°C compared to 330°C under nitrogen. The final mass residue is lower (45 %) under an air atmosphere.

7.2.2 TGA of tetra-*n*-butylammonium octa-*para*-tolyloctasilsesquioxane fluoride cage

The TGA plot (in pink) and the DTA curve (in blue) of the (*para*-tolyl)$_8$T$_8$-TBAF under a nitrogen atmosphere are shown in Figure 87. The TGA curve shows no weight loss at around 100°C which demonstrates that the compound is anhydrous. The TGA/DTA plot shows again two distinctive mass-loss regions at 300-360°C and 450-680°C which suggest a complicated degradation process.

The first mass loss step between 300-360°C represents 18.5 % of weight loss and confirms the loss of TBA (MW = 242 which represents 17.2 % of the total weight of the (*para*-tolyl)$_8$T$_8$-TBAF, MW = 1407) with a corresponding endothermic peak at 345°C.

The mass loss between 450 and 680°C (35 %) exhibits a weak inflexion point at 585°C. The former rapid weight loss (28 %) between 450 and 585°C does not lead to an obvious endothermic peak in the DTA curve. The later rapid weight loss (7 %) between 585 and 680°C is associated to a broad weak endothermic peak at 600-630°C. This weight loss can be ascribed to the decomposition and loss of organic *para*-tolyl groups followed by subsequent cross-linking reactions that lead to the formation of a SiO_xC_y network. The residue weight (43 % at 900°C) is thus higher than the inorganic fraction (Si_8O_{12}) of the original compound (30%), indicative of the incorporation of a small fraction of organic matter being trapped in the larger siloxane network. On completion of the thermal analysis the residue was completely black.

The thermal stability and degradation behaviour of the tetra-*n*-butylammonium octa-*para*-tolyloctasilsesquioxane fluoride cage is very similar to the tetra-*n*-butylammonium octaphenyl octasilsesquioxane fluoride cage. This result confirms the loss of the tetra-*n*-butylammonium ion in the first step, then the degradation and loss of organic groups before

the formation of a cross-linked siloxane structure. However, we observed that the (*para*-tolyl)$_8$T$_8$-TBAF cage lost TBAF at a lower temperature (300°C) than the Ph$_8$T$_8$-TBAF cage (320°C) which demonstrates the higher thermal stability of the Ph$_8$T$_8$-TBAF cage.

Figure 87 TGA of the (*para*-tolyl)$_8$T$_8$-TBAF cage under N_2

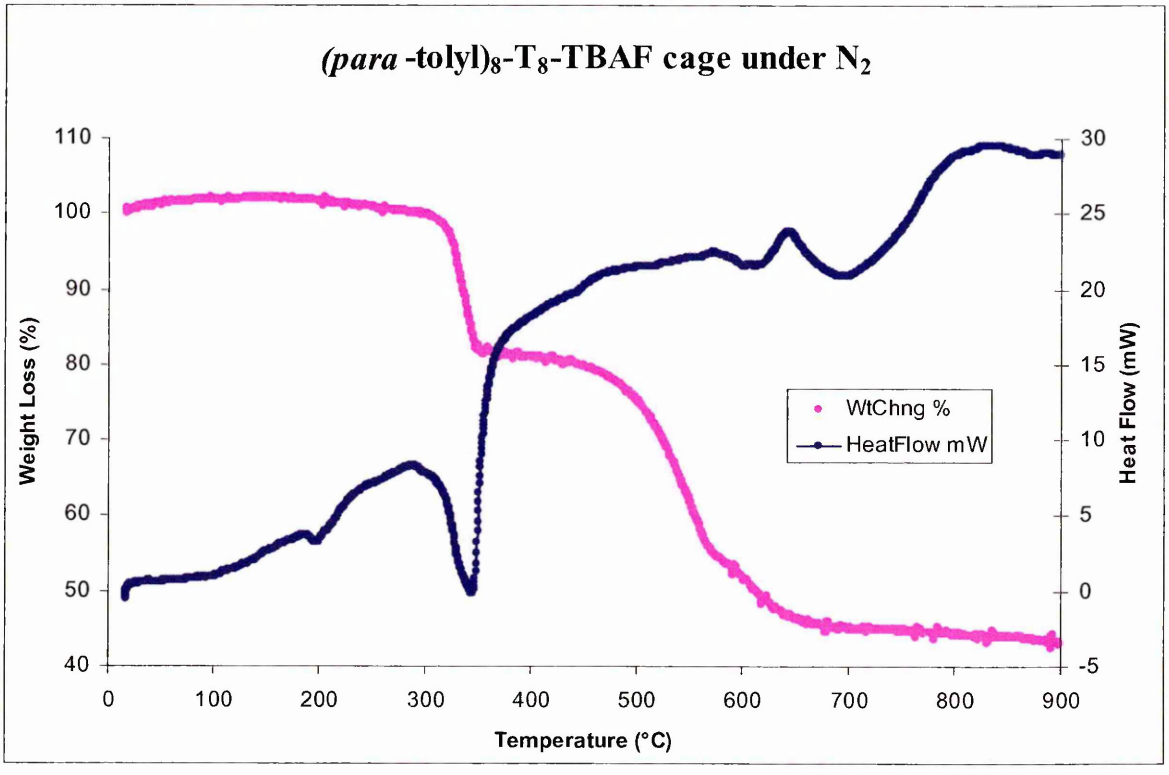

7.2.3 TGA of tetra-*n*-butylammonium octavinyloctasilsesquioxane fluoride cage

The TGA plot (in pink) and the DTA curve (in blue) of the $(vinyl)_8T_8$-TBAF under a nitrogen atmosphere are shown in Figure 88. The TGA/DTA plot shows again two distinctive mass-loss regions at 55-85°C and 120-300°C which suggest a reduction in the thermal stability of the $(vinyl)_8T_8$-TBAF cage with respect to the Ph_8T_8-TBAF and $(para\text{-}tolyl)_8T_8$-TBAF cages.

The first mass loss step between 55-85°C represents 8 % of weight loss which does not correspond to the loss of TBA (MW = 242 which represents 27 % of the total weight of the $(vinyl)_8T_8$-TBAF, MW = 895). This first weight loss corresponds to an endothermic peak at 70°C. We can explain this mass loss at very low temperature by the presence of solvent in the crystals. We thus need to consider that the initial weight of the compound is the weight at 100°C and recalculate all the % weight loss from there. The mass loss between 120 and 300°C (28 % corrected to 30 %) exhibits a weak inflexion point at 190°C. The former rapid weight loss (13 % corrected to 14 %) between 120 and 190°C is associated with a broad endothermic peak at 130-170°C in the DTA curve. The later rapid weight loss (15 % corrected to 16 %) between 190 and 300°C does not show an endothermic peak in the DTA curve. This weight loss can be ascribed to the loss of TBAF (MW = 261 which represents 29 % of the total weight of the $(vinyl)_8T_8$-TBAF, MW = 895). We will see later in the discussion that the TGA of TBAF hydrate has a similar behaviour with the major loss of weight happening in a rapid and slower loss separated by an inflexion point. This behaviour could indicate the loss of TBAF in two steps, first loss of butane then loss of tributylamine (b.p. = 216°C). As the percentage of the two step loss are not perfectly reflecting this hypothesis, that could also be explained by the presence of two different TBAF in the

crystal. These suggest that further investigations would be needed to fully explain the mechanism of this complex thermal decomposition behaviour. We can also observe a third region between 450 and 750°C with a low weight loss which corresponds to a very broad endothermic peat at 500-750°C. This might be explained by a small loss of vinyl group together with the polymerization and cross-linking reaction of the vinyl arms between the cages which will lead to the formation of a SiO_xC_y network. The residue weight (57% corrected to 62 % at 900°C) is thus higher than the inorganic fraction (Si_8O_{12}) of the original compound (46%) and much higher that in the case of the Ph_8T_8-TBAF and (*para*-tolyl)$_8T_8$-TBAF cages, which confirms the probable polymerization of the vinyl groups in a larger siloxane network. In contrast with Ph_8T_8-TBAF and (*para*-tolyl)$_8T_8$-TBAF cages, the vinyl$_8T_8$-TBAF cage contains functionalities useful in polymerization that may also play a role in subsequent thermal decomposition pathways. On completion of the thermal analysis the residue was completely black.

The thermal stability and degradation behaviour of the tetra-*n*-butylammonium octavinyloctasilsesquioxane fluoride cage is different from the two previous cages. In fact, no loss of TBAF has been observed and the high weight of the residue demonstrates the high organic content at higher temperatures. Additionally, the vinyl$_8T_8$-TBAF cage degrades at a much lower temperature and proved to have a lower thermal stability than the Ph_8T_8-TBAF and (*para*-tolyl)$_8T_8$-TBAF cages.

Figure 88 TGA of the $(Vinyl)_8T_8$-TBAF cage under N_2

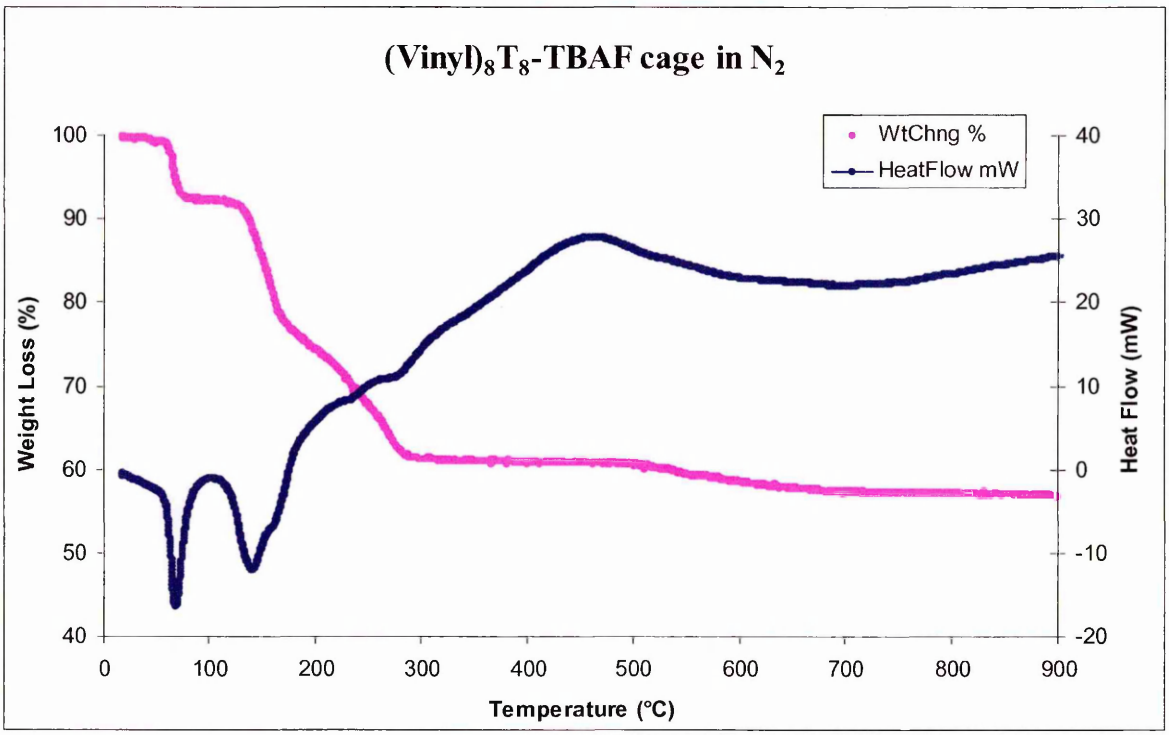

Since we have obtained single crystals of the $(vinyl)_{12}$-T_{12} cage from some of the experiments, we also carried out thermogravimetric analysis on these samples. The TGA/DTA plot for the $(vinyl)_{12}$-T_{12} (Figure 89) shows two distinctive mass-loss regions at 215-400°C and 510-690°C. There is a large broad endothermic peak at 50-200°C with no corresponding weight loss which might suggest some polymerization processes occuring at low temperature. The first mass loss step (30 %) between 215 and 400°C can be ascribed to the decomposition and loss of the organic vinyl groups together with a cross-linking reaction that leads to the formation of a SiO_xC_y network. The second mass loss step (4 %) between 510 and 690°C can be ascribed to a rearrangement of the siloxane network. The residue weight (67 % at 900°C) is very close to the inorganic fraction ($Si_{12}O_{18}$) of the original compound (65%) which confirms that the compound decomposes primarily through partial loss of the organic substituents followed by subsequent cross-linking reactions that

incorporate the remaining organic matter into a SiO_xC_y network. Such a decomposition pattern is certainly due to the fact that the vinyl$_{12}$T$_{12}$-TBAF cage contains functionalities useful for polymerizations which occur during the thermal decomposition of the material.

Figure 89 TGA of the (vinyl)$_{12}$-T$_{12}$ cage under N_2

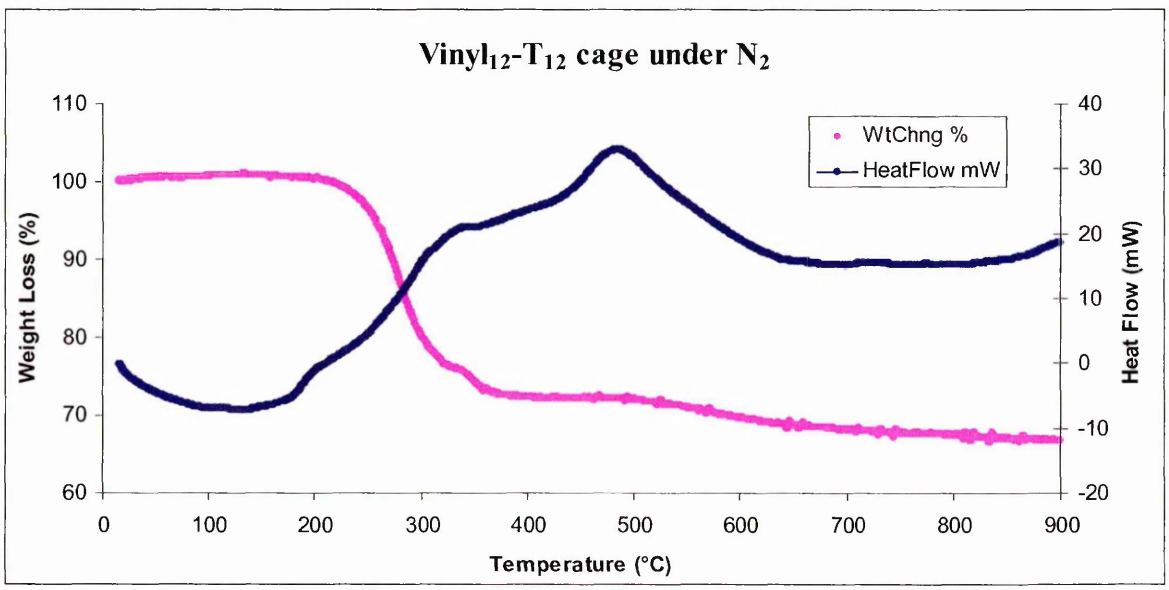

7.2.4 TGA of tetra-*n*-butylammonium fluoride hydrate 98 %

We were interested in looking at the thermal degradation behaviour of tetra-*n*-butylammonium fluoride itself. We used TBAF as solid hydrate 98 %. The TGA plot (in pink) and the DTA curve (in blue) of the TBAF hydrate under a nitrogen atmosphere are shown in Figure 90. The TGA/DTA plot shows a distinctive mass-loss region between 40-125°C and a more complex region between 125-370°C.

Figure 90 TGA of TBAF Hydrate 98 % under N_2

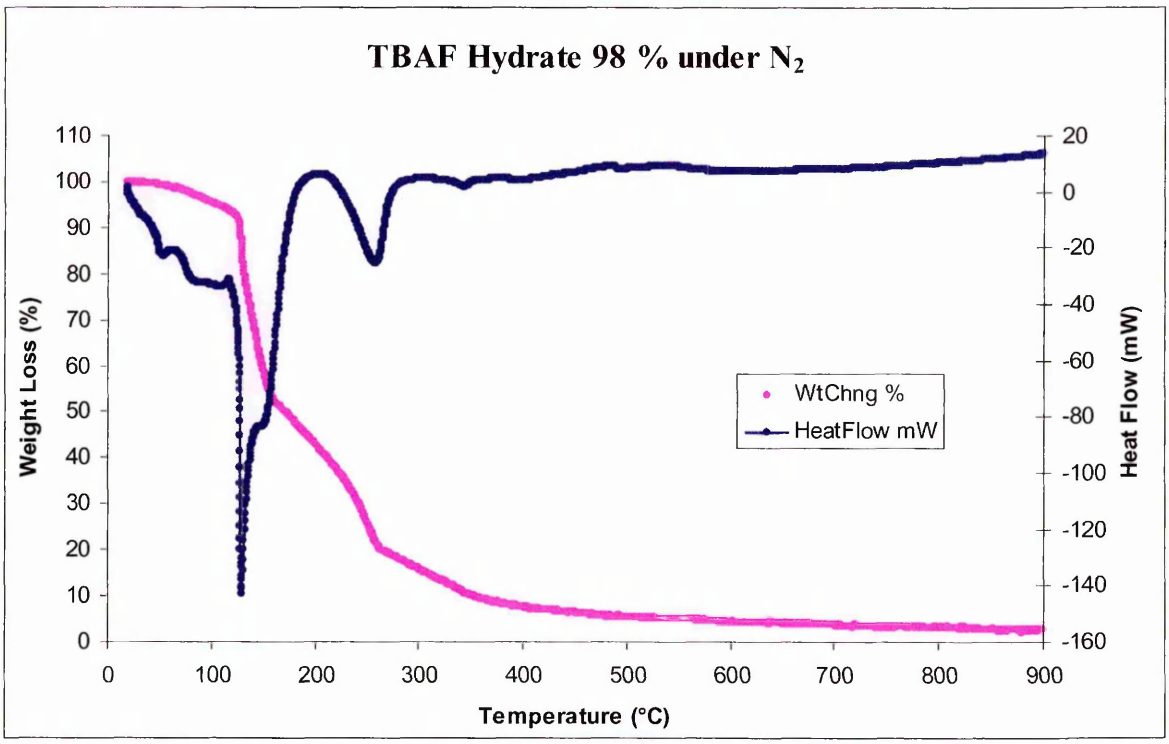

The first mass loss step between 40-125°C represents 8 % of the weight loss which might be ascribed to the loss of water contained in the sample. This initial weight loss corresponds to an endothermic broad peak at 40-120°C. We thus need to calculate the weight loss considering that the initial weight of the compound is the weight at 125°C. The mass loss between 125 and 370°C (85% corrected to 92%) exhibits two inflexion points at 160 and 270°C. The first rapid weight loss (40% corrected to 43 %) between 125 and 160°C presents an endothermic peak at 125-160°C in the DTA curve. The latter rapid weight loss (30% corrected to 33 %) between 160 and 270°C corresponds to an endothermic peak at 260°C in the DTA curve. The last mass-loss region from 270 to 400°C represents a low weight loss of 11 %. On completion of the thermal analysis the residue represents only 2 % of the initial weight. The weight loss between 125 and 160°C could have been ascribed to the loss of HF (MW = 20) and butene (MW = 56.1) through a Hoffmann's elimination, as shown in the

Scheme 2 below, but the additional relative weight should have been 29% and not 43%. Then the second weight loss would have arised from the loss of the tributylamine (MW = 185.4, b.p. = 216°C) but again the weight loss should have been 71% and not 33%.

Scheme 2

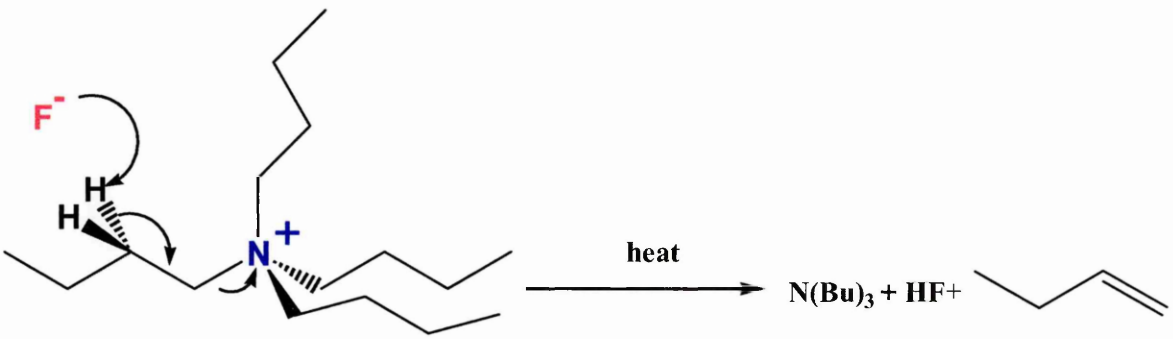

We cannot extrapolate the thermal behaviour of free TBAF to the behaviour of tetrabutyl ammonium fluoride which is in close contact with an octasilsesquioxane cage with the fluoride being within the cage, although the TGA plot and the characteristic weight loss in two steps with an inflexion point has been observed in TGA of the tetra-*n*-butylammonium octasilsesquioxane cages. However, this experiment highlights the complex mechanism of degradation of a simple molecule and thus warns against simple conclusions in the degradation of very complex molecules which have different packing network as in octasilsesquioxane cages.

7.3 TGA studies of conventional octasilsesquioxane cages and comparison with the tetra-*n*-butylammonium octasilsesquioxane fluoride cages

7.3.1 TGA of PhenylT$_6$, PhenylT$_8$ and PhenylT$_{12}$ cages and comparison with Ph$_8$T$_8$-TBAF

We have not found any reports of TGA studies of phenylsilsesquioxane cages in the literature except for the poly(phenylsilsesquioxane) (PPSQ) which has been widely studied and characterized [55,73,44,41]. The PPSQ is generally characterized by an outstanding thermal stability until 450°C at which temperature the thermal reduction of the siloxane network begins with the loss of the organic moieties-phenyl groups [89].

As the conventional phenyl-T$_8$ cage has been described as a "rock", we wanted to examine its thermal degradation behaviour and compare it with our Ph$_8$T$_8$-TBAF cage. The experiment was carried out under a nitrogen atmosphere using a sample provided by the Dow Corning Corporation. The TGA plot (in pink) and the DTA curve (in blue) of the (Phenyl)$_8$T$_8$ are shown in Figure 91. The TGA/DTA plot shows a mass-loss region at 400-700°C (25 %) with an endothermic peak at 470°C and an exothermic peak at 590°C. This weight loss can be ascribed to the decomposition and loss of organic phenyl groups together with cross-linking reactions that lead to the formation of a SiO_xC_y network.

Figure 91 TGA of PhenylT$_8$ from Dow Corning under N_2

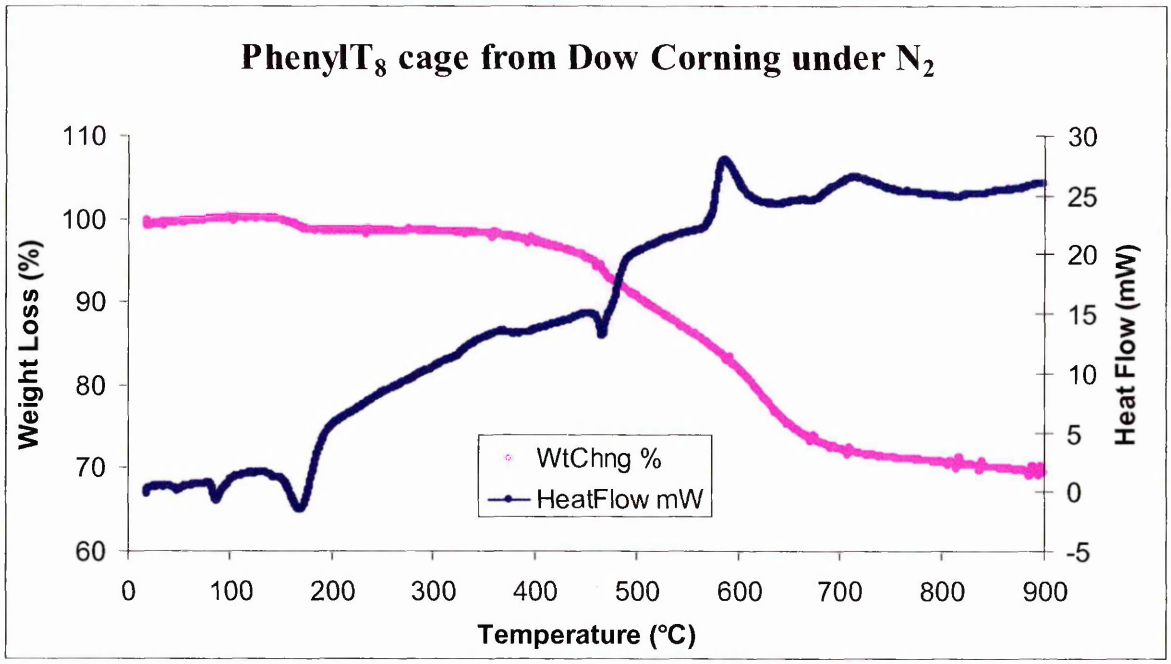

The residue weight (70 % at 900°C) is thus higher than the inorganic fraction (Si_8O_{12}) of the original compound (40%) and much higher than in the case of the Ph_8T_8-TBAF (55 %). On completion of the thermal analysis the residue was completely black.

Unexpectedily, the thermal stability of the conventional PhenylT$_8$ cage is quite similar to the Ph_8T_8-TBAF. However, the conventional cage starts to degrade after 400°C whereas the Ph_8T_8-TBAF cage starts at 350°C which denotes the higher thermal stability for the conventional PhenylT$_8$ cage. Despite the presence of a fluoride anion at the center of the cage, the thermal stability and thermal degradation are not drastically reduced and the Ph_8T_8-TBAF retains its outstanding thermal stability.

We also conducted thermogravimetric analysis on $(Phenyl)_6T_6$ and $(Phenyl)_{12}T_{12}$ cages. The experiments were carried out under nitrogen atmosphere. The $(Phenyl)_6T_6$ was synthesized

by Marina Maesano and the $(Phenyl)_{12}T_{12}$ had crystalized out in one of our experiment (MP152), the crystals were ground into a fine powder before performing the TGA.

The TGA/DTA plot for the $(Phenyl)_6T_6$ sample (Figure 92) shows a mass-loss region at 290-600°C (90 %) with an endothermic peak at 260°C and an exothermic peak at 520°C. The total weight loss exceeds 92% and is thus greater than the organic fraction of the material. We thus observed that the $(Phenyl)_6T_6$ cage sublimed at 350°C. The residue (8 %) might be composed by larger siloxane structures which had been formed by the decomposition and rearrangement of the material. Alternatively the $(Phenyl)_6T_6$ sample may have been inpure and contained larger cages that did not sublime. It is interesting to see the difference in thermal behaviour between the $(Phenyl)_6T_6$ and the $(Phenyl)_8T_8$ where the T_6 sublimed at 350°C and the T_8 decomposed at 400°C to lead to the formation of a SiO_xC_y network. Such a difference was not observed between the (*cyclo*-hexyl)$_6T_6$ and the (*cyclo*-hexyl)$_8T_8$ where both compounds were reported to sublime at 360 and 460°C respectively under nitrogen [90].

Figure 92 TGA of $(Phenyl)_6T_6$ cage under N_2

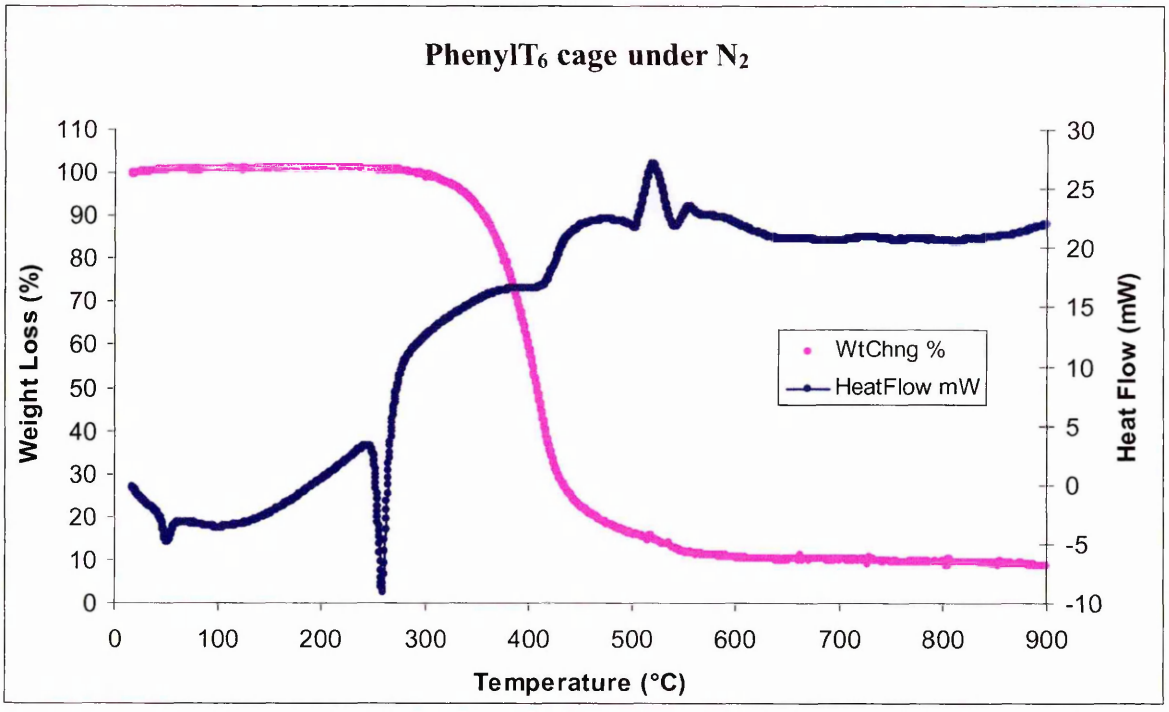

The TGA/DTA plot for the $(Phenyl)_{12}T_{12}$ sample (Figure 93) shows two distinctive mass-loss regions at 80-190°C and 420-680°C. The first mass loss step (12 %) between 80 and 190°C corresponds to an endothermic peak at 180°C. This first weight loss can be explained by the loss of water or solvent present in the crystal. The second mass loss step (30 %) between 420 and 680°C corresponds to an endothermic broad peak at 570-670°C. This weight loss can be ascribed to the decomposition and loss of the organic phenyl groups together with a cross-linking reaction that lead to the formation of a SiO_xC_y network. The residue weight (57 % at 900°C) is thus higher than the inorganic fraction ($Si_{12}O_{18}$) of the original compound (40%) which confirms that the compound decomposes primarily through partial loss of the organic substituents followed by subsequent cross-linking reactions that incorporate the remaining organic matter into a SiO_xC_y network. Such a decomposition pattern seems to be prefered because of the higher bond strength of the silicon-oxygen bond

(128 kcal/mol) in comparison with the silicon-carbon bond strength (88 kcal/mol) as reported by Walsh [8].

Figure 93 TGA of $(Phenyl)_{12}T_{12}$ cage under N_2

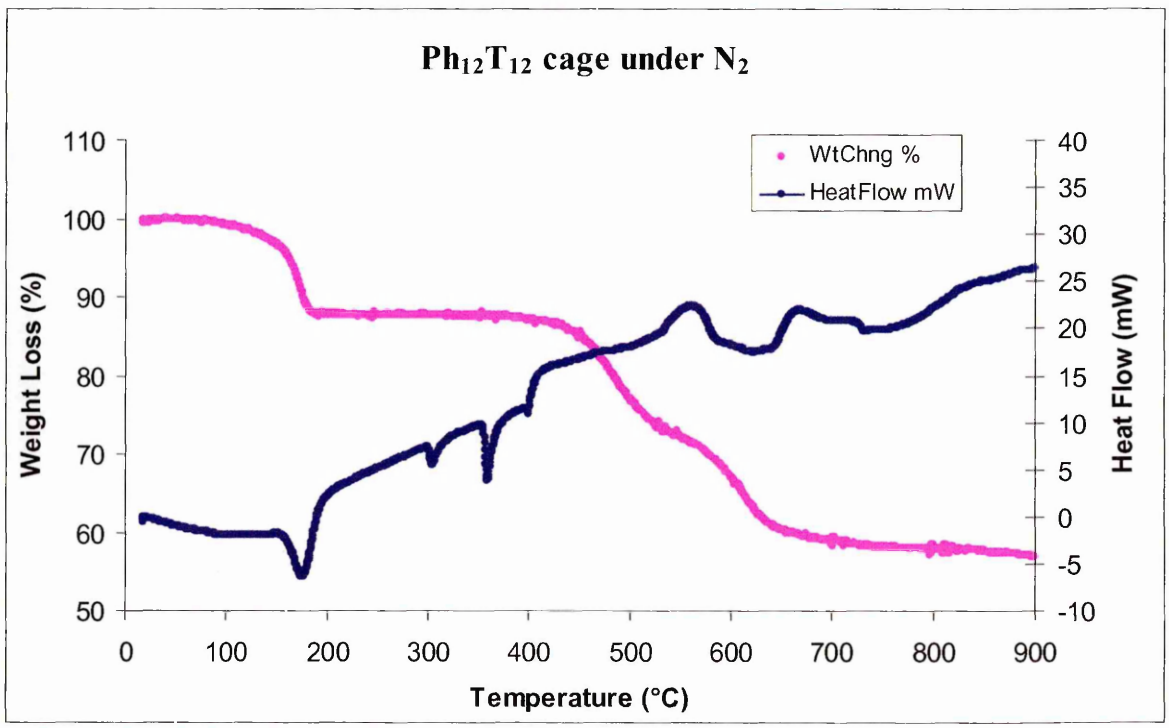

7.4 TGA of $Q_8(OEt)_8$-TBAF and comparison with other Q_8 cage systems

7.4.1 TGA of $Q_8(OEt)_8$-TBAF cage

The TGA plot (in pink) and the DTA curve (in blue) of the $Q_8(OEt)_8$-TBAF (MP300: as we have not been able to obtain pure crystal of this compound, we have to be aware that the sample which we analysed is certainly still containing some solvent, TBAF or some impurity even though the NMR analysis revealed only more TBAF than the expected cage: TBAF ratio of 1:1) under a nitrogen atmosphere are shown in Figure 94. The TGA curve shows an initial weight loss (9 %) between 20 and 120°C which confirms that the compound contains some water or solvent. The TGA/DTA plot shows two distinctive mass-loss regions at 120-280°C and 280-380°C which are separated by a weak inflexion point at 280°C. This thermal decomposition behaviour is as discussed previously characteristic for the loss of TBAF.

The mass loss between 120-380°C represents 58% (after recalculation of the initial weight at 120°C) of weight loss and may be due in part to the loss of TBAF together with the loss of the ethoxy groups (MW_{TBAF} = 261 which represents 25 % of the total weight of the $Q_8(OEt)_8$-TBAF cage, MW = 1038) with two corresponding endothermic peaks at 180°C and 330°C. At 380°C, the remaining weight (42 %) is lower than the weight of the inorganic part (Si_8O_{20}) of the initial material (MW_{Si8O20} = 544 which represent 52 % of $MW_{Q_8(OEt)_{20}\text{-}TBAF}$ = 1038). This again confirms that the initial material contained some solvent and an excess of TBAF. During the first step (120-380°C) we also suggest the loss of some inorganic groups followed by subsequent rearrangement and cross-linking reactions that lead to the formation of a Si_xO_y network. The residue total weight (38 % at 900°C) is

thus much lower than the inorganic fraction of the materials (52 %), indicative of the rearrangement and formation of a larger silica structure residue.

Figure 94 TGA of $Q_8(OEt)_8$-TBAF cage under N_2

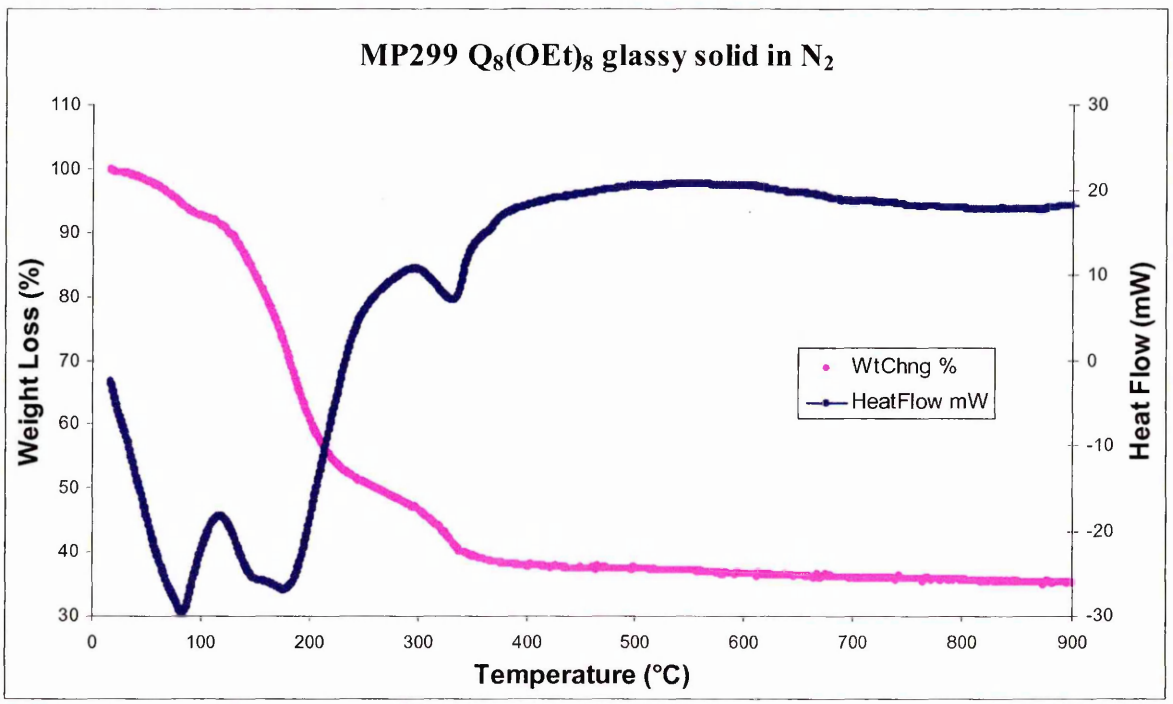

7.4.2 TGA of Q_8M_8 cage

The TGA plot (in pink) and the DTA curve (in blue) of the Q_8M_8 under a nitrogen atmosphere are shown in Figure 95. The TGA curve shows that the Q_8M_8 partially sublimes with a weight loss of 96 % between 200 and 310°C. No marked decomposition is shown and two corresponding endothermic peaks at 200 and 290°C are displayed in the DTA curve. The TGA plot also revealed a carbonaceous residue (3.5 %) at 315°C.

This thermal behaviour is very different from our $Q_8(OEt)_8$-TBAF cage which turned out to be less thermostable but did not undergo sublimation and left a higher residue at 900°C. This might suggest some interesting properties and new areas of research for this class of compound which are the building block of zeolites.

Figure 95 TGA of Q_8M_8 cage under N_2

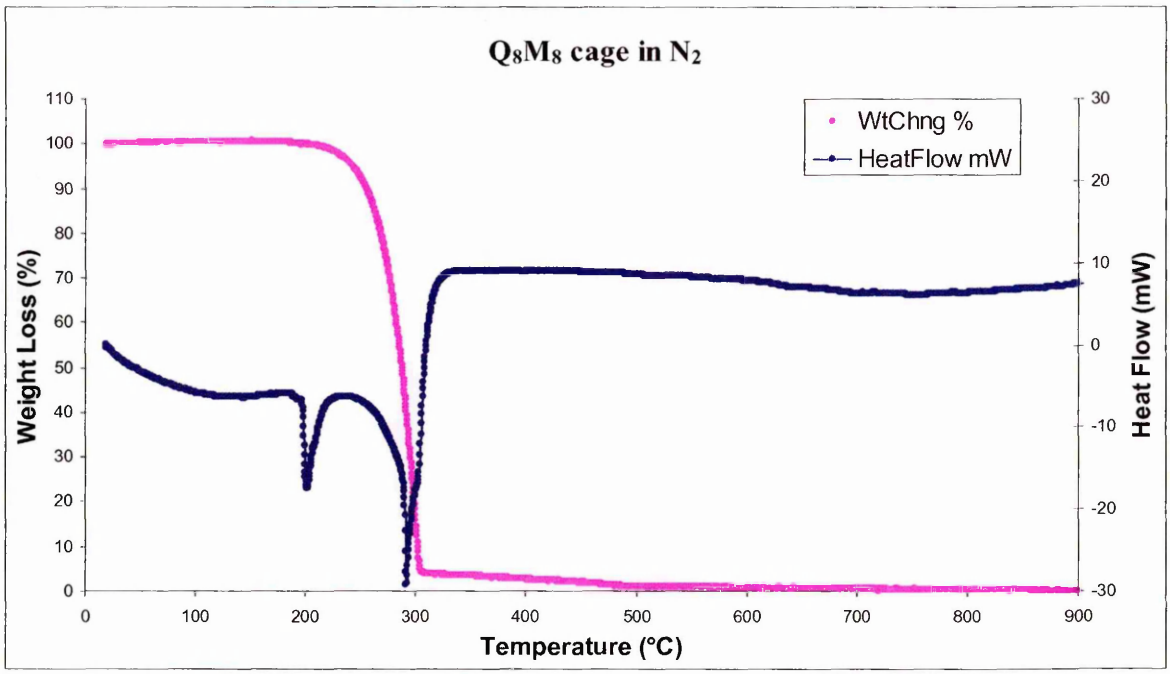

7.5 TGA of T_8H_8

Since we had studied the thermal decomposition behaviour of numerous T_8 and Q_8 systems, we noticed that no study had yet been performed on the simplest of the T_8 cage systems: the T_8H_8 cage. Based on the low molecular weight of this compound we might expect a sublimation mechanism.

The TGA plot (in pink) and the DTA curve (in blue) of the Q_8H_8 under a nitrogen atmosphere are shown in Figure 96. The TGA curve shows that the Q_8H_8 sublimes with a weight loss of 98 % between 130 and 245°C. No marked decomposition is shown and a corresponding endothermic peak at 230°C is displayed in the DTA curve. The TGA plot also revealed a carbonaceous residue (2 %) at 245°C.

Figure 96 TGA of Q_8H_8 cage under N_2

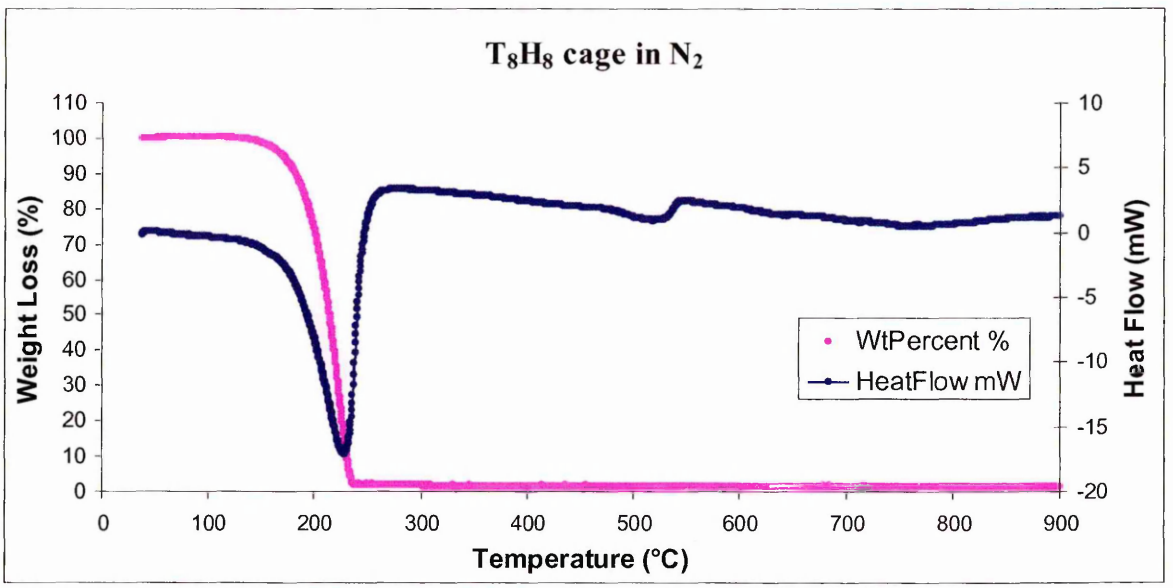

7.6 Conclusion

This TGA experiments showed that our new class of compound, tetra-*n*-butylammonium octasilsesquioxane fluoride cages, do not have very different thermal decomposition behaviour from the corresponding conventional octasilsesquioxane cages. We had thought that the presence of a fluoride anion in the middle of the cage could have been a major destabilizing factor in the thermal stability of these compounds. Unexpectedly, the tetra-*n*-butylammonium octasilsesquioxane fluoride cages seem to have a reasonable thermal stability, particularly the Ph_8T_8-TBAF and (*para*-tolyl)$_8T_8$-TBAF cages. Thus, this new class of compound demonstrates some interesting physical properties which are promising for possible future applications.

Chapter 8: Experimental

8.1 General Notes

8.1.1 NMR spectroscopy

All NMR spectra were obtained using either a JEOL EX 400 NMR or a JEOL lambda 300 NMR spectrometer. The pulse delay for ^{29}Si spectra was standardised at 20 seconds unless stated otherwise.

Unless stated otherwise all spectra was recorded at room temperature (25°C) using deuterated chloroform ($CDCl_3$) dried over 4 Å molecular sieves as solvent. The NMR external reference compound was TMS for ^{1}H, ^{13}C and ^{29}Si NMR spectra and $CFCl_3$ for ^{19}F NMR spectra. The spectral data point position of these compounds was accurately located before acquisition. All coupling constants are quoted in Hz.

8.1.2 Micro-analysis

Microanalysis was performed by MEDAC Ltd. of Brunel University. Where possible, elemental analysis have been reported. Work within the group over a number of years has shown that it is often very difficult to get accurate elemental analysis for some organosilicon compounds, in particular the silsesquioxane cage compounds, despite repeated submission of samples that have passed every other purity test, silicon carbide formation leads to percentages of silicon and carbon that are consistently less than expected. Thus many of the compounds have one figure which falls short of ideal values and have not been quoted.

8.1.3 Mass Spectrometry

Where possible, the mass spectrum has been reported. Work within the group over a number of years has shown that it can be very difficult to get mass spectra (ESI, FAB negative ion and MALDI-TOF) for some organosilicon compounds and in particular cages, which do not dissolve in the solvent or matrix used for analysis and thus showed no evidence of the expected parent ion.

Lower resolution mass spectra were recorded on a VG 20-250 mass spectrometer or performed by the National Mass Spectrometry Service Centre based at the University of Wales, Swansea. Matrix Assisted Laser Desorption/Ionisation - Time of Flight (MALDI-TOF) has been found to be a particularly useful mass spectrometric technique for cage compounds and analysis have been carried out by the University of Southampton. Unless stated otherwise the analysis used (DBH) as a matrix and dichloromethane as a solvent.

8.1.4 Melting Point

These were determined on an Electrothermal Digital melting point apparatus and are uncorrected.

8.1.5 FT-IR

Infrared spectra were obtained as neat samples or nujol mulls using sodium chloride plates using a Nicolet 205 FT-IR spectrometer or Perkin-Elmer 1710 Infrared Fourier Transform Spectrometer.

8.1.6 Thermogravimetric Analysis

Thermogravimetric analysis was performed using a Rheometric Scientific STA 1500 system. The sample was crushed to a fine powder, placed (5 mg) in a ceramic crucible and heated under nitrogen gas (50 cm^3/min) over the temperature range 20-900°C at a rate of 20°C/min.

8.1.7 X-Ray Crystallography

The X-ray crystallographic analysis of compounds was performed using the EPSRC X-ray crystallography service at the University of Southampton.

8.1.8 Solvents

The following solvents were dried before use:

Diethyl ether - dried over sodium wire.

Chloroform - dried using magnesium sulphate or 4Å molecular sieves.

Acetone - dried using magnesium sulphate.

THF - dried by distillation from sodium wire containing benzophenone and stored under nitrogen before use.

8.1.9 Chemicals

All chemical handling, reactions and work-up were performed in an efficient fume cupboard. Reagents were obtained primarily from the Aldrich Chemical Company, Lancaster Ltd. and Gelest Ltd. Reagents and many silanes were stored under nitrogen, the transfer of moisture sensitive liquid reagents was achieved by appropriate syringes fitted with needles with point tips to minimise damage to septa seals.

Unless state otherwise TBAF was a 1 molar solution in THF containing 5% of water and the platinum catalyst was a 0.02 molar solution of H_2PtCl_6 in *iso*-propyl alcohol.

Full experimental data are reported only for new compounds and those not reported are in agreement with literature data. All new compounds from this work are highlighted with an asterix " * " at the end of the title.

8.2 Experimental

8.2.1 Synthesis of octaalkyloctasilsesquioxanes and tetra-*n*-butylammonium octaphenyloctasilsesquioxane fluoride

Synthesis of (c-C_5H_9)Si(OEt)$_3$ (MP02):

Ethanol (46 g.mol^{-1}; 11g; in excess) and cyclopentyltrichlorosilane (203.35 g.mol^{-1}; 10g; 49.18 mmol) were dissolved in dry THF (200 ml); a solution of triethylamine (101 g.mol^{-1}; 22 g; 217.80 mmol) in dry THF (100 ml) was added to the mixture very slowly. The mixture was stirred for one and a half hours during which time a white solid precipitated out. The mixture was filtered under vacuum and the filtrate collected. A brownish liquid was obtained after distillation (10.20 g, 84 %). **^{1}H NMR** (300 MHz, $CDCl_3$, 25°C)/ppm: δ = 0.92 (m, vbr, 1H, C**H** of Cp), 1.14 (t, 9H, C**H**$_3$), 1.60 (m, 4H, C**H**$_2$ of Cp), 1.77 (m, 4H, C**H**$_2$ of Cp), 3.75 (q, 6H, OC**H**$_2$); **^{13}C NMR** (75.5 MHz, $CDCl_3$, 25°C)/ppm: δ = 18.9 (s, **C**H$_3$), 22.5 (s, **C**H of Cp), 26.7 (s, **C**H$_2$ of Cp), 27.3 (s, **C**H$_2$ of Cp), 58.3 (s, O**C**H$_2$); **^{29}Si NMR** (79.3 MHz, $CDCl_3$, 25°C)/ppm: δ = -45.8. All spectra data were in agreement with published data[71].

Reaction of (c-C_5H_9)Si(OEt)$_3$ with TBAF (MP04):

Cyclopentyltriethoxysilane (232 g.mol^{-1}; 1.20 g; 5.17 mmol) was dissolved in acetone, then TBAF (2.5 ml of a 1M solution in THF with 5% water) was added. This mixture was stirred at room temperature for 24 hours. A white solid precipitated out. After filtration under

vacuum, a white solid was obtained (0.60 g, 96%). **^{1}H NMR** (300 MHz, $CDCl_3$, 25°C)/ppm: δ = 0.92 (m, vbr, 1H, **CH** of Cp), 1.50 (m, vbr, 4H, **CH_2** of Cp), 1.80 (m, vbr, 4H, **CH_2** of Cp); **^{13}C NMR** (75.5 MHz, $CDCl_3$, 25°C)/ppm: δ = 22.3 (s, **C**HSi), 27.3 (s, **CH_2** of Cp), 27.5 (s, **CH_2** of Cp); **^{29}Si NMR** (79.3 MHz, $CDCl_3$, 25°C)/ppm: δ = 66.6; **Solid State ^{29}Si NMR** (79.3 MHz, 25°C)/ppm: δ = -65.8. The spectral data were consistent with the product being octa-*cyclo*-pentyloctasilsesquioxane[71].

Synthesis of (c-C_5H_9)Si(OCH_3)$_3$ (MP05):

Methanol (32 g.mol^{-1}; 8 g; in excess) and cyclopentyltrichlorosilane (203.35 g.mol^{-1}; 10.3 g; 50.65 mmol) were dissolved in dry THF (200 ml); a solution of triethylamine (101 g.mol^{-1}; 22 g; 217.8 mmol) in dry THF (100 ml) was added to the mixture very slowly. The mixture was stirred for one and a half hours during which time a white solid precipitated out. The mixture was filtered under vacuum and the filtrate collected. A brown liquid was obtained after distillation (7.40 g, 87%). **^{1}H NMR** (300 MHz, $CDCl_3$, 25°C)/ppm: δ = 1.1 (m, vbr, 1H, **CH** of Cp), 1.60 (m, vbr, 4H, **CH_2** of Cp), 1.85 (m, vbr, 4H, **CH_2** of Cp), 3.62 (s, 9H, **OCH_3**); **^{13}C NMR** (75.5 MHz, $CDCl_3$, 25°C)/ppm: δ = 21.7 (s, **C**H of Cp), 27.0 (s, **CH_2** of Cp), 27.5 (s, **CH_2** of Cp), 50.7 (s, **OCH_3**); **^{29}Si NMR** (79.3 MHz, $CDCl_3$, 25°C)/ppm: δ = -45.4. All spectra data were in agreement with the product being *cyclo*-pentyltrimethoxysilane.

Reaction of (c-C_5H_9)Si(OCH_3)$_3$ with TBAF (MP06):

Cyclopentyltrimethoxysilane (190 g.mol^{-1}; 1 g; 5.26 mmol) was dissolved in acetone (20 ml), then TBAF (2.5 ml of a 1M solution in THF with 5% water) was added. This mixture was stirred at room temperature for 24 hours. A white solid precipitated out. After filtration under vacuum, a white solid was obtained (0.44 g, 69%). **^{1}H NMR** (300 MHz, $CDCl_3$, 25°C)/ppm: δ = 0.92 (m, vbr, 1H, **CH** of Cp), 1.50 (m, vbr, 4H, **CH_2** of Cp), 1.80 (m, vbr, 4H, **CH_2** of Cp); **^{13}C NMR** (75.5 MHz, $CDCl_3$, 25°C)/ppm: δ = 22.5 (s, **C**HSi), δ 27.3 (s, **CH_2** of Cp), 27.6 (s, **CH_2** of Cp); **^{29}Si NMR** (79.3 MHz, $CDCl_3$, 25°C)/ppm: δ = -66.6. The spectral data were consistent with the product being octa-*cyclo*-pentyloctasilsesquioxane[71].

Synthesis of (c-C_5H_9)Si($OCH_2CH_2CH_3$)$_3$ (MP07):

Propan-1-ol (60.10 g.mol^{-1}; 19.7 g; in excess) and cyclopentyltrichlorosilane (203.35 g.mol^{-1}; 10.08 g; 49.57 mmol) were dissolved in dry THF (200 ml); a solution of triethylamine (101 g.mol^{-1}; 22 g; 217.8 mmol) in dry THF (100 ml) was added to the mixture very slowly. The mixture was stirred for one and a half hours during which time a white solid precipitated out. The mixture was filtered under vacuum and the filtrate collected. A brown liquid was obtained after distillation (9.35 g, 68%). **^{1}H NMR** (300 MHz, $CDCl_3$, 25°C)/ppm: δ = 0.95 (t, 9H, CH_3), 1.08 (m, vbr, 1H, CH of Cp), 1.55 (m, vbr, 4H, CH_2 of Cp), 1.61 (m, vbr, 6H, CH_2), 1.85 (m, 4H, CH_2 of Cp), 3.76 (t, 6H, OCH_2); **^{13}C NMR** (75.5 MHz, $CDCl_3$, 25°C)/ppm: δ = 10.6 (s, CH_3), 22.3 (s, CH of Cp), 25.8 (s, CH_2), 27.0 (s, CH_2 of Cp), 27.7 (s, CH_2 of Cp), 64.6 (s, OCH_2); **^{29}Si NMR** (79.3 MHz, $CDCl_3$, 25°C)/ppm: δ = -46.3. All spectra data were in agreement with the product being *cyclo*-pentyltripropoxysilane.

Reaction of (c-C_5H_9)Si($OCH_2CH_2CH_3$)$_3$ with TBAF (MP08):

Cyclopentyltripropoxysilane (274 g.mol^{-1}; 1.05 g; 3.83 mmol) was dissolved in dry acetone (20 ml), then TBAF (2.5 ml of a 1M solution in THF with 5% water) was added. This mixture was stirred at room temperature for 24 hours. A white solid precipitated out. After filtration under vacuum, a white solid was obtained (0.44 g, 94.9%). **^{1}H NMR** (300 MHz, $CDCl_3$, 25°C)/ppm: δ = 0.92 (m, vbr, 1H, CH of Cp), 1.50 (m, vbr, 4H, CH_2 of Cp), 1.80 (m, vbr, 4H, CH_2 of Cp); **^{13}C NMR** (75.5 MHz, $CDCl_3$, 25°C)/ppm: δ = 22.5 (s, CHSi), 27.3 (s, CH_2 of Cp), 27.6 (s, CH_2 of Cp); **^{29}Si NMR** (79.3 MHz, $CDCl_3$, 25°C)/ppm: δ = -66.6. The spectral data were consistent with the product being octa-*cyclo*-pentyloctasilsesquioxane[71].

Synthesis of (c-C_5H_9)Si(OCH_2CH_2 CH_2CH_3)$_3$ (MP09):

Butan-1-ol (74.12 g.mol^{-1}; 20.05 g; in excess) and *cyclo*-pentyltrichlorosilane (203.35 g.mol^{-1}; 10.25 g; 50.41 mmol) were dissolved in dry THF (200 ml); a solution of triethylamine (101 g.mol^{-1}; 22 g; 217.8 mmol) in dry THF (100 ml) was added to the mixture very slowly. The mixture was stirred for one and a half hours during which time a white solid precipitated out. The mixture was filtered under vacuum and the filtrate collected. A brownish liquid was obtained after distillation (9.85 g, 62%). **^{1}H NMR** (300

MHz, $CDCl_3$, 25°C)/ppm: δ = 0.87 (t, vbr, 9H, CH_3), 0.92 (m, vbr, 1H, CH of Cp), 1.30 (m, 6H, CH_2), 1.50 (m, 6H, CH_2), 1.55 (m, vbr, 4H, CH_2 of Cp), 1.75 (m, vbr, 4H, CH_2 of Cp), 3.68 (t, 6H, OCH_2); **^{13}C NMR** (75.5 MHz, $CDCl_3$, 25°C)/ppm: δ = 13.8 (s, CH_3), 19.1 (s, CH_2CH_3), 21.7 (s, CH of Cp), 26.5 (s, CH_2 of Cp), 27.5 (s, CH_2 of Cp), 34.9 (s, CH_2), 62.7 (s, OCH_2); **^{29}Si NMR** (79.3 MHz, $CDCl_3$, 25°C) /ppm: δ = -46.2. All spectra data were in agreement with the product being *cyclo*-pentyltributoxysilane.

Reaction of (c-C_5H_9)Si(OCH_2CH_2 CH_2CH_3)$_3$ with TBAF (MP10):

Cyclopentyltributoxysilane (316 g.mol^{-1}; 1.09 g; 3.45 mmol) was dissolved in acetone (20 ml), then TBAF (2.5 ml of a 1M solution in THF with 5% water) was added. This mixture was stirred at room temperature for 24 hours. A white solid precipitated out. After filtration under vacuum, a white solid was obtained (0.39 g, 93%). **^{1}H NMR** (300 MHz, $CDCl_3$, 25°C)/ppm: δ = 0.92 (m, vbr, 1H, CH of Cp), 1.50 (m, vbr, 4H, CH_2 of Cp), 1.80 (m, vbr, 4H, CH_2 of Cp); **^{13}C NMR** (75.5 MHz, $CDCl_3$, 25°C)/ppm: δ = 22.2 (s, CHSi), 27.0 (s, CH_2 of Cp), 27.3 (s, CH_2 of Cp); **^{29}Si NMR** (79.3 MHz, $CDCl_3$, 25°C)/ppm: δ = -66.6. The spectral data were consistent with the product being octa-*cyclo*-pentyloctasilsesquioxane[71].

Synthesis of (c-C_5H_9)$_8$$Si_8O_{12}$ cage from (c-C_5H_9)Si($OCH_2CH_2CH_3$)$_3$ (MP62):

Cyclopentyltripropoxysilane (274 g.mol^{-1}; 1.18 g; 4.31 mmol) was dissolved in dry pyridine (20 ml), then TBAF (2.5 ml of a 1M solution in THF with 5% water) was added. This mixture was stirred at room temperature for 24 hours. A white solid precipitated out and after filtration under vacuum, a white solid (0.36 g, 68.4%) and a red liquid (the filtrate) were obtained. **White powder**: **^{1}H NMR** (300 MHz, $CDCl_3$, 25°C)/ppm: δ = 0.92 (m, vbr, 1H, CH of Cp), 1.50 (m, vbr, 4H, CH_2 of Cp), 1.80 (m, vbr, 4H, CH_2 of Cp); **^{13}C NMR** (75.5 MHz, $CDCl_3$, 25°C)/ppm: δ = 22.3 (s, CHSi), 27.0 (s, CH_2 of Cp), 27.3 (s, CH_2 of Cp); **^{29}Si NMR** (79.3 MHz, $CDCl_3$, 25°C)/ppm: δ = -66.6. The spectral data were consistent with the product being octa-*cyclo*-pentyloctasilsesquioxane[71].

Red liquid: **^{29}Si NMR** (79.3 MHz, $CDCl_3$, 25°C)/ppm: δ = -66.6, -69.3

Synthesis of $C_6H_5Si(OCH_3)_3$ (MP11):

Methanol (32 g.mol^{-1}; 15 g; in excess) and phenyltrichlorosilane (211.55 g.mol^{-1}; 10.3 g; 48.69 mmol) were dissolved in dry THF (200 ml); a solution of triethylamine (101 g.mol^{-1};

22 g; 217.8 mmol) in dry THF (100 ml) was added to the mixture very slowly. The mixture was stirred for one and a half hours during which time a white solid precipitated out. The mixture was filtered under vacuum and the filtrate collected. A brown liquid was obtained after distillation (6.54 g, 68%). **^{1}H NMR** (300 MHz, $CDCl_3$, 25°C)/ppm: δ = 3.26 (s, 9H, OCH_3), 7.00 (m, vbr, 3H, Ar-**H**), 7.27 (m, 2H, Ar-**H**); **^{13}C NMR** (75.5 MHz, $CDCl_3$, 25°C)/ppm: δ = 50.6 (s, OCH_3), 127.8 (s, *o*-**C** of Ar), 130.4 (s, *i*-**C** of Ar); 134.6 (s, *m*-**C** of Ar), 138.2 (s, *p*-**C** of Ar); **^{29}Si NMR** (79.3 MHz, $CDCl_3$, 25°C)/ppm: δ = -54.4. All spectra data were in agreement with the product being phenyltrimethoxysilane.

Reaction of $C_6H_5Si(OCH_3)_3$ with TBAF (MP12)*:

Phenyltrimethoxysilane (198.30 g.mol^{-1}; 1.20 g; 6.05 mmol) was dissolved in acetone (20 ml), then TBAF (2.5 ml of a 1M solution in THF with 5% water) was added. This mixture was stirred at room temperature for 24 hours. A yellow viscous liquid was obtained after removal of the solvent. Dry chloroform was added and a white powder was obtained after filtration together with a yellow-brown liquid. The powder dissolved in acetone (0.05 g, 6.4%).

Yellow viscous liquid: ^{29}Si NMR (79.3 MHz, d_6 acetone, 25°C)/ppm: δ = -79.6, -81.4

White powder: **^{1}H NMR** (300 MHz, d_6 acetone, 25°C)/ppm: δ = 0.86 (t, 15H, CH_3), 1.30 (m, 10H, CH_2), 1.68 (m, 10H, CH_2), 3.30 (t, 10H, CH_2), 7.18 (m, 30H, Ar-**H**), 7.68 (m, 20H, Ar-**H**); **^{13}C NMR** (75.5 MHz, d_6 acetone, 25°C)/ppm: δ = 13.8 (s, CH_3), 20.3 (s, -CH_2-), 24.3 (s, -CH_2-), 49.8 (s, N-CH_2), 128.1 (s, *o*-**C** of Ar), 129.7 (s, *i*-**C** of Ar), 134.9 (s, *m*-**C** of Ar), 138.3 (s, *p*-**C** of Ar); **^{29}Si NMR** (79.3 MHz, d_6 acetone, 25°C)/ppm: δ = -80.6. This compound is not the anticipated Ph_8T_8 cage[71]. However, this was subsequently shown to be the tetra-*n*-butylammonium octaphenyloctasilsesquioxane fluoride cage (see experimental MP19).

Synthesis of $(C_6H_5)Si(OEt)_3$ (MP13):

Ethanol (46 g.mol^{-1}; 10 g; in excess) and phenyltrichlorosilane (211.55 g.mol^{-1}; 11.20g; 52.94 mmol) were dissolved in dry THF (200 ml); a solution of triethylamine (101 g.mol^{-1}; 22 g; 217.8 mmol) in dry THF (100 ml) was added to the mixture very slowly. The mixture was stirred for one and a half hours during which time a white solid precipitated out. The mixture was filtered under vacuum and the filtrate collected. A yellow liquid was obtained

after distillation (9.34 g, 73.4%). **^{1}H NMR** (300 MHz, $CDCl_3$, 25°C)/ppm: δ = 0.89 (t, 9H, CH_3), 3.52 (q, 6H, OCH_2), 7.03 (m, 3H, Ar-**H**), 7.33 (m, 2H, Ar-**H**); **^{13}C NMR** (75.5 MHz, $CDCl_3$, 25°C)/ppm: δ = 18.1 (s, CH_3), 58.6 (s, OCH_2), δ 127.7 (s, *o*-**C** of Ar), 130.1 (s, *i*-**C** of Ar), 134.6 (s, *m*-**C** of Ar), 138.2 (s, *p*-**C** of Ar); **^{29}Si NMR** (79.3 MHz, $CDCl_3$, 25°C)/ppm: δ = -57.6. All spectra data were in agreement with the product being phenyltriethoxysilane.

Reaction of $(C_6H_5)Si(OEt)_3$ with TBAF (MP14)*:

Phenyltriethoxysilane (240.3 g.mol^{-1}; 1.06 g; 4.41 mmol) was dissolved in acetone (20 ml), then TBAF (2.5 ml of a 1M solution in THF with 5% water) was added. This mixture was stirred at room temperature for 24 hours. A yellow viscous liquid was obtained after removal of the solvent. Dry chloroform was added and a white powder was obtained after filtration together with a yellow liquid. The powder dissolved in acetone (0.02 g, 3.5%). **White powder**: **^{1}H NMR** (300 MHz, d_6 acetone, TMS)/ppm: δ = 7.81-7.78 (dd, $^3J(H_2,H_1)$ = 2.0 Hz, $^3J(H_2,H_3)$ = 1.1 Hz, 2H; *m*-C**H** of Ar-**H**), 7.79 (t, $^3J(H_3,H_2)$ = 1.1 Hz, 1H; *p*-C**H** of Ar-**H**), 7.29 (d, $^3J(H_1,H_2)$ = 2.0 Hz, 2H; *o*-C**H** of Ar-**H**), 3.39-3.34 (t, $^3J(H_4,H_5)$ = 8.26 Hz, 2H; N-CH_2), 1.75-1.85 (quintuplet, $^3J(H_5,H_4)$ = 8.26 Hz, $^3J(H_5,H_6)$ = 7.33 Hz, 2H; CH_2), 1.36-1.48 (m, 2H; CH_2), 0.95-0.99 (t, $^3J(H_7,H_6)$ = 7.54 Hz, 3H, CH_3); **^{13}C NMR** (75.5 MHz, d_6 Acetone, TMS)/ppm: δ = 138.4 (*p*-**C** of Ar), 134.9 (*m*-**C** of Ar), 129.7 (*i*-**C** of Ar), 128.1 (*o*-**C** of Ar), 49.8 (N-**C**), 24.3 (CH_2), 20.3 (CH_2), 13.8 (CH_3); **^{29}Si NMR** (79.30 MHz, d_6 acetone, TMS)/ppm: δ = -80.6; **^{19}F NMR** (376 MHz, d_6 acetone)/ppm: δ = -26.4. This compound is not the anticipated Ph_8T_8 cage[71]. However, this was subsequently shown to be the tetra-*n*-butylammonium octaphenyloctasilsesquioxane fluoride cage (see experimental MP19).

Yellow liquid solved in chloroform: ^{29}Si NMR (79.3 MHz, $CDCl_3$, 25°C)/ppm: δ = -81.4

Synthesis of $(C_6H_5)Si(OCH_2CH_2CH_3)_3$ (MP15):

Propan-1-ol (60.10 g.mol^{-1}; 13 g; in excess) and phenyltrichlorosilane (211.55 g.mol^{-1}; 10.93 g; 51.67 mmol) were dissolved in dry THF (200 ml); a solution of triethylamine (101 g.mol^{-1}; 22 g; 217.8 mmol) in dry THF (100 ml) was added to the mixture very slowly. The mixture was stirred for one and a half hours during which time a white solid precipitated out. The mixture was filtered under vacuum and the filtrate collected. A yellow liquid was

obtained after distillation (12.55 g, 86%). **^{1}H NMR** (300 MHz, $CDCl_3$, 25°C)/ppm: δ = 0.57 (t, 9H, **CH_3**), 1.26 (m, 6H, **CH_2**), 3.41 (m, 6H, **OCH_2**), 7.06 (m, 3H, Ar-**H**), 7.33 (m, 2H, Ar-**H**); **^{13}C NMR** (75.5 MHz, $CDCl_3$, 25°C)/ppm: δ = 10.2 (s, **CH_3**), 25.6 (s, **CH_2**), 64.7 (s, OCH_2), 127.8 (s, *o*-**C** of Ar), 130.2 (s, *i*-**C** of Ar), 134.8 (s, *m*-**C** of Ar), 138.2 (*p*-**C** of Ar); **^{29}Si NMR** (79.3 MHz, $CDCl_3$, 25°C)/ppm: δ = -57.9. All spectra data were in agreement with the product being phenyltripropoxysilane.

Reaction of $C_6H_5Si(OCH_3)_3$ with TBAF (MP17):

Phenyltrimethoxysilane (198.30 g.mol^{-1}; 1.10 g; 5.55 mmol) was dissolved in chloroform (20 ml), then TBAF (2.5 ml of a 1M solution in THF with 5% water) was added. This mixture was stirred at room temperature for 24 hours. A yellow viscous solid that could not be characterised was obtained after removal of the solvent (0.08 g, resin).

Reaction of $(C_6H_5)Si(OEt)_3$ with TBAF (MP18):

Phenyltriethoxysilane (240.3 g.mol^{-1}; 1 g; 4.46 mmol) was dissolved in chloroform (20 ml), then TBAF (2.5 ml of a 1M solution in THF with 5% of water) was added. This mixture was stirred at room temperature for 24 hours. A yellow viscous liquid that could not be characterised was obtained after removal of the solvent (1.58 g, resin).

Synthesis of tetra-*n*-butylammonium octaphenyloctasilsesquioxane fluoride (MP19)*:

Phenyltriethoxysilane (1.02 g, 4.2 mmol) was dissolved in dry tetrahydrofuran (20 cm^3), then tetra-*n*-butylammonium fluoride (2.5 cm^3 of a 1M solution in THF with 5% water) was added. The mixture was stirred at room temperature for 24 hours and a yellow viscous liquid obtained after removal of the solvent. Dry chloroform (10 cm^3) was added and a white powder was obtained after filtration. Recrystallisation from acetone afforded colourless crystals (1.25 g, 46%). **IR** (KBr disc): ν/cm^{-1} 3085 (ν_{C-H}), 2990 (ν_{C-H}), 2935 (ν_{C-H}), 1410 (m), 1120 ($\nu_{as(Si-O-Si)}$), 1050, 1000, 750, 700, 510 ($\nu_{s(Si-O-Si)}$), 410 ($\delta_{(O-Si-O)}$); **^{1}H NMR** (300 MHz, d_6 acetone, TMS)/ppm: δ = 7.81-7.78 (dd, $^3J(H_2,H_1)$ = 2.0 Hz, $^3J(H_2,H_3)$ = 1.1 Hz, 2H; *m*-C**H**), 7.79 (t, $^3J(H_3,H_2)$ = 1.1 Hz, 1H; *p*-C**H**), 7.29 (d, $^3J(H_1,H_2)$ = 2.0 Hz, 2H; *o*-C**H**), 3.39-3.34 (t, $^3J(H_4,H_5)$ = 8.26 Hz, 2H; N-**CH_2**), 1.75-1.85 (quintuplet, $^3J(H_5,H_4)$ = 8.26 Hz, $^3J(H_5,H_6)$ = 7.33 Hz, 2H; **CH_2**), 1.36-1.48 (m, 2H; **CH_2**), 0.95-0.99 (t, $^3J(H_7,H_6)$ = 7.54 Hz, 3H, **CH_3**); **^{13}C NMR** (75.5 MHz, d_6 acetone, TMS)/ppm: δ = 138.4 (*p*-**C** of Ar), 134.9 (*m*-**C**

of Ar), 129.7 (*i*-**C** of Ar), 128.1 (*o*-**C** of Ar), 49.8 (N-**C**), 24.3 (**C**H_2), 20.3 (**C**H_2), 13.8 (**C**H_3); **^{29}Si NMR** (79.30 MHz, d_6 acetone, TMS)/ppm: δ = -80.6; **^{19}F NMR** (376 MHz, d_6 acetone)/ppm: δ = -26.4; **MS** (MALDI-TOF): *m/z* (%): 1294.5 [M^-], 1052.5 (35) [M^- -$C_{16}H_{36}N$], 1034 (100) [M^-- $C_{16}H_{36}NF$], 242.3 (99) [$C_{16}H_{36}N^+$], 19 [F^-]. **TGA**: m.p. 342°C. **Anal. Calc. for $C_{64}H_{76}FNO_{12}Si_8$ (1294.98)**: %C = 59.36, %H = 5.92, %N = 1.08, %F = 1.47; % Found: % C = 58.29, %H = 5.81, %N = 0.86, %F = 1.40

This compound has been fully characterised and X-ray data are reported in the appendix.

Reaction of $(C_6H_5)Si(OCH_2CH_2CH_3)_3$ with TBAF (MP21)*:

Phenyltripropoxysilane (282.3 g.mol^{-1}; 1.07 g; 3.79 mmol) was dissolved in n-hexane (20 ml), then TBAF (2.5 ml of a 1M solution in THF with 5% water) was added. This mixture was stirred at room temperature for 24 hours. A yellow viscous liquid was obtained after removal of the solvent. Dry chloroform was added and a white powder was obtained after filtration together with a yellow-brown liquid. The powder dissolved in acetone (0.01 g, 2%).

White powder: All spectral data were in agreement with those given in the previous experiment (MP19).

Yellow-brown liquid: ^{29}Si NMR (79.3 MHz, $CDCl_3$, 25°C)/ppm: δ = -79.8, -81.5

Synthesis of $(C_6H_5)Si(OCH_2CH_2\ CH_2CH_3)_3$ (MP22):

Butan-1-ol (74.12 g.mol^{-1}; 16.85 g; in excess) and phenyltrichlorosilane (203.35 g.mol^{-1}; 10.73 g; 52.77 mmol) were dissolved in dry THF (200 ml); a solution of triethylamine (101 g.mol^{-1}; 22 g; 217.8 mmol) in dry THF (100 ml) was added to the mixture very slowly. The mixture was stirred for one and a half hours during which time a white solid precipitated out. The mixture was filtered under vacuum and the filtrate collected. A brown liquid was obtained after distillation (13.34 g, 78%). **^{1}H NMR** (300 MHz, $CDCl_3$, 25°C)/ppm: δ = 0.56 (t, vbr, 9H, C**H**$_3$), 1.04 (m, 6H, C**H**$_2$CH$_3$), 1.22 (m, 6H, C**H**$_2$), 3.46 (m, 3H, OC**H**$_2$), 7.04 (m, 3H, Ar-**H**), 7.32 (m, 2H, Ar-**H**); **^{13}C NMR** (75.5 MHz, $CDCl_3$, 25°C)/ppm: δ = 13.7 (s, **C**H$_3$), 18.8 (s, **C**H$_2$), 34.4 (s, **C**H$_2$), 62.6 (s, O**C**H$_2$), 127.6 (s, *o*-**C** of Ar), 130.1 (s, *i*-**C** of Ar), 134. 7 (s, *m*-**C** of Ar), 138.1 (*p*-**C** of Ar); **^{29}Si NMR** (79.3 MHz, $CDCl_3$, 25°C)/ppm: δ = -57.8. All spectra data were in agreement with the product being phenyltributoxysilane.

Reaction of $(C_6H_5)Si(OCH_2CH_2CH_3)_3$ with TBAF (MP23):

Phenyltripropoxysilane (282.3 $g.mol^{-1}$; 1.14 g; 4.04 mmol) was dissolved in chloroform (20 ml), then TBAF (2.5 ml of a 1M solution in THF with 5% water) was added. This mixture was stirred at room temperature for 24 hours. A yellow viscous solid that could not be characterised was obtained after removal of the solvent (resin).

Reaction of $(C_6H_5)Si(OCH_2CH_2CH_2CH_3)_3$ with TBAF (MP24):

Phenyltributoxysilane (324.3 $g.mol^{-1}$; 1.14 g; 3.51 mmol) was dissolved in chloroform (20 ml), then TBAF (2.5 ml of a 1M solution in THF with 5% water) was added. This mixture was stirred at room temperature for 24 hours. A yellow viscous solid that could not be characterised was obtained after removal of the solvent (resin).

Reaction of $(C_6H_5)Si(OCH_2CH_2CH_3)_3$ with TBAF (MP25)*:

Phenyltripropoxysilane (282.3 $g.mol^{-1}$; 1.24 g; 4.39 mmol) was dissolved in toluene (20 ml), then TBAF (2.5 ml of a 1M solution in THF with 5% water) was added. This mixture was stirred at room temperature for 48 hours. A yellow viscous liquid was obtained after the removal of the solvent. Dry chloroform was added and a white powder was obtained after filtration together with a yellow liquid. The powder dissolved in acetone (0.07 g, 12%).

White powder: All spectral data were in agreement with those given in experiment MP19.

Reaction of $(C_6H_5)Si(OCH_2CH_2CH_3)_3$ with TBAF (MP26)*:

Phenyltripropoxysilane (282.3 $g.mol^{-1}$; 1.14 g; 4.04 mmol) was dissolved in pyridine (20 ml), then TBAF (2.5 ml of a 1M solution in THF with 5% water) was added. This mixture was stirred at room temperature for 48 hours. A yellow viscous liquid was obtained after removal of the solvent. Dry chloroform was added and a white powder was obtained after filtration together with a yellow-brown liquid. The powder dissolved in acetone (0.32 g, 61%).

White powder: All spectral data were in agreement with those given in experiment MP19.

Reaction of $(C_6H_5)Si(OEt)_3$ with TBAF (MP27)*:

Phenyltriethoxysilane (240.3 $g.mol^{-1}$; 1.21 g; 5.04 mmol) was dissolved in pyridine (20 ml), then TBAF (2.5 ml of a 1M solution in THF with 5% water) was added. This mixture was stirred at room temperature for 24 hours. A yellow viscous solid was obtained after removal

of the solvent. Dry chloroform was added and a white powder was obtained after filtration together with a yellow-brown liquid. The powder dissolved in acetone (0.25 g, 38.5%).
White powder: All spectral data were in agreement with those given in experiment MP19.

Reaction of $(C_6H_5)Si(OCH_2CH_2CH_2CH_3)_3$ with TBAF (MP28)*:

Phenyltributoxysilane (324.3 $g.mol^{-1}$; 1.06 g; 3.27 mmol) was dissolved in dry pyridine (20 ml), then TBAF (2.5 ml of a 1M solution in THF with 5% water) was added. This mixture was stirred at room temperature for 24 hours. A yellow viscous solid was obtained after removal of the solvent. Dry chloroform was added and a white powder was obtained after filtration together with a yellow liquid. The powder dissolved in acetone (0.16 g, 38%).
White powder: All spectral data were in agreement with those given in experiment MP19.

Reaction of $(C_6H_5)Si(OCH_2CH_2CH_2CH_3)_3$ with TBAF (MP29):

Phenyltributoxysilane (324.3 $g.mol^{-1}$; 1.01 g; 3.11 mmol) was dissolved in dry THF (20 ml), then TBAF (2.5 ml of a 1M solution in THF with 5% water) was added. This mixture was stirred at room temperature for 24 hours. A yellow viscous solid that could not be characterised was obtained after removal of the solvent.

Reaction of $(C_6H_5)Si(OCH_2CH_2CH_3)_3$ with TBAF (MP30)*:

Phenyltripropoxysilane (282.3 $g.mol^{-1}$; 1.08 g; 3.83 mmol) was dissolved in dry THF (20 ml), then TBAF (2.5 ml of a 1M solution in THF with 5% water) was added. This mixture was stirred at room temperature for 48 hours. A yellow viscous liquid was obtained after removal of the solvent. Dry chloroform was added and a white powder was obtained after filtration together with a yellow-brown liquid. The powder dissolved in acetone (0.10 g, 20%).
White powder: All spectral data were in agreement with those given in experiment MP19.
Yellow-brown liquid: ^{29}Si NMR (79.3 MHz, d_6 acetone, 25°C)/ppm: δ = -79.7, -81.6

Reaction of $C_6H_5Si(OCH_3)_3$ with TBAF (MP31)*:

Phenyltrimethoxysilane (198.30 $g.mol^{-1}$; 1.09 g; 5.50 mmol) was dissolved in THF (20 ml), then TBAF (2.5 ml of a 1M solution in THF with 5% water) was added. This mixture was stirred at room temperature for 24 hours. A yellow viscous solid was obtained after removal

of the solvent. Dry chloroform was added and a white powder was obtained after filtration together with a yellow-brown liquid. The powder dissolved in acetone (0.23 g, 32.5%).

White powder: All spectral data were in agreement with those given in experiment MP19.

Yellow-brown liquid: ^{29}**Si NMR** (79.3 MHz, d_6 acetone, 25°C)/ppm: δ = -79.7, -81.7

Reaction of $(C_6H_5)Si(OCH_2CH_2CH_2CH_3)_3$ with TBAF (MP32):

Phenyltributoxysilane (324.3 g.mol^{-1}; 1.09 g; 3.36 mmol) was dissolved in chloroform (20 ml), then TBAF (2.5 ml of a 1M solution in THF with 5% water) was added. The solution was cloudy after 24 hours. This mixture was stirred at room temperature for 48 hours. A white solid precipitated out which after filtration under vacuum gave a white solid. The powder did not dissolve in any solvent which is consistent with a Ph_8T_8 cage[71, 82, 83] (0.35 g, 80.7%).

Solid State ^{29}**Si NMR** (79.3 MHz, 25°C)/ppm: δ = -76.4, -79.6, -81.2

Reaction of $(C_6H_5)Si(OCH_2CH_2CH_3)_3$ with TBAF (MP33):

Phenyltripropoxysilane (282.3 g.mol^{-1}; 1.19 g; 4.21 mmol) was dissolved in chloroform (20 ml), then TBAF (2.5 ml of a 1M solution in THF with 5% water) was added. This mixture was stirred at room temperature for 48 hours. A white solid precipitated out which after filtration under vacuum gave a white solid. The powder did not dissolve in any solvent which is consistent with a Ph_8T_8 cage[71, 82, 83] (0.10 g, 18.4%).

Reaction of $(C_6H_5)Si(OEt)_3$ with TBAF (MP34):

Phenyltriethoxysilane (240.3 g.mol^{-1}; 1.09 g; 4.54 mmol) was dissolved in chloroform (20 ml), then TBAF (2.5 ml of a 1M solution in THF with 5% water) was added. This mixture was stirred at room temperature for 48 hours. A white solid precipitated out and after filtration under vacuum gave a white solid. The powder did not dissolve in any solvent which is consistent with a Ph_8T_8 cage[71, 82, 83] (0.07 g, 12.3%).

Reaction of $C_6H_5Si(OCH_3)_3$ with TBAF (MP35):

Phenyltrimethoxysilane (198.30 g.mol^{-1}; 0.91 g; 4.59 mmol) was dissolved in chloroform (20 ml), then TBAF (2.5 ml of a 1M solution in THF with 5% water) was added. The solution was cloudy after 24 hours. This mixture was stirred at room temperature for 48

hours. A white solid precipitated out which after filtration under vacuum gave a white solid. The powder did not dissolve in any solvent which is consistent with a Ph_8T_8 cage[71, 82, 83] (0.48 g, 81%).

Solid State ^{29}Si NMR (79.3 MHz, d_6 acetone, 25°C)/ppm: δ = -76.3, -77.0, -79.7

Reaction of $(C_6H_5)Si(OCH_2CH_2CH_3)_3$ with TBAF (MP61)*:

Phenyltripropoxysilane (282.3 g.mol^{-1}; 1.20 g; 4.251 mmol) was dissolved in pyridine (20 ml), then TBAF (2.5 ml of a 1M solution in THF with 5% water) was added. This mixture was stirred at room temperature for 48 hours. A yellow viscous liquid was obtained after removal of the solvent. Dry chloroform was added and a white powder was obtained after filtration together with a yellow liquid. The powder dissolved in acetone (0.38 g, 69.8%).

White powder: All spectral data were in agreement with those given in experiment MP19.

Red liquid: ^{29}Si NMR (79.3 MHz, d_6 acetone, 25°C)/ppm: δ = -81.4

Reaction of $(C_6H_5)Si(OCH_2CH_2CH_3)_3$ with TBAF (MP73)*:

Phenyltripropoxysilane (282.3 g.mol^{-1}; 1.39 g; 4.92 mmol) was dissolved in pyridine (20 ml), then TBAF (2.5 ml of a 1M solution in THF with 5% water) was added. This mixture was stirred at room temperature for 24 hours. A yellow viscous liquid was obtained after removal of the solvent. Dry chloroform was added and a white powder was obtained after filtration together with a yellow-brown liquid. The powder dissolved in acetone (0.17 g, 31.2%). **Yellow viscous liquid after removing the solvent: ^{29}Si NMR** (79.3 MHz, d_6 acetone, 25°C)/ppm: δ = -81.5; **^{19}F NMR** (376 MHz, d_6 acetone, 25°C)/ppm: δ = -26.4, -115.4, -120.1, -124.1, -129.4, -134.3;

White powder: All spectral data were in agreement with those given in experiment MP19.

Red liquid: ^{29}Si NMR (79.3 MHz, d_6 acetone, 25°C)/ppm: δ = -77.1, -79.6, -81.4

Reaction of $(C_6H_5)Si(OCH_2CH_2CH_3)_3$ with TBAF (MP112)*:

Phenyltripropoxysilane (282.3 g.mol^{-1}; 0.30 g; 1.06 mmol) was dissolved in d_6 acetone (5 ml), then TBAF (0.6 ml of aM solution in THF with 5% water) was added. This mixture was stirred at room temperature for 48 hours. The reaction was followed over time using ^{29}Si NMR spectroscopy. The solvent was removed at first without heating and subsequently

with heating. A yellow viscous liquid was obtained after the removal of the solvent. The results are described in section 2.3.

Reaction of $(C_6H_5)Si(OCH_2CH_2CH_3)_3$ with TBAF under anhydrous conditions (MP176)*:

Solid TBAF.xH_2O was used as the catalyst which was dried overnight under high vacuum. 0.65g of dry TBAF (261.47 g.mol^{-1}; 2.5 mmol) was then placed in a sealed round bottom flask that had been previously dried in an oven. The air was immediately replaced by nitrogen gas in the flask. 2.5ml of dry THF was added with a syringe to the flask to obtain 2.5ml of an anhydrous TBAF solution (1M) in THF (No water was added). 20ml of dry toluene was then added with a syringe to the flask before adding phenyltripropoxysilane (282.3 g.mol^{-1}; 1.38 g; 4.90 mmol). This mixture was stirred at room temperature for 24 hours. The solvent was removed on a rotary evaporator. A viscous liquid was obtained after the removal of the solvent. Only peaks arising from the starting material were observed in the NMR spectra.

Reaction of $(C_6H_5)Si(OCH_2CH_2CH_3)_3$ with TBAF and 2.5% water (MP177)*:

Solid TBAF.xH_2O was used as the catalyst which was dried overnight under high vacuum. 0.65g of dry TBAF (261.47 g.mol^{-1}; 2.5 mmol) was then placed in a sealed round bottom flask that had been previously dried in an oven. The air was immediately replaced by nitrogen gas in the flask. 2.5ml of dry THF was added with a syringe to the flask to obtain 2.5ml of an anhydrous TBAF solution (1M) in THF. 2.5% distilled water was added with a syringe into the flask. 20ml of dry toluene was then added with a syringe to the flask before adding phenyltripropoxysilane (282.3 g.mol^{-1}; 1.38 g; 4.90 mmol). This mixture was stirred at room temperature for 24 hours. The solvent was removed on a rotary evaporator. A viscous yellow liquid was obtained after the removal of the solvent. The mixture showed a number of peaks around -78 ppm in the ^{29}Si NMR indicative of a resin but no Ph_8T_8-TBAF peaks were observed.

Reaction of $(C_6H_5)Si(OCH_2CH_2CH_3)_3$ with TBAF and 5% water (MP178)*:

Solid TBAF.xH_2O was used as the catalyst which was dried overnight under high vacuum. 0.65g of dry TBAF (261.47 g.mol^{-1}; 2.5 mmol) was then placed in a sealed round bottom flask that had been previously dried in an oven. The air was immediately replaced by

nitrogen gas in the flask. 2.5ml of dry THF was added with a syringe into the flask to obtain 2.5ml of an anhydrous TBAF solution (1M) in THF. 5% distilled water was added with a syringe into the flask. 20ml of dry toluene was then added with a syringe to the flask before adding phenyltripropoxysilane (282.3 $g.mol^{-1}$; 1.38 g; 4.90 mmol). This mixture was stirred at room temperature for 24 hours. The solvent was removed on a rotary evaporator. A viscous liquid was obtained after the removal of the solvent.

Viscous liquid after removing the solvent: **^{29}Si NMR** (79.3 MHz, d_6 acetone, 25°C)/ppm: δ = -79, -81.5; **^{19}F NMR** (376 MHz, d_6 acetone, 25°C)/ppm: δ = -26.4, -115.4, -120.1, -124.1, -129.4, -134.3

Reaction of $(C_6H_5)Si(OCH_2CH_2CH_3)_3$ with TBAF and 7.5% water (MP179)*:

Solid TBAF.xH_2O was used as the catalyst which was dried overnight under high vacuum. 0.65g of dry TBAF (261.47 $g.mol^{-1}$; 2.5 mmol) was then placed in a sealed round bottom flask that had been previously dried in an oven. The air was immediately replaced by nitrogen gas in the flask. 2.5ml of dry THF was added with a syringe to the flask to obtain 2.5ml of an anhydrous TBAF solution (1M) in THF. 7.5% distilled water was added with a syringe to the flask. 20ml of dry toluene was then added with a syringe to the flask before adding phenyltripropoxysilane (282.3 $g.mol^{-1}$; 1.38 g; 4.90 mmol). This mixture was stirred at room temperature for 24 hours. The solvent was removed on a rotary evaporator. A viscous liquid was obtained after the removal of the solvent. The mixture showed a number of peaks around -78 ppm in the ^{29}Si NMR indicative of a resin but no Ph_8T_8-TBAF peaks were observed.

Reaction of $(C_6H_5)Si(OCH_2CH_2CH_3)_3$ with TBAF (MP154)*:

Phenyltripropoxysilane (282.3 $g.mol^{-1}$; 1.39 g; 4.92 mmol) was dissolved in acetone (20 ml), then TBAF (2.5 ml of a 1M solution in THF with 5% water) was added. This mixture was stirred at room temperature. After 24 hours, the reaction was stopped and the solvent removed at 50°C and 400 mbar on a rotary evaporator. A yellow solid gel was obtained.

Yellow solid gel after removing the solvent: **^{29}Si NMR** (79.3 MHz, d_6 acetone, 25°C)/ppm: δ = -79.7; **^{19}F NMR** (376 MHz, d_6 acetone, 25°C)/ppm: δ = -115.4, -120.1, -124.1, -129.4, -134.3. The results of this experiment are described in section 2.4.

Reaction of $(C_6H_5)Si(OCH_2CH_2CH_3)_3$ with TBAF (MP168)*:

Phenyltripropoxysilane (282.3 $g.mol^{-1}$; 1.40 g; 4.96 mmol) was dissolved in THF (20 ml), then TBAF (2.5 ml of a 1M solution in THF with 5% water) was added. This mixture was stirred at room temperature. After 24 hours, the reaction was stopped and the solvent removed at 55°C and 375 mbar on a rotary evaporator. A yellow solid gel was obtained.

Yellow solid gel after removing the solvent: ^{29}Si NMR (79.3 MHz, d_6 acetone, 25°C)/ppm: -78.4, -79.5, -79.6, -81.4; **^{19}F NMR** (376 MHz, d_6 acetone, 25°C)/ppm: δ = -115.4, -120.1, -124.1, -129.4, -134.3. The results of this experiment are described in section 2.4.

Reaction of $(C_6H_5)Si(OCH_2CH_2CH_3)_3$ with TBAF (MP153)*:

Phenyltripropoxysilane (282.3 $g.mol^{-1}$; 1.39 g; 4.92 mmol) was dissolved in toluene (20 ml), then TBAF (2.5 ml of a 1M solution in THF with 5% water) was added. This mixture was stirred at room temperature. After 24 hours, the reaction was stopped and the solvent removed at 90°C and 200 mbar on a rotary evaporator. A yellow solid gel was obtained.

Yellow solid gel after removing the solvent: ^{29}Si NMR (79.3 MHz, d_6 acetone, 25°C)/ppm: δ = -127.3 ($PhSiF_4^-$, quintet, J_{SiF} 206 Hz); **^{19}F NMR** (376 MHz, d_6 acetone, 25°C)/ppm: δ = -115.4, -120.1, -124.1, -129.4, -134.3. The results of this experiment are described in section 2.4.

Reaction of $(C_6H_5)Si(OCH_2CH_2CH_3)_3$ with TBAF (MP187)*:

Phenyltripropoxysilane (282.3 $g.mol^{-1}$; 1.38 g; 4.89 mmol) was dissolved in acetone (20 ml), then TBAF (2.5 ml of a 1M solution in THF with 5% water) was added. This mixture was stirred at room temperature. After 24 hours, the reaction was stopped and the solvent removed at 50°C and 400 mbar for about 10 minutes. A yellow solid gel, **A**, was obtained. The gel A was redissolved in toluene and stirred for 10 minutes. The toluene was removed at 73 mbar and 85°C for 10 minutes. A yellow solid gel, **B**, was obtained.

Gel A: ^{29}Si NMR (79.3 MHz, d_6 acetone, 25°C)/ppm: δ = -80.6; **^{19}F NMR** (376 MHz, d_6 acetone, 25°C)/ppm: δ = -26.6, -115.4, -120.1, -124.1, -129.4, -134.3;

Gel B: ^{29}Si NMR (79.3 MHz, d_6 acetone, 25°C)/ppm: δ = -79.4, -80.6, -128 (triplet, J_{SiF} 206 Hz); **^{19}F NMR** (376 MHz, d_6 acetone, 25°C)/ppm: δ = -26.6, -115.4, -120.1, -124.1, -129.4, -134.3. The results of this experiment are described in section 2.4.

Reaction of $(C_6H_5)Si(OCH_2CH_2CH_3)_3$ with TBAF (MP189)*:

Phenyltripropoxysilane (282.3 $g.mol^{-1}$; 1.41 g; 4.99 mmol) was dissolved in toluene (20 ml), then TBAF (2.5 ml of a 1M solution in THF with 5% water) was added. This mixture was stirred at room temperature. After 24 hours, the reaction was stopped and the solvent removed at 73 mbar and at 60°C to 90°C over 25 minutes. A yellow solid gel, **A**, was obtained. The gel A was redissolved in toluene and stirred for 10 minutes. The toluene was removed at 79 mbar and 60°C over 15 minutes and heated at 70°C and at 79 mbar for a further 15 minutes. A yellow solid gel **B** was obtained.

Gel A: **^{29}Si NMR** (79.3 MHz, d_6 acetone, 25°C)/ppm: δ = -68.9, -77.7, -78.5, -80.6; **^{19}F NMR** (376 MHz, d_6 acetone, 25°C)/ppm: δ = -26.6, -115.4, -120.1, -124.1, -129.4, -134.3; **Gel B**: **^{29}Si NMR** (79.3 MHz, d_6 acetone, 25°C)/ppm: δ = -80.6, -127.3 ($PhSiF_4^-$, quintet, J_{SiF} 206 Hz); **^{19}F NMR** (376 MHz, d_6 acetone, 25°C)/ppm: δ = -26.6. The results of this experiment are described in section 2.4.

Reaction of $(C_6H_5)Si(OCH_2CH_2CH_3)_3$ with TBAF (MP192)*:

Phenyltripropoxysilane (282.3 $g.mol^{-1}$; 1.38 g; 4.89 mmol) was dissolved in toluene (20 ml), then TBAF (2.5 ml of a 1M solution in THF with 5% water) was added. This mixture was stirred at room temperature. After 24 hours, the reaction was stopped and the solvent removed at 80°C and 73 mbar for 15 minutes using a rotary evaporator. A yellow solid gel was obtained which was then extracted with chloroform to give a white solid after filtration. **White powder**: **^{29}Si NMR** (79.3 MHz, d_6 acetone, 25°C)/ppm: δ = -80.6; **^{19}F NMR** (376 MHz, d_6 acetone, 25°C)/ppm: δ = -26.6. All spectral data were in agreement with the formation of Ph_8T_8-TBAF as described in experiment MP19.

Reaction of $(C_6H_5)Si(OCH_2CH_2CH_3)_3$ with TBAF (MP237)*:

Phenyltripropoxysilane (282.3 $g.mol^{-1}$; 1.39 g; 4.92 mmol) was dissolved in toluene (20 ml), then TBAF (2.5 ml of a 1M solution in THF with 5% water) was added. The mixture reaction was stirred and heated at 80°C for an hour before removing the solvent under vacuum distillation. A white solid gel was obtained.

White powder: **^{29}Si NMR** (79.3 MHz, d_6 acetone, 25°C)/ppm: δ = -80.6; **^{19}F NMR** (376 MHz, d_6 acetone, 25°C)/ppm: δ = -26.6. All spectral data were in agreement with the formation of Ph_8T_8-TBAF as described in experiment MP19.

8.2.2 Synthesis of tetra-*n*-butylammonium octavinyloctasilsesquioxane fluoride

Synthesis of tetra-*n*-butylammonium octavinyloctasilsesquioxane fluoride (MP205)*:

Vinyltriethoxysilane (190.3 $g.mol^{-1}$; 1.04 g, 5.46 mmol) was dissolved in dry toluene (20 cm^3), then tetra-*n*-butylammonium fluoride (2.5 cm^3 of a 1M solution in THF with 5% water) was added. The mixture was stirred at room temperature. After 24 hours, the reaction was stopped and the solvent removed on a rotary evaporator with a temperature gradient from 30°C to 80°C over 10 minutes, then leaving at 80°C and a vacuum of 70 mbar for 15 minutes. A yellow solid gel was obtained. Recrystallisation from acetone afforded colourless crystals (0.46 g, 60 %).

Gel: ^{1}H NMR (300 MHz, d_6 acetone)/ppm: δ = 5.98 (m, 24H, vinyl-**H**), 3.47-3.41 (m, 8H; N-C**H**$_2$), 1.80-1.70 (m, 8H; C**H**$_2$), 1.50-1.38 (m, 8H; C**H**$_2$), 0.98 (t, $^3J_{HH}$ = 7.4 Hz, 12H, C**H**$_3$); **^{13}C NMR** (75.5 MHz, d_6 acetone)/ppm: δ = 136.7 (Si-**C**H$_{vinyl}$), 132.0 (H$_2$**C**$_{vinyl}$), 59.3 (N-**C**H$_2$), 24.4 (**C**H$_2$), 20.3 (**C**H$_2$), 13.8 (**C**H$_3$); **^{29}Si NMR** (79.30 MHz, d_6 acetone)/ppm: δ = -82.9; **^{19}F NMR** (376 MHz, d_6 acetone)/ppm: δ = - 25.4, - 27.3, - 61.2, -108.4, -116.4, -117.8, -123.4, -124.6, -124.8, -149.6;

Crystals data: ^{1}H NMR (300 MHz, d_6 acetone)/ppm: δ = 5.98 (m, 24H, vinyl-H), 3.47-3.41 (m, 8H; N-CH$_2$), 1.80-1.70 (m, 8H; CH$_2$), 1.50-1.38 (m, 8H; CH$_2$), 0.98 (t, $^3J_{HH}$ = 7.4 Hz, 12H, CH$_3$); **^{13}C NMR** (75.5 MHz, d_6 acetone)/ppm: δ = 136.7 (Si-**C**H$_{vinyl}$), 132.0 (H$_2$**C**$_{vinyl}$), 59.3 (N-**C**H$_2$), 24.4 (**C**H$_2$), 20.3 (**C**H$_2$), 13.8 (**C**H$_3$); **^{29}Si NMR** (79.30 MHz, d_6 acetone)/ppm: δ = -82.9; **^{19}F NMR** (376 MHz, d_6 acetone)/ppm: δ = -25.4; **solid state ^{19}F NMR:** δ = -23.0 ppm; **MS** (ESI): *m/z* (%): 651.0 (100%) [M^-], 242.3 (100%) [$C_{16}H_{36}N^+$]. **TGA**: mp 150°C. **Anal. Calc. for $C_{32}H_{60}FNO_{12}Si_8$ (894.53)**: %C = 42.97, %H = 6.76, %N = 1.57, %F = 2.12; % Found: % C = 43.19, %H = 6.70, %N = 1.54

This compound has been fully characterised and X-ray data are reported in the appendix.

Synthesis of tetra-*n*-butylammonium octavinyloctasilsesquioxane fluoride (MP209)*:

Vinyltriethoxysilane (1.24 g, 6.52 mmol) was dissolved in dry toluene (20 cm^3), then tetra-*n*-butylammonium fluoride (2.5 cm^3 of a 1M solution in THF with 5% water) was added. The mixture was stirred at room temperature. After 24 hours, the reaction was stopped and

the solvent removed at room temperature and 95 mbar on a rotary evaporator. A yellow solid gel **A** was obtained. The gel A was redissolved in toluene, stirred for ten minutes and the solvent removed using a temperature gradient from 30°C to 80°C for 10 minutes, then leaving at 80°C and a vacuum of 70 mbar for 15 minutes. A yellow solid, gel **B**, was obtained.

Gel A: **^{29}Si NMR** (79.30 MHz, d_6 acetone)/ppm: δ = -63.6, -71, -74.2, -79.8, -81.6, -82.3, -82.4, -82.9; **^{19}F NMR** (376 MHz, d_6 acetone)/ppm: δ = -25.4, -27.0, -61.2, -108.4, -118.3, -124.3, -125.2, -126.0, -126.2, -150.0;

Gel B: **^{29}Si NMR** (79.30 MHz, d_6 acetone)/ppm: δ = -82.9; **^{19}F NMR** (376 MHz, d_6 acetone)/ppm: δ = -25.4, -27.0, -61.2, -108.4, -118.3, -124.3, -125.2, -126.0, -126.2, -150.0. The results of this experiment are described in section 3.2.

Synthesis of tetra-*n*-butylammonium octavinyloctasilsesquioxane fluoride (MP271)*:

Vinyltriethoxysilane (190.3 g.mol^{-1}; 1.04 g, 5.46 mmol) was dissolved in dry toluene (20 cm^3), then tetra-*n*-butylammonium fluoride (2.5 cm^3 of a 1M solution in THF with 5% water) was added. The mixture was stirred at room temperature. After 24 hours, the reaction was stopped and the solvent removed on a rotary evaporator at 90°C and a vacuum of 100 mbar for 15 minutes. A yellow solid gel was obtained. **^{29}Si NMR** (79.30 MHz, d_6 acetone)/ppm: δ = -74.2, -79.4, -79.6, -81.1, -81.7, -82.1, -82.5, -82.9, -84.0, -84.4; **^{19}F NMR** (376 MHz, d_6 acetone)/ppm: δ = -25.3, -26.4, -27.1, - 61.2, -108.4, -118.3, -124.3, -125.2, -126.0, -126.2, -150.0. The results of this experiment are described in section 3.2.

Synthesis of tetra-*n*-butylammonium octavinyloctasilsesquioxane fluoride (MP277B)*:

Vinyltriethoxysilane (190.3 g.mol^{-1}; 1.01 g, 5.31 mmol) was dissolved in dry toluene (20 cm^3), then tetrabutylammonium fluoride (2.5 cm^3 of a 1M solution in THF with 5% water) was added. The mixture was stirred at room temperature. After 24 hours, the reaction was stopped and the solvent removed on a rotary evaporator at 90°C and a vacuum of 90 mbar for 15 minutes. A yellow solid gel was obtained. **^{29}Si NMR** (79.30 MHz, d_6 acetone)/ppm: δ = -79.4, -79.6, -81.1, -81.7, -82.1, -82.5, -82.9, -84.0, -84.4; **^{19}F NMR** (376 MHz, d_6 acetone)/ppm: δ = -25.3, -26.4, -27.1, -61.2, -108.4, -118.3, -124.3, -125.2, -126.0, -126.2, -150.0. The results of this experiment are described in section 3.2.

Synthesis of tetra-*n*-butylammonium octavinyloctasilsesquioxane fluoride (MP293)*:

Vinyltriethoxysilane (190.3 $g.mol^{-1}$; 1.03 g, 5.41 mmol) was dissolved in dry toluene (20 cm^3), then tetra-*n*-butylammonium fluoride (2.5 cm^3 of a 1M solution in THF with 5% water) was added. The mixture was stirred at room temperature. After 24 hours, the reaction was stopped and the solvent removed on a rotary evaporator at 90°C and a vacuum of 80 mbar for 15 minutes. A yellow solid gel was obtained. **^{29}Si NMR** (79.30 MHz, d_6 acetone)/ppm: δ = -79.4, -79.6, -81.1, -82.9, -84.0, -84.4; **^{19}F NMR** (376 MHz, d_6 acetone)/ppm: δ = -25.3, -26.4, -27.1, -61.2, -108.4, -118.3, -124.3, -125.2, -126.0, -126.2, -150.0. The results of this experiment are described in section 3.2.

Synthesis of tetra-*n*-butylammonium octavinyloctasilsesquioxane fluoride (MP236)*:

Vinyltriethoxysilane (190.3 $g.mol^{-1}$; 1.05 g, 5.52 mmol) was dissolved in dry toluene (20 cm^3), then tetra-*n*-butylammonium fluoride (2.5 cm^3 of a 1M solution in THF with 5% water) was added. The mixture reaction was stirred and heated at 80°C for an hour before removing the solvent under vacuum distillation. A yellow solid gel was obtained. **^{29}Si NMR** (79.30 MHz, d_6 acetone)/ppm: δ = -82.9; **^{19}F NMR** (376 MHz, d_6 acetone)/ppm: δ = -25.3, -26.4, -27.1, -61.2, -108.4, -118.3, -124.3, -125.2, -126.0, -126.2, -150.0. The results of this experiment are described in section 3.2.

Synthesis of tetrabutylammonium octavinyloctasilsesquioxane fluoride (MP333)*:

Vinyltriethoxysilane (190.3 $g.mol^{-1}$; 1.04 g, 5.46 mmol) was dissolved in dry toluene (20 cm^3), then tetra-*n*-butylammonium fluoride (2.5 cm^3 of a 1M solution in THF with 5% water) was added. The mixture was stirred at room temperature. Six ^{19}F NMR spectroscopy measurements were then performed at different times for the same reaction: at time t = 0 (gel **A**) and at time t = 24h after 10 minutes (gel **B**) on the rotary evaporator at 70°C, and then after removal of 25% (gel **C**), 50% (gel **D**) and 75% (gel **E**) of the solvent, and finally after complete removal of the solvent (gel **F**).

Gel A: **^{19}F NMR** (376 MHz, d_6 acetone)/ppm: δ = -25.1, -26.8;

Gel B: **^{19}F NMR** (376 MHz, d_6 acetone)/ppm: δ = -25.1, -26.8;

Gel C: **^{29}Si NMR** (79.30 MHz, d_6 acetone)/ppm: δ = -70.7, -79.5, -80.3, -82.7; **^{19}F NMR** (376 MHz, d_6 acetone)/ppm: δ = -25.1, -26.8;

Gel D: **^{19}F NMR** (376 MHz, d_6 acetone)/ppm: δ = -25.1, -26.8;

Gel E: ^{29}**Si NMR** (79.30 MHz, d_6 acetone)/ppm: δ = -82.7; ^{19}**F NMR** (376 MHz, d_6 acetone)/ppm: δ = -25.1, -26.8;

Gel F: ^{29}**Si NMR** (79.30 MHz, d_6 acetone)/ppm: δ = -82.7; ^{19}**F NMR** (376 MHz, d_6 acetone)/ppm: δ = -25.1. The results of this experiment are described in section 3.2.

8.2.3 Synthesis of tetrabutylammonium octa-*para*-tolyloctasilsesquioxane fluoride

Reaction of *para*-tolyltripropoxysilane with TBAF (MP252)*:

Para-tolyltripropoxysilane (296.5 g.mol^{-1}; 1.06 g, 3.57 mmol) was dissolved in chloroform (20 cm^3), then tetra-*n*-butylammonium fluoride (2.5 cm^3 of a 1M solution in THF with 5% water) was added. The mixture was stirred at room temperature for 24 hours. The solvent was removed on a rotary evaporator with a temperature gradient from 30°C to 50°C over 10 minutes and a vacuum of 500 mbar for 15 minutes. A yellow solid gel was obtained. ^{29}**Si NMR** (79.30 MHz, d_6 acetone)/ppm: δ = -78.1, -79.5, -81.0; ^{19}**F NMR** (376 MHz, d_6 acetone)/ppm: δ = -108.4, -118.3, -124.3, -125.2, -126.0, -126.2, -150.0

This compound was subsequently shown to be the tetrabutylammonium octa-*para*-tolyloctasilsesquioxane cage.

Synthesis of tetrabutylammonium octa-*para*-tolyloctasilsesquioxane fluoride (MP265)*:

Para-tolyltrimethoxysilane (212.3 g.mol^{-1}; 1.05 g, 4.95 mmol) was dissolved in dry toluene (20 cm^3), then tetra-*n*-butylammonium fluoride (2.5 cm^3 of a 1M solution in THF with 5% water) was added. The mixture was stirred at room temperature for 24 hours. The solvent was removed on a rotary evaporator with a temperature gradient from 25°C to 87°C over 10 minutes and a vacuum of 100 mbar for 15 minutes. A brown gel was obtained. Recrystallisation from acetone afforded colourless crystals (0.56 g, 55 %).

Gel: ^{29}**Si NMR** (79.30 MHz, d_6 acetone)/ppm: δ = -68.5, -71.6, -77.4, -78.1, -79.4, -80.0, -80.4; ^{19}**F NMR** (376 MHz, d_6 acetone)/ppm: δ = -26.5, -26.8, -27.8, -108.4, -118.3, -124.3, -125.2, -126.0, -126.2, -150.0;

Crystals: ^{1}**H NMR** (300 MHz, d_6 acetone)/ppm: δ = 7.60 (d, $^3J_{HH}$ = 7.8 Hz, 16H, Ar-**H**), 7.02 (d, $^3J_{HH}$ = 7.8 Hz, 16H; Ar-**H**), 3.40-3.35 (m, 8H; N- **CH**$_2$), 2.20 (s, 24H, Ar-**CH**$_3$), 1.80-1.70 (m, 8H; **CH**$_2$), 1.43-1.30 (m, 8H; **CH**$_2$), 0.91 (t, $^3J_{HH}$ = 7.3 Hz, 12H, **CH**$_3$); ^{13}**C**

NMR (75.5 MHz, d_6 acetone)/ppm: δ = 139.0 (*p*-**C** of Ar), 135.2 (*i*-**C** of Ar), 135.0 (*m*-**C**H of Ar), 128.7 (*o*-**C**H of Ar), 59.3 (N-**C**H_2), 24.4 (**C**H_2), 21.5 (Ar-**C**H_3), 20.4 (**C**H_2), 13.8 (**C**H_3); **^{29}Si NMR** (79.30 MHz, d_6 acetone)/ppm: δ = -80.4; **^{19}F NMR** (376 MHz, d_6 acetone)/ppm: δ = -26.8; **MS** (MALDI-TOF): *m/z* (%): 1164.4 [M^-], 242.3 (100) [$C_{16}H_{36}N^+$]. **TGA**: mp 340-345°C. **Anal. Calc. for $C_{72}H_{92}FNO_{12}Si_8$ (1407.19)**: %C = 61.45, %H = 6.59, %N = 1.00, %F = 1.47; % Found: % C = 61.75, %H = 6.83, %N = 0.86 This compound has been fully characterised and X-ray data are reported in the appendix.

Reaction of *para*-tolyltrimethoxysilane with TBAF (MP266)*:

Para-tolyltrimethoxysilane (212.3 g.mol^{-1}; 1.43 g, 6.73 mmol) was dissolved in dry toluene (20 cm^3), then tetra-*n*-butylammonium fluoride (2.5 cm^3 of a 1M solution in THF with 5% water) was added. The mixture was stirred at room temperature for 24 hours. The solvent was removed on a rotary evaporator with a temperature gradient from 25°C to 87°C over 10 minutes and a vacuum of 100 mbar for 15 minutes. A brown gel was obtained. **^{29}Si NMR** (79.30 MHz, d_6 acetone)/ppm: δ = -80.4; **^{19}F NMR** (376 MHz, d_6 acetone)/ppm: δ = -26.8. All spectral data were in agreement with experiment MP265.

Reaction of *para*-tolyltripropoxysilane with TBAF (MP239) *:

Para-tolyltripropoxysilane (296.5 g.mol^{-1}; 1.22 g, 4.11 mmol) was dissolved in toluene (20 cm^3), then tetra-*n*-butylammonium fluoride (2.5 cm^3 of a 1M solution in THF with 5% water) was added. The mixture was stirred at room temperature for 24 hours. The solvent was removed on a rotary evaporator with a temperature gradient from 25°C to 87°C over 10 minutes and a vacuum of 100 mbar for 15 minutes. A brown gel was obtained. **^{29}Si NMR** (79.30 MHz, d_6 acetone)/ppm: δ = -68.5, -77.4, -78.1, -80.4; **^{19}F NMR** (376 MHz, d_6 acetone)/ppm: δ = -26.4, -27.7, -108.4, -118.3, -124.3, -125.2, -126.0, -126.2, -150.0. The results of this experiment are described in section 3.3.

Reaction of *para*-tolyltripropoxysilane with TBAF (MP267)*:

Para-tolyltripropoxysilane (296.5 g.mol^{-1}; 1.41 g, 4.76 mmol) was dissolved in toluene (20 cm^3), then tetra-*n*-butylammonium fluoride (2.5 cm^3 of a 1M solution in THF with 5% water) was added. The mixture was stirred at room temperature. After 24 hours, the reaction was stopped and the solvent removed on a rotary evaporator with a temperature gradient

from 25°C to 87°C over 10 minutes and a vacuum of 100 mbar for 15 minutes. A brown gel was obtained. Recrystallisation from acetone afforded colourless crystals.

Gel: ^{29}Si NMR (79.30 MHz, d_6 acetone)/ppm: δ = -68.5, -77.4, -78.1, -80.4; **^{19}F NMR** (376 MHz, d_6 acetone)/ppm: δ = -26.0, -26.3, -108.4, -118.3, -124.3, -125.2, -126.0, -126.2, -150.0;

Crystals: ^{1}H NMR (300 MHz, d_6 acetone)/ppm: δ = 7.60 (d, $^{3}J_{HH}$ = 7.8 Hz, 16H, Ar-**H**), 7.02 (d, $^{3}J_{HH}$ = 7.8 Hz, 16H; Ar-**H**), 3.40-3.35 (m, 8H; N-C**H**$_2$), 2.20 (s, 24H, Ar-C**H**$_3$), 1.80-1.70 (m, 8H; C**H**$_2$), 1.43-1.30 (m, 8H; C**H**$_2$), 0.91 (t, $^{3}J_{HH}$ = 7.3 Hz, 12H, C**H**$_3$); **^{13}C NMR** (75.5 MHz, d_6 acetone)/ppm: δ = 139.0 (*p*-**C** of Ar), 135.2 (*i*-**C** of Ar), 135.0 (*m*-CH of Ar), 128.7 (*o*-CH of Ar), 59.3 (N-**C**H$_2$), 24.4 (**C**H$_2$), 21.5 (Ar-**C**H$_3$), 20.4 (**C**H$_2$), 13.8 (**C**H$_3$); **^{29}Si NMR** (79.30 MHz, d_6 acetone)/ppm: δ = -80.4; **^{19}F NMR** (376 MHz, d_6 acetone)/ppm: δ = -26.8. All spectral data were in agreement with experiment MP265.

8.2.4 Synthesis of tetrabutylammonium octa-*para*-chloromethylphenyloctasilsesquioxane fluoride

Reaction of *para*-chloromethylphenyltrimethoxysilane with TBAF (MP201)*:

Para-chloromethylphenyltrimethoxysilane (246.8 g.mol^{-1}; 1.03 g, 4.17 mmol) was dissolved in acetone (20 cm^3), then tetra-*n*-butylammonium fluoride (2.5 cm^3 of a 1M solution in THF with 5% water) was added. The mixture was stirred at room temperature. After 24 hours, the reaction was stopped and the solvent removed on a rotary evaporator at a temperature of 40°C and a vacuum of 80 mbar over 15 minutes. A pink-red gel was obtained. **^{29}Si NMR** (79.30 MHz, d_6 acetone)/ppm: δ = -78.7, -80.8; **^{19}F NMR** (376 MHz, d_6 acetone)/ppm: δ = -26.5, -108.4, -118.3, -124.3, -125.2, -126.0, -126.2, -150.0. This compound was subsequently shown to be the tetra-n-butylammonium octa-*para*-chloromethylphenyloctasilsesquioxane (see experiment MP314).

Reaction of *para*-chloromethylphenyltrimethoxysilane with TBAF (MP227)*:

Para-chloromethylphenyltrimethoxysilane (246.8 g.mol^{-1}; 1.30 g, 5.28 mmol) was dissolved in toluene (20 cm^3), then tetrabutylammonium fluoride (2.5 cm^3 of a 1M solution in THF with 5% water) was added. The mixture was stirred at room temperature. After 24 hours, the

reaction was stopped and the solvent removed on a rotary evaporator with a temperature of 80°C and a vacuum of 70 mbar for 20 minutes. A yellow gel was obtained. **^{1}H NMR** (300 MHz, d_6 acetone)/ppm: δ = 7.82 (d, $^3J_{HH}$ = 7.7 Hz, 2H, Ar-**H**), 7.75 (d, $^3J_{HH}$ = 7.7 Hz, 2H; Ar-**H**), 4.63 (s, 2**H**; Cl-C**H**$_2$), 3.38 (t, 1H, N-C**H**$_2$), 1.68 (m, 1H; C**H**$_2$), 1.36 (m, 1H; C**H**$_2$), 0.93 (t, $^3J_{HH}$ = 7.3 Hz, 1.5H, C**H**$_3$); **^{13}C NMR** (75.5 MHz, d_6 acetone)/ppm: δ = 139.2 (*p*-**C** of Ar), 129.6 (*i*-**C** of Ar), 128.9 (*m*-**C**H of Ar), 126.0 (*o*-**C**H of Ar), 59.1 (N-**C**H$_2$), 46.9 (Cl-**C**H$_2$), 24.4 (**C**H$_2$), 20.3 (**C**H$_2$), 13.9 (**C**H$_3$); **^{29}Si NMR** (79.30 MHz, d_6 acetone)/ppm: δ = -80.8; **^{19}F NMR** (376 MHz, d_6 acetone)/ppm: δ = -26.3, -118.3, -150.0, -208.2. This compound was subsequently shown to be the tetra-n-butylammonium octa-*para*-chloromethylphenyloctasilsesquioxane (see experiment MP314).

Reaction of *para*-chloromethylphenyltrimethoxysilane with TBAF (MP314)*:

Para-chloromethylphenyltrimethoxysilane (246.8 g.mol^{-1}; 1.57 g, 6.36 mmol) was dissolved in toluene (20 cm^3), then tetrabutylammonium fluoride (2.5 cm^3 of a 1M solution in THF with 5% water) was added. The mixture was stirred at room temperature. After 24 hours, the reaction was stopped and the solvent removed on a rotary evaporator at a temperature of 76°C and a vacuum of 170 mbar for 20 minutes. A yellow gel was obtained. **^{1}H NMR** (300 MHz, d_6 acetone)/ppm: δ = 7.82 (d, $^3J_{HH}$ = 7.7 Hz, 2H, Ar-**H**), 7.75 (d, $^3J_{HH}$ = 7.7 Hz, 2H; Ar-**H**), 4.63 (s, 2H; Cl-C**H**$_2$), 3.38 (t, 1H, N-C**H**$_2$), 1.68 (m, 1H; C**H**$_2$), 1.36 (m, 1H; C**H**$_2$), 0.93 (t, $^3J_{HH}$ = 7.3 Hz, 1.5H, C**H**$_3$); **^{13}C NMR** (75.5 MHz, d_6 acetone)/ppm: δ = 139.2 (*p*-**C** of Ar), 129.6 (*i*-**C** of Ar), 128.9 (*m*-**C**H of Ar), 126.0 (*o*-**C**H of Ar), 59.1 (N-**C**H$_2$), 46.9 (Cl-**C**H$_2$), 24.4 (**C**H$_2$), 20.3 (**C**H$_2$), 13.9 (**C**H$_3$); **^{29}Si NMR** (79.30 MHz, d_6 acetone)/ppm: δ = -80.8; **^{19}F NMR** (376 MHz, d_6 acetone)/ppm: δ = -26.2, -118.3, -150.0, -208.2; **MS** (MALDI-TOF): *m/z* (%): 1440.1 (80%) ($C_{56}H_{48}FCl_8O_{12}Si_8^-$) [M$^-$] (calculated: 1440.3), 1421.2 (70%) ($C_{56}H_{49}FCl_7O_{13}Si_8^-$) [M$^-$] (calculated: 1421.8), 1403.2 (70%) ($C_{56}H_{50}FCl_6O_{14}Si_8^-$) [M$^-$] (calculated: 1403.4), 1385.2 (35%) ($C_{56}H_{51}FCl_5O_{15}Si_8^-$) [M$^-$] (calculated: 1385.0), 1366.2 (25%) ($C_{56}H_{52}FCl_4O_{16}Si_8^-$) [M$^-$] (calculated: 1366.5), 242.3 (100%) ($C_{16}H_{36}N^+$) [M$^+$]

Reaction of *para*-chloromethylphenyltrimethoxysilane with TBAF (MP242)*:

Para-chloromethylphenyltrimethoxysilane (246.8 g.mol^{-1}; 1.09 g, 4.42 mmol) was dissolved in toluene (20 cm^3), then tetrabutylammonium fluoride (2.5 cm^3 of a 1M solution in THF

with 5% water) was added. The reaction mixture was stirred and heated at 95 °C under nitrogen. After 1 hour, the reaction was stopped and the solvent removed by distillation under vacuum at 95°C and a vacuum of 120 mbar. A yellow gel was obtained. **^{1}H NMR** (300 MHz, d_6 acetone)/ppm: δ = 7.82 (d, $^{3}J_{HH}$ = 7.7 Hz, 2H, Ar-**H**), 7.75 (d, $^{3}J_{HH}$ = 7.7 Hz, 2H; Ar-**H**), 4.63 (s, 2H; Cl-C**H**$_2$), 3.38 (t, 1H, N-C**H**$_2$), 1.68 (m, 1H; C**H**$_2$), 1.36 (m, 1H; C**H**$_2$), 0.93 (t, $^{3}J_{HH}$ = 7.3 Hz, 1.5H, C**H**$_3$); **^{13}C NMR** (75.5 MHz, d_6 acetone)/ppm: δ = 139.2 (*p*-**C** of Ar), 129.6 (*i*-**C** of Ar), 128.9 (*m*-**C**H of Ar), 126.0 (*o*-**C**H of Ar), 59.1 (N-**C**H$_2$), 46.9 (Cl-**C**H$_2$), 24.4 (**C**H$_2$), 20.3 (**C**H$_2$), 13.9 (**C**H$_3$); **^{29}Si NMR** (79.30 MHz, d_6 acetone)/ppm: δ = -80.8; **^{19}F NMR** (376 MHz, d_6 acetone)/ppm: δ = -26.2, -118.9, -150.0, -207.2. All spectral data were in agreement with experiment MP314.

8.2.5 What about the encapsulation of different anions using other catalysts ?

Reaction of phenyltripropoxysilane with tetrabutylammonium bromide (MP64):

Phenyltripropoxysilane (282.3 g.mol^{-1}; 1.41 g; 4.99 mmol) was dissolved in pyridine (20 ml), then 0.81g of TBABr (322.4 g.mol^{-1}; 2.51 mmol) was added. This mixture was stirred at room temperature. After stirring for 24 hours, the reaction was stopped and the solvent removed at 80°C and 70 mbar. A liquid was obtained.

Liquid after removing the solvent: ^{29}Si NMR (79.3 MHz, d_6 acetone, 25°C)/ppm: δ = -58.7. All spectral data were in agreement with phenyltripropoxysilane as described in experiment MP15.

Reaction of phenyltripropoxysilane with tetrabutylammonium bromide and TBAF (MP65)*:

Phenyltripropoxysilane (282.3 g.mol^{-1}; 1.41 g; 4.99 mmol) was dissolved in pyridine (20 ml), then 0.40g of TBABr (322.4 g.mol^{-1}; 1.25 mmol) and 1.25ml of TBAF (1M solution in THF with 5% water, 1.25 mmol) was added. This mixture was stirred at room temperature. After stirring for 24 hours, the reaction was stopped and the solvent removed at 80°C and 70 mbar. A gel was obtained.

Gel after removing the solvent: **^{29}Si NMR** (79.3 MHz, d_6 acetone, 25°C)/ppm: δ = -80.6; **^{19}F NMR** (376 MHz, d_6 acetone, 25°C)/ppm: δ = -26.6. All spectral data were in agreement with the formation of Ph_8T_8-TBAF as described in experiment MP19.

Reaction of phenyltripropoxysilane with tetrabutylammonium chloride (MP66):

Phenyltripropoxysilane (282.3 g.mol^{-1}; 1.41 g; 4.99 mmol) was dissolved in pyridine (20 ml), then 0.70g of TBACl (277.9 g.mol^{-1}; 2.51 mmol) was added. This mixture was stirred at room temperature. After stirring for 24 hours, the reaction was stopped and a liquid was obtained after removal of the solvent at 80°C and 70 mbar.

Liquid after removing the solvent: **^{29}Si NMR** (79.3 MHz, d_6 acetone, 25°C)/ppm: δ = -58.7. All spectral data were in agreement with phenyltripropoxysilane as described in experiment MP15.

Reaction of phenyltripropoxysilane with tetrabutylammonium chloride and TBAF (MP72)*:

Phenyltripropoxysilane (282.3 g.mol^{-1}; 1.40 g; 4.96 mmol) was dissolved in pyridine (20 ml), then 0.35g of TBACl (277.9 g.mol^{-1}; 1.26 mmol) and 1.25ml of TBAF (1M solution in THF with 5% water, 1.25 mmol) was added. This mixture was stirred at room temperature. After stirring for 24 hours, the reaction was stopped and the solvent removed at 80°C and 70 mbar. A gel was obtained and redissolved in chloroform. After filtration, a white solid was obtained. **White solid:** **^{29}Si NMR** (79.3 MHz, d_6 acetone, 25°C)/ppm: δ = -80.6; **^{19}F NMR** (376 MHz, d_6 acetone, 25°C)/ppm: δ = -26.6;

Filtrate: **^{29}Si NMR** (79.3 MHz, d_6 acetone, 25°C)/ppm: δ = -81.4

All spectral data were in agreement with the formation of Ph_8T_8-TBAF as described in experiment MP19.

Reaction of phenyltripropoxysilane with tetrabutylammonium iodide (MP71):

Phenyltripropoxysilane (282.3 g.mol^{-1}; 1.39 g; 4.92 mmol) was dissolved in pyridine (20 ml), then 0.92g of TBAI (369.4 g.mol^{-1}; 2.49 mmol) was added. This mixture was stirred at room temperature. After stirring for 24 hours, the reaction was stopped and the solvent removed at 80°C and 70 mbar. A liquid was obtained.

Liquid after removing the solvent: **^{29}Si NMR** (79.3 MHz, d_6 acetone, 25°C)/ppm: δ = -58.7. All spectral data were in agreement with phenyltripropoxysilane as described in experiment MP15.

Reaction of phenyltripropoxysilane with tetrabutylammonium iodide and TBAF (MP78)*:

Phenyltripropoxysilane (282.3 g.mol^{-1}; 1.40 g; 4.96 mmol) was dissolved in pyridine (20 ml), then 0.46g of TBAI (369.4 g.mol^{-1}; 1.25 mmol) and 1.25ml of TBAF (1M solution in THF with 5% water, 1.25 mmol) was added. This mixture was stirred at room temperature. After stirring for 24 hours, the reaction was stopped and the solvent removed at 80°C and 70 mbar. After filtration, a white solid was obtained.

White solid: **^{29}Si NMR** (79.3 MHz, d_6 acetone, 25°C)/ppm: δ = -80.6; **^{19}F NMR** (376 MHz, d_6 acetone, 25°C)/ppm: δ = -26.6. All spectral data were in agreement with the formation of Ph_8T_8-TBAF as described in experiment MP19.

Reaction of vinyltriethoxysilane with tetraethylammonium hydroxide (MP389)*:

Vinyltriethoxysilane (190.3 g.mol^{-1}; 1.44 g; 7.60 mmol) was dissolved in toluene (10 ml), then 0.86 g of a solution of TEAOH with 35% water (147.3 g.mol^{-1}; 3.8 mmol) was added. This mixture was stirred at room temperature for 24 hours. The reaction was stopped and the solvent removed at 80°C and 70 mbar.

Gel: **^{1}H NMR** (300 MHz, d_6 acetone)/ppm: δ = 6.40 (s, vbr, $\mathbf{H_2O}$), 5.98 (m, 8H, vinyl-**H**), 3.42-3.35 (q, 8H; N-$\mathbf{CH_2}$), 1.78 (s, 0.4H), 1.28 (t, 12H, $\mathbf{CH_3}$); **^{13}C NMR** (75.5 MHz, d_6 acetone)/ppm: δ = 136.7 (Si-$\mathbf{CH_{vinyl}}$), 132.0 ($\mathbf{H_2C_{vinyl}}$), 52.9 (N-$\mathbf{CH_2}$), 8.0 ($\mathbf{CH_3}$); **^{29}Si NMR** (79.3 MHz, d_6 acetone, 25°C)/ppm: δ = -62.7, -71.1, -72.0, -73.1, -73.3, -79.6, -82.5. The results of this experiment are described in section 4.2.

Reaction of phenyltripropoxysilane with caesium fluoride (MP152):

Caesium fluoride was dried in an oven. 3.80 g of caesium fluoride (151.9 g.mol^{-1}; 2.5 mmol) with phenyltripropoxysilane (282.3 g.mol^{-1}; 1.40 g; 4.96 mmol) were placed in a sealed flask. 20 ml of dry acetone were then added with a serynge together with a controlled amount (1 ml, 5%) of water. After the reaction was stirred and heated (30°C) under a nitrogen atmosphere for 24 hours, the solvent was removed and a liquid obtained. **^{29}Si NMR**

(79.3 MHz, d_6 acetone, 25°C)/ppm: δ = -58.7; **^{19}F NMR** (376 MHz, d_6 acetone, 25°C)/ppm: no peak. All spectral data were in agreement with phenyltripropoxysilane as described in experiment MP15.

Recation of *para*-tolyltrimethoxysilane with lithium fluoride (MP92):

Para-tolyltrimethoxysilane (212.3 g.mol^{-1}; 2.08 g, 9.80 mmol) was placed with 0.13g of LiF (25.94 g.mol^{-1}, 5.0 mmol) in a sealed flask. 20 ml of dry acetone were then added with a serynge together with a controlled amount (1 ml, 5%) of water. After the reaction was stirred and heated (30°C) under a nitrogen atmosphere for 24 hours, the solvent was removed and a liquid obtained. **^{29}Si NMR** (79.3 MHz, d_6 acetone, 25°C)/ppm: δ = -58.7; **^{19}F NMR** (376 MHz, d_6 acetone, 25°C)/ppm: no peak. All spectral data were in agreement with phenyltripropoxysilane as described in experiment MP15.

Reaction of vinyltriethoxysilane with Tris(dimethylamino)sulfonium difluorotrimethylsilicate (TASF) (MP316):

Vinyltriethoxysilane (190.3 g.mol^{-1}; 0.55 g; 2.90 mmol) was dissolved in dry THF (20 ml), then 0.40 g of TASF (275.5 g.mol^{-1}, 1.45 mmol) was added. This mixture was stirred at room temperature under nitrogen for 24 hours. The solvent was removed at 375 mbar and at 55°C and a liquid obtained. **^{29}Si NMR** (79.3 MHz, d_6 acetone, 25°C)/ppm: δ = -59.1. All spectral data were in agreement with vinyltriethoxysilane.

Reaction of vinyltriethoxysilane with Tris(dimethylamino)sulfonium difluorotrimethylsilicate (TASF) (MP317):

Vinyltriethoxysilane (190.3 g.mol^{-1}; 0.55 g; 2.90 mmol) was dissolved in dry THF (20 ml) in a sealed flask, then 0.40 g of TASF (275.5 g.mol^{-1}, 1.45 mmol) was added. 1 ml of distilled water was then added with a serynge. This mixture was stirred at room temperature under nitrogen. After stirring for 24 hours, the reaction was stopped and the solvent removed at 375 mbar and at 55°C. Two liquid layers were obtained.

Upper layer: **^{29}Si NMR** (79.3 MHz, d_6 acetone, 25°C)/ppm: δ = -59.1, -66.5, -66.6, -74.2, -74.3; **^{19}F NMR** (376 MHz, d_6 acetone, 25°C)/ppm: no peak.

Lower layer: **^{1}H NMR** (300 MHz, d_6 acetone)/ppm: δ = 5.85 (m, 3H, vinyl-**H**), 2.93 (s, 12H, $S(N(CH_3)_2)_3$), 1.04 (t, 6H, Si-CH_3); **^{13}C NMR** (75.5 MHz, d_6 acetone)/ppm: δ = 136.4

($Si\text{-}CH_{vinyl}$), 131.9 (H_2C_{vinyl}), 56.9 ($N\text{-}CH_3$), 38.4 ($Si\text{-}CH_3$); **^{29}Si NMR** (79.3 MHz, d_6 acetone, 25°C)/ppm: δ = -82.87; **^{19}F NMR** (376 MHz, d_6 acetone, 25°C)/ppm: no peak. The results of this experiment are described in section 4.3.

Reaction of vinyltriethoxysilane with tetraethylammonium fluoride (MP286)*:

Vinyltriethoxysilane (190.3 g.mol^{-1}; 1.20 g, 6.30 mmol) was dissolved in dry acetone (20 cm^3), then tetraethylammonium fluoride (2.5 cm^3 of a 1M solution in THF with 5% water) was added. The mixture was stirred at room temperature. After 24 hours, the reaction was stopped and the solvent removed on a rotary evaporator at 400 mbar and at 55°C. A yellow solid gel was obtained.

Gel: **^{1}H NMR** (300 MHz, d_6 acetone)/ppm: δ = 5.85 (m, 24H, vinyl-**H**), 3.50 (m, 8H; $N\text{-}CH_2$), 1.06 (t, 12H, CH_3); **^{13}C NMR** (75.5 MHz, d_6 acetone)/ppm: δ = 136.7 ($Si\text{-}CH_{vinyl}$), 132.5 (H_2C_{vinyl}), 57.0 ($N\text{-}CH_2$), 19.3 (CH_3); **^{29}Si NMR** (79.30 MHz, d_6 acetone)/ppm: δ = -82.8; **^{19}F NMR** (376 MHz, d_6 acetone)/ppm: δ = -25.1. The results of this experiment are described in section 4.3.

Reaction of Ph_8T_8-TBAF with caesium iodide (MP82)*:

Ph_8T_8-TBAF (1294.98 g.mol^{-1}, 0.30 g, 0.23 mmol) was dissolved in dry acetone (20 cm^3), then caesium fluoride (259.81 g.mol^{-1}, 0.13 g, 0.5 mmol) was added. The mixture was stirred at room temperature. After 12 hours, the reaction was stopped and the solvent removed at 80°C and 73 mbar for 15 minutes using a rotary evaporator. A yellow solid gel was obtained which was then extracted with chloroform to give a white solid after filtration.

White powder: **^{29}Si NMR** (79.3 MHz, d_6 acetone, 25°C)/ppm: δ = -80.6; **^{19}F NMR** (376 MHz, d_6 acetone, 25°C)/ppm: δ = -26.7. All spectral data were in agreement with experiment MP19.

Reaction of Ph_8T_8-TBAF with sodium iodide (MP249)*:

Ph_8T_8-TBAF (1294.98 g.mol^{-1}, 0.30 g, 0.23 mmol) was dissolved in dry acetone (20 cm^3), then sodium fluoride (149.89 g.mol^{-1}, 0.075 g, 0.5 mmol) was added. The mixture was stirred at room temperature. After 12 hours, the reaction was stopped and the solvent removed at 80°C and 73 mbar for 15 minutes using a rotary evaporator. A yellow solid gel was obtained which was then extracted with chloroform to give a white solid after filtration.

White powder: **^{29}Si NMR** (79.3 MHz, d_6 acetone, 25°C)/ppm: δ = -80.6; **^{19}F NMR** (376 MHz, d_6 acetone, 25°C)/ppm: δ = -26.7. All spectral data were in agreement with experiment MP19.

Reaction of VinylT$_8$-TBAF with lithium iodide (MP291):

VinylT$_8$-TBAF (894.53 g.mol^{-1}, 0.40 g, 0.45 mmol) was dissolved in dry acetone (15 cm^3), then lithium fluoride (133.85 g.mol^{-1}, 0.12 g, 0.9 mmol) in 5ml of dry acetone was added. The mixture was stirred at room temperature. After 12 hours, the reaction was stopped and the solvent removed at 80°C and 70 mbar for 15 minutes using a rotary evaporator. A yellow solid gel was obtained.

Gel: **^{29}Si NMR** (79.3 MHz, d_6 acetone, 25°C)/ppm: δ = -79.8, -81.2; **^{19}F NMR** (376 MHz, d_6 acetone, 25°C)/ppm: no peak. The results of this experiment are described in section 4.4.

Reaction of VinylT$_8$-TBAF with lithium tetraphenylborate (MP298)*:

VinylT$_8$-TBAF (894.53 g.mol^{-1}, 0.95 g, 1.06 mmol) was dissolved in dry acetone (15 cm^3), then lithium tetraphenylborate ($LiPh_4B$) (326.17 g.mol^{-1}, 0.6 g, 1.85 mmol) in 5ml of dry acetone was added. The mixture was stirred at room temperature. After 12 hours, the reaction was stopped and the solvent removed at 80°C and 70 mbar for 15 minutes using a rotary evaporator. A yellow solid gel was obtained. **Gel:** **^{29}Si NMR** (79.3 MHz, d_6 acetone, 25°C)/ppm: δ = -82.8; **^{19}F NMR** (376 MHz, d_6 acetone, 25°C)/ppm: δ = -25.4. All spectral data were in agreement with experiment MP205.

8.2.6 Is the encapsulation of a fluoride anion possible when the R group on the silicon atom is attached by an sp3 carbon atom ?

Reaction of *cyclo*-hexyltripropoxysilane with TBAF (MP113):

Cyclo-hexyltripropoxysilane (288.5 g.mol^{-1}; 1.17 g, 4.06 mmol) was dissolved in pyridine (20 cm^3), then tetrabutylammonium fluoride (2.5 cm^3 of a 1M solution in THF with 5% water) was added. The mixture was stirred at room temperature. After 24 hours, the reaction was stopped and the solvent removed on a rotary evaporator at a temperature of 80°C and a vacuum of 80 mbar for 15 minutes. A brown-red gel was obtained. **^{1}H NMR** (300 MHz,

$CDCl_3$)/ppm: δ = 1.70 (m, 40H, CH_2), 1.19 (m, 40H, CH_2), 0.72 (m, 8H, CH); **^{13}C NMR** (75.5 MHz, $CDCl_3$)/ppm: δ = 23.2 (CH), 26.7 (CH_2), 27.5 (CH_2); **^{29}Si NMR** (79.30 MHz, $CDCl_3$)/ppm: δ = -69.0; **^{19}F NMR** (376 MHz, $CDCl_3$)/ppm: no peak. The spectral data were consistent with the product being octa-*cyclo*-hexyloctasilsesquioxane [47,71].

Reaction of *cyclo*-hexyltripropoxysilane with TBAF (MP216):

Cyclo-hexyltripropoxysilane (288.5 g.mol^{-1}; 1.08 g, 3.74 mmol) was dissolved in toluene (20 cm^3), then tetrabutylammonium fluoride (2.5 cm^3 of a 1M solution in THF with 5% water) was added. The mixture was stirred at room temperature. After 24 hours, the reaction was stopped and the solvent removed by distillation under vacuum at a temperature of 80°C. A brown-red gel was obtained. **^{1}H NMR** (300 MHz, $CDCl_3$)/ppm: δ = 1.70 (m, 40H, CH_2), 1.19 (m, 40H, CH_2), 0.72 (m, 8H, CH); **^{13}C NMR** (75.5 MHz, $CDCl_3$)/ppm: δ = 23.2 (CH), 26.7 (CH_2), 27.5 (CH_2); **^{29}Si NMR** (79.30 MHz, $CDCl_3$)/ppm: δ = -68.7; **^{19}F NMR** (376 MHz, $CDCl_3$)/ppm: no peak. The spectral data were consistent with the product being octa-*cyclo*-hexyloctasilsesquioxane [47,71].

Reaction of *cyclo*-pentyltripropoxysilane with TBAF (MP74):

Cyclo-pentyltripropoxysilane (274.5 g.mol^{-1}; 1.18 g, 4.30 mmol) was dissolved in pyridine (20 cm^3), then tetrabutylammonium fluoride (2.5 cm^3 of a 1M solution in THF with 5% water) was added. The mixture was stirred at room temperature. After 24 hours, the reaction was stopped and the solvent removed on a rotary evaporator at a temperature of 80°C and a vacuum of 80 mbar for 15 minutes. A brown-red gel was obtained. **^{1}H NMR** (300 MHz, $CDCl_3$)/ppm: δ = 1.70 (m, 16H, CH_2), 1.44 (m, 48H, CH_2), 0.90 (m, 8H, CH); **^{13}C NMR** (75.5 MHz, $CDCl_3$)/ppm: δ = 22.3 (CH), 27.0 (CH_2), 27.3 (CH_2); **^{29}Si NMR** (79.30 MHz, $CDCl_3$)/ppm: δ = -66.6; **^{19}F NMR** (376 MHz, $CDCl_3$)/ppm: no peak. The spectral data were consistent with the product being octa-*cyclo*-pentyloctasilsesquioxane [47,71].

Reaction of *cyclo*-pentyltripropoxysilane with TBAF (MP196):

Cyclo-pentyltripropoxysilane (274.5 g.mol^{-1}; 1.09 g, 4.00 mmol) was dissolved in toluene (20 cm^3), then tetrabutylammonium fluoride (2.5 cm^3 of a 1M solution in THF with 5% water) was added. The mixture was stirred at room temperature. After 24 hours, the reaction was stopped and the solvent removed on a rotary evaporator at a temperature of 80°C and a vacuum of 100 mbar for 15 minutes. A brown-red gel was obtained. **^{1}H NMR** (300 MHz,

$CDCl_3$)/ppm: δ = 1.70 (m, 16H, CH_2), 1.44 (m, 48H, CH_2), 0.90 (m, 8H, CH); **^{13}C NMR** (75.5 MHz, $CDCl_3$)/ppm: δ = 22.3 (CH), 27.0 (CH_2), 27.3 (CH_2); **^{29}Si NMR** (79.30 MHz, $CDCl_3$)/ppm: δ = -66.6; **^{19}F NMR** (376 MHz, $CDCl_3$)/ppm: no peak. The spectral data were consistent with the product being octa-*cyclo*-pentyloctasilsesquioxane [47, 71].

Reaction of *iso*-butyltripropoxysilane with TBAF (MP203):

Iso-butyltrimethoxysilane (178.3 g.mol^{-1}; 1.02 g, 5.7 mmol) was dissolved in toluene (20 cm^3), then tetrabutylammonium fluoride (2.5 cm^3 of a 1M solution in THF with 5% water) was added. The mixture was stirred at room temperature. After 24 hours, the reaction was stopped and the solvent removed on a rotary evaporator at a temperature of 80°C and a vacuum of 75 mbar for 15 minutes. A brown gel was obtained. Recrystallisation from acetone afforded colourless crystals (0.42 g, 67% yield). **^{1}H NMR** (300 MHz, $CDCl_3$)/ppm: δ = 0.18 (d, J_{HH} = 6.96 Hz, 16H, CH_2), 0.54 (d, J_{HH} = 6.60 Hz, 48H, CH_3), 1.35-1.53 (m, 8H, CH); **^{13}C NMR** (75.5 MHz, $CDCl_3$)/ppm: δ = 22.5 (CH_2), 23.9 (CH), 25.7 (CH_3); **^{29}Si NMR** (79.30 MHz, $CDCl_3$)/ppm: δ = -67.9; **^{19}F NMR** (376 MHz, $CDCl_3$)/ppm: no peak. The spectral data were consistent with the product being octa-*iso*-butyloctasilsesquioxane [82]. X-ray: details are given in the appendix.

Reaction of 5-*bicyclo*-heptenyltributoxysilane with TBAF (MP54):

5-*bicyclo*-heptenyltributoxysilane (340.6 g.mol^{-1}; 0.98 g, 2.9 mmol) was dissolved in acetone (20 cm^3), then tetrabutylammonium fluoride (2.5 cm^3 of a 1M solution in THF with 5% water) was added. The mixture was stirred at room temperature. After 24 hours, the reaction was stopped. A white solid was obtained after removing the solvent on a rotary evaporator at a temperature of 40°C and a vacuum of 80 mbar for 15 minutes. **^{1}H NMR** (300 MHz, $CDCl_3$)/ppm: *exo*-5-*bicyclo*-heptenyl group: δ = 0.40 (1H, m, SiCH), 1.25 (2H, m, SiCHCH_2), 1.70 (1H, m, SiCHCH_2CH), 2.90 (2H, m, SiCHCHCH_2), 5.95 (1H, m, C*H*=C*H*), 6.12 (1H, m, C*H*=C*H*); *endo*-5-*bicyclo*-heptenyl group: δ = 1.11 (2H, m, SiCHCH_2), 1.29 (1H, m, SiCHCH_2CH), 1.83 (1H, m, SiCH), 2.90 (1H, m, SiCHCHCH_2), 3.00 (1H, m, SiCHCHCH_2), 5.95 (2H, m, C*H*=C*H*); **^{13}C NMR** (75.5 MHz, $CDCl_3$)/ppm: *exo*-5-*bicyclo*-heptenyl group: δ = 21.3 (SiCH), 26.4 (SiCHCH_2), 42.3 (SiCHCH), 42.8 (SiCHCH_2CH-), 46.9 (SiCHCHCH_2), 133.9 (*CH*=CH) and 137.6 (*CH*=CH); *endo*-5-*bicyclo*-heptenyl group: δ = 21.4 (SiCH), 26.8 (SiCHCH_2), 42.5 (SiCHCH), 44.3 (SiCHCH_2CH-), 50.7 (SiCHCHCH_2), 133.8 (*CH*=CH) and 135.6 (*CH*=CH); **^{29}Si NMR**

(79.30 MHz, $CDCl_3$)/ppm: δ = -67.6, -68.4; **^{19}F NMR** (376 MHz, $CDCl_3$)/ppm: no peak. The spectral data were consistent with the product being octa-5-*bicyclo*-heptenyloctasilsesquioxane [82].

Reaction of 5-*bicyclo*-heptenyltripropoxysilane with TBAF (MP57):

5-*bicyclo*-heptenyltripropoxysilane (298.5 g.mol^{-1}; 0.39 g, 1.3 mmol) was dissolved in acetone (20 cm^3), then tetrabutylammonium fluoride (2.5 cm^3 of a 1M solution in THF with 5% water) was added. The mixture was stirred at room temperature. After 24 hours, the reaction was stopped. A white solid [82] was obtained after removing the solvent on a rotary evaporator at a temperature of 40°C and a vacuum of 80 mbar for 15 minutes. All data are in agreement with those previously obtained for MP54

Reaction of 3-*para*-methoxyphenylpropyltriethoxysilane with TBAF (MP50):

3-*para*-methoxyphenylpropyltriethoxysilane (312.5 g.mol^{-1}; 1.63 g, 5.2 mmol) was dissolved in THF (20 cm^3), then tetrabutylammonium fluoride (2.5 cm^3 of a 1M solution in THF with 5% water) was added. The mixture was stirred at room temperature. After 24 hours, the reaction was stopped and the solvent removed on a rotary evaporator at a temperature of 80°C and a vacuum of 80 mbar for 15 minutes. A brown-red gel was obtained. **^{1}H NMR** (300 MHz, $CDCl_3$)/ppm: δ = 0.31 (16H, t, $SiCH_2$), 1.10 (16H, m, $SiCH_2CH_2CH_2Ar$), 3.15 (16H, t, $SiCH_2CH_2CH_2Ar$), 3.17 (24H, s, CH_3OAr), 6.17 (16H, d, CH=CH), 6.50 (16H, d, CH=CH); **^{13}C NMR** (75.5 MHz, $CDCl_3$)/ppm: δ = 13.8 ($SiCH_2$); 28.9 ($SiCH_2CH_2$); 38.6 ($ArCH_2$), 55.0 (CH_3), 113.4 (*o*-C of Ar), 129.1 (*i*-C of Ar), 134.5 (*m*-C of Ar) and 157.4 (*p*-C of Ar); **^{29}Si NMR** (79.30 MHz, $CDCl_3$)/ppm: δ = -68.7; **^{19}F NMR** (376 MHz, $CDCl_3$)/ppm: no peak. The spectral data were consistent with the product being octa-3-*para*-methoxyphenylpropyl-octasilsesquioxane [47, 71].

Reaction of 3-*para*-methoxyphenylpropyltripropoxysilane with TBAF (MP80):

3-*para*-methoxyphenylpropyltripropoxysilane (354.6 g.mol^{-1}; 1.09 g, 3.1 mmol) was dissolved in acetone (20 cm^3), then tetrabutylammonium fluoride (2.5 cm^3 of a 1M solution in THF with 5% water) was added. The mixture was stirred at room temperature. After 24 hours, the reaction was stopped and the solvent removed on a rotary evaporator at a temperature of 40°C and a vacuum of 80 mbar for 15 minutes. A brown-red gel was obtained [71]. **^{29}Si NMR** (79.30 MHz, $CDCl_3$)/ppm: δ = -66.9, -68.6, -68.7, -71.2; **^{19}F NMR**

(376 MHz, $CDCl_3$)/ppm: no peak. The results of this experiment are described in section 5.6.

Reaction of 3-*para*-methoxyphenylpropyltripropoxysilane with TBAF (MP85):

3-*para*-methoxyphenylpropyltripropoxysilane (354.6 $g.mol^{-1}$; 1.11 g, 3.1 mmol) was dissolved in toluene (20 cm^3), then tetrabutylammonium fluoride (2.5 cm^3 of a 1M solution in THF with 5% water) was added. The mixture was stirred at room temperature. After 24 hours, the reaction was stopped and the solvent removed on a rotary evaporator at a temperature of 80°C and a vacuum of 80 mbar for 15 minutes. A brown-red gel was obtained [71]. **^{29}Si NMR** (79.30 MHz, $CDCl_3$)/ppm: δ = -66.9, -68.7; **^{19}F NMR** (376 MHz, $CDCl_3$)/ppm: no peak. The results of this experiment are described in section 5.6.

Reaction of methyltripropoxysilane with TBAF (MP243):

Methyltripropoxysilane (220.4 $g.mol^{-1}$; 1.04 g, 4.7 mmol) was dissolved in toluene (20 cm^3), then tetrabutylammonium fluoride (2.5 cm^3 of a 1M solution in THF with 5% water) was added. The mixture was stirred at room temperature. After 24 hours, the reaction was stopped and the solvent removed on a rotary evaporator at a temperature of 80°C and a vacuum of 80 mbar for 15 minutes. An insoluble gel was obtained which is in agreement with the product being resin [18, 71].

Reaction of allyltriethoxysilane with TBAF (MP222):

Allyltriethoxysilane (204.3 $g.mol^{-1}$; 1.04 g, 5.1 mmol) was dissolved in toluene (20 cm^3), then tetrabutylammonium fluoride (2.5 cm^3 of a 1M solution in THF with 5% water) was added. The mixture was stirred at room temperature. After 24 hours, the reaction was stopped and the solvent removed on a rotary evaporator at a temperature of 80°C and a vacuum of 80 mbar for 15 minutes. A yellow gel was obtained. **^{1}H NMR** (300 MHz, $CDCl_3$)/ppm: δ = 0.86-1.12 (16H, m, $SiCH_2$), 4.26-4.55 (16H, m, $SiCH_2CHCH_2$), 5.07-5.12 (8H, m, $SiCH_2CHCH_2$); **^{13}C NMR** (75.5 MHz, $CDCl_3$)/ppm: δ = 13.8 ($SiCH_2$), 114.6 ($SiCH_2CHCH_2$), 131.7 ($SiCH_2CHCH_2$); **^{29}Si NMR** (79.30 MHz, $CDCl_3$)/ppm: δ = -71.5, -73.4, -73.6, -76.1; **^{19}F NMR** (376 MHz, $CDCl_3$)/ppm: no peak. The spectral data were consistent with the product being octaallyloctasilsesquioxane [47, 71].

Reaction of *n*-hexyltriethoxysilane with TBAF (MP229):

n-hexyltriethoxysilane (248.4 g.mol^{-1}; 1.07 g, 4.3 mmol) was dissolved in toluene (20 cm^3), then tetrabutylammonium fluoride (2.5 cm^3 of a 1M solution in THF with 5% water) was added. The mixture was stirred at room temperature. After 24 hours, the reaction was stopped and the solvent removed on a rotary evaporator at a temperature of 80°C and a vacuum of 80 mbar for 15 minutes. A gel was obtained. **^{1}H NMR** (300 MHz, $CDCl_3$)/ppm: δ = 0.61 (16H, t, $SiCH_2$ CH_2), 0.89 (24H, t, CH_2CH_3), 1.31 (64H, m, $SiCH_2CH_2CH_2CH_2CH_2CH_3$); **^{13}C NMR** (75.5 MHz, $CDCl_3$)/ppm: δ = 11.9 ($SiCH_2$), 14.1 (CH_2CH_3), 22.5 ($SiCH_2CH_2CH_2CH_2CH_2CH_3$), 22.6 ($SiCH_2CH_2CH_2CH_2CH_2CH_3$), 31.5 ($SiCH_2CH_2CH_2CH_2CH_2CH_3$), 32.4 ($SiCH_2CH_2CH_2CH_2CH_2CH_3$); **^{29}Si NMR** (79.30 MHz, $CDCl_3$)/ppm: δ = -66.6; **^{19}F NMR** (376 MHz, $CDCl_3$)/ppm: no peak. The spectral data were consistent with the product being octa-*n*-hexyloctasilsesquioxane [24, 22].

Reaction of 2-chloroethyltriethoxysilane with TBAF (MP230):

2-chloroethyltriethoxysilane (226.8 g.mol^{-1}; 1.10 g, 4.9 mmol) was dissolved in toluene (20 cm^3), then tetrabutylammonium fluoride (2.5 cm^3 of a 1M solution in THF with 5% water) was added. The mixture was stirred at room temperature. After 24 hours, the reaction was stopped and the solvent removed on a rotary evaporator at a temperature of 80°C and a vacuum of 80 mbar for 15 minutes. An insoluble gel was obtained which is in agreement with the product being resin [82].

Reaction of benzyltributoxysilane with TBAF (MP46):

Benzyltributoxysilane (338.6 g.mol^{-1}; 1.06 g, 3.1 mmol) was dissolved in chloroform (20 cm^3), then tetrabutylammonium fluoride (2.5 cm^3 of a 1M solution in THF with 5% water) was added. The mixture was stirred at room temperature. After 24 hours, the reaction was stopped and the solvent removed on a rotary evaporator at a temperature of 50°C and a vacuum of 80 mbar for 15 minutes. A yellow gel was obtained [47]. **^{1}H NMR** (300 MHz, $CDCl_3$)/ppm: δ = 1.66 (20H, s, $SiCH_2$), 6.21 (20H, m, Ar-H), 6.45 (30H, m, Ar-H); **^{13}C NMR** (75.5 MHz, $CDCl_3$)/ppm: δ = 21.2 ($SiCH_2$), 124.7 (*o*-C of Ar), 128.2 (*i*-C of Ar), 128.7 (*m*-C of Ar), 136.6 (*p*-C of Ar); **^{29}Si NMR** (79.30 MHz, $CDCl_3$)/ppm: δ = -71.3, -73.0, -73.1, -75.6; **^{19}F NMR** (376 MHz, $CDCl_3$)/ppm: no peak. The results of this experiment are described in section 5.11.

Reaction of benzyltripropoxysilane with TBAF (MP84):

Benzyltripropoxysilane (296.5 $g.mol^{-1}$; 1.17 g, 3.9 mmol) was dissolved in acetone (20 cm^3), then tetrabutylammonium fluoride (2.5 cm^3 of a 1M solution in THF with 5% water) was added. The mixture was stirred at room temperature. After 24 hours, the reaction was stopped and the solvent removed on a rotary evaporator at a temperature of 40°C and a vacuum of 80 mbar for 15 minutes. A yellow gel was obtained. **^{1}H NMR** (300 MHz, $CDCl_3$)/ppm: δ = 1.66 (20H, s, $SiCH_2$), 6.21 (20H, m, Ar-**H**), 6.45 (30H, m, Ar-**H**); **^{13}C NMR** (75.5 MHz, $CDCl_3$)/ppm: δ = 21.2 ($SiCH_2$), 124.7 (*o*-**C** of Ar), 128.2 (*i*-**C** of Ar), 128.7 (*m*-**C** of Ar), 136.6 (*p*-**C** of Ar); **^{29}Si NMR** (79.30 MHz, $CDCl_3$)/ppm: δ = -73.2; **^{19}F NMR** (376 MHz, $CDCl_3$)/ppm: no peak. The spectral data were consistent with the product being octabenzyloctasilsesquioxane [47].

Reaction of benzyltriethoxysilane with TBAF (MP275):

Benzyltriethoxysilane (254.4 $g.mol^{-1}$; 1.27 g, 5.0 mmol) was dissolved in toluene (20 cm^3), then tetrabutylammonium fluoride (2.5 cm^3 of a 1M solution in THF with 5% water) was added. The mixture was stirred at room temperature. After 24 hours, the reaction was stopped and the solvent removed on a rotary evaporator at a temperature of 70°C and a vacuum of 100 mbar for 15 minutes. A yellow gel was obtained. **^{29}Si NMR** (79.30 MHz, d_6 acetone)/ppm: δ = -99.8; **^{19}F NMR** (376 MHz, d_6 acetone)/ppm: δ = -28.2, -29.7, -31.1, -32.6, -34.1, -35.6, -36.0. The results of this experiment are described in section 5.11.

Reaction of benzyltriethoxysilane with TBAF (MP282):

Benzyltriethoxysilane (254.4 $g.mol^{-1}$; 0.78 g, 3.1 mmol) was dissolved in chloroform (20 cm^3), then tetrabutylammonium fluoride (2.5 cm^3 of a 1M solution in THF with 5% water) was added. The mixture was stirred at room temperature. After 24 hours, the reaction was stopped and the solvent removed on a rotary evaporator at a temperature of 40°C and a vacuum of 80 mbar for 15 minutes. A yellow gel was obtained [47]. **^{29}Si NMR** (79.30 MHz, d_6 acetone)/ppm: δ = -70.5, -70.7, -70.9, -71.1, -73.0, -74.5, -75.5, -76.2; **^{19}F NMR** (376 MHz, d_6 acetone)/ppm: δ = -26.5, -29.0. The results of this experiment are described in section 5.11.

8.2.7 Is the encapsulation of a fluoride anion possible when the R group on the silicon atom is attached by an sp carbon atom ?

Synthesis of phenylacetylenetriethoxysilane (MP140)

Granular sodium amide, $NaNH_2$ (2.6g, 67.5 mmol), was rapidly placed in a mortar with dry toluene and crushed to a fine suspension. The suspension was added to 50 ml of dry toluene in a three neck round bottom flask with a condenser under nitrogen. Phenylacetylene was then added slowly (4.6 g, 45 mmol). The reaction flak was placed in an ice bath and the reaction mixture stirred for 4 hours. $Si(OEt)_4$ was added dropwise (20.8 g, 0.1 mol), to react with the phenylacetylene and neutralize the unreacted sodium amide. As it was an exothermic reaction, the flask was placed in a ice bath and the reaction mixture stirred overnight. After 12 hours, the reaction was stopped to give a brown reaction mixture. $Si(OEt)_4$ was added to neutralize any unreacted sodium amide. After filtration, the filtrate was then distilled under vacuum. We would expect the phenylacetylenetriethoxysilane to be formed and collected after distillation. **^{29}Si NMR** (79.30 MHz, d_6 acetone)/ppm: no peaks

8.2.8 Synthesis of tetrabutylammonium octaethoxyoctasilsesquioxane fluoride

Reaction of tetraethylorthosilicate with TBAF (MP292)*:

Tetraethylorthosilicate (208.3 g.mol^{-1}; 2.11 g, 10.1 mmol) was dissolved in toluene (20 cm^3), then tetrabutylammonium fluoride (2.5 cm^3 of a 1M solution in THF with 5% water) was added. The mixture was stirred at room temperature. Samples from the reaction mixture were taken after 24 hours, 120 hours and 10 days, and in each sample the solvent was removed on a rotary evaporator at a temperature of 50°C and a vacuum of 70 mbar for 15 minutes. A yellow gel was obtained for each sample. **^{1}H NMR** (300 MHz, d_6 acetone)/ppm: δ = 0.96 (t, $^3J_{HH}$ = 7.3 Hz, 3H, **C**H_3), 1.08 (t, $^3J_{HH}$ = 6.9 Hz, 3H, **C**H_3), 1.10-1.19 (2H, vbr, m, **C**H_2), 1.35-47 (2H, vbr, m, **C**H_2), 3.34 (t, $^3J_{HH}$ = 8.4 Hz, 2H, N-**C**H_2), 3.48-3.55 (q, $^3J_{HH}$ = 6.9 Hz, 2H, O-**C**H_2); **^{13}C NMR** (75.5 MHz, d_6 acetone)/ppm: δ = 14.1 (**C**H_3), 19.2 (-**C**H_2-), 24.5 (-**C**H_2-), 26.3 (**C**H_3), 57.1 (N-**C**H_2-), 58.9 (O-**C**H_2-); **^{29}Si NMR** (79.30 MHz, d_6 acetone)/ppm: δ = -81.9, -88.7, -88.8, -99.7, -99.9, -106.7, -106.9; **^{19}F NMR** (376 MHz, d_6

acetone)/ppm: δ = -35.5, -36.0, -36.5. The results of this experiment are discussed in section 6.2.

Reaction of tetraethylorthosilicate with TBAF (MP299)*:

Tetraethylorthosilicate (208.3 $g.mol^{-1}$; 1.10 g, 5.3 mmol) was dissolved in dry THF (20 cm^3), then tetrabutylammonium fluoride (1.0 cm^3 of a 1M solution in THF with 5% water) was added. The mixture was stirred at room temperature. After 24 hours, the reaction was stopped and the solvent removed on a rotary evaporator at a temperature of 55°C and a vacuum of 95 mbar for 15 minutes. A yellow gel was obtained. **^{1}H NMR** (300 MHz, d_6 acetone)/ppm: δ = 0.96 (t, $^3J_{HH}$ = 7.3 Hz, 3H, CH_3), 1.08 (t, $^3J_{HH}$ = 6.9 Hz, 3H, CH_3), 1.10-1.19 (2H, vbr, m, CH_2), 1.35-47 (2H, vbr, m, CH_2), 3.34 (t, $^3J_{HH}$ = 8.4 Hz, 2H, N-CH_2), 3.48-3.55 (q, $^3J_{HH}$ = 6.9 Hz, 2H, O-CH_2); **^{13}C NMR** (75.5 MHz, d_6 acetone)/ppm: δ = 14.1 (CH_3), 19.2 (-CH_2-), 24.5 (-CH_2-), 26.3 (CH_3), 57.1 (N-CH_2-), 58.9 (O-CH_2-); **^{29}Si NMR** (79.30 MHz, d_6 acetone)/ppm: δ = -81.9, -88.3, -88.7, -99.7, -99.9, -106.9, -107.1; **^{19}F NMR** (376 MHz, d_6 acetone)/ppm: -35.7, -36.4, -36.6, -36.7, -37.1; **MS** (ESI): *m/z* (%): 795.4 (100%) ($C_{16}H_{40}FO_{20}Si_8^-$) [$M^-$] (calculated: 795.0), 242.3 (100%) ($C_{16}H_{36}N^+$) [M^+] (calculated: 242.3); **MS** (MALDI-TOF): *m/z* (%): 795.0 (70%) ($C_{16}H_{40}FO_{20}Si_8^-$) [$M^-$] (calculated: 795.0), 242.3 (100%) ($C_{16}H_{36}N^+$) [M^+] (calculated: 242.3); **MS** (FAB negative ion): *m/z* (%):795.3 (35%) ($C_{16}H_{40}FO_{20}Si_8^-$) [$M^-$] (calculated: 795.0). The results of this experiment are discussed in section 6.2.

Reaction of tetraethylorthosilicate with TBAF (MP300)*:

Tetraethylorthosilicate (208.3 $g.mol^{-1}$; 1.10 g, 5.3 mmol) was dissolved in dry THF (20 cm^3), then tetrabutylammonium fluoride (2.5 cm^3 of a 1M solution in THF with 5% water) was added. The mixture was stirred at room temperature. After 24 hours, the reaction was stopped and the solvent removed on a rotary evaporator at a temperature of 55°C and a vacuum of 95 mbar for 15 minutes. A yellow gel was obtained. 1 g of this yellow gel was redissolved in dry THF and 0.60 g of lithium tetraphenylborate, $LiPh_4B$, was added. The reaction was stirred for 24 hours. After removing the solvent, a white solid was obtained.

Gel: ^{1}H NMR (300 MHz, d_6 acetone)/ppm: 0.96 (t, $^3J_{HH}$ = 7.3 Hz, 3H, CH_3), 1.08 (t, $^3J_{HH}$ = 6.9 Hz, 3H, CH_3), 1.10-1.19 (2H, vbr, m, CH_2), 1.35-47 (2H, vbr, m, CH_2), 3.34 (t, $^3J_{HH}$ = 8.4 Hz, 2H, N-CH_2), 3.48-3.55 (q, $^3J_{HH}$ = 6.9 Hz, 2H, O-CH_2); **^{13}C NMR** (75.5 MHz, d_6

acetone)/ppm: δ = 14.1 ($\mathbf{C}H_3$), 19.2 (-$\mathbf{C}H_2$-), 24.5 (-$\mathbf{C}H_2$-), 26.3 ($\mathbf{C}H_3$), 57.1 (N-$\mathbf{C}H_2$-), 58.9 (O-$\mathbf{C}H_2$-); **^{29}Si NMR** (79.30 MHz, d_6 acetone)/ppm: δ = -99.8, -100.0; **^{19}F NMR** (376 MHz, d_6 acetone)/ppm: δ = -35.7, -36.1;

White solid: ^{29}Si NMR (79.30 MHz, d_6 acetone)/ppm: δ = -99.7; **^{19}F NMR** (376 MHz, d_6 acetone)/ppm: δ = -33.3, -35.8, -35.85, -36.1. The results of this experiment are discussed in section 6.2.

Reaction of tetraethylorthosilicate with TBAF (MP295)*:

Tetraethylorthosilicate (208.3 g.mol^{-1}; 20 g, 96 mmol) was dissolved in toluene (20 cm^3), then tetrabutylammonium fluoride (25 cm^3 of a 1M solution in THF with 5% water) was added. The mixture was stirred at room temperature. After 24 hours, the reaction was stopped and the solvent removed on a rotary evaporator at a temperature of 55°C and a vacuum of 95 mbar for 15 minutes. A yellow gel was obtained.

Gel: ^{1}H NMR (300 MHz, d_6 acetone)/ppm: 0.96 (t, $^3J_{HH}$ = 7.3 Hz, 3H, $\mathbf{C}H_3$), 1.08 (t, $^3J_{HH}$ = 6.9 Hz, 3H, $\mathbf{C}H_3$), 1.10-1.19 (2H, vbr, m, $\mathbf{C}H_2$), 1.35-47 (2H, vbr, m, $\mathbf{C}H_2$), 3.34 (t, $^3J_{HH}$ = 8.4 Hz, 2H, N-$\mathbf{C}H_2$), 3.48-3.55 (q, $^3J_{HH}$ = 6.9 Hz, 2H, O-$\mathbf{C}H_2$); **^{13}C NMR** (75.5 MHz, d_6 acetone)/ppm: δ = 14.1 ($\mathbf{C}H_3$), 19.2 (-$\mathbf{C}H_2$-), 24.5 (-$\mathbf{C}H_2$-), 26.3 ($\mathbf{C}H_3$), 57.1 (N-$\mathbf{C}H_2$-), 58.9 (O-$\mathbf{C}H_2$-); **^{29}Si NMR** (79.30 MHz, d_6 acetone)/ppm: δ = -99.7, -99.9; **^{19}F NMR** (376 MHz, d_6 acetone)/ppm: δ = -35.9, -36.3, -36.8. The results of this experiment are discussed in section 6.2.

8.2.9 Synthesis of tetrabutylammonium octapropoxyoctasilsesquioxane fluoride

Reaction of tetrapropylorthosilicate with TBAF (MP343)*:

Tetrapropylorthosilicate (264.4 g.mol^{-1}; 1.38 g, 5.2 mmol) was dissolved in toluene (20 cm^3), then tetrabutylammonium fluoride (25 cm^3 of a 1M solution in THF with 5% water) was added. The mixture was stirred at room temperature. After 24 hours, the reaction was stopped and the solvent removed on a rotary evaporator at a temperature of 55°C and a vacuum of 95 mbar for 15 minutes. A yellow gel was obtained.

Gel: ^{29}**Si NMR** (79.30 MHz, d_6 acetone)/ppm: δ = -99.7, -99.8; ^{19}**F NMR** (376 MHz, d_6 acetone)/ppm: δ = -33.2, -35.5, -35.9. The results of this experiment are discussed in section 6.3.

References

1. I. M. Baney R. H., Sakakibara A., Suzuki T., *Chem. Rev.*, 1995, **95**, 1409.
2. A. R. Bassindale and M. Borbaruah, *Journal of the Chemical Society - Chemical Communications*, 1991, 1499.
3. A. R. Bassindale and M. Borbaruah, *Journal of the Chemical Society - Chemical Communications*, 1991, 1501.
4. J. Boyer, C. Breliere, R. J. P. Corriu, A. Kpoton, M. Poirier, and G. Royo, *Journal of Organometallic Chemistry*, 1986, **311**, C39.
5. M. Kira, K. Sato, and H. Sakurai, *Journal of Organic Chemistry*, 1987, **52**, 948.
6. A. Boudin, G. Cerveau, C. Chuit, R. J. P. Corriu, and C. Reye, *Organometallics*, 1988, **7**, 1165.
7. P. G. Harrison, *Journal of Organometallic Chemistry*, 1997, **542**, 141.
8. R. Walsh and R. Becerra, in 'Thermochemistry', ed. Rappoport Z. and A. Y., Chichester, 1998.
9. T. L. Simpson and B. E. Volcani, 'Silicon and Siliceous Structures in Biological Systems', ed. Simpson T. L. and V. B. E., Springer-Verlag, 1981.
10. F. S. Kipping, *J. Chem. Soc.*, 1907, 209.
11. F. S. Kipping, *J. Chem. Soc.*, 1908, 457.
12. C. Eaborn and W. Bott, in 'Synthesis and Reaction of the Silicon-Carbon Bond', ed. A. G. MacDairmid, NewYork, 1968.
13. O. B. Young and C. E. Dickerman, *Industrial and Engineering Chemistry*, 1954, **46**, 364.
14. M. S. Beevers, in 'Dielectric Properties of Siloxanes', ed. S. J. Clarson and J. A. Semlyen, Englewood Cliffs, NJ, 1993.
15. M. J. Owen, in 'Siloxane Surface Activity', ed. J. M. Zeigler and F. W. G. Fearon, Washington D.C., 1990.
16. T. Owaga, T. Suzuki, and I. Mita, *Macromol. Chem. Phys.*, 1994, **195**, 1973.
17. D. R. Thomas, in 'Crosslinking of silicones', ed. S. J. Clarson and J. A. Semlyen, Englewood Cliffs, NJ, 1993.
18. M. G. Voronkov and V. I. Lavrent'yev, *Top. Curr. Chem.*, 1982, **102**, 199.
19. R. H. Baney, M. Itoh, A. Sakakibara, and T. Suzuki, *Chem. Rev.*, 1995, **95**, 1409.
20. P. R. Eisenberg, R. Erra-balsells, Y. Ishikawa, J. C. Lucas, A. N. Mauri, H. Nonami, C. C. Riccardi, and R. J. J. Williams, *Macromolecules*, 2000, **33**, 1940.
21. A. R. Bassindale and T. Gentle, *Journal of Organometallic Chemistry*, 1996, **521**, 391.
22. A. R. Bassindale and T. E. Gentle, *Journal of Materials Chemistry*, 1993, **3**, 1319.
23. T. E. Gentle and A. R. Bassindale, *Journal of Inorganic and Organometallic Polymers*, 1995, **5**, 281.
24. G. Calzaferri, D. Herren, and H. Burgy, *Helvetica Chimica Acta*, 1991, **74**, 24.
25. M. M. Sprung and F. O. Guenther, *Journal of the American Chemical Society*, 1955, **77**, 6045.
26. K. Larsson, *Arki. Chemi.*, 1960, **16**, 215.
27. C. Eaborn, 'Organosilicon Compounds', Butterworths, 1960.
28. F. J. Feher, *Journal of the American Chemical Society*, 1986, **108**, 3850.

29. F. J. Feher and R. L. Blanski, *Journal of the Chemical Society - Chemical Communications*, 1990, 1614.
30. I. M. Saez and J. W. Goodby, *Liquid Crystals*, 1999, **26**, 1101.
31. R. Elsasser, G. H. Mehl, J. W. Goodby, and D. J. Photinos, *Chemical Communications*, 2000, 851.
32. F. J. Feher, K. D. Wyndham, M. A. Scialdone, and Y. Hamuro, *Chemical Communications*, 1998, 1469.
33. F. J. Feher and K. D. Wyndham, *Chemical Communications*, 1998, 323.
34. R. Muller, *J. Prakt. Chem.*, 1959, **9**, 71.
35. C. L. Frye and W. T. Collins, *Journal of the American Chemical Society*, 1970, **92**, 5586.
36. P. A. Agaskar, *Inorg. Chem.*, 1991, **30**, 2707.
37. D. W. Scott, *J. Am. Chem. Soc.*, 1946, **68**, 356.
38. M. M. Sprung and F. O. Guenther, *Journal of the American Chemical Society*, 1955, **77**, 3990.
39. M. M. Sprung and F. O. Guenther, *Journal of the American Chemical Society*, 1955, **77**, 3996.
40. A. J. Barry, W. H. Daudt, J. J. Domicone, and J. W. Gilkey, *Journal of the American Chemical Society*, 1955, **77**, 4248.
41. K. Olsson, *Arki. Kemi.*, 1958, **13**, 367.
42. K. Larsson, *Arki. Chemi.*, 1960, **16**, 209.
43. L. H. Vogt and J. F. Brown, *Inorganic Chemistry*, 1963, **2**, 189.
44. J. F. Brown, L. H. Vogt, and P. I. Prescott, *Journal of the American Chemical Society*, 1964, **86**, 1120.
45. T. N. Martynova, V. P. Korchkov, and P. P. Semyannikov, *Journal of Organometallic Chemistry*, 1983, **258**, 277.
46. F. J. Feher and T. A. Budzichowski, *Journal of Organometallic Chemistry*, 1989, **379**, 33.
47. F. J. Feher and T. A. Budzichowski, *Journal of Organometallic Chemistry*, 1989, **373**, 153.
48. M. G. Voronkov and V. I. Lavrent'yev, *Zh. Obshch. Khim.*, 1979, **49**, 1522.
49. P. G. Harrison and C. Hall, *Main Group Metal Chemistry*, 1997, **20**, 515.
50. M. Unno, T. Matsumoto, K. Mochizuki, K. Higuchi, M. Goto, and H. Matsumoto, *Journal of Organometallic Chemistry*, 2003, **685**, 156.
51. A. R. Bassindale, Z. H. Liu, I. A. MacKinnon, P. G. Taylor, Y. X. Yang, M. E. Light, P. N. Horton, and M. B. Hursthouse, *Dalton Transactions*, 2003, 2945.
52. M. M. Sprung and F. O. Guenther, *Journal of Polymer Science*, 1958, **28**, 17.
53. R. J. Chambers and A. Marfat, *Journal of Heterocyclic Chemistry*, 1995, **32**, 1401.
54. A. R. Bassindale, H. P. Chen, Z. H. Liu, L. A. MacKinnon, D. J. Parker, P. G. Taylor, Y. X. Yang, M. E. Light, P. N. Horton, and M. B. Hursthouse, *Journal of Organometallic Chemistry*, 2004, **689**, 3287.
55. J. F. Brown, *Journal of the American Chemical Society*, 1965, **87**, 4317.
56. V. I. Lavrent'yev, V. M. Kovrigin, and G. G. Treer, *Zh. Obshch. Khim.*, 1981, **51**, 124.
57. J. F. Brown and L. H. Vogt, *Journal of the American Chemical Society*, 1965, **87**, 4313.
58. V. I. Lavrent'yev and V. M. Kovrigin, *Zh. Obshch. Khim.*, 1989, **59**, 377.
59. F. Liebau, H. Gies, R. P. Gunawardane, and B. Marler, *Zeolites*, 1986, **6**, 373.

60. M. Pourny, 'Characterization of Fe-MCM-22', Universita degli Studi di Torino, Turin, Italy, 2000.
61. H. Kessler, J. Patarin, and C. Schottdarie, in 'The Opportunities of the Fluoride Route in the Synthesis of Microporous Materials', 1994.
62. P. Caullet, J. L. Guth, J. Hazm, J. M. Lamblin, and H. Gies, *European Journal of Solid State and Inorganic Chemistry*, 1991, **28**, 345.
63. P. Caullet, L. Schreyeck, J. C. Mougenel, J. Patarin, and J. L. Paillaud, *Microporous Materials*, 1997, **11**, 161.
64. P. Caullet, L. Schreyeck, F. Dagosto, J. Stumbe, and J. C. Mougenel, *Chemical Communications*, 1997, 1241.
65. H. W. Roesky, Y. Yang, J. Pinkas, and M. Schafer, *Angewandte Chemie-International Edition*, 1998, **37**, 2650.
66. J. Patarin, A. Matijasic, and J. L. Paillaud, *Journal of Materials Chemistry*, 2000, **10**, 1345.
67. J. Patarin, P. Reinert, and B. Marler, *Chemical Communications*, 1998, 1769.
68. L. A. Villaescusa, P. Lightfoot, and R. E. Morris, *Chemical Communications*, 2002, 2220.
69. C. R. A. Catlow and A. R. George, *Zeolites*, 1997, **18**, 67.
70. R. Stosser and M. Pach, *Journal of Physical Chemistry A*, 1997, **101**, 8360.
71. Y. Yang, 'Synthesis and Rearrangement of Silsesquioxane Cages', The Open University, Milton Keynes, UK, 2001.
72. H. C. Marsmann and E. Rikowski, *Polyhedron*, 1997, **16**, 3357.
73. J. F. Brown, L. H. Vogt, and P. P. I., *J. Am. Chem. Soc.*, 1963, **86**, 1120.
74. J. F. Brown, L. H. Vogt, A. Katchman, J. W. Eustance, and K. M. Kiser, *Journal of the American Chemical Society*, 1960, **82**, 6194.
75. E. Wiberg and W. Simmler, *Zeitschrift Fur Anorganische Und Allgemeine Chemie*, 1955, **282**, 330.
76. P. G. Jones, *Chemistry in Britain*, 1981, **17**, 222.
77. Q. Chen and Z. J., *J. Chem. Soc., Chem. Comm.*, 1994, 2663.
78. Q. Chen and J. Zubieta, *J. Chem. Soc., Chem. Comm.*, 1994, 1635.
79. A. Shibato, Y. Itagaki, E. Tayama, Y. Hokke, N. Asao, and K. Maruoka, *Tetrahedron*, 2000, **56**, 5373.
80. N. Asao, A. Shibato, Y. Itagaki, F. Jourdan, and K. Maruoka, *Tetrahedron Letters*, 1998, **39**, 3177.
81. A. R. Bassindale, I. A. MacKinnon, M. G. Maesano, and P. G. Taylor, *Chemical Communications*, 2003, 1382.
82. Z. H. Liu, 'Synthesis and Reactions of Novel Silsesquioxane Cages', The Open University, Milton Keynes, UK, 2004.
83. M. A. Hossain, M. B. Hursthouse, and K. M. A. Malik, *Acta Crystallographica Section B-Structural Science*, 1979, **35**, 2258.
84. S. S. Park, C. Y. Xiao, F. Hagelberg, D. Hossain, C. U. Pittman, and S. Saebo, *Journal of Physical Chemistry A*, 2004, **108**, 11260.
85. T. E. Gentle, 'Octopus and Dendrimer Molecules with Silsesquioxane Cores', The Open University, Milton Keynes, UK, 1995.
86. W. R. Roush, T. D. Bannister, M. D. Wendt, M. S. VanNieuwenhze, D. J. Gustin, G. J. Dilley, G. C. Lane, K. A. Scheidt, and W. J. Smith, *Journal of Organic Chemistry*, 2002, **67**, 4284.
87. K. A. Scheidt, H. Chen, B. C. Follows, S. R. Chemler, D. S. Coffey, and W. R. Roush, *Journal of Organic Chemistry*, 1998, **63**, 6436.

88. M. A. Brook, 'Silicon in Organic, Organometallic, and Polymer Chemistry', Wiley, 2000.
89. S. Liu, X. Lang, H. Ye, S. Zhang, and J. Zhao, *European Polymer Journal*, 2005, **41**, 996.
90. R. A. Mantz, P. F. Jones, K. P. Chaffee, J. D. Lichtenhan, J. W. Gilman, I. M. K. Ismail, and M. J. Burmeister, *Chemistry of Materials*, 1996, **8**, 1250.

Appendix of crystallographic data

This section summarises the key instrument parameters and crystal data for the single crystal X-ray structures presented in this thesis. The appendix is split into 6 parts, one for each structure.

Part 1:	Ph_8T_8-TBAF
Part 2:	Vinyl-T_8-TBAF
Part 3:	*p*-tolyl-T_8-TBAF
Part 4:	Ph_8T_8
Part 5:	$Ph_{12}T_{12}$
Part 6:	*Iso*-butylT_8

The layout of each part is as follow:

Section A: Summary of crystal parameters, instrument condition and data refinement information.

Section B: Listing of atomic coordinates and thermal parameters for non-hydrogen atoms.

Section C: Structure diagrams. Hydrogens normally omitted for clarity.

Section D: Listing of key bond lengths and angles (data for C-H bonds omitted).

Part1: Ph_8T_8-TBAF

Section A. Crystal data and structure refinement.

Identification code	01SRC394
Empirical formula	$C_{64}H_{76}FNO_{12}Si_8$
Formula weight	1294.98
Temperature	120(2) K
Wavelength	0.71073 Å
Crystal system	Monoclinic
Space group	*C2/c*
Unit cell dimensions	$a = 23.8267(4)$ Å
	$b = 12.9976(3)$ Å $\quad \beta = 108.1550(12)°$
	$c = 22.1794(5)$ Å
Volume	6526.8(2) Å^3
Z	4
Density (calculated)	1.318 Mg / m^3
Absorption coefficient	0.228 mm^{-1}
F(000)	2736
Crystal	Colourless Prism
Crystal size	0.30 × 0.20 × 0.10 mm^3
θ range for data collection	3.01 – 25.03°
Index ranges	$-28 \le h \le 28, -15 \le k \le 15, -25 \le l \le 26$
Reflections collected	16965
Independent reflections	5719 [$R_{int} = 0.0555$]
Completeness to $\theta = 25.03°$	99.1 %
Max. and min. transmission	0.9775 and 0.9347
Refinement method	Full-matrix least-squares on F^2
Data / restraints / parameters	5719 / 0 / 389
Goodness-of-fit on F^2	1.032
Final *R* indices [$F^2 > 2\sigma(F^2)$]	*R1* = 0.0397, *wR2* = 0.1050
R indices (all data)	*R1* = 0.0560, *wR2* = 0.1134
Largest diff. peak and hole	0.503 and –0.387 e Å^{-3}

Diffractometer: *Nonius KappaCCD* area detector (ϕ scans and ω scans to fill *Ewald* sphere). **Cell determination:** DirAx (Duisenberg, A.J.M.(1992). J. Appl. Cryst. 25, 92-96.) **Data collection:** Collect (Collect: Data collection software, R. Hooft, Nonius B.V., 1998). **Data reduction and cell refinement**: *Denzo* (Z. Otwinowski & W. Minor, *Methods in Enzymology* (1997) Vol. **276**: *Macromolecular Crystallography*, part A, pp. 307–326; C. W. Carter, Jr. & R. M. Sweet, Eds., Academic Press). **Absorption correction**: *SORTAV* (R. H. Blessing, Acta Cryst. A**51** (1995) 33–37; R. H. Blessing, J. Appl. Cryst. **30** (1997) 421–426). **Structure solution**: *SHELXS97* (G. M. Sheldrick, Acta Cryst. (1990) A**46** 467–473). **Structure refinement**: *SHELXL97* (G. M. Sheldrick (1997), University of Göttingen, Germany). **Graphics:** Cameron - A Molecular Graphics Package. (D. M. Watkin, L. Pearce and C. K. Prout, Chemical Crystallography Laboratory, University of Oxford, 1993).

Special details: All hydrogen atoms were placed in idealised positions and refined using a riding model.

Section B. Atomic coordinates [$\times 10^4$], equivalent isotropic displacement parameters [$Å^2 \times 10^3$] and site occupancy factors. U_{eq} is defined as one third of the trace of the orthogonalized U^{ij} tensor.

Atom	*x*	*y*	*z*	U_{eq}	*S.o.f.*
C1	1197(1)	6893(2)	4020(1)	16(1)	1
C2	992(1)	6053(2)	4281(1)	20(1)	1
C3	1376(1)	5355(2)	4678(1)	25(1)	1
C4	1982(1)	5489(2)	4825(1)	25(1)	1
C5	2197(1)	6325(2)	4581(1)	26(1)	1
C6	1810(1)	7016(2)	4186(1)	23(1)	1
C7	1141(1)	6911(2)	1705(1)	16(1)	1
C8	941(1)	6016(2)	1361(1)	20(1)	1
C9	1323(1)	5330(2)	1208(1)	28(1)	1
C10	1922(1)	5544(2)	1396(1)	32(1)	1
C11	2131(1)	6437(2)	1724(1)	37(1)	1
C12	1747(1)	7109(2)	1879(1)	28(1)	1
C13	1085(1)	10946(2)	1633(1)	16(1)	1
C14	1002(1)	10856(2)	981(1)	24(1)	1
C15	1263(1)	11527(2)	665(1)	29(1)	1
C16	1621(1)	12312(2)	993(1)	29(1)	1
C17	1718(1)	12411(2)	1638(1)	31(1)	1
C18	1450(1)	11735(2)	1949(1)	24(1)	1
C19	−1148(1)	10934(2)	949(1)	17(1)	1
C20	−1102(1)	10815(2)	338(1)	26(1)	1
C21	−1377(1)	11476(2)	−153(1)	32(1)	1
C22	−1701(1)	12300(2)	−43(1)	34(1)	1
C23	−1757(1)	12435(2)	556(1)	32(1)	1
C24	−1488(1)	11754(2)	1041(1)	23(1)	1
O1	866(1)	8917(1)	3633(1)	17(1)	1
O2	828(1)	7458(1)	2756(1)	17(1)	1
O3	−23(1)	7434(1)	1617(1)	17(1)	1
O4	819(1)	8924(1)	1886(1)	18(1)	1
O5	868(1)	10397(1)	2766(1)	17(1)	1
O6	−23(1)	10391(1)	1658(1)	17(1)	1
Si1	693(1)	7740(1)	3409(1)	14(1)	1
Si2	654(1)	7748(1)	2008(1)	14(1)	1
Si3	662(1)	10100(1)	2015(1)	14(1)	1
Si4	−700(1)	10095(1)	1599(1)	14(1)	1
C25	−15(1)	3186(2)	1948(1)	18(1)	1
C26	−42(1)	3706(2)	1334(1)	37(1)	1
C27	−29(1)	2951(2)	836(1)	29(1)	1
C28	−50(1)	3392(2)	203(1)	36(1)	1
C29	538(1)	4603(2)	2667(1)	18(1)	1
C30	1136(1)	4089(2)	2826(1)	32(1)	1
C31	1627(1)	4868(2)	3025(1)	24(1)	1
C32	2243(1)	4421(2)	3186(1)	40(1)	1
N1	0	3895(2)	2500	16(1)	1
F1	0	8922(1)	2500	20(1)	1

Section C. Bond lengths [Å] and angles [°].

C1–C2	1.394(3)	C23–C24	1.386(3)
C1–C6	1.402(3)	O1–Si1	1.6224(15)
C1–Si1	1.864(2)	O1–Si4^{i}	1.6240(15)
C2–C3	1.391(3)	O2–Si1	1.6213(15)
C3–C4	1.388(3)	O2–Si2	1.6241(15)
C4–C5	1.381(3)	O3–Si2	1.6264(15)
C5–C6	1.386(3)	O3–Si1^{i}	1.6284(15)
C7–C8	1.392(3)	O4–Si3	1.6198(15)
C7–C12	1.396(3)	O4–Si2	1.6227(15)
C7–Si2	1.863(2)	O5–Si3	1.6291(15)
C8–C9	1.388(3)	O5–Si4^{i}	1.6295(15)
C9–C10	1.384(4)	O6–Si3	1.6211(15)
C10–C11	1.378(4)	O6–Si4	1.6222(15)
C11–C12	1.383(3)	Si1–O3^{i}	1.6284(15)
C13–C18	1.385(3)	Si4–O1^{i}	1.6240(15)
C13–C14	1.402(3)	Si4–O5^{i}	1.6295(15)
C13–Si3	1.863(2)	C25–C26	1.503(3)
C14–C15	1.382(3)	C25–N1	1.525(2)
C15–C16	1.382(3)	C26–C27	1.484(3)
C16–C17	1.383(3)	C27–C28	1.504(3)
C17–C18	1.389(3)	C29–C30	1.513(3)
C19–C24	1.392(3)	C29–N1	1.526(2)
C19–C20	1.402(3)	C30–C31	1.505(3)
C19–Si4	1.858(2)	C31–C32	1.515(3)
C20–C21	1.383(3)	N1–C29^{i}	1.526(2)
C21–C22	1.384(4)	N1–C25^{i}	1.525(2)
C22–C23	1.387(4)		

C2–C1–C6	116.9(2)	C20–C19–Si4	119.10(17)
C2–C1–Si1	122.32(17)	C21–C20–C19	122.2(2)
C6–C1–Si1	120.42(16)	C22–C21–C20	119.7(2)
C3–C2–C1	121.8(2)	C21–C22–C23	119.5(2)
C4–C3–C2	119.9(2)	C24–C23–C22	120.2(2)
C5–C4–C3	119.5(2)	C23–C24–C19	121.7(2)
C4–C5–C6	120.2(2)	Si1–O1–Si4^{i}	141.11(10)
C5–C6–C1	121.7(2)	Si1–O2–Si2	143.36(10)
C8–C7–C12	117.0(2)	Si2–O3–Si1^{i}	139.11(10)
C8–C7–Si2	122.72(17)	Si3–O4–Si2	141.11(10)
C12–C7–Si2	119.96(17)	Si3–O5–Si4^{i}	138.56(10)
C9–C8–C7	122.2(2)	Si3–O6–Si4	143.88(10)
C10–C9–C8	119.3(2)	O2–Si1–O1	112.55(8)
C11–C10–C9	119.8(2)	O2–Si1–O3^{i}	112.21(8)
C10–C11–C12	120.3(2)	O1–Si1–O3^{i}	113.27(8)
C11–C12–C7	121.4(2)	O2–Si1–C1	104.69(8)
C18–C13–C14	116.6(2)	O1–Si1–C1	106.86(9)
C18–C13–Si3	123.41(17)	O3^{i}–Si1–C1	106.54(9)
C14–C13–Si3	119.81(16)	O4–Si2–O2	112.98(8)
C15–C14–C13	122.0(2)	O4–Si2–O3	113.55(8)
C14–C15–C16	120.0(2)	O2–Si2–O3	112.40(8)
C17–C16–C15	119.3(2)	O4–Si2–C7	106.22(9)
C16–C17–C18	120.1(2)	O2–Si2–C7	104.11(8)
C13–C18–C17	122.0(2)	O3–Si2–C7	106.71(9)
C24–C19–C20	116.8(2)	O4–Si3–O6	112.75(8)
C24–C19–Si4	123.81(17)	O4–Si3–O5	113.00(8)

O6–Si3–O5	112.45(8)	C27–C26–C25	111.8(2)
O4–Si3–C13	106.81(9)	C26–C27–C28	116.1(2)
O6–Si3–C13	104.18(9)	C30–C29–N1	116.70(18)
O5–Si3–C13	106.91(9)	C31–C30–C29	111.12(19)
O6–Si4–O1^{i}	112.84(8)	C30–C31–C32	114.8(2)
O6–Si4–O5^{i}	112.36(8)	C29–N1–C29^{i}	105.9(2)
O1^{i}–Si4–O5^{i}	113.50(8)	C29–N1–C25	111.56(12)
O6–Si4–C19	103.86(9)	C29^{i}–N1–C25	111.19(12)
O1^{i}–Si4–C19	106.44(9)	C29–N1–C25^{i}	111.19(12)
O5^{i}–Si4–C19	107.00(9)	C29^{i}–N1–C25^{i}	111.56(12)
C26–C25–N1	116.05(18)	C25–N1–C25^{i}	105.6(2)

Symmetry transformations used to generate equivalent atoms:
(i) –x,y,–z+1/2

Section D. Anisotropic displacement parameters [$Å^2 \times 10^3$]. The anisotropic displacement factor exponent takes the form: $-2\pi^2[h^2a^{*2}U^{11} + \cdots + 2\,h\,k\,a^*\,b^*\,U^{12}]$.

Atom	U^{11}	U^{22}	U^{33}	U^{23}	U^{13}	U^{12}
C1	18(1)	17(1)	12(1)	−2(1)	6(1)	1(1)
C2	18(1)	23(1)	19(1)	1(1)	8(1)	0(1)
C3	29(1)	24(1)	24(1)	7(1)	13(1)	1(1)
C4	28(1)	25(1)	18(1)	4(1)	4(1)	8(1)
C5	17(1)	32(1)	27(1)	1(1)	3(1)	0(1)
C6	22(1)	22(1)	23(1)	4(1)	5(1)	−2(1)
C7	18(1)	19(1)	12(1)	4(1)	6(1)	2(1)
C8	21(1)	24(1)	17(1)	0(1)	7(1)	2(1)
C9	37(2)	23(1)	24(1)	−3(1)	11(1)	5(1)
C10	33(2)	41(2)	28(1)	1(1)	16(1)	18(1)
C11	18(1)	56(2)	37(2)	−9(1)	12(1)	3(1)
C12	21(1)	35(1)	30(1)	−10(1)	11(1)	−4(1)
C13	15(1)	15(1)	21(1)	2(1)	9(1)	4(1)
C14	27(1)	24(1)	25(1)	−4(1)	13(1)	−4(1)
C15	37(2)	32(1)	25(1)	2(1)	21(1)	0(1)
C16	31(1)	25(1)	40(2)	6(1)	24(1)	−2(1)
C17	29(1)	28(1)	37(2)	−2(1)	13(1)	−11(1)
C18	22(1)	29(1)	21(1)	−1(1)	9(1)	−2(1)
C19	15(1)	17(1)	18(1)	−1(1)	4(1)	−3(1)
C20	32(1)	24(1)	21(1)	0(1)	6(1)	5(1)
C21	39(2)	38(2)	16(1)	2(1)	4(1)	−1(1)
C22	35(2)	32(2)	28(1)	13(1)	−1(1)	4(1)
C23	30(1)	29(1)	35(2)	6(1)	7(1)	12(1)
C24	21(1)	25(1)	23(1)	3(1)	7(1)	3(1)
O1	19(1)	16(1)	18(1)	0(1)	5(1)	0(1)
O2	19(1)	18(1)	15(1)	2(1)	7(1)	3(1)
O3	15(1)	19(1)	18(1)	−3(1)	6(1)	0(1)
O4	20(1)	16(1)	19(1)	0(1)	9(1)	0(1)
O5	17(1)	19(1)	16(1)	−1(1)	6(1)	−4(1)
O6	15(1)	18(1)	19(1)	4(1)	6(1)	0(1)
Si1	14(1)	14(1)	14(1)	0(1)	6(1)	0(1)
Si2	14(1)	14(1)	14(1)	0(1)	6(1)	0(1)
Si3	14(1)	15(1)	14(1)	1(1)	6(1)	−1(1)
Si4	15(1)	15(1)	13(1)	0(1)	5(1)	1(1)
C25	20(1)	16(1)	19(1)	−3(1)	7(1)	0(1)
C26	71(2)	22(1)	23(1)	0(1)	23(1)	2(1)
C27	45(2)	24(1)	22(1)	−1(1)	16(1)	0(1)
C28	51(2)	37(2)	23(1)	1(1)	17(1)	4(1)
C29	19(1)	15(1)	22(1)	−2(1)	8(1)	−3(1)
C30	21(1)	23(1)	51(2)	0(1)	9(1)	0(1)
C31	20(1)	26(1)	25(1)	0(1)	7(1)	−1(1)
C32	23(1)	41(2)	54(2)	−2(1)	10(1)	2(1)
N1	19(1)	14(1)	17(1)	0	7(1)	0
F1	22(1)	20(1)	18(1)	0	8(1)	0

Section E. Hydrogen coordinates [$\times 10^4$] and isotropic displacement parameters [$Å^2 \times 10^3$].

Atom	*x*	*y*	*z*	U_{eq}	*S.o.f.*
H2	578	5954	4186	24	1
H3	1225	4787	4848	30	1
H4	2246	5010	5091	30	1
H5	2611	6427	4685	32	1
H6	1966	7588	4022	27	1
H8	530	5870	1226	24	1
H9	1174	4721	977	33	1
H10	2188	5075	1300	39	1
H11	2540	6593	1843	44	1
H12	1899	7717	2110	33	1
H14	759	10319	750	29	1
H15	1196	11448	222	34	1
H16	1799	12778	777	35	1
H17	1967	12942	1869	37	1
H18	1520	11815	2392	28	1
H20	−875	10260	259	31	1
H21	−1345	11367	−565	38	1
H22	−1882	12769	−375	41	1
H23	−1982	12995	633	38	1
H24	−1536	11850	1446	27	1
H25A	342	2746	2077	22	1
H25B	−362	2728	1869	22	1
H26A	−409	4117	1185	44	1
H26B	297	4182	1407	44	1
H27A	−369	2478	771	35	1
H27B	335	2535	996	35	1
H28A	−34	2832	−87	54	1
H28B	288	3852	256	54	1
H28C	−418	3779	27	54	1
H29A	496	5074	2305	22	1
H29B	531	5029	3035	22	1
H30A	1179	3587	3173	39	1
H30B	1165	3709	2449	39	1
H31A	1592	5243	3401	29	1
H31B	1573	5375	2679	29	1
H32A	2534	4978	3310	59	1
H32B	2287	4064	2814	59	1
H32C	2307	3934	3538	59	1

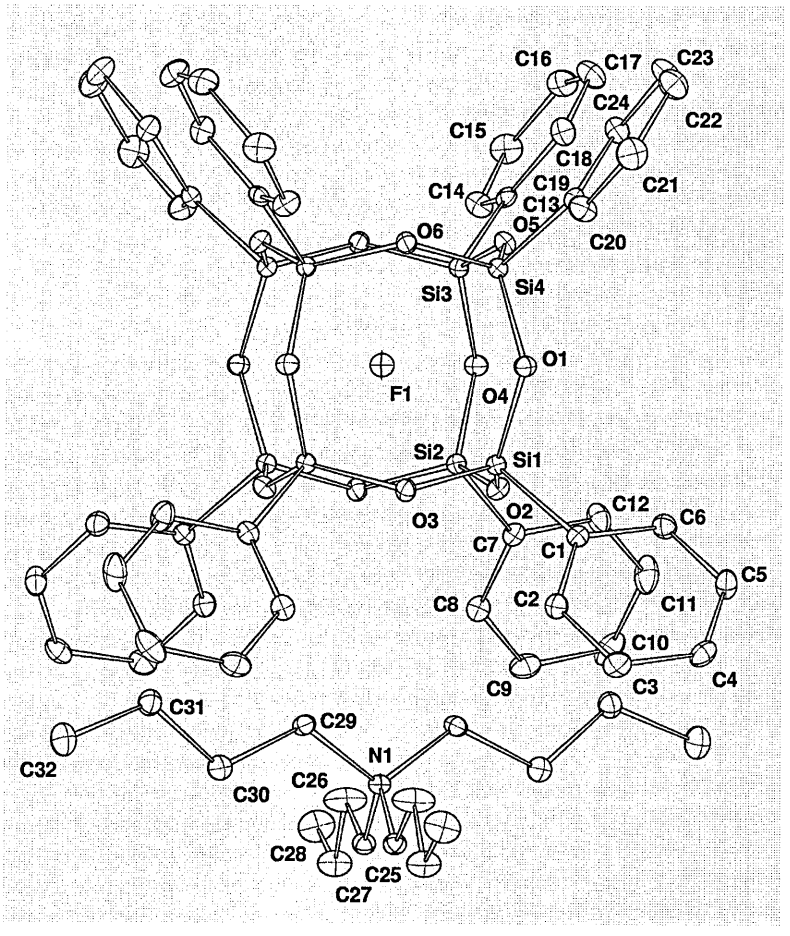
C16
C17
C23
C24
C22
C15
C18
C21
C14
C19
C13
C20
O6
O5
Si3
Si4
O1
F1
O4
Si2
Si1
O3
O2
C12
C6
C7
C1
C5
C8
C2
C11
C10
C9
C3
C4
C31
C29
N1
C32
C30
C26
C28
C25
C27

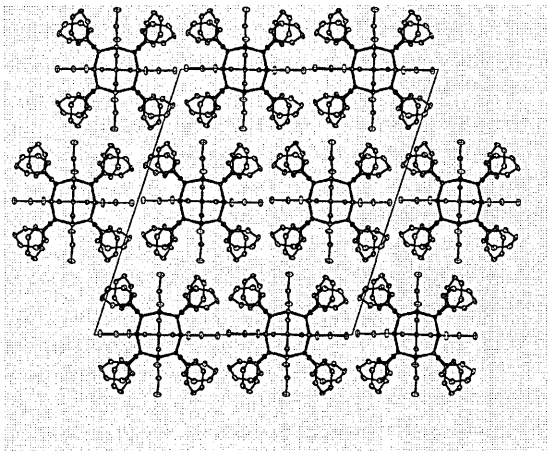

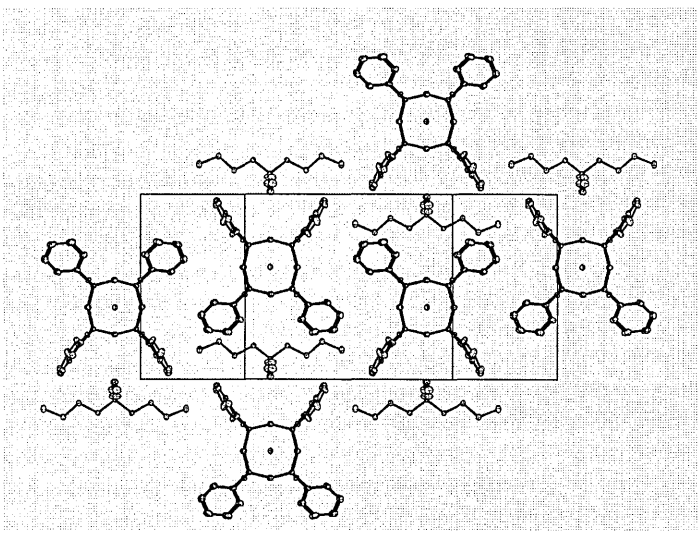

Part 2: Vinyl-T_8-TBAF

Section A. Crystal data and structure refinement.

Identification code	**02src587**	
Empirical formula	$C_{32}H_{60}FNO_{12}Si_8$	
Formula weight	894.53	
Temperature	120(2) K	
Wavelength	0.71073 Å	
Crystal system	Monoclinic	
Space group	$P2_1/n$	
Unit cell dimensions	$a = 12.15090(10)$ Å	$\alpha = 90°$
	$b = 18.2072(2)$ Å	$\beta = 96.9900(10)°$
	$c = 20.6679(2)$ Å	$\gamma = 90°$
Volume	4538.45(8) Å^3	
Z	4	
Density (calculated)	1.309 Mg / m^3	
Absorption coefficient	0.295 mm^{-1}	
F(000)	1904	
Crystal	Block; Colourless	
Crystal size	0.80 × 0.60 × 0.30 mm^3	
θ range for data collection	2.98 – 27.47°	
Index ranges	$-15 \le h \le 15, -23 \le k \le 21, -26 \le l \le 26$	
Reflections collected	48660	
Independent reflections	10362 [$R_{int} = 0.0603$]	
Completeness to $\theta = 27.47°$	99.6 %	
Absorption correction	Semi–empirical from equivalents	
Max. and min. transmission	0.9167 and 0.7983	
Refinement method	Full-matrix least-squares on F^2	
Data / restraints / parameters	10362 / 0 / 502	
Goodness-of-fit on F^2	1.027	
Final R indices [$F^2 > 2\sigma(F^2)$]	$R1 = 0.0403$, $wR2 = 0.1041$	
R indices (all data)	$R1 = 0.0578$, $wR2 = 0.1124$	
Largest diff. peak and hole	0.527 and –0.477 e Å^{-3}	

Diffractometer: *Nonius KappaCCD* area detector (ϕ scans and ω scans to fill *asymmetric unit* sphere). **Cell determination:** DirAx (Duisenberg, A.J.M.(1992). J. Appl. Cryst. 25, 92-96.) **Data collection:** Collect (Collect: Data collection software, R. Hooft, Nonius B.V., 1998). **Data reduction and cell refinement**: *Denzo* (Z. Otwinowski & W. Minor, *Methods in Enzymology* (1997) Vol. **276**: *Macromolecular Crystallography*, part A, pp. 307–326; C. W. Carter, Jr. & R. M. Sweet, Eds., Academic Press). **Absorption correction**: *SORTAV* (R. H. Blessing, Acta Cryst. A**51** (1995) 33–37; R. H. Blessing, J. Appl. Cryst. **30** (1997) 421–426). **Structure solution**: *SHELXS97* (G. M. Sheldrick, Acta Cryst. (1990) A**46** 467–473). **Structure refinement**: *SHELXL97* (G. M. Sheldrick (1997), University of Göttingen, Germany). **Graphics:** Cameron - A Molecular Graphics Package. (D. M. Watkin, L. Pearce and C. K. Prout, Chemical Crystallography Laboratory, University of Oxford, 1993).

Special details:

All hydrogen atoms are fixed.
One butyl group of the TBA ion is disordered over 2 sites.

Section B. Atomic coordinates [$\times 10^4$], equivalent isotropic displacement parameters [$Å^2 \times 10^3$] and site occupancy factors. U_{eq} is defined as one third of the trace of the orthogonalized U^{ij} tensor.

Atom	*x*	*y*	*z*	U_{eq}	*S.o.f.*
Si1	7790(1)	−656(1)	7213(1)	18(1)	1
Si2	6869(1)	−1979(1)	7883(1)	18(1)	1
Si3	6964(1)	−1107(1)	9155(1)	17(1)	1
Si4	7903(1)	217(1)	8483(1)	18(1)	1
Si5	5433(1)	−95(1)	6815(1)	19(1)	1
Si6	4510(1)	−1411(1)	7480(1)	18(1)	1
Si7	4595(1)	−549(1)	8750(1)	16(1)	1
Si8	5533(1)	777(1)	8079(1)	17(1)	1
F1	6169(1)	−604(1)	7951(1)	22(1)	1
O1	7597(1)	−1500(1)	7426(1)	21(1)	1
O2	7128(1)	−1769(1)	8650(1)	20(1)	1
O3	7696(1)	−390(1)	9026(1)	20(1)	1
O4	8271(1)	−144(1)	7823(1)	21(1)	1
O5	6725(1)	−299(1)	6773(1)	20(1)	1
O6	5553(1)	−1969(1)	7621(1)	22(1)	1
O7	5668(1)	−913(1)	9176(1)	19(1)	1
O8	6851(1)	765(1)	8327(1)	20(1)	1
O9	4659(1)	−795(1)	6931(1)	21(1)	1
O10	4110(1)	−1067(1)	8140(1)	20(1)	1
O11	4795(1)	290(1)	8523(1)	20(1)	1
O12	5269(1)	584(1)	7306(1)	21(1)	1
N1	2909(2)	−3108(1)	9119(1)	26(1)	1
C1	8904(2)	−680(1)	6673(1)	26(1)	1
C2	8856(2)	−347(1)	6108(1)	42(1)	1
C3	7295(2)	−2949(1)	7821(1)	28(1)	1
C4	7670(2)	−3361(1)	8314(1)	48(1)	1
C5	7505(2)	−1443(1)	9975(1)	25(1)	1
C6	8073(2)	−2054(1)	10091(1)	39(1)	1
C7	9078(2)	780(1)	8851(1)	26(1)	1
C8	9489(2)	736(1)	9469(1)	38(1)	1
C9	4910(2)	232(1)	5984(1)	26(1)	1
C10	4096(2)	−96(1)	5606(1)	36(1)	1
C11	3353(2)	−1996(1)	7109(1)	25(1)	1
C12	3481(2)	−2675(1)	6906(1)	35(1)	1
C13	3511(2)	−519(1)	9306(1)	21(1)	1
C14	3673(2)	−726(1)	9922(1)	28(1)	1
C15	5119(2)	1744(1)	8181(1)	25(1)	1
C16	4429(2)	1973(1)	8582(1)	38(1)	1
C21	2750(2)	−3860(1)	8794(1)	30(1)	1
C22	3210(2)	−3949(1)	8147(1)	34(1)	1
C23	2979(2)	−4730(1)	7890(1)	37(1)	1
C24	3419(2)	−4862(2)	7246(1)	49(1)	1
C25	2267(2)	−2522(1)	8705(1)	24(1)	1
C26	1030(2)	−2655(1)	8552(1)	33(1)	1
C27	456(2)	−1960(1)	8259(1)	36(1)	1
C28	339(2)	−1364(1)	8760(1)	37(1)	1
C29	2481(2)	−3183(1)	9777(1)	35(1)	1
C30	2513(2)	−2489(1)	10188(1)	37(1)	1
C31	2131(2)	−2650(1)	10849(1)	45(1)	1
C32	950(3)	−2906(2)	10809(1)	61(1)	1
C33	4108(2)	−2873(1)	9192(1)	42(1)	1
C34A	4764(6)	−3421(4)	9719(4)	45(1)	0.486(4)

C35A	5469(5)	−3215(3)	10099(4)	56(1)	0.486(4)
C36A	6463(11)	−3753(10)	10354(9)	58(2)	0.486(4)
C34B	5067(5)	−3364(4)	9449(3)	45(1)	0.514(4)
C35B	5983(5)	−3200(3)	9744(3)	56(1)	0.514(4)
C36B	6757(11)	−3685(10)	10177(8)	58(2)	0.514(4)

Section C. Bond lengths [Å] and angles [°].

Si1–O4	1.6194(14)	C10–H10A	0.9500
Si1–O5	1.6232(14)	C10–H10B	0.9500
Si1–O1	1.6237(14)	C11–C12	1.321(3)
Si1–C1	1.857(2)	C11–H11	0.9500
Si2–O2	1.6232(14)	C12–H12A	0.9500
Si2–O1	1.6246(14)	C12–H12B	0.9500
Si2–O6	1.6252(14)	C13–C14	1.320(3)
Si2–C3	1.849(2)	C13–H13	0.9500
Si3–O3	1.6190(14)	C14–H14A	0.9500
Si3–O7	1.6193(14)	C14–H14B	0.9500
Si3–O2	1.6230(13)	C15–C16	1.316(3)
Si3–C5	1.847(2)	C15–H15	0.9500
Si4–O3	1.6183(14)	C16–H16A	0.9500
Si4–O8	1.6213(14)	C16–H16B	0.9500
Si4–O4	1.6249(14)	C21–C22	1.519(3)
Si4–C7	1.845(2)	C21–H21A	0.9900
Si5–O9	1.6194(14)	C21–H21B	0.9900
Si5–O5	1.6268(14)	C22–C23	1.531(3)
Si5–O12	1.6273(14)	C22–H22A	0.9900
Si5–C9	1.855(2)	C22–H22B	0.9900
Si6–O9	1.6201(14)	C23–C24	1.512(3)
Si6–O6	1.6219(14)	C23–H23A	0.9900
Si6–O10	1.6280(13)	C23–H23B	0.9900
Si6–C11	1.854(2)	C24–H24A	0.9800
Si7–O7	1.6228(13)	C24–H24B	0.9800
Si7–O11	1.6237(14)	C24–H24C	0.9800
Si7–O10	1.6279(14)	C25–C26	1.517(3)
Si7–C13	1.8499(19)	C25–H25A	0.9900
Si8–O8	1.6215(14)	C25–H25B	0.9900
Si8–O11	1.6229(13)	C26–C27	1.533(3)
Si8–O12	1.6297(14)	C26–H26A	0.9900
Si8–C15	1.850(2)	C26–H26B	0.9900
N1–C33	1.508(3)	C27–C28	1.519(3)
N1–C29	1.520(3)	C27–H27A	0.9900
N1–C25	1.522(2)	C27–H27B	0.9900
N1–C21	1.526(3)	C28–H28A	0.9800
C1–C2	1.311(3)	C28–H28B	0.9800
C1–H1	0.9500	C28–H28C	0.9800
C2–H2A	0.9500	C29–C30	1.521(3)
C2–H2B	0.9500	C29–H29A	0.9900
C3–C4	1.303(3)	C29–H29B	0.9900
C3–H3	0.9500	C30–C31	1.523(3)
C4–H4A	0.9500	C30–H30A	0.9900
C4–H4B	0.9500	C30–H30B	0.9900
C5–C6	1.316(3)	C31–C32	1.501(4)
C5–H5	0.9500	C31–H31A	0.9900
C6–H6A	0.9500	C31–H31B	0.9900
C6–H6B	0.9500	C32–H32A	0.9800
C7–C8	1.316(3)	C32–H32B	0.9800
C7–H7	0.9500	C32–H32C	0.9800
C8–H8A	0.9500	C33–C34B	1.511(7)
C8–H8B	0.9500	C33–C34A	1.613(8)
C9–C10	1.326(3)	C33–H33A	0.9900
C9–H9	0.9500	C33–H33B	0.9900

C34A–C35A	1.152(10)	C34B–C35B	1.239(9)
C34A–H34A	0.9900	C34B–H34C	0.9900
C34A–H34B	0.9900	C34B–H34D	0.9900
C35A–C36A	1.593(18)	C35B–C36B	1.504(18)
C35A–H35A	0.9900	C35B–H35C	0.9900
C35A–H35B	0.9900	C35B–H35D	0.9900
C36A–H36A	0.9800	C36B–H36D	0.9800
C36A–H36B	0.9800	C36B–H36E	0.9800
C36A–H36C	0.9800	C36B–H36F	0.9800

O4–Si1–O5	113.11(7)	O11–Si8–C15	106.25(8)
O4–Si1–O1	112.59(7)	O12–Si8–C15	107.02(8)
O5–Si1–O1	113.55(7)	Si1–O1–Si2	140.56(9)
O4–Si1–C1	105.13(8)	Si3–O2–Si2	141.06(9)
O5–Si1–C1	105.23(9)	Si4–O3–Si3	143.06(9)
O1–Si1–C1	106.31(8)	Si1–O4–Si4	140.96(9)
O2–Si2–O1	112.77(7)	Si1–O5–Si5	140.40(9)
O2–Si2–O6	112.92(7)	Si6–O6–Si2	141.49(9)
O1–Si2–O6	112.54(7)	Si3–O7–Si7	142.62(9)
O2–Si2–C3	105.64(9)	Si4–O8–Si8	142.71(9)
O1–Si2–C3	107.13(8)	Si5–O9–Si6	139.91(9)
O6–Si2–C3	105.10(9)	Si7–O10–Si6	139.13(9)
O3–Si3–O7	112.61(7)	Si8–O11–Si7	142.19(9)
O3–Si3–O2	112.35(7)	Si5–O12–Si8	138.66(9)
O7–Si3–O2	112.04(7)	C33–N1–C29	111.52(18)
O3–Si3–C5	106.01(8)	C33–N1–C25	106.29(16)
O7–Si3–C5	106.66(8)	C29–N1–C25	110.93(16)
O2–Si3–C5	106.62(8)	C33–N1–C21	111.57(17)
O3–Si4–O8	111.92(7)	C29–N1–C21	105.96(16)
O3–Si4–O4	112.81(7)	C25–N1–C21	110.66(16)
O8–Si4–O4	111.89(7)	C2–C1–Si1	124.60(18)
O3–Si4–C7	105.70(9)	C2–C1–H1	117.7
O8–Si4–C7	107.03(8)	Si1–C1–H1	117.7
O4–Si4–C7	106.99(8)	C1–C2–H2A	120.0
O9–Si5–O5	114.19(7)	C1–C2–H2B	120.0
O9–Si5–O12	112.90(7)	H2A–C2–H2B	120.0
O5–Si5–O12	113.50(7)	C4–C3–Si2	124.84(18)
O9–Si5–C9	104.51(9)	C4–C3–H3	117.6
O5–Si5–C9	104.35(8)	Si2–C3–H3	117.6
O12–Si5–C9	106.21(8)	C3–C4–H4A	120.0
O9–Si6–O6	114.07(7)	C3–C4–H4B	120.0
O9–Si6–O10	112.94(7)	H4A–C4–H4B	120.0
O6–Si6–O10	113.35(7)	C6–C5–Si3	124.53(18)
O9–Si6–C11	104.58(8)	C6–C5–H5	117.7
O6–Si6–C11	104.55(9)	Si3–C5–H5	117.7
O10–Si6–C11	106.22(8)	C5–C6–H6A	120.0
O7–Si7–O11	113.67(7)	C5–C6–H6B	120.0
O7–Si7–O10	111.97(7)	H6A–C6–H6B	120.0
O11–Si7–O10	111.94(7)	C8–C7–Si4	123.35(18)
O7–Si7–C13	105.18(8)	C8–C7–H7	118.3
O11–Si7–C13	107.16(8)	Si4–C7–H7	118.3
O10–Si7–C13	106.28(8)	C7–C8–H8A	120.0
O8–Si8–O11	113.98(7)	C7–C8–H8B	120.0
O8–Si8–O12	112.02(7)	H8A–C8–H8B	120.0
O11–Si8–O12	112.39(7)	C10–C9–Si5	123.27(18)
O8–Si8–C15	104.43(8)	C10–C9–H9	118.4

Si5–C9–H9	118.4	C27–C26–H26B	109.7
C9–C10–H10A	120.0	H26A–C26–H26B	108.2
C9–C10–H10B	120.0	C28–C27–C26	113.40(19)
H10A–C10–H10B	120.0	C28–C27–H27A	108.9
C12–C11–Si6	123.83(18)	C26–C27–H27A	108.9
C12–C11–H11	118.1	C28–C27–H27B	108.9
Si6–C11–H11	118.1	C26–C27–H27B	108.9
C11–C12–H12A	120.0	H27A–C27–H27B	107.7
C11–C12–H12B	120.0	C27–C28–H28A	109.5
H12A–C12–H12B	120.0	C27–C28–H28B	109.5
C14–C13–Si7	123.78(16)	H28A–C28–H28B	109.5
C14–C13–H13	118.1	C27–C28–H28C	109.5
Si7–C13–H13	118.1	H28A–C28–H28C	109.5
C13–C14–H14A	120.0	H28B–C28–H28C	109.5
C13–C14–H14B	120.0	N1–C29–C30	115.91(19)
H14A–C14–H14B	120.0	N1–C29–H29A	108.3
C16–C15–Si8	125.13(18)	C30–C29–H29A	108.3
C16–C15–H15	117.4	N1–C29–H29B	108.3
Si8–C15–H15	117.4	C30–C29–H29B	108.3
C15–C16–H16A	120.0	H29A–C29–H29B	107.4
C15–C16–H16B	120.0	C29–C30–C31	110.6(2)
H16A–C16–H16B	120.0	C29–C30–H30A	109.5
C22–C21–N1	116.34(18)	C31–C30–H30A	109.5
C22–C21–H21A	108.2	C29–C30–H30B	109.5
N1–C21–H21A	108.2	C31–C30–H30B	109.5
C22–C21–H21B	108.2	H30A–C30–H30B	108.1
N1–C21–H21B	108.2	C32–C31–C30	113.8(2)
H21A–C21–H21B	107.4	C32–C31–H31A	108.8
C21–C22–C23	109.48(19)	C30–C31–H31A	108.8
C21–C22–H22A	109.8	C32–C31–H31B	108.8
C23–C22–H22A	109.8	C30–C31–H31B	108.8
C21–C22–H22B	109.8	H31A–C31–H31B	107.7
C23–C22–H22B	109.8	C31–C32–H32A	109.5
H22A–C22–H22B	108.2	C31–C32–H32B	109.5
C24–C23–C22	112.6(2)	H32A–C32–H32B	109.5
C24–C23–H23A	109.1	C31–C32–H32C	109.5
C22–C23–H23A	109.1	H32A–C32–H32C	109.5
C24–C23–H23B	109.1	H32B–C32–H32C	109.5
C22–C23–H23B	109.1	N1–C33–C34B	124.1(3)
H23A–C23–H23B	107.8	N1–C33–C34A	106.5(3)
C23–C24–H24A	109.5	C34B–C33–C34A	26.1(3)
C23–C24–H24B	109.5	N1–C33–H33A	110.4
H24A–C24–H24B	109.5	C34B–C33–H33A	114.2
C23–C24–H24C	109.5	C34A–C33–H33A	110.4
H24A–C24–H24C	109.5	N1–C33–H33B	110.4
H24B–C24–H24C	109.5	C34B–C33–H33B	85.3
C26–C25–N1	115.63(17)	C34A–C33–H33B	110.4
C26–C25–H25A	108.4	H33A–C33–H33B	108.6
N1–C25–H25A	108.4	C35A–C34A–C33	121.7(7)
C26–C25–H25B	108.4	C35A–C34A–H34A	106.9
N1–C25–H25B	108.4	C33–C34A–H34A	106.9
H25A–C25–H25B	107.4	C35A–C34A–H34B	106.9
C25–C26–C27	110.03(19)	C33–C34A–H34B	106.9
C25–C26–H26A	109.7	H34A–C34A–H34B	106.7
C27–C26–H26A	109.7	C34A–C35A–C36A	119.8(10)
C25–C26–H26B	109.7	C34A–C35A–H35A	107.4

C36A–C35A–H35A	107.4	C34B–C35B–H35C	105.4
C34A–C35A–H35B	107.4	C36B–C35B–H35C	105.4
C36A–C35A–H35B	107.4	C34B–C35B–H35D	105.4
H35A–C35A–H35B	106.9	C36B–C35B–H35D	105.4
C35B–C34B–C33	129.6(6)	H35C–C35B–H35D	106.0
C35B–C34B–H34C	104.9	C35B–C36B–H36D	109.5
C33–C34B–H34C	104.9	C35B–C36B–H36E	109.5
C35B–C34B–H34D	104.9	H36D–C36B–H36E	109.5
C33–C34B–H34D	104.9	C35B–C36B–H36F	109.5
H34C–C34B–H34D	105.8	H36D–C36B–H36F	109.5
C34B–C35B–C36B	127.6(8)	H36E–C36B–H36F	109.5

Symmetry transformations used to generate equivalent atoms:

Section D. Anisotropic displacement parameters [$Å^2 \times 10^3$]. The anisotropic displacement factor exponent takes the form: $-2\pi^2[h^2a^{*2}U^{11} + \cdots + 2\,h\,k\,a^*\,b^*\,U^{12}]$.

Atom	U^{11}	U^{22}	U^{33}	U^{23}	U^{13}	U^{12}
Si1	19(1)	17(1)	19(1)	−1(1)	6(1)	−1(1)
Si2	22(1)	13(1)	20(1)	−1(1)	5(1)	1(1)
Si3	19(1)	16(1)	16(1)	1(1)	1(1)	1(1)
Si4	17(1)	16(1)	20(1)	−2(1)	3(1)	−2(1)
Si5	21(1)	20(1)	16(1)	2(1)	3(1)	0(1)
Si6	19(1)	19(1)	17(1)	−2(1)	3(1)	−3(1)
Si7	17(1)	17(1)	16(1)	0(1)	4(1)	0(1)
Si8	20(1)	14(1)	18(1)	1(1)	4(1)	2(1)
F1	24(1)	20(1)	21(1)	−1(1)	4(1)	0(1)
O1	24(1)	16(1)	23(1)	0(1)	8(1)	1(1)
O2	26(1)	16(1)	19(1)	1(1)	2(1)	4(1)
O3	21(1)	19(1)	19(1)	0(1)	2(1)	−2(1)
O4	19(1)	22(1)	22(1)	−4(1)	6(1)	−2(1)
O5	22(1)	21(1)	19(1)	2(1)	6(1)	0(1)
O6	24(1)	17(1)	24(1)	−3(1)	3(1)	−2(1)
O7	20(1)	21(1)	17(1)	2(1)	3(1)	1(1)
O8	21(1)	14(1)	25(1)	−1(1)	4(1)	−1(1)
O9	23(1)	25(1)	17(1)	1(1)	2(1)	−3(1)
O10	20(1)	23(1)	18(1)	−3(1)	5(1)	−4(1)
O11	22(1)	18(1)	20(1)	1(1)	6(1)	1(1)
O12	26(1)	18(1)	18(1)	2(1)	3(1)	3(1)
N1	31(1)	20(1)	27(1)	1(1)	−2(1)	2(1)
C1	25(1)	25(1)	30(1)	−5(1)	11(1)	−2(1)
C2	44(1)	42(1)	43(2)	1(1)	24(1)	0(1)
C3	35(1)	18(1)	31(1)	−4(1)	11(1)	4(1)
C4	69(2)	27(1)	50(2)	2(1)	19(1)	19(1)
C5	26(1)	30(1)	19(1)	3(1)	1(1)	1(1)
C6	48(2)	43(1)	26(1)	9(1)	0(1)	11(1)
C7	22(1)	22(1)	35(1)	−6(1)	6(1)	−4(1)
C8	31(1)	37(1)	45(1)	−8(1)	−8(1)	−7(1)
C9	30(1)	29(1)	19(1)	3(1)	5(1)	4(1)
C10	35(1)	50(2)	22(1)	2(1)	1(1)	6(1)
C11	23(1)	33(1)	20(1)	−1(1)	3(1)	−8(1)
C12	39(1)	36(1)	30(1)	−9(1)	7(1)	−18(1)
C13	19(1)	21(1)	25(1)	−3(1)	6(1)	−2(1)
C14	33(1)	30(1)	23(1)	−5(1)	12(1)	−4(1)
C15	29(1)	21(1)	24(1)	4(1)	3(1)	4(1)
C16	42(1)	27(1)	47(1)	0(1)	12(1)	14(1)
C21	39(1)	19(1)	31(1)	−2(1)	2(1)	2(1)
C22	41(1)	28(1)	34(1)	−5(1)	6(1)	−2(1)
C23	38(1)	31(1)	43(1)	−10(1)	4(1)	1(1)
C24	56(2)	46(2)	44(2)	−17(1)	7(1)	2(1)
C25	29(1)	20(1)	22(1)	4(1)	2(1)	2(1)
C26	31(1)	28(1)	37(1)	−4(1)	−6(1)	−1(1)
C27	33(1)	37(1)	34(1)	−5(1)	−6(1)	9(1)
C28	30(1)	37(1)	42(1)	−2(1)	1(1)	7(1)
C29	59(2)	24(1)	23(1)	4(1)	1(1)	4(1)
C30	53(2)	27(1)	29(1)	−1(1)	1(1)	7(1)
C31	74(2)	36(1)	24(1)	3(1)	2(1)	19(1)
C32	94(3)	51(2)	42(2)	4(1)	29(2)	1(2)
C33	28(1)	34(1)	59(2)	−11(1)	−9(1)	7(1)
C34A	33(3)	47(2)	52(4)	3(3)	−1(2)	9(2)

C35A	33(2)	52(2)	82(4)	12(2)	1(2)	−6(2)
C36A	37(6)	50(3)	81(8)	13(4)	−14(4)	3(4)
C34B	33(3)	47(2)	52(4)	3(3)	−1(2)	9(2)
C35B	33(2)	52(2)	82(4)	12(2)	1(2)	−6(2)
C36B	37(6)	50(3)	81(8)	13(4)	−14(4)	3(4)

Section E. Hydrogen coordinates [$\times 10^4$] and isotropic displacement parameters [$Å^2 \times 10^3$].

Atom	*x*	*y*	*z*	U_{eq}	*S.o.f.*
H1	9555	–953	6816	31	1
H2A	8218	–69	5949	50	1
H2B	9460	–383	5857	50	1
H3	7237	–3161	7399	33	1
H4A	7740	–3168	8744	57	1
H4B	7873	–3856	8243	57	1
H5	7364	–1154	10339	30	1
H6A	8230	–2356	9738	47	1
H6B	8327	–2193	10526	47	1
H7	9405	1118	8580	31	1
H8A	9178	403	9750	46	1
H8B	10096	1039	9634	46	1
H9	5243	655	5822	31	1
H10A	3750	–520	5757	43	1
H10B	3859	94	5183	43	1
H11	2626	–1796	7061	31	1
H12A	4198	–2891	6947	41	1
H12B	2855	–2948	6719	41	1
H13	2796	–345	9138	26	1
H14A	4380	–903	10103	34	1
H14B	3084	–699	10184	34	1
H15	5429	2104	7923	30	1
H16A	4102	1630	8848	46	1
H16B	4259	2481	8606	46	1
H21A	3102	–4233	9100	36	1
H21B	1946	–3968	8724	36	1
H22A	4019	–3857	8206	41	1
H22B	2857	–3589	7828	41	1
H23A	3324	–5086	8215	45	1
H23B	2168	–4817	7835	45	1
H24A	3057	–4524	6918	73	1
H24B	3263	–5370	7107	73	1
H24C	4221	–4778	7298	73	1
H25A	2379	–2045	8934	29	1
H25B	2587	–2478	8289	29	1
H26A	717	–2791	8956	39	1
H26B	897	–3066	8239	39	1
H27A	886	–1763	7921	43	1
H27B	–290	–2093	8044	43	1
H28A	–133	–1541	9079	55	1
H28B	1	–927	8541	55	1
H28C	1072	–1237	8984	55	1
H29A	2923	–3566	10030	42	1
H29B	1705	–3359	9703	42	1
H30A	2025	–2112	9957	44	1
H30B	3278	–2292	10251	44	1
H31A	2619	–3031	11072	54	1
H31B	2216	–2199	11118	54	1
H32A	472	–2571	10530	91	1
H32B	718	–2913	11247	91	1
H32C	890	–3402	10624	91	1
H33A	4182	–2359	9347	50	1

H33B	4410	–2910	8770	50	1
H34A	4202	–3650	9964	54	0.486(4)
H34B	5076	–3819	9471	54	0.486(4)
H35A	5128	–3047	10485	67	0.486(4)
H35B	5797	–2777	9913	67	0.486(4)
H36A	6336	–4235	10149	86	0.486(4)
H36B	6503	–3805	10829	86	0.486(4)
H36C	7162	–3549	10243	86	0.486(4)
H34C	4748	–3720	9737	54	0.514(4)
H34D	5237	–3649	9066	54	0.514(4)
H35C	5845	–2768	10015	67	0.514(4)
H35D	6424	–3016	9405	67	0.514(4)
H36D	6734	–3546	10634	86	0.514(4)
H36E	7514	–3625	10067	86	0.514(4)
H36F	6528	–4198	10114	86	0.514(4)

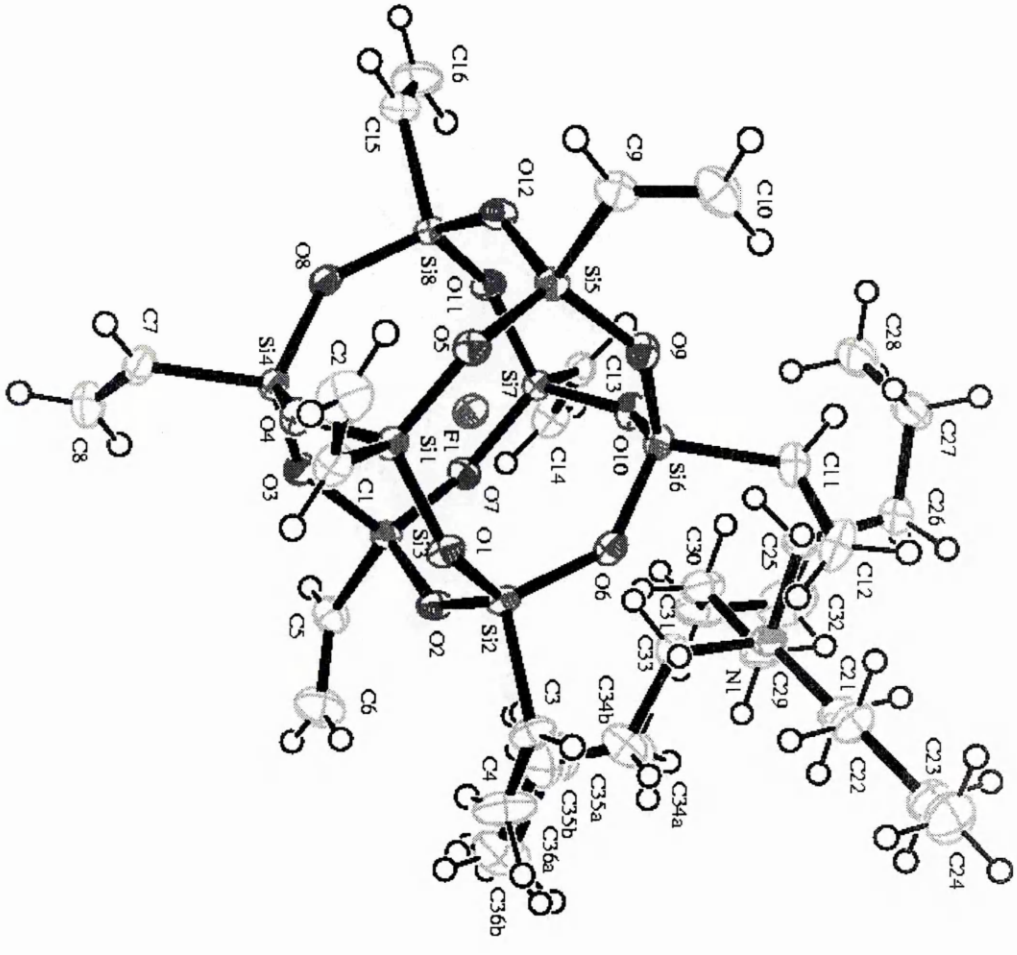
Cl6
Cl5
O12
C9
C10
O8
Si8
O11
Si5
C7
O5
O9
C28
Si4
C2
Si7
Cl3
C27
C8
O4
F1
Si1
O10
Si6
Cl1
O3
Cl4
O7
C26
C1
O1
C30
C25
Cl2
Si3
O6
C31
C32
C5
O2
Si2
C33
N1
C29
C21
C3
C34b
C6
C4
C35a
C34a
C22
C23
C35b
C36a
C24
C36b

Part 3: *para*-tolyl-T8-TBAF

Section A. Crystal data and structure refinement.

Identification code	**03src0097**	
Empirical formula	$C_{72}H_{92}FNO_{12}Si_8$	
Formula weight	1407.19	
Temperature	120(2) K	
Wavelength	0.71073 Å	
Crystal system	Tetragonal	
Space group	*I*–4	
Unit cell dimensions	a = 12.64760(10) Å	α = 90°
	b = 12.64760(10) Å	β = 90°
	c = 22.6513(6) Å	γ = 90°
Volume	3623.34(10) Å^3	
Z	2	
Density (calculated)	1.290 Mg / m^3	
Absorption coefficient	0.211 mm^{-1}	
F(000)	1496	
Crystal	Shard; Colourless	
Crystal size	0.30 × 0.22 × 0.08 mm^3	
θ range for data collection	3.14 – 27.49°	
Index ranges	$-16 \le h \le 16$, $-16 \le k \le 16$, $-29 \le l \le 25$	
Reflections collected	10458	
Independent reflections	4040 [R_{int} = 0.0697]	
Completeness to θ = 27.49°	99.8 %	
Absorption correction	Semi–empirical from equivalents	
Max. and min. transmission	0.9833 and 0.9393	
Refinement method	Full-matrix least-squares on F^2	
Data / restraints / parameters	4040 / 0 / 216	
Goodness-of-fit on F^2	1.039	
Final *R* indices [$F^2 > 2\sigma(F^2)$]	*R1* = 0.0489, *wR2* = 0.1141	
R indices (all data)	*R1* = 0.0632, *wR2* = 0.1242	
Absolute structure parameter	–0.07(16)	
Extinction coefficient	0.0063(7)	
Largest diff. peak and hole	0.324 and –0.343 e Å^{-3}	

Diffractometer: *Nonius KappaCCD* area detector (ϕ scans and ω scans to fill *asymmetric unit* sphere). **Cell determination:** DirAx (Duisenberg, A.J.M.(1992). J. Appl. Cryst. 25, 92-96.) **Data collection:** Collect (Collect: Data collection software, R. Hooft, Nonius B.V., 1998). **Data reduction and cell refinement**: *Denzo* (Z. Otwinowski & W. Minor, *Methods in Enzymology* (1997) Vol. **276**: *Macromolecular Crystallography*, part A, pp. 307–326; C. W. Carter, Jr. & R. M. Sweet, Eds., Academic Press). **Absorption correction**: *SORTAV* (R. H. Blessing, Acta Cryst. A**51** (1995) 33–37; R. H. Blessing, J. Appl. Cryst. **30** (1997) 421–426). **Structure solution**: *SHELXS97* (G. M. Sheldrick, Acta Cryst. (1990) A**46** 467–473). **Structure refinement**: *SHELXL97* (G. M. Sheldrick (1997), University of Göttingen, Germany). **Graphics:** Cameron - A Molecular Graphics Package. (D. M. Watkin, L. Pearce and C. K. Prout, Chemical Crystallography Laboratory, University of Oxford, 1993).

Special details:

All hydrogen atoms were fixed.
Absolute structure cannot be accurately determined.

Section B. Atomic coordinates [$\times 10^4$], equivalent isotropic displacement parameters [$Å^2 \times 10^3$] and site occupancy factors. U_{eq} is defined as one third of the trace of the orthogonalized U^{ij} tensor.

Atom	*x*	*y*	*z*	U_{eq}	*S.o.f.*
C1	3522(2)	7518(2)	6325(1)	21(1)	1
C2	2883(2)	7828(2)	5852(1)	25(1)	1
C3	2561(2)	7107(2)	5428(1)	24(1)	1
C4	2848(2)	6048(2)	5457(1)	27(1)	1
C5	3454(3)	5728(2)	5939(2)	33(1)	1
C6	3778(2)	6447(2)	6367(1)	30(1)	1
C7	2558(3)	5309(2)	4957(2)	40(1)	1
C8	7478(2)	8461(2)	6350(1)	21(1)	1
C9	7465(2)	7357(2)	6313(1)	24(1)	1
C10	8223(2)	6801(2)	5986(1)	26(1)	1
C11	9013(2)	7328(2)	5683(1)	28(1)	1
C12	9036(2)	8432(2)	5708(1)	29(1)	1
C13	8278(2)	8983(2)	6038(1)	24(1)	1
C14	9832(2)	6726(3)	5337(2)	41(1)	1
O1	5364(1)	8533(2)	6666(1)	22(1)	1
O2	3519(2)	9630(1)	6655(1)	21(1)	1
O3	3897(1)	8155(1)	7501(1)	21(1)	1
F1	5000	10000	7500	25(1)	1
Si1	4112(1)	8528(1)	6825(1)	19(1)	1
Si2	6470(1)	9122(1)	6823(1)	18(1)	1
C15	9061(2)	5252(2)	7896(1)	31(1)	1
C16	8073(2)	5637(2)	7579(2)	34(1)	1
C17	7114(3)	5581(2)	7990(2)	36(1)	1
C18	6118(2)	5996(2)	7692(2)	39(1)	1
N1	10000	5000	7500	28(1)	1

Section C. Bond lengths [Å] and angles [°].

C1–C6	1.396(4)	C14–H14A	0.9800
C1–C2	1.399(4)	C14–H14B	0.9800
C1–Si1	1.863(3)	C14–H14C	0.9800
C2–C3	1.386(4)	O1–Si1	1.6235(19)
C2–H2	0.9500	O1–Si2	1.6242(19)
C3–C4	1.389(4)	O2–Si2^{i}	1.624(2)
C3–H3	0.9500	O2–Si1	1.6286(19)
C4–C5	1.394(5)	O3–Si1	1.624(2)
C4–C7	1.514(4)	O3–Si2^{ii}	1.629(2)
C5–C6	1.391(4)	Si2–O2^{i}	1.624(2)
C5–H5	0.9500	Si2–O3^{iii}	1.629(2)
C6–H6	0.9500	C15–C16	1.521(4)
C7–H7A	0.9800	C15–N1	1.522(3)
C7–H7B	0.9800	C15–H15A	0.9900
C7–H7C	0.9800	C15–H15B	0.9900
C8–C9	1.399(4)	C16–C17	1.530(4)
C8–C13	1.400(4)	C16–H16A	0.9900
C8–Si2	1.864(3)	C16–H16B	0.9900
C9–C10	1.399(4)	C17–C18	1.522(5)
C9–H9	0.9500	C17–H17A	0.9900
C10–C11	1.383(4)	C17–H17B	0.9900
C10–H10	0.9500	C18–H18A	0.9800
C11–C12	1.398(4)	C18–H18B	0.9800
C11–C14	1.506(4)	C18–H18C	0.9800
C12–C13	1.402(4)	N1–C15^{iv}	1.522(3)
C12–H12	0.9500	N1–C15^{v}	1.522(3)
C13–H13	0.9500	N1–C15^{vi}	1.522(3)

C6–C1–C2	117.2(3)	C9–C8–Si2	118.4(2)
C6–C1–Si1	122.1(2)	C13–C8–Si2	124.9(2)
C2–C1–Si1	120.4(2)	C8–C9–C10	121.7(3)
C3–C2–C1	121.1(3)	C8–C9–H9	119.2
C3–C2–H2	119.4	C10–C9–H9	119.2
C1–C2–H2	119.4	C11–C10–C9	121.0(3)
C2–C3–C4	121.6(3)	C11–C10–H10	119.5
C2–C3–H3	119.2	C9–C10–H10	119.5
C4–C3–H3	119.2	C10–C11–C12	118.4(3)
C3–C4–C5	117.5(3)	C10–C11–C14	120.8(3)
C3–C4–C7	119.7(3)	C12–C11–C14	120.8(3)
C5–C4–C7	122.7(3)	C11–C12–C13	120.3(3)
C6–C5–C4	121.1(3)	C11–C12–H12	119.9
C6–C5–H5	119.4	C13–C12–H12	119.9
C4–C5–H5	119.4	C8–C13–C12	121.9(3)
C5–C6–C1	121.3(3)	C8–C13–H13	119.0
C5–C6–H6	119.3	C12–C13–H13	119.0
C1–C6–H6	119.3	C11–C14–H14A	109.5
C4–C7–H7A	109.5	C11–C14–H14B	109.5
C4–C7–H7B	109.5	H14A–C14–H14B	109.5
H7A–C7–H7B	109.5	C11–C14–H14C	109.5
C4–C7–H7C	109.5	H14A–C14–H14C	109.5
H7A–C7–H7C	109.5	H14B–C14–H14C	109.5
H7B–C7–H7C	109.5	Si1–O1–Si2	142.47(13)
C9–C8–C13	116.6(3)	Si2^{i}–O2–Si1	140.49(13)

Si1–O3–Si2^{ii}	140.53(11)	C15–C16–H16B	109.6
O1–Si1–O3	111.92(10)	C17–C16–H16B	109.6
O1–Si1–O2	113.14(9)	H16A–C16–H16B	108.1
O3–Si1–O2	113.29(10)	C18–C17–C16	111.8(3)
O1–Si1–C1	104.96(11)	C18–C17–H17A	109.3
O3–Si1–C1	107.85(11)	C16–C17–H17A	109.3
O2–Si1–C1	104.93(12)	C18–C17–H17B	109.3
O1–Si2–O2^{i}	113.69(9)	C16–C17–H17B	109.3
O1–Si2–O3^{iii}	112.13(9)	H17A–C17–H17B	107.9
O2^{i}–Si2–O3^{iii}	112.86(9)	C17–C18–H18A	109.5
O1–Si2–C8	104.91(11)	C17–C18–H18B	109.5
O2^{i}–Si2–C8	107.17(11)	H18A–C18–H18B	109.5
O3^{iii}–Si2–C8	105.25(11)	C17–C18–H18C	109.5
C16–C15–N 1	115.5(2)	H18A–C18–H18C	109.5
C16–C15–H15A	108.4	H18B–C18–H18C	109.5
N1–C15–H15A	108.4	C15^{iv}–N1–C15	107.8(2)
C16–C15–H15B	108.4	C15^{iv}–N1–C15^{v}	110.34(12)
N1–C15–H15B	108.4	C15–N1–C15^{v}	110.34(12)
H15A–C15–H15B	107.5	C15^{iv}–N1–C15^{vi}	110.34(12)
C15–C16–C17	110.5(3)	C15–N1–C15^{vi}	110.34(12)
C15–C16–H16A	109.6	C15^{v}–N1–C15^{vi}	107.8(2)
C17–C16–H16A	109.6		

Symmetry transformations used to generate equivalent atoms:
(i) –x+1,–y+2,z (ii) y–1/2,–x+3/2,–z+3/2 (iii) –y+3/2,x+1/2,–z+3/2
(iv) –x+2,–y+1,z (v) –y+3/2,x–1/2,–z+3/2 (vi) y+1/2,–x+3/2,–z+3/2

Section D. Anisotropic displacement parameters [$Å^2 \times 10^3$]. The anisotropic displacement factor exponent takes the form: $-2\pi^2[h^2a^{*2}U^{11} + \cdots + 2\,h\,k\,a^*\,b^*\,U^{12}]$.

Atom	U^{11}	U^{22}	U^{33}	U^{23}	U^{13}	U^{12}
C1	19(1)	24(1)	20(2)	−1(1)	1(1)	−3(1)
C2	22(1)	24(1)	28(2)	−2(1)	0(1)	−2(1)
C3	24(1)	27(1)	22(2)	1(1)	−2(1)	−3(1)
C4	30(1)	28(1)	24(2)	−4(1)	2(1)	−7(1)
C5	42(2)	21(1)	37(2)	−2(1)	−6(2)	0(1)
C6	37(2)	25(1)	27(2)	0(1)	−8(1)	1(1)
C7	56(2)	31(2)	34(2)	−8(2)	−2(2)	−5(2)
C8	21(1)	26(1)	18(2)	0(1)	0(1)	1(1)
C9	23(1)	27(1)	23(2)	0(1)	2(1)	2(1)
C10	25(1)	28(1)	24(2)	−3(1)	−1(1)	3(1)
C11	24(1)	40(2)	18(1)	−5(1)	0(1)	6(1)
C12	24(1)	38(2)	24(2)	3(1)	4(1)	−2(1)
C13	23(1)	27(1)	22(1)	2(1)	−1(1)	−2(1)
C14	29(2)	53(2)	39(2)	−9(2)	9(2)	5(1)
O1	20(1)	24(1)	21(1)	−4(1)	2(1)	−2(1)
O2	21(1)	21(1)	22(1)	1(1)	−1(1)	−1(1)
O3	24(1)	22(1)	17(1)	0(1)	−1(1)	−3(1)
F1	27(1)	27(1)	21(2)	0	0	0
Si1	19(1)	19(1)	17(1)	−2(1)	0(1)	−1(1)
Si2	18(1)	20(1)	17(1)	0(1)	0(1)	0(1)
C15	39(2)	30(1)	23(2)	1(1)	5(1)	1(1)
C16	37(2)	41(2)	25(2)	4(1)	8(2)	0(1)
C17	43(2)	33(2)	32(2)	2(1)	9(2)	0(1)
C18	36(2)	34(2)	46(2)	−4(1)	12(1)	−4(1)
N1	33(1)	33(1)	17(2)	0	0	0

Section E. Hydrogen coordinates [$\times 10^4$] and isotropic displacement parameters [$Å^2 \times 10^3$].

Atom	*x*	*y*	*z*	U_{eq}	*S.o.f.*
H2	2666	8545	5820	30	1
H3	2133	7342	5109	29	1
H5	3649	5005	5976	40	1
H6	4181	6205	6693	36	1
H7A	2684	4576	5079	60	1
H7B	2992	5472	4611	60	1
H7C	1809	5400	4858	60	1
H9	6929	6974	6514	29	1
H10	8194	6051	5972	31	1
H12	9568	8810	5501	34	1
H13	8308	9733	6050	29	1
H14A	9491	6142	5125	61	1
H14B	10365	6442	5608	61	1
H14C	10172	7201	5053	61	1
H15A	8878	4608	8123	37	1
H15B	9280	5799	8184	37	1
H16A	7945	5194	7226	41	1
H16B	8179	6376	7447	41	1
H17A	6999	4839	8112	43	1
H17B	7257	6004	8349	43	1
H18A	5969	5574	7339	58	1
H18B	6222	6737	7579	58	1
H18C	5521	5943	7966	58	1

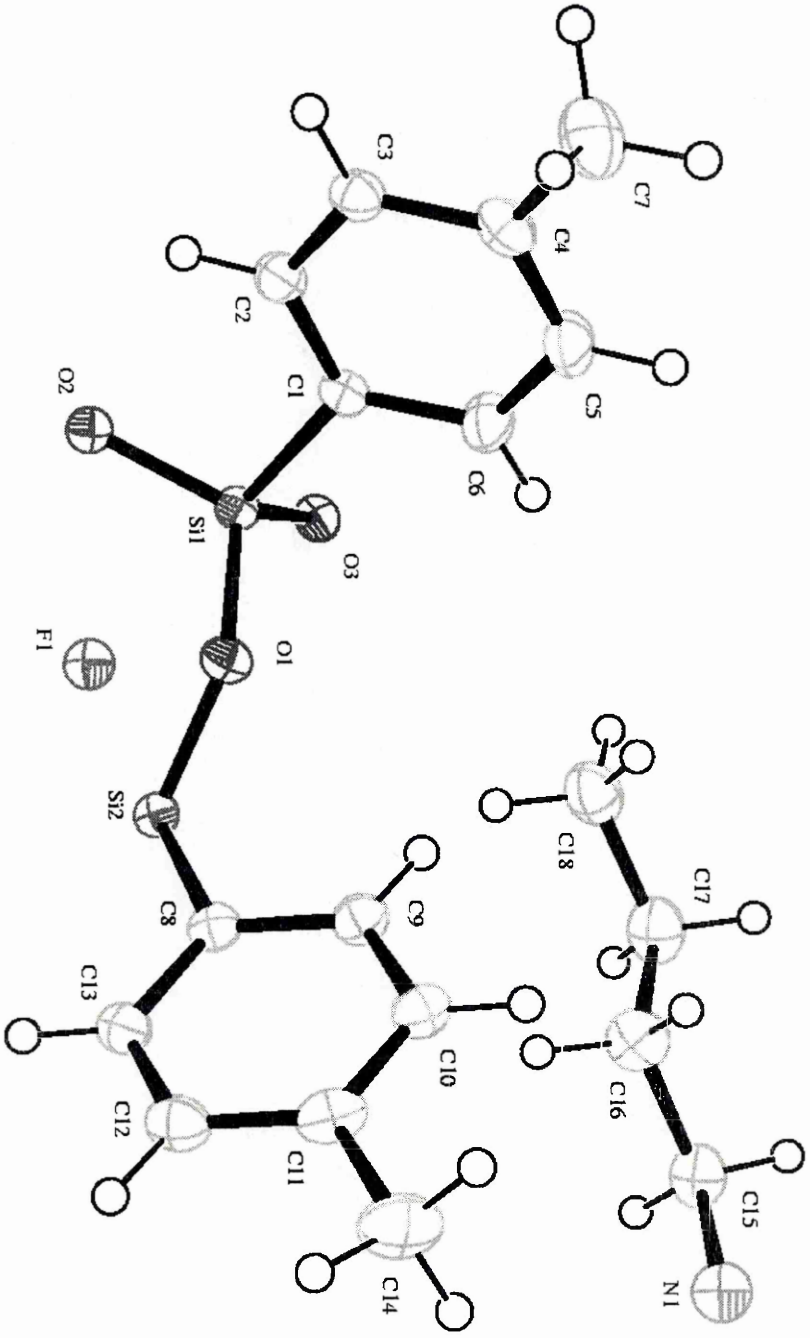
C3
C7
C4
C2
C1
C5
O2
C6
Si1
O3
F1
O1
Si2
C18
C17
C8
C9
C13
C10
C16
C12
C11
C15
C14
N1

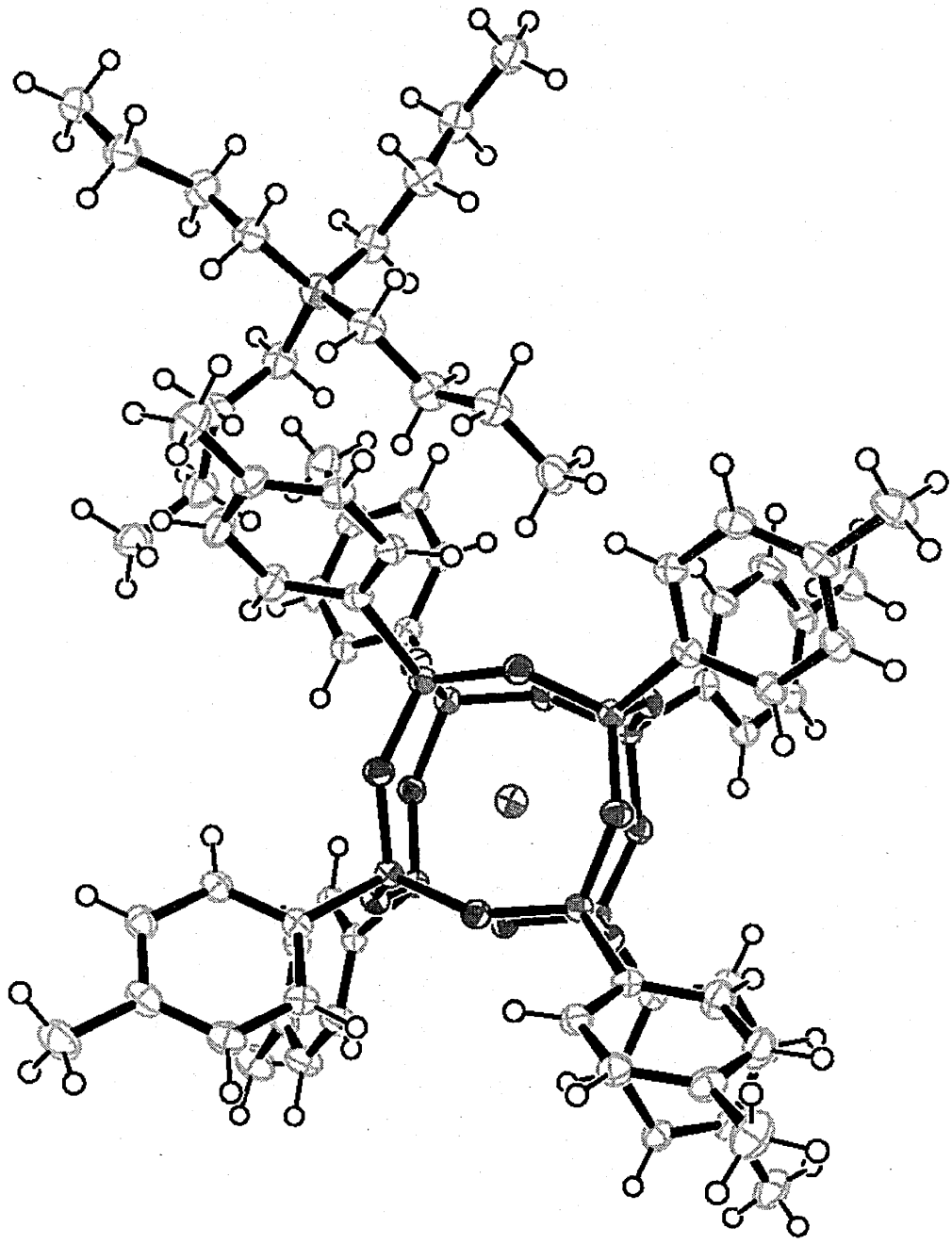

Part 4: Ph_8T_8

Section A. Crystal data and structure refinement.

Identification code	01SRC1029
Empirical formula	$C_{48}H_{40}O_{12}Si_8 \cdot 2H_2O$
Formula weight	1069.55
Temperature	120(2) K
Wavelength	0.71073 Å
Crystal system	Tetragonal
Space group	*P4/n*
Unit cell dimensions	a = 14.4556(6) Å
	b = 14.4556(6) Å
	c = 12.8151(10) Å
Volume	2677.9(3) $Å^3$
Z	2
Density (calculated)	1.326 Mg / m^3
Absorption coefficient	0.262 mm^{-1}
F(000)	1112
Crystal	Colourless Block
Crystal size	0.20 × 0.10 × 0.10 mm^3
θ range for data collection	3.18 – 25.02°
Index ranges	$-17 \le h \le 17, -12 \le k \le 12, -15 \le l \le 14$
Reflections collected	4373
Independent reflections	2366 [R_{int} = 0.0660]
Completeness to θ = 25.02°	99.7 %
Max. and min. transmission	0.9742 and 0.9494
Refinement method	Full-matrix least-squares on F^2
Data / restraints / parameters	2366 / 9 / 170
Goodness-of-fit on F^2	1.066
Final R indices [$F^2 > 2\sigma(F^2)$]	*R1* = 0.0933, *wR2* = 0.2639
R indices (all data)	*R1* = 0.1688, *wR2* = 0.3332
Largest diff. peak and hole	1.570 and –0.423 e $Å^{-3}$

Diffractometer: *Nonius KappaCCD* area detector (ϕ scans and ω scans to fill *asymmetric unit* sphere). **Cell determination:** DirAx (Duisenberg, A.J.M.(1992). J. Appl. Cryst. 25, 92-96.) **Data collection:** Collect (Collect: Data collection software, R. Hooft, Nonius B.V., 1998). **Data reduction and cell refinement**: *Denzo* (Z. Otwinowski & W. Minor, *Methods in Enzymology* (1997) Vol. **276**: *Macromolecular Crystallography*, part A, pp. 307–326; C. W. Carter, Jr. & R. M. Sweet, Eds., Academic Press). **Absorption correction**: *SORTAV* (R. H. Blessing, Acta Cryst. A**51** (1995) 33–37; R. H. Blessing, J. Appl. Cryst. **30** (1997) 421–426). **Structure solution**: *SHELXS97* (G. M. Sheldrick, Acta Cryst. (1990) A**46** 467–473). **Structure refinement**: *SHELXL97* (G. M. Sheldrick (1997), University of Göttingen, Germany). **Graphics:** Cameron - A Molecular Graphics Package. (D. M. Watkin, L. Pearce and C. K. Prout, Chemical Crystallography Laboratory, University of Oxford, 1993).

Special details: All hydrogen atoms were placed in idealised positions and refined using a riding model.

Section B. Atomic coordinates [$\times 10^4$], equivalent isotropic displacement parameters [$Å^2 \times 10^3$] and site occupancy factors. U_{eq} is defined as one third of the trace of the orthogonalized U^{ij} tensor.

Atom	*x*	*y*	*z*	U_{eq}	*S.o.f.*
Si1	1990(120)	1060(120)	9610(140)	30(60)	1
Si2	1960(120)	1070(120)	7210(140)	30(60)	1
O1	3100(300)	1300(300)	9800(400)	40(130)	1
O2	1900(300)	700(300)	8400(300)	40(130)	1
O3	3000(300)	1300(300)	7000(400)	40(130)	1
O1W	−1300(600)	−2100(500)	7100(600)	0(200)	0.50
C1	1700(500)	100(400)	10500(500)	30(160)	1
C2	2300(600)	−600(500)	10700(700)	100(200)	1
C3	2200(600)	−1300(600)	11400(800)	100(300)	1
C4	1300(700)	−1300(600)	11900(700)	100(300)	1
C5	700(600)	−700(600)	11700(600)	100(200)	1
C6	900(500)	100(500)	11000(700)	100(200)	1
C7	1600(400)	100(400)	6400(500)	30(160)	1
C8	1300(600)	−700(500)	6700(600)	0(200)	1
C9	1000(700)	−1400(600)	6100(800)	100(300)	1
C10	1000(600)	−1300(700)	5000(800)	100(300)	1
C11	1200(600)	−400(600)	4600(700)	100(200)	1
C12	1500(500)	300(500)	5300(600)	40(190)	1

Section C. Bond lengths [Å] and angles [°].

Si1–O2	1.6(5)	C3–H3	0.9500
Si1–O1^{i}	1.6(4)	C4–C5	1.4(12)
Si1–O1	1.6(5)	C4–H4	0.9500
Si1–C1	1.8(7)	C5–C6	1.4(11)
Si2–O3	1.6(4)	C5–H5	0.9500
Si2–O3^{i}	1.6(4)	C6–H6	0.9500
Si2–O2	1.6(5)	C7–C12	1.4(10)
Si2–C7	1.8(7)	C7–C8	1.4(9)
O1–Si1^{ii}	1.6(4)	C8–C9	1.4(11)
O3–Si2^{ii}	1.6(4)	C8–H8	0.9500
O1W–H2W	1(3)	C9–C10	1.4(13)
O1W–H1W	1(3)	C9–H9	0.9500
C1–C2	1.4(10)	C10–C11	1.4(12)
C1–C6	1.4(10)	C10–H10	0.9500
C2–C3	1.4(12)	C11–C12	1.4(11)
C2–H2	0.9500	C11–H11	0.9500
C3–C4	1.4(12)	C12–H12	0.9500

O2–Si1–O1^{i}	108(10)	C5–C4–H4	120.2
O2–Si1–O1	109(10)	C3–C4–H4	120.2
O1^{i}–Si1–O1	110(10)	C4–C5–C6	121(10)
O2–Si1–C1	111(10)	C4–C5–H5	119.5
O1^{i}–Si1–C1	111(10)	C6–C5–H5	119.7
O1–Si1–C1	108(10)	C1–C6–C5	120(10)
O3–Si2–O3^{i}	109(10)	C1–C6–H6	119.8
O3–Si2–O2	108(10)	C5–C6–H6	119.7
O3^{i}–Si2–O2	110(10)	C12–C7–C8	119(10)
O3–Si2–C7	112(10)	C12–C7–Si2	120(10)
O3^{i}–Si2–C7	108(10)	C8–C7–Si2	121(10)
O2–Si2–C7	110(10)	C7–C8–H8	119.6
Si1^{ii}–O1–Si1	152(10)	C9–C8–H8	119.7
Si1–O2–Si2	145(10)	C8–C9–C10	120(10)
Si2–O3–Si2$^{i\ i}$	151(10)	C8–C9–H9	120.1
H2W–O1W–H1W	125(10)	C10–C9–H9	120.1
C2–C1–C6	118(10)	C11–C10–C9	119(10)
C2–C1–Si1	119(10)	C11–C10–H10	120.3
C6–C1–Si1	123(10)	C9–C10–H10	120.2
C1–C2–C3	121(10)	C10–C11–C12	119(10)
C1–C2–H2	119.7	C10–C11–H11	120.3
C3–C2–H2	119.7	C12–C11–H11	120.5
C4–C3–C2	120(10)	C7–C12–C11	122(10)
C4–C3–H3	119.7	C7–C12–H12	118.8
C2–C3–H3	119.8	C11–C12–H12	118.9
C5–C4–C3	120(10)		

Symmetry transformations used to generate equivalent atoms:
(i) y,–x+1/2,z (ii) –y+1/2,x,z

Section D. Anisotropic displacement parameters [$Å^2 \times 10^3$]. The anisotropic displacement factor exponent takes the form: $-2\pi^2[h^2a^{*2}U^{11} + \cdots + 2\,h\,k\,a^*\,b^*\,U^{12}]$.

Atom	U^{11}	U^{22}	U^{33}	U^{23}	U^{13}	U^{12}
Si1	30(110)	30(110)	30(120)	0(80)	0(80)	0(80)
Si2	30(110)	30(110)	30(120)	0(80)	0(80)	0(80)
O1	0(300)	0(300)	0(300)	0(200)	0(200)	0(200)
O2	0(300)	0(300)	0(300)	0(200)	0(200)	0(200)
O3	0(200)	0(300)	0(300)	0(200)	0(200)	0(200)
O1W	0(400)	0(300)	0(300)	0(300)	0(300)	0(300)
C1	0(400)	0(400)	0(400)	0(300)	0(300)	0(300)
C2	0(500)	0(500)	100(600)	0(500)	0(400)	0(400)
C3	100(600)	100(600)	100(900)	0(600)	0(500)	0(500)
C4	100(600)	0(500)	100(600)	0(400)	0(500)	0(500)
C5	100(500)	100(600)	0(500)	0(400)	0(400)	0(500)
C6	0(500)	100(500)	100(500)	0(400)	0(400)	0(400)
C7	0(300)	0(400)	0(400)	0(300)	0(300)	0(300)
C8	100(600)	0(400)	0(500)	0(400)	0(400)	0(400)
C9	100(700)	0(500)	100(700)	0(500)	0(500)	0(500)
C10	100(600)	100(600)	100(700)	0(500)	0(500)	0(500)
C11	100(500)	100(600)	0(500)	0(400)	0(400)	0(500)
C12	0(400)	0(400)	0(500)	0(400)	0(400)	0(400)

Section E. Hydrogen coordinates [$\times 10^4$] and isotropic displacement parameters [$Å^2 \times 10^3$].

Atom	*x*	*y*	*z*	U_{eq}	*S.o.f.*
H2	2906	–579	10294	69	1
H3	2634	–1732	11558	88	1
H4	1199	–1852	12342	72	1
H5	120	–698	12100	69	1
H6	403	519	10926	61	1
H8	1398	–848	7462	60	1
H9	841	–2004	6353	80	1
H10	768	–1734	4535	80	1
H11	1100	–264	3891	64	1
H12	1624	885	5036	53	1
H2W	–2000(3000)	–2000(8000)	7000(8000)	50	0.50
H1W	–1000(7000)	–2000(4000)	7000(9000)	50	0.50

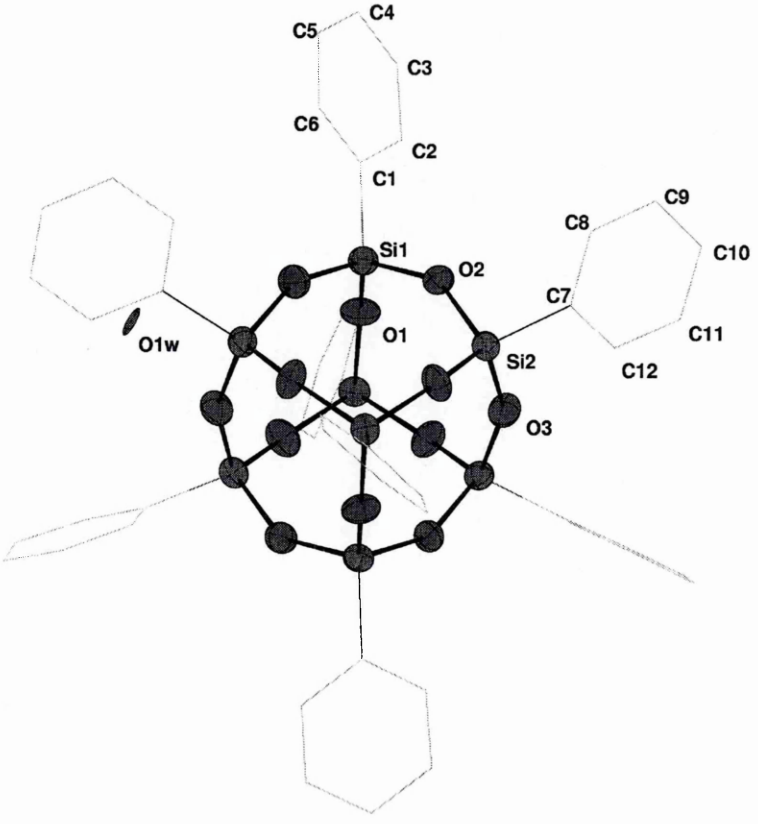
C4
C5
C3
C6
C2
C1
C9
C8
C10
Si1
O2
C7
O1w
O1
C11
Si2
C12
O3

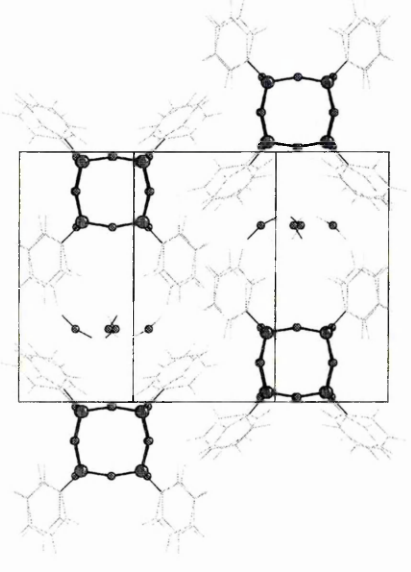

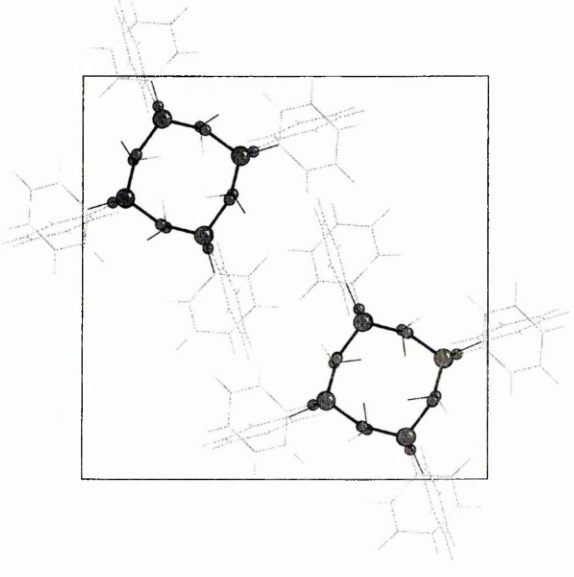

Part 5: $Ph_{12}T_{12}$

Section A. Crystal data and structure refinement.

Identification code	**01SRC332**
Empirical formula	$C_{72}H_{60}O_{18}Si_{12}$
Formula weight	1550.28
Temperature	120(2) K
Wavelength	0.71073 Å
Crystal system	Tetragonal
Space group	*P4/n*
Unit cell dimensions	a = 17.2605(2) Å
	b = 17.2605(2) Å
	c = 13.9608(2) Å
Volume	4159.27(9) $Å^3$
Z	2
Density (calculated)	1.238 Mg / m^3
Absorption coefficient	0.249 mm^{-1}
F(000)	1608
Crystal	Colourless block
Crystal size	0.02 × 0.02 × 0.02 mm^3
θ range for data collection	2.92 – 25.02°
Index ranges	$-20 \le h \le 20$, $-20 \le k \le 20$, $-16 \le l \le 16$
Reflections collected	32444
Independent reflections	3679 [R_{int} = 0.1228]
Completeness to θ = 25.02°	99.8 %
Max. and min. transmission	0.9950 and 0.9950
Refinement method	Full-matrix least-squares on F^2
Data / restraints / parameters	3679 / 0 / 196
Goodness-of-fit on F^2	1.530
Final R indices [$F^2 > 2\sigma(F^2)$]	*R1* = 0.1628, *wR2* = 0.4486
R indices (all data)	*R1* = 0.2092, *wR2* = 0.4691
Extinction coefficient	0.002(2)
Largest diff. peak and hole	2.400 and –0.514 e $Å^{-3}$

Diffractometer: *Nonius KappaCCD* area detector (ϕ scans and ω scans to fill *Ewald* sphere). **Cell determination:** DirAx (Duisenberg, A.J.M.(1992). J. Appl. Cryst. 25, 92-96.) **Data collection:** Collect (Collect: Data collection software, R. Hooft, Nonius B.V., 1998). **Data reduction and cell refinement**: *Denzo* (Z. Otwinowski & W. Minor, *Methods in Enzymology* (1997) Vol. **276**: *Macromolecular Crystallography*, part A, pp. 307–326; C. W. Carter, Jr. & R. M. Sweet, Eds., Academic Press). **Absorption correction**: *SORTAV* (R. H. Blessing, Acta Cryst. A**51** (1995) 33–37; R. H. Blessing, J. Appl. Cryst. **30** (1997) 421–426). **Structure solution**: *SHELXS97* (G. M. Sheldrick, Acta Cryst. (1990) A**46** 467–473). **Structure refinement**: *SHELXL97* (G. M. Sheldrick (1997), University of Göttingen, Germany). **Graphics:** Cameron - A Molecular Graphics Package. (D. M. Watkin, L. Pearce and C. K. Prout, Chemical Crystallography Laboratory, University of Oxford, 1993).

Special details: All hydrogen atoms were placed in idealised positions and refined using a riding model.

Section B. Atomic coordinates [$\times 10^4$], equivalent isotropic displacement parameters [$Å^2 \times 10^3$] and site occupancy factors. U_{eq} is defined as one third of the trace of the orthogonalized U^{ij} tensor.

Atom	*x*	*y*	*z*	U_{eq}	*S.o.f.*
O1	2125(4)	8828(4)	3332(7)	57(2)	1
O2	2500	7500	2482(11)	73(4)	1
O3	1133(4)	7674(4)	3274(7)	63(3)	1
O4	3400(4)	8545(4)	4307(7)	66(3)	1
O5	2353(4)	9464(4)	5025(7)	60(2)	1
Si1	1811(1)	8109(1)	2701(3)	56(1)	1
Si2	860(1)	6983(1)	3994(3)	58(1)	1
Si3	2761(2)	9201(1)	4046(3)	60(1)	1
C1	1425(4)	8491(4)	1548(5)	56(3)	1
C2	1301(4)	9280(3)	1415(6)	69(4)	1
C3	984(5)	9548(3)	562(7)	75(4)	1
C4	791(5)	9027(5)	−159(5)	71(4)	1
C5	915(5)	8238(4)	−26(6)	70(4)	1
C6	1232(4)	7971(3)	827(7)	73(4)	1
C7	110(4)	6392(4)	3384(7)	62(4)	1
C8	−108(5)	6545(5)	2444(7)	90(5)	1
C9	−672(5)	6094(6)	2004(7)	93(5)	1
C10	−1018(5)	5489(5)	2504(8)	92(5)	1
C11	−800(5)	5336(4)	3444(8)	91(5)	1
C12	−236(5)	5788(5)	3884(7)	83(5)	1
C13	3189(4)	10070(3)	3461(8)	78(5)	1
C14	3399(5)	10705(4)	4016(8)	89(5)	1
C15	3699(5)	11365(4)	3581(10)	145(11)	1
C16	3788(5)	11389(4)	2592(10)	106(7)	1
C17	3577(6)	10754(6)	2038(8)	125(8)	1
C18	3278(5)	10095(5)	2472(8)	93(5)	1

Section C. Bond lengths [Å] and angles [°].

O1–Si1	1.614(8)	C2–C3	1.3900
O1–Si3	1.618(8)	C3–C4	1.3900
O2–Si1^{i}	1.616(4)	C4–C5	1.3900
O2–Si1	1.616(4)	C5–C6	1.3900
O3–Si1	1.605(8)	C7–C8	1.3900
O3–Si2	1.630(8)	C7–C12	1.3900
O4–Si3	1.622(7)	C8–C9	1.3900
O4–Si2^{i}	1.628(7)	C9–C10	1.3900
O5–Si3	1.603(9)	C10–C11	1.3900
O5–Si2^{ii}	1.612(10)	C11–C12	1.3900
Si1–C1	1.863(8)	C13–C14	1.3900
Si2–O5^{iii}	1.612(10)	C13–C18	1.3900
Si2–O4^{i}	1.628(7)	C14–C15	1.3900
Si2–C7	1.854(7)	C15–C16	1.3900
Si3–C13	1.860(7)	C16–C17	1.3900
C1–C2	1.3900	C17–C18	1.3900
C1–C6	1.3900		

Si1–O1–Si3	150.4(5)	C2–C1–Si1	121.1(4)
Si1^{i}–O2–Si1	158.2(11)	C6–C1–Si1	118.8(4)
Si1–O3–Si2	149.4(5)	C1–C2–C3	120.0
Si3–O4–Si2^{i}	149.7(7)	C4–C3–C2	120.0
Si3–O5–Si2^{ii}	143.2(4)	C3–C4–C5	120.0
O3–Si1–O1	109.4(5)	C6–C5–C4	120.0
O3–Si1–O2	109.1(4)	C5–C6–C1	120.0
O1–Si1–O2	110.9(4)	C8–C7–C12	120.0
O3–Si1–C1	109.6(4)	C8–C7–Si2	121.2(5)
O1–Si1–C1	108.6(4)	C12–C7–Si2	118.8(5)
O2–Si1–C1	109.3(6)	C7–C8–C9	120.0
O5^{iii}–Si2–O4 ^{i}	105.5(5)	C10–C9–C8	120.0
O5^{iii}–Si2–O3	109.5(4)	C11–C10–C9	120.0
O4^{i}–Si2–O3	110.4(4)	C12–C11–C10	120.0
O5^{iii}–Si2–C7	111.5(4)	C11–C12–C7	120.0
O4^{i}–Si2–C7	111.3(4)	C14–C13–C18	120.0
O3–Si2–C7	108.7(5)	C14–C13–Si3	119.7(5)
O5–Si3–O1	109.8(4)	C18–C13–Si3	120.3(5)
O5–Si3–O4	107.8(5)	C15–C14–C13	120.0
O1–Si3–O4	108.8(4)	C14–C15–C16	120.0
O5–Si3–C13	108.6(4)	C17–C16–C15	120.0
O1–Si3–C13	108.7(5)	C18–C17–C16	120.0
O4–Si3–C13	113.1(4)	C17–C18–C13	120.0
C2–C1–C6	120.0		

Symmetry transformations used to generate equivalent atoms:
(i) –x+1/2,–y+3/2,z (ii) y–1/2,–x+1,–z+1 (iii) –y+1,x+1/2,–z+1

Section D. Anisotropic displacement parameters [$Å^2 \times 10^3$]. The anisotropic displacement factor exponent takes the form: $-2\pi^2[h^2a^{*2}U^{11} + \cdots + 2\,h\,k\,a^*\,b^*\,U^{12}]$.

Atom	U^{11}	U^{22}	U^{33}	U^{23}	U^{13}	U^{12}
O1	26(3)	21(3)	124(7)	1(4)	−4(4)	0(3)
O2	27(5)	28(5)	164(12)	0	0	10(4)
O3	19(3)	27(3)	143(8)	12(4)	−1(4)	−2(3)
O4	24(3)	21(3)	153(8)	−3(4)	−9(4)	3(3)
O5	28(3)	19(3)	131(7)	−3(4)	6(4)	2(3)
Si1	17(1)	16(1)	135(3)	3(2)	1(2)	0(1)
Si2	17(1)	18(1)	138(3)	3(2)	2(2)	−1(1)
Si3	19(1)	15(1)	146(4)	−1(2)	1(2)	−1(1)
C1	18(4)	28(5)	122(10)	−2(6)	4(5)	3(4)
C2	46(6)	33(6)	129(12)	−3(7)	6(7)	7(5)
C3	66(8)	40(7)	119(12)	9(8)	4(8)	14(6)
C4	52(7)	54(7)	109(11)	−1(8)	3(7)	13(6)
C5	55(7)	45(7)	109(11)	−9(7)	−11(8)	2(5)
C6	44(6)	29(6)	146(14)	−11(7)	−1(8)	−5(5)
C7	31(5)	22(5)	133(12)	−4(6)	10(6)	−5(4)
C8	46(7)	82(10)	142(15)	14(10)	−4(9)	−32(7)
C9	85(11)	87(11)	105(13)	−22(9)	10(9)	−32(9)
C10	55(8)	68(9)	151(16)	−34(10)	12(9)	−33(7)
C11	67(9)	59(8)	148(15)	−18(10)	9(10)	−35(7)
C12	46(7)	42(7)	162(15)	4(8)	9(8)	−22(6)
C13	22(5)	17(5)	195(17)	2(7)	5(7)	−3(4)
C14	61(8)	31(6)	176(16)	3(8)	−23(9)	−18(6)
C15	50(9)	28(7)	360(40)	17(13)	−1(15)	−18(6)
C16	58(9)	40(8)	220(20)	35(11)	43(12)	−1(6)
C17	76(10)	75(11)	220(20)	33(13)	79(13)	−8(9)
C18	71(9)	63(9)	147(15)	12(10)	53(10)	−15(7)

Section E. Hydrogen coordinates [$\times 10^4$] and isotropic displacement parameters [$Å^2 \times 10^3$].

Atom	*x*	*y*	*z*	U_{eq}	*S.o.f.*
H2	1433	9636	1908	83	1
H3	900	10087	471	90	1
H4	575	9210	−742	86	1
H5	783	7882	−519	84	1
H6	1316	7432	918	87	1
H8	129	6959	2103	108	1
H9	−821	6198	1362	111	1
H10	−1403	5181	2204	110	1
H11	−1036	4923	3785	110	1
H12	−87	5684	4526	100	1
H14	3338	10689	4692	107	1
H15	3842	11799	3960	174	1
H16	3992	11840	2295	127	1
H17	3638	10771	1362	150	1
H18	3134	9661	2094	112	1

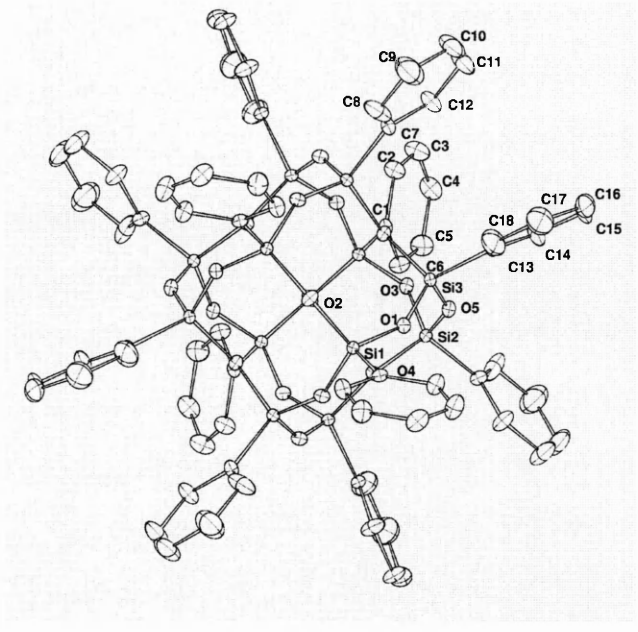
C10
C9
C11
C8
C12
C7
C3
C2
C4
C1
C17
C16
C18
C15
C5
C14
C13
C6
O3
Si3
O2
O5
O1
Si2
Si1
O4

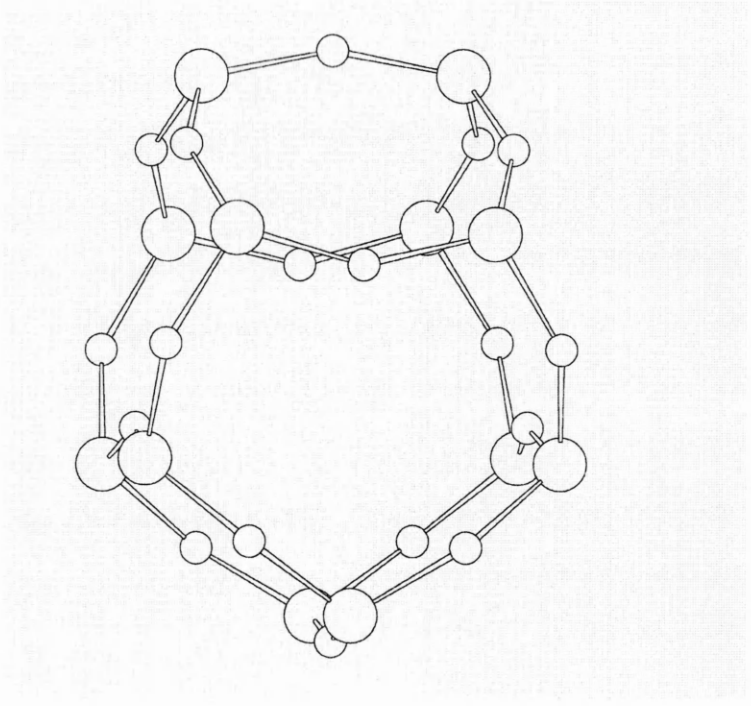

Part 6: iso-butylT$_8$

Section A. Crystal data and structure refinement.

Identification code	**02src624**	
Empirical formula	$C_{32}H_{72}O_{12}Si_8$	
Formula weight	873.62	
Temperature	120(2) K	
Wavelength	0.71073 Å	
Crystal system	Triclinic	
Space group	*P*–1	
Unit cell dimensions	a = 10.0114(3) Å	α = 96.7560(10)°
	b = 10.8285(3) Å	β = 91.1600(10)°
	c = 10.9746(3) Å	γ = 99.3190(10)°
Volume	1164.95(6) Å^3	
Z	1	
Density (calculated)	1.245 Mg / m^3	
Absorption coefficient	0.282 mm^{-1}	
F(000)	472	
Crystal	Shard; Colourless	
Crystal size	0.40 × 0.30 × 0.20 mm^3	
θ range for data collection	3.04 – 27.44°	
Index ranges	$-12 \le h \le 12$, $-14 \le k \le 13$, $-14 \le l \le 14$	
Reflections collected	20992	
Independent reflections	5262 [R_{int} = 0.0401]	
Completeness to θ = 27.44°	99.2 %	
Absorption correction	Semi–empirical from equivalents	
Max. and min. transmission	0.9458 and 0.8956	
Refinement method	Full-matrix least-squares on F^2	
Data / restraints / parameters	5262 / 0 / 379	
Goodness-of-fit on F^2	1.030	
Final *R* indices [$F^2 > 2\sigma(F^2)$]	*R1* = 0.0345, *wR2* = 0.0854	
R indices (all data)	*R1* = 0.0481, *wR2* = 0.0914	
Largest diff. peak and hole	0.331 and –0.333 e Å^{-3}	

Diffractometer: *Nonius KappaCCD* area detector (ϕ scans and ω scans to fill *asymmetric unit* sphere). **Cell determination:** DirAx (Duisenberg, A.J.M.(1992). J. Appl. Cryst. 25, 92-96.) **Data collection:** Collect (Collect: Data collection software, R. Hooft, Nonius B.V., 1998). **Data reduction and cell refinement**: *Denzo* (Z. Otwinowski & W. Minor, *Methods in Enzymology* (1997) Vol. **276**: *Macromolecular Crystallography*, part A, pp. 307–326; C. W. Carter, Jr. & R. M. Sweet, Eds., Academic Press). **Absorption correction**: *SORTAV* (R. H. Blessing, Acta Cryst. A**51** (1995) 33–37; R. H. Blessing, J. Appl. Cryst. **30** (1997) 421–426). **Structure solution**: *SHELXS97* (G. M. Sheldrick, Acta Cryst. (1990) A**46** 467–473). **Structure refinement**: *SHELXL97* (G. M. Sheldrick (1997), University of Göttingen, Germany). **Graphics:** Cameron - A Molecular Graphics Package. (D. M. Watkin, L. Pearce and C. K. Prout, Chemical Crystallography Laboratory, University of Oxford, 1993).

Special details:

Section B. Atomic coordinates [$\times 10^4$], equivalent isotropic displacement parameters [$Å^2 \times 10^3$] and site occupancy factors. U_{eq} is defined as one third of the trace of the orthogonalized U^{ij} tensor.

Atom	*x*	*y*	*z*	U_{eq}	*S.o.f.*
Si1	1375(1)	4117(1)	−1918(1)	14(1)	1
Si2	2353(1)	4426(1)	860(1)	14(1)	1
Si3	−492(1)	3210(1)	1529(1)	14(1)	1
Si4	−1475(1)	2901(1)	−1247(1)	14(1)	1
O1	2216(1)	4184(1)	−627(1)	21(1)	1
O2	1140(1)	3499(1)	1416(1)	20(1)	1
O3	−1181(1)	2730(1)	175(1)	21(1)	1
O4	−39(1)	3135(1)	−1917(1)	20(1)	1
O5	1018(1)	5500(1)	−2063(1)	20(1)	1
O6	2205(1)	5875(1)	1298(1)	21(1)	1
C1	2427(2)	3552(2)	−3157(1)	19(1)	1
C2	1884(2)	3424(2)	−4496(2)	25(1)	1
C3	2682(2)	2615(2)	−5339(2)	37(1)	1
C4	1921(3)	4704(2)	−4950(2)	44(1)	1
C5	3987(2)	4142(2)	1473(2)	19(1)	1
C6	4263(2)	2776(2)	1318(2)	24(1)	1
C7	4454(2)	2314(2)	−20(2)	39(1)	1
C8	5505(2)	2670(2)	2098(2)	39(1)	1
C9	−896(2)	2028(2)	2601(1)	17(1)	1
C10	−458(2)	737(2)	2270(2)	21(1)	1
C11	−513(2)	22(2)	3390(2)	32(1)	1
C12	−1337(3)	−53(2)	1215(2)	38(1)	1
C13	−2627(2)	1489(2)	−1975(2)	19(1)	1
C14	−3571(2)	1696(2)	−3031(2)	27(1)	1
C15	−4724(2)	580(2)	−3308(2)	40(1)	1
C16	−2772(3)	1939(2)	−4173(2)	42(1)	1

Section C. Bond lengths [Å] and angles [°].

Si1–O5	1.6200(11)	C6–C7	1.521(3)
Si1–O1	1.6214(11)	C6–C8	1.523(3)
Si1–O4	1.6269(11)	C6–H6	0.92(2)
Si1–C1	1.8442(16)	C7–H7A	0.95(2)
Si2–O6	1.6168(11)	C7–H7B	1.01(2)
Si2–O1	1.6215(11)	C7–H7C	0.96(3)
Si2–O2	1.6229(11)	C8–H8A	0.99(3)
Si2–C5	1.8417(16)	C8–H8B	0.96(3)
Si3–O3	1.6175(11)	C8–H8C	0.98(3)
Si3–O5^{i}	1.6216(11)	C9–C10	1.538(2)
Si3–O2	1.6225(11)	C9–H9A	0.95(2)
Si3–C9	1.8419(15)	C9–H9B	0.91(2)
Si4–O3	1.6201(11)	C10–C11	1.525(2)
Si4–O6^{i}	1.6202(11)	C10–C12	1.525(3)
Si4–O4	1.6253(11)	C10–H10	0.99(2)
Si4–C13	1.8460(16)	C11–H11A	0.95(2)
O5–Si3^{i}	1.6216(11)	C11–H11B	0.98(3)
O6–Si4^{i}	1.6202(11)	C11–H11C	0.98(2)
C1–C2	1.540(2)	C12–H12A	0.95(3)
C1–H1A	0.94(2)	C12–H12B	0.96(3)
C1–H1B	0.97(2)	C12–H12C	1.02(3)
C2–C4	1.523(3)	C13–C14	1.540(2)
C2–C3	1.527(3)	C13–H13A	1.01(2)
C2–H2	0.98(2)	C13–H13B	0.92(2)
C3–H3A	0.99(3)	C14–C16	1.526(3)
C3–H3B	0.94(2)	C14–C15	1.527(3)
C3–H3C	1.00(3)	C14–H14	1.05(2)
C4–H4A	1.04(3)	C15–H15A	1.06(3)
C4–H4B	0.97(2)	C15–H15B	1.09(3)
C4–H4C	0.98(3)	C15–H15C	1.04(3)
C5–C6	1.539(2)	C16–H16A	0.95(2)
C5–H5A	0.98(2)	C16–H16B	0.98(3)
C5–H5B	0.99(2)	C16–H16C	0.99(3)

O5–Si1–O1	108.93(6)	O6^{i}–Si4–O4	108.74(6)
O5–Si1–O4	108.35(6)	O3–Si4–C13	108.74(7)
O1–Si1–O4	109.66(6)	O6^{i}–Si4–C13	108.96(7)
O5–Si1–C1	112.58(7)	O4–Si4–C13	112.68(7)
O1–Si1–C1	107.63(7)	Si1–O1–Si2	151.92(8)
O4–Si1–C1	109.68(7)	Si3–O2–Si2	143.14(7)
O6–Si2–O1	108.59(6)	Si3–O3–Si4	152.73(8)
O6–Si2–O2	109.09(6)	Si4–O4–Si1	143.08(7)
O1–Si2–O2	108.93(6)	Si1–O5–Si3^{i}	152.11(8)
O6–Si2–C5	108.46(7)	Si2–O6–Si4^{i}	152.35(8)
O1–Si2–C5	112.90(7)	C2–C1–Si1	118.77(12)
O2–Si2–C5	108.81(7)	C2–C1–H1A	109.8(11)
O3–Si3–O5^{i}	108.86(6)	Si1–C1–H1A	103.3(11)
O3–Si3–O2	108.66(6)	C2–C1–H1B	109.6(12)
O5^{i}–Si3–O2	109.10(6)	Si1–C1–H1B	107.5(12)
O3–Si3–C9	112.24(7)	H1A–C1–H1B	107.3(17)
O5^{i}–Si3–C9	109.38(7)	C4–C2–C3	109.86(16)
O2–Si3–C9	108.56(7)	C4–C2–C1	111.85(15)
O3–Si4–O6^{i}	108.98(6)	C3–C2–C1	110.80(15)
O3–Si4–O4	108.68(6)	C4–C2–H2	109.2(12)

C3–C2–H2	106.5(11)
C1–C2–H2	108.5(11)
C2–C3–H3A	110.8(14)
C2–C3–H3B	109.0(14)
H3A–C3–H3B	108(2)
C2–C3–H3C	109.8(14)
H3A–C3–H3C	110(2)
H3B–C3–H3C	109.3(19)
C2–C4–H4A	108.5(15)
C2–C4–H4B	111.0(14)
H4A–C4–H4B	106(2)
C2–C4–H4C	112.2(15)
H4A–C4–H4C	108(2)
H4B–C4–H4C	111(2)
C6–C5–Si2	117.54(11)
C6–C5–H5A	110.2(12)
Si2–C5–H5A	103.6(12)
C6–C5–H5B	107.0(11)
Si2–C5–H5B	110.4(11)
H5A–C5–H5B	107.7(16)
C7–C6–C8	110.00(17)
C7–C6–C5	111.38(15)
C8–C6–C5	110.40(16)
C7–C6–H6	106.8(12)
C8–C6–H6	107.8(12)
C5–C6–H6	110.4(12)
C6–C7–H7A	113.8(14)
C6–C7–H7B	109.1(13)
H7A–C7–H7B	104.8(19)
C6–C7–H7C	110.0(15)
H7A–C7–H7C	106.6(19)
H7B–C7–H7C	112(2)
C6–C8–H8A	110.6(15)
C6–C8–H8B	111.0(15)
H8A–C8–H8B	107(2)
C6–C8–H8C	109.4(14)
H8A–C8–H8C	112(2)
H8B–C8–H8C	107(2)
C10–C9–Si3	117.54(11)
C10–C9–H9A	108.5(12)
Si3–C9–H9A	110.6(12)
C10–C9–H9B	113.3(13)
Si3–C9–H9B	102.4(13)
H9A–C9–H9B	103.5(17)
C11–C10–C12	109.91(16)
C11–C10–C9	110.24(14)
C12–C10–C9	111.72(14)
C11–C10–H10	107.8(11)
C12–C10–H10	108.8(11)
C9–C10–H10	108.3(11)
C10–C11–H11A	108.7(13)
C10–C11–H11B	111.7(16)
H11A–C11–H11B	106(2)
C10–C11–H11C	111.4(11)
H11A–C11–H11C	106.6(18)
H11B–C11–H11C	111.8(19)
C10–C12–H12A	105.9(15)
C10–C12–H12B	113.1(16)
H12A–C12–H12B	113(2)
C10–C12–H12C	108.2(16)
H12A–C12–H12C	113(2)
H12B–C12–H12C	104(2)
C14–C13–Si4	116.13(11)
C14–C13–H13A	111.7(11)
Si4–C13–H13A	104.9(11)
C14–C13–H13B	108.6(13)
Si4–C13–H13B	111.3(13)
H13A–C13–H13B	103.5(17)
C16–C14–C15	111.34(16)
C16–C14–C13	110.69(16)
C15–C14–C13	110.93(16)
C16–C14–H14	108.3(12)
C15–C14–H14	106.2(12)
C13–C14–H14	109.3(11)
C14–C15–H15A	110.3(13)
C14–C15–H15B	107.2(14)
H15A–C15–H15B	110.7(19)
C14–C15–H15C	112.6(15)
H15A–C15–H15C	106.5(19)
H15B–C15–H15C	109(2)
C14–C16–H16A	111.4(13)
C14–C16–H16B	107.8(14)
H16A–C16–H16B	106.8(19)
C14–C16–H16C	110.3(15)
H16A–C16–H16C	114(2)
H16B–C16–H16C	106(2)

Symmetry transformations used to generate equivalent atoms:
(i) −x,−y+1,−z

Section D. Anisotropic displacement parameters [$Å^2 \times 10^3$]. The anisotropic displacement factor exponent takes the form: $-2\pi^2[h^2a^{*2}U^{11} + \cdots + 2\,h\,k\,a^*\,b^*\,U^{12}]$.

Atom	U^{11}	U^{22}	U^{33}	U^{23}	U^{13}	U^{12}
Si1	14(1)	15(1)	13(1)	2(1)	1(1)	4(1)
Si2	13(1)	15(1)	14(1)	3(1)	0(1)	4(1)
Si3	14(1)	14(1)	14(1)	4(1)	1(1)	3(1)
Si4	14(1)	14(1)	14(1)	2(1)	0(1)	3(1)
O1	19(1)	31(1)	14(1)	2(1)	−1(1)	8(1)
O2	14(1)	21(1)	25(1)	9(1)	2(1)	3(1)
O3	26(1)	22(1)	15(1)	4(1)	−3(1)	1(1)
O4	17(1)	19(1)	22(1)	−1(1)	3(1)	1(1)
O5	24(1)	17(1)	22(1)	5(1)	5(1)	8(1)
O6	20(1)	16(1)	26(1)	1(1)	−2(1)	6(1)
C1	19(1)	21(1)	18(1)	2(1)	4(1)	6(1)
C2	26(1)	30(1)	18(1)	1(1)	3(1)	5(1)
C3	45(1)	43(1)	21(1)	−3(1)	10(1)	10(1)
C4	72(2)	43(1)	22(1)	9(1)	5(1)	20(1)
C5	17(1)	20(1)	19(1)	4(1)	0(1)	5(1)
C6	14(1)	21(1)	40(1)	11(1)	4(1)	6(1)
C7	39(1)	31(1)	47(1)	−5(1)	0(1)	18(1)
C8	26(1)	42(1)	56(1)	20(1)	−2(1)	15(1)
C9	17(1)	18(1)	18(1)	5(1)	2(1)	4(1)
C10	23(1)	19(1)	22(1)	7(1)	4(1)	6(1)
C11	46(1)	24(1)	31(1)	13(1)	4(1)	11(1)
C12	59(2)	21(1)	35(1)	0(1)	−8(1)	9(1)
C13	19(1)	18(1)	21(1)	2(1)	0(1)	2(1)
C14	25(1)	29(1)	26(1)	0(1)	−7(1)	1(1)
C15	30(1)	46(1)	39(1)	−4(1)	−9(1)	−7(1)
C16	50(1)	47(1)	25(1)	9(1)	−8(1)	−5(1)

Section E. Hydrogen coordinates [$\times 10^4$] and isotropic displacement parameters [$Å^2 \times 10^3$].

Atom	*x*	*y*	*z*	U_{eq}	*S.o.f.*
H1A	2558(19)	2754(19)	–2953(17)	25(5)	1
H1B	3310(20)	4100(20)	–3066(19)	35(5)	1
H2	950(20)	2980(19)	–4544(17)	28(5)	1
H3A	2620(30)	1760(30)	–5090(20)	57(7)	1
H3B	3600(20)	2990(20)	–5280(20)	42(6)	1
H3C	2340(20)	2560(20)	–6210(20)	53(7)	1
H4A	2920(30)	5140(30)	–4940(20)	63(8)	1
H4B	1590(20)	4610(20)	–5790(20)	47(6)	1
H4C	1430(30)	5250(30)	–4430(20)	61(7)	1
H5A	3990(20)	4463(19)	2350(19)	30(5)	1
H5B	4750(20)	4660(18)	1106(17)	28(5)	1
H6	3540(20)	2241(19)	1571(18)	31(5)	1
H7A	4630(20)	1470(20)	–150(20)	43(6)	1
H7B	5280(20)	2850(20)	–320(20)	47(6)	1
H7C	3640(30)	2330(20)	–510(20)	53(7)	1
H8A	5360(20)	2910(20)	2970(20)	54(7)	1
H8B	5680(20)	1820(20)	2020(20)	51(7)	1
H8C	6300(30)	3190(20)	1810(20)	48(6)	1
H9A	–1830(20)	1896(19)	2746(18)	29(5)	1
H9B	–510(20)	2450(20)	3326(19)	33(5)	1
H10	490(20)	879(18)	2018(17)	27(5)	1
H11A	–1420(20)	–100(20)	3660(20)	39(6)	1
H11B	50(30)	500(30)	4080(30)	63(8)	1
H11C	–280(20)	–820(20)	3186(17)	30(5)	1
H12A	–990(30)	–820(30)	1070(20)	57(7)	1
H12B	–1370(30)	370(30)	490(20)	62(8)	1
H12C	–2320(30)	–190(30)	1480(30)	73(9)	1
H13A	–3150(20)	1145(19)	–1280(18)	31(5)	1
H13B	–2160(20)	860(20)	–2249(18)	32(5)	1
H14	–4030(20)	2480(20)	–2763(19)	37(5)	1
H15A	–5280(20)	440(20)	–2510(20)	54(7)	1
H15B	–4270(30)	–240(30)	–3620(20)	66(8)	1
H15C	–5410(30)	720(20)	–3980(20)	61(7)	1
H16A	–2110(20)	2670(20)	–4020(20)	43(6)	1
H16B	–3400(30)	2090(20)	–4810(20)	56(7)	1
H16C	–2410(30)	1170(30)	–4500(20)	60(8)	1

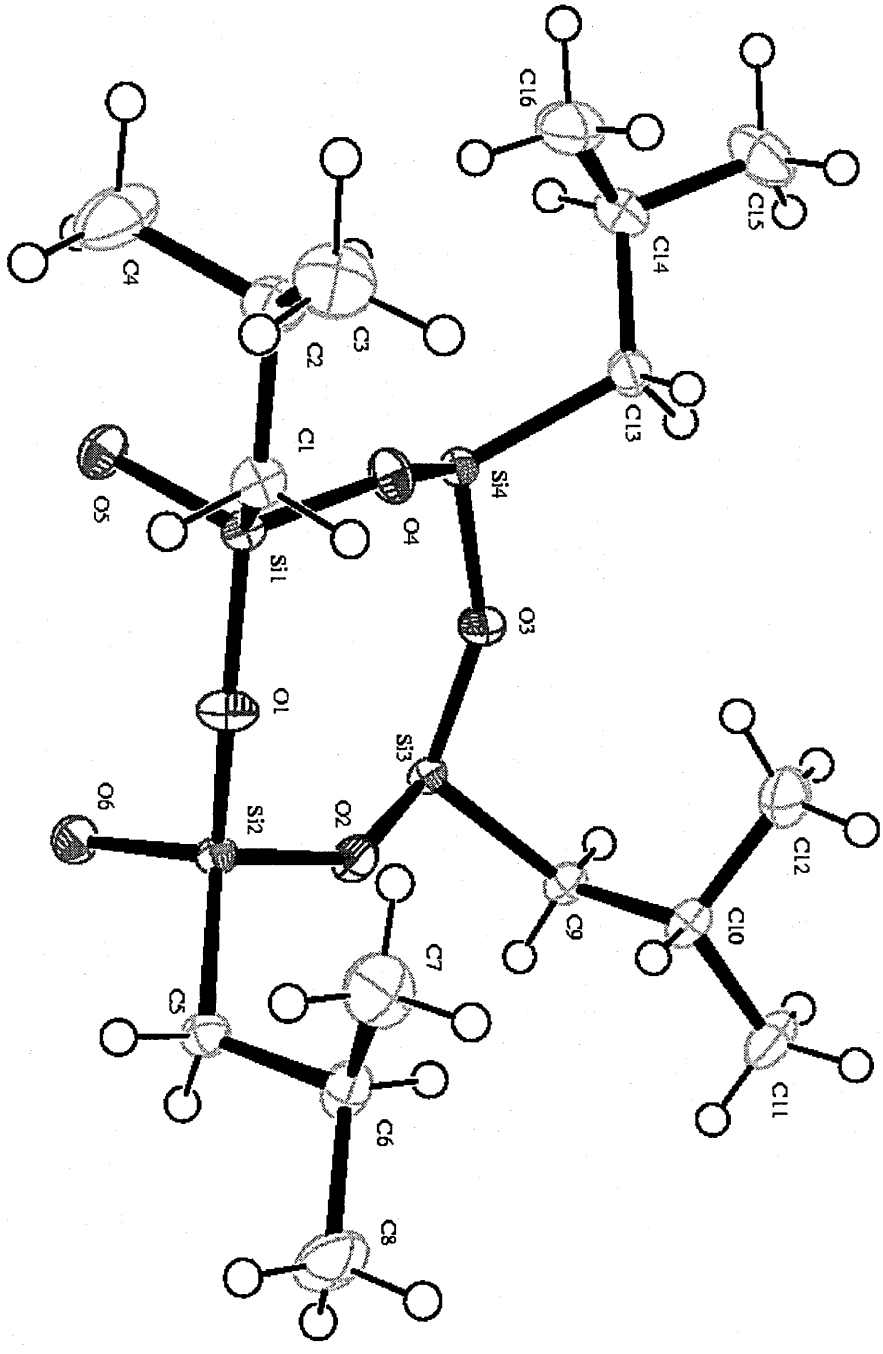
C16
C15
C14
C4
C3
C2
C13
C1
O5
Si4
O4
Si1
O3
O1
Si3
O6
Si2
O2
C12
C9
C10
C7
C5
C11
C6
C8